

University of Nottingham  
School of Chemical, Environmental and Mining Engineering

**Tray Efficiency Effects in Batch Distillation**

by

Chibuikwe Igbokwe Ukeje-Eloagu  
B.Sc., M.Sc.

Thesis submitted to the University of Nottingham for the degree of  
Doctor of Philosophy

May 1998

This work is dedicated to my parents, Mr Ukeje O. Eloagu

Mrs. Florence M. Ukeje-Eloagu

And to my siblings Nneoma

Ngozi

Ihuarulam (Wawam)

Onyekachi

# ACKNOWLEDGEMENTS

I would like to express my gratitude to my supervisor Dr. J.A. Wilson for his guidance and support throughout the project and also to Dr. Richard Pulley and Prof. B.J. Azzopardi. Thanks to the Chemical Engineering department for their financial assistance.

A special word of gratitude to my parents Mr. & Mrs. Ukeje O. Eloagu for their support, love and faith. Without you, I couldn't have done this.

I would also like to express my gratitude to:

- Mr & Mrs A.C. Madubuko, my 'parents' in England.
- Mr. & Mrs. D.A. Ochemba for their love and support.
- Dr. & Mrs. E.O. Ogbonna and family for their love and guidance.
- Emma Rowe for her listening ear, her support, motivation and invaluable assistance throughout.
- Dr. D. Rees, Dr. C. Watkins, Dr. & Mrs. Rowe, Tunde Kazeem, Jacob Madubuko, Dr. Ahmed Bellah, Luca Letizia, Dr. Claudio Martinez, Dr. Avtar Barhey, Dr. Adrian Holt, Sue Rea, Cristiane Sodre, Mr. John Luger, Mr. Derek Wood, Adam Dodgheson, Sahana Nayak, Ugochi Ofurum, Okey Ajikere, Dr. Seema Agrawal and other friends who have contributed to my progress in their different ways.
- The technical staff in the Chemical Engineering laboratory.
- Staff and postgraduates in the Chemical Engineering department.
- The Nottingham Salseros, especially the University Staff Club dance class.
- The Nottingham University Volley club.

## SUMMARY

Computer simulation has long been recognised as a useful tool in improved process operation and design studies. Commercial simulation packages now available for batch distillation studies typically assume constant tray efficiency. Here, on the basis of both practical work and computer simulation, the effects of tray efficiency variation with tray liquid composition on model accuracy and column performance are investigated.

Detailed modelling studies were carried out on a pilot batch distillation unit and tray efficiency was found to be an important factor affecting the model fidelity. Distillation of different methanol/water mixtures revealed that tray efficiency varies with the mixture composition on the tray, the form of the variation being for the efficiency to pass through a minimum at intermediate compositions.

This variation of tray efficiency with tray composition is a known phenomenon, which has not been included in batch distillation simulations even though tray compositions change significantly during a batch run. The model developed in this work (Variable Efficiency Model) includes the tray efficiency variation with mixture composition and results in an evident improvement in model accuracy for methanol/water distillation.

The potential effects of strong tray efficiency dependence on mixture composition, at a more general level, are investigated using two case studies, based on hypothetical extensions of the tray efficiency concentration dependence observed for methanol/water mixtures. In extreme cases, the efficiency-composition dependence could introduce a significant additional non-linearity to the process behaviour, resulting in unexpected composition and temperature movements. To quantify the potential significance of these effects, the economic performance of a column based on simulation using the Variable Efficiency Model was compared with its performance, using an

overall column efficiency (which is the common practice). Using fixed column efficiency was found to under-predict column performance for low purity products and over-predict performance for high purity products.

# CONTENTS

<b>CHAPTER 1. INTRODUCTION</b>	<b>1</b>
<b>CHAPTER 2. LITERATURE REVIEW</b>	<b>7</b>
2.1 APPLICATION OF BATCH DISTILLATION	8
2.1.1 Azeotropic Batch Distillation	8
2.1.2 Reactive Batch Distillation	11
2.2 COLUMN CONFIGURATIONS	12
2.3 OPERATION OF BATCH DISTILLATION COLUMNS	14
2.3.1 Constant Reflux Ratio Operation	14
2.3.2 Variable Reflux Ratio Operation	15
2.3.3 Optimum Reflux Ratio Operation	15
2.3.4 Other Operating Strategies	16
2.3.4.1 Accumulated Product Strategy	16
2.3.4.2 Intermittent Distillate Scheme	17
2.3.4.3 Slop Handling Strategies	17
2.3.5 Optimisation	19
2.4 MODELLING & SIMULATION	20
2.4.1 Simplified / Shortcut Models	23
2.4.2 Rigorous Models	25
2.4.3 State Estimation	27
2.5 FACTORS AFFECTING BATCH DISTILLATION	27
2.5.1 Tray Holdup	28
2.5.2 Reflux Ratio	30
2.5.3 Tray Efficiency	31
2.5.3.1 Non-Equilibrium Stage Models	33
2.5.3.2 Murphree Vapour Phase Tray Efficiency	34
2.5.3.3 Tray Efficiency Variation	35
2.5.3.4 Estimating Tray Efficiency	37
2.6 FACTORS AFFECTING TRAY EFFICIENCY	39

2.6.1	Hole Size and Outlet Weir Height	39
2.6.2	Reflux Ratio and Tray Holdup	40
2.6.3	Fluid Flow Regime	41
2.6.4	Liquid Viscosity	41
2.6.5	Surface Tension Effects	42
2.6.6	Concentration Effects	45
2.7	SUMMARY	48
<b>CHAPTER 3. THE KESTNER COLUMN</b>		<b>50</b>
3.1	THE STILL / BOILER	50
3.2	THE COLUMN	53
3.3	THE CONDENSER	55
3.4	EXPERIMENTAL PROCEDURE	55
3.4.1	Sampling Procedure	57
<b>CHAPTER 4. THE SIMULATION MODEL</b>		<b>58</b>
4.1	MODEL SPECIFICATIONS	58
4.2	MODEL ASSUMPTIONS	59
4.3	MODEL EQUATIONS	61
4.3.1	Main Column Equations	61
4.3.2	Vapour Liquid Equilibrium	64
4.3.3	The Heat Input and Fluid Flow Rates.	66
4.3.4	Variable Tray Efficiency	68
4.4	SIMULATION USING THE MODEL	69
4.5	LIMITATIONS OF THE MODEL	70
<b>CHAPTER 5. THE CONSTANT EFFICIENCY MODEL</b>		<b>72</b>
5.1	METHANOL/WATER MIXTURE DISTILLATION	72
5.1.1	Runs 1 and 2	72
5.1.2	Run 3	75
5.1.3	Run 4	79
5.1.4	Runs 5, 6 and 7	82
5.2	MODEL VERIFICATION USING OTHER FEED MIXTURES	86

5.2.1	Simulating the Experimental Work of Dribika (1986)	87
5.2.2	Simulating the Experimental Work of Domench et al (1974)	91
5.3	SUMMARY	94
<b>CHAPTER 6. THE VARIABLE EFFICIENCY MODEL</b>		<b>96</b>
6.1	TRAY EFFICIENCY VS CONCENTRATION CURVES	96
6.2	MODEL VERIFICATION	98
<b>CHAPTER 7. CASE STUDIES</b>		<b>107</b>
7.1	CASE STUDY –1	108
7.1.1	Case Study –1 Simulations	110
7.1.1.1	Fixed Reflux Ratio Simulation For Case Study –1	110
7.1.1.2	Fixed Distillate Composition Simulation for Case Study –1	125
7.2	CASE STUDY –2	128
7.2.1	Case Study –2 Simulations	130
7.2.1.1	Fixed Reflux Ratio Simulation For Case Study –2	130
7.2.1.2	Fixed Distillate Composition Simulation For Case Study –2	135
7.3	ECONOMIC PERFORMANCE IMPLICATIONS OF THE TRAY EFFICIENCY-COMPOSITION DEPENDENCE	137
<b>CHAPTER 8. RESULTS ANALYSIS</b>		<b>146</b>
8.1	MODEL BEHAVIOUR AND ACCURACY	146
8.1.1	Equilibration Time	148
8.1.2	Slope of the Equilibrium Line.	149
8.1.3	Temperature and Composition Profiles	151
8.2	COLUMN PERFORMANCE ANALYSIS	154
<b>CHAPTER 9. CONCLUSIONS</b>		<b>157</b>
<b>CHAPTER 10. FURTHER WORK.</b>		<b>162</b>
<b>NOMENCLATURE</b>		<b>163</b>

<b>REFERENCES</b>	<b>166</b>
<b>APPENDIX A: COLUMN TEST RUNS AND SUMMARY OF FEED AND OPERATING CONDITIONS FOR ALL THE EXPERIMENTAL RUNS</b>	<b>182</b>
A.1 WATER TEST RUNS	182
A.2 METHANOL/WATER TEST RUNS	183
A.2.1 Run T1	184
A.2.2 Runs T2 and T3	185
A.3 SUMMARY OF THE FEED AND OPERATING CONDITIONS FOR THE EXPERIMENTAL AND SIMULATION RUNS	188
<b>APPENDIX B: PROGRAM LISTING, INPUT DATA AND OUTPUT FILES</b>	<b>190</b>
B.1 PROGRAM LISTING	190
B.2 SAMPLE INPUT DATA AND OUTPUT FILES	213
<b>APPENDIX C: PROPERTIES OF COMPONENTS</b>	<b>221</b>

# LIST OF FIGURES

Figure 2.1: Equilibrium Curve for an Azeotropic Mixture.	9
Figure 2.2: Different Configurations of Batch Distillation Columns (Davidyan et. al. (1994)).	13
Figure 2.3: Interfacial Contacting on a Perforated Plate for a Positive and a Negative System (from Ellis & Legg (1962)).	43
Figure 3.1: The Kestner Distillation Column.	51
Figure 3.2: Bubble Cap Tray Details.	52
Figure 4.1: Column Section for Arbitrary Trays, n, n-1 and Top of Column.	62
Figure 4. 2: Flowchart of Program Algorithm	69
Figure 5.1: Steady State Temperature and Composition Profiles for Run 1 and Run 2	74
Figure 5.2: Column Steady State Profiles for Run 3 after Initial Total Reflux Startup and after Timed Product Withdrawal.	77
Figure 5.3: Temperature and Composition Movements in the Column during Product Withdrawal for Run 3	78
Figure 5.4: Column Steady State Profiles and Temperature Movements during Product Withdrawal for Run 4.	81
Figure 5.5: Column Steady State Profiles and Temperature Movements during Product Withdrawal for Run 5	83
Figure 5.6: Column Steady State Profiles and Temperature Movements during Product Withdrawal for Run 6	84
Figure 5.7: Column Steady State Profiles and Temperature Movements during Product Withdrawal for Run 7	85
Figure 5.8: Constant Efficiency Model Profiles at Steady State Compared with Profiles from Dribika (1986) for the Drib -1 example	88
Figure 5.9: Constant Efficiency Model Profiles at Steady State Compared with Profiles from Dribika (1986) for the Drib -2 example	89

Figure 5.10: Constant Efficiency Model Profiles at Steady State Compared with Profiles from Dribika (1986) for the Drib –3 example	90
Figure 5.11: Cyclohexane-Toluene Distillation results - Example 1 (Domench et al (1974)).	93
Figure 5.12: Cyclohexane-Toluene Distillation results - Example 2 (Domench et al (1974)).	93
Figure 6.1: Tray Efficiency vs. Concentration for Runs 3 to 7.	97
Figure 6.2: Polynomial Best-Fit Curve for Tray Efficiency as a Function of Methanol Concentration	97
Figure 6.3: Constant & Variable Efficiency Model Steady State Temperature and Composition Profiles for Run 3.	99
Figure 6.4: Constant & Variable Efficiency Model Steady State Temperature and Composition Profiles for Run 5	100
Figure 6.5: Constant & Variable Efficiency Model Steady State Temperature and Composition Profiles for Run 6	101
Figure 6.6: Constant & Variable Efficiency Model Steady State Temperature and Composition Profiles for Run 7	102
Figure 6.7: Experimental and Simulation (Variable and Constant Efficiency) Temperature Movements on Trays 2, 3, 4 and 5 between the Initial and Final Steady States for Run 3.	103
Figure 6.8: Experimental and Simulation (Variable and Constant Efficiency) Temperature Movements on Trays 7, 8, 9 and 10 between the Initial and Final Steady States for Run 4.	103
Figure 6.9: Experimental and Simulation (Variable and Constant Efficiency) Temperature Movements on Trays 3, 4, 5 and 6 between the Initial and Final Steady States for Run 5	104
Figure 6.10: Experimental and Simulation (Variable and Constant Efficiency) Temperature Movements on Trays 3, 4, 5 and 6 between the Initial and Final Steady States for Run 6	104
Figure 6.11: Experimental and Simulation (Variable and Constant Efficiency) Temperature Movements on Trays 3, 4, 5 and 6 between the Initial and Final Steady States for Run 7	105

Figure 7.1: Efficiency-Concentration Relationship for an Ethanol-Water Mixture (Mostafa (1979)).	107
Figure 7.2: Assumed Tray Efficiency-Concentration Relationship used for Case Study –1.(Note: Values in legend represent the maximum efficiency values at the ends of composition range)	109
Figure 7.3: Initial and Final Steady State Temperature Profiles for the Case Study -1 Efficiency Curves with Different Severities of Tray Efficiency-Concentration Relationship.	112
Figure 7.4: Overhead composition profile for 25min Distillate Withdrawal from Steady State for Case Study –1 Efficiency Curves	113
Figure 7.5: Total Reflux Initial Steady State McCabe-Thiele Plots for the Case Study –1 Efficiency Curves.	114
Figure 7.6: Distillate Composition Movements for Continuous Distillate Withdrawal after Steady State using Case Study –1 Efficiency Curves	116
Figure 7.7: Transient Temperature Profile for Each Tray from Startup until All the Methanol Charged to the Column is Distilled off. Offtake Starts at Time, $t = 2.0$ hours.	120
Figure 7.8: Distillate Composition Profile For Product Withdrawal When Distillate Composition is Over 92% Methanol.	124
Figure 7.9: Case Study 1 Distillate Composition and Reflux Ratio Profiles For 92% MeOH Product - Fixed Distillate Composition Policy	127
Figure 7.10: Case Study 1 Distillate Composition and Reflux Ratio Profiles For 99% MeOH Product - Fixed Distillate Composition Policy	127
Figure 7.11: Assumed Tray Efficiency-Concentration Relationship used for Case Study –2 (Note: Values in legend link to “equivalent” values in Figure 7.2.	129
Figure 7.12: Initial and Final Steady State Temperature Profiles for Case Study -2 Efficiency Curves with Different Severities of Tray Efficiency-Concentration Relationship.	131
Figure 7.13: Transient Composition Profiles for Distillate and Trays 1, 3, 5, 7, 9 using Efficiency curves E1.7 and E1.7q	132
Figure 7.14: Transient Composition Profiles for Distillate and Trays 1, 3, 5, 7, 9 using Efficiency curves E2.0 and E2.0q	132

Figure 7.15: Distillate Composition Profiles for Case Study 2 with Distillate Withdrawal Start Time, $t=2.0$ hrs at Reflux Ratio of 4.5.	134
Figure 7.16: Composition Trajectory on All Trays during Product Withdrawal until all Methanol is Distilled for Efficiency Curve E2.0q.	134
Figure 7.17: Case Study 2 Distillate Composition & Reflux Ratio Profiles For 92% MeOH Product - Fixed Distillate Composition Operation	136
Figure 7.18: Case Study 2 Distillate Composition & Reflux Ratio Profiles For 99% MeOH Product - Fixed Distillate Composition Operation	136
Figure 7.19: Product and Steam Utilities for Simulation Using the Different Efficiency Curves for a 92% Methanol Specification	143
Figure 7.20: Product and Steam Utilities for Simulation Using the Different Efficiency Curves for a 99% Methanol Specification	144
Figure 7.21: Annual Performance of the Different Efficiency Curves for a 92% and a 99% Methanol Specification.	145
Figure A.1: Steam and Vapour Boilup Rates for the Column Using Water as a Test Fluid.	183
Figure A.2: Experimental and Simulation Steady State Temperature and Composition Profiles for Runs T2 and T3	187
Figure B.1: Main Program Listing.	193
Figure B.2: Bubble Point Temperature Subroutine Listing.	197
Figure B.3: Subroutine INITIAL Listing for Column Data Initialisation	199
Figure B.4: Subroutine HOLDUP Listing.	202
Figure B.5: Subroutine REBOIL, Fluid rates and Reflux Ratio Calculation Listing.	203
Figure B.6: Subroutine ENTH, Enthalpy Calculations Listing.	204
Figure B.7: Subroutine DERIV Listing	204
Figure B.8: Subroutine Euler Numerical Integration Program Listing.	205
Figure B.9: Subroutine DYNEFF Listing.	207
Figure B.10: Subroutine DRAWDIST Listing.	208
Figure B.11: Subroutine PRES Listing for Output of Simulation Results.	211

Figure B.12: Subroutine PDRG Listing, for Output of Composition Results	212
Figure B.13: Subroutine HEADER Listing for Writing Output File Headers	213

# LIST OF TABLES

Table 3. 1: Dimensions of Tray Details	52
Table 5.1: Murphree Tray Efficiencies for Methanol in Run 1 and Run2	75
Table 5.2: Murphree Tray Efficiency Values for Run 3	76
Table 5.3: Product Withdrawn From The Column For Run 4	80
Table 5.4: Size and Concentration of Charge for Rig Runs.	82
Table 5.5: Sample Experimental Run Details From Dribika (1986)	87
Table 7.1: Equilibration Time Under Total Reflux for the Different Efficiency Curves.	115
Table 7.2: Duration of Distillate Composition Oscillation after Start of Product Withdrawal and the Distillate Composition at which Oscillations Apparently Stop.	117
Table 7.3: Product Details For Offtake When Distillate Composition is Over 92%	124
Table 7.4: Production details for Fixed Distillate Composition Simulation for Case Study 1	128
Table 7.5: Production details for Fixed Distillate Composition Simulation for Case Study 2	137
Table 7.6: Product and Utilities for 92% Methanol Purity Specification Using Case Study 1 Efficiency Curves	140
Table 7.7: Product and Utilities for 99% Methanol Purity Specification Using Case Study 1 Efficiency Curves	140
Table 7.8: Product and Utilities for 92% Methanol Purity Specification Using Case Study 2 Efficiency Curves	141
Table 7.9: Product and Utilities for 99% Methanol Purity Specification Using Case Study 2 Efficiency Curves	141
Table 8.1: Liquid and Vapour Composition at Near-Pinch Situation for the Efficiency Curves of Case Studies-1 and Case Study –2 with the Most Severe Composition Dependence (E2.0 and E2.0q).	150
Table A.1: Mixture Compositions at Measured Temperatures for Run T1	184

Table A.2: Feed and Operating Conditions and Results of Experimental Runs and Equivalent Simulation Runs.	189
Table B. 1: Sample Data File for the Simulation	215
Table B. 2: Sample Output File T1-3.ANS	218
Table B. 3: Sample Output File T1-3.DRG	220
Table C.1: Table of Antoine Constants (Coulson and Richardson (1993))	221
Table C.2: Physical Properties of the Mixture Components	221
Table C.3: Wilson Coefficients, $\Lambda_{ij}$ for Methanol-Water System (Hirata et al (1975))	222
Table C.4: Wilson Coefficients, $\Lambda_{ij}$ for Methanol-Ethanol-Propanol System (Hirata et al (1975))	222
Table C.5: Wilson Coefficients, $\Lambda_{ij}$ for Cyclohexane-Toluene System (Hirata et al (1975))	222

# CHAPTER ONE.

## INTRODUCTION

In the chemical process industry, various processing units such as chemical reactors, evaporators, distillation columns, phase separators, extractors, heat exchangers, etc. or a combination of these units are used to transform raw materials and energy into finished products. This is done discretely, continuously or batchwise.

Discrete processes are generally used in the manufacture of consumer goods (e.g. cars, computers, furniture, etc) while continuous processes are more widely used in the bulk chemical and petrochemical process industries. Batch processing on the other hand, finds more widespread use in pharmaceutical, dyestuff, specialty chemicals and agrochemical industries. Compared with continuous processes, batch processes have attracted relatively little attention from the academic world, and have not been associated with large investments in industrial process technology research despite its immense contribution to wealth creation (Sharratt (1997)). Currently however, the spread of continuous processing for bulk chemicals production appears to be in reverse in the developed world. This point is highlighted by Freshwater (1994) who points out that while profitability in petrochemicals (a continuous process sector) fell by 25% in 1992, pharmaceuticals was the fastest growing area with an increase of 20% in the same year.

Continuous and batch processes (including distillation) offer a number of contrasts, reflected in the technical and economic factors, which govern the choice between them. One major advantage of continuous processing is economy of scale (Sawyer (1993)). High volume production of a standard product generally yields a good return on the initial capital investment and if product requirements do not change significantly, the process will require a

minimum of modification during its working life. Other potential advantages include: less space requirement, less material handling involved, lower manning levels needed, less bulk storage required and lower energy consumption, compared to a batch process of the same capacity.

For batch processing on the other hand, the key advantages include:

- Flexibility. This flexibility allows the handling of different feed compositions and the supply of different grades of product without having to change the equipment or construct new plants.
- The processing of materials with high solid content or substances that become very viscous on concentration, favours batch processing because solids or the thick, viscous fluids settle to the bottom of the processing units and can be removed at the end of the batch.
- Batch plants are more robust than their continuous counterparts because incorrect design is often less serious in batch processing. For example, a batch reaction can easily be left for longer if it is incomplete or more reagents added if a test result is out of specification. A continuous process would more likely require major modifications to the plant.
- Most importantly, a number of different products can be produced in a single batch plant. In the case of a continuous processing plant, major modification to existing process units or the construction of a new plant may be required, if a new product is to be produced from an existing plant.

This last point mentioned above is the driving force behind the construction and use of multipurpose and multiproduct plants. Such plants are designed to be easily and quickly configured for new products, using generic process units. It is however, not uncommon for a dedicated plant to be adapted for a new process after its original product is discontinued. Intelligent reuse of process plants can bring savings of 15% on capital costs and 30% on project timescale (Hirst (1996)).

The outlook on bulk chemicals (continuous process) production is changing as a result of falling profit margins, changing markets and strong competition from emerging nations, often with cheaper raw materials and labour costs. The technological advantages available to chemical companies in developed nations no longer overcome the lower wage costs, growing markets and desire for new industry in the developing nations. Such threats to profitability have led major companies to try to move back into the specialty and fine chemicals sector where products have higher added value, for larger profit margins.

In the fine chemicals industry for instance, recent estimates of annual worldwide production are in the range US \$26-64 billion, with the world market for fine chemicals in 1995 estimated at US \$42 billion (Sharratt (1997)). Of this, 30% was used as pharmaceutical intermediates, 35% for pesticides, 23% for flavours and fragrances and 12% for other uses. Growth is expected mainly in the pharmaceutical sector at 6% annually, with pesticides growing at about 1%, and the average growth in the production of fine chemicals continuing at about 5% (Sharratt (1997)).

In these process and chemicals industries, separation is a vital unit operation used for waste treatment, product concentration, etc. Numerous novel separation methods and techniques have been developed to date but distillation, which is one of the oldest methods, still remains the most important and widely used separation method.

Distillation columns constitute a significant fraction of the capital investment in chemical plants and refineries around the world. The operating costs of these columns often constitute a major proportion of the total operating cost of many processes e.g. distillation columns consume some 95% of the total energy used in separation and this amounts to roughly 3% of the total energy consumed in the United States alone (Ognisty (1995)). It is becoming of great economic importance to run a distillation column as optimally as possible.

The aggressive nature of the market and strong competition makes it essential to reduce lead times between decision to invest and first production since the first product to corner a market is usually the most successful. One useful technique in reducing this lead-time (at the process design stage), which has also found wide applicability in control and operation studies, is dynamic simulation. This involves the construction of a mathematical model, based on time-dependent differential equations that represent the changes in a process with time.

Early models, for example distillation models, include the McCabe-Thiele steady state model, which is restricted to binary distillation. The level of detail in this and other early models was very much constrained by the rigours of the computations involved and was thus greatly simplified. Advances in computer power and in modelling methods have rendered obsolete many of the simplifications and special modifications which were necessary in earlier models. Until recently however, much of the development in computer simulation has been in the area of steady state, continuous process simulators, with batch, dynamic simulation receiving very little attention in comparison.

Computer models permit the handling of greater degrees of complexity in the design and analysis of the operation of batch separation. Commercial simulation packages exist for the modelling of batch process plants or process units, including distillation. These models can be used to augment or replace experimental studies, depending on the complexity and accuracy of the model used. The effort and investment devoted to producing exact models must be balanced by the benefits realised from its use.

Recent focus in batch processes has been directed at improved simulation techniques and the automation of aspects of batch processing by use of expert systems. Most of the techniques used attempt to transfer the philosophies and methodologies of continuous processing for use in batch processing without full consideration of the realm and constraints under which batch processes operate.

If simulation models are to replace experimental studies and find use in control and optimisation studies, operational research and the safe investigation of hazardous operations (e.g. possible runaway reactions), such models must accurately predict the behaviour of the actual experimental unit. Much work has been carried out recently in the field of dynamic optimisation of batch processes yet, as highlighted by Terwiesch et al (1994), industrial implementation of operating profiles based on dynamic models and mathematical optimisation is still rare today. This can be attributed to the level of fidelity of these models and their inherent simplifications and assumptions.

One such simplification, in batch distillation, is the use of equilibrium stage models. In most other models where tray efficiencies are employed, they are usually treated as tuning parameters to match model predictions with experimental results. Investigating the effect of tray efficiency on distillation, Bidulph and Ashton (1977), Mostafa (1979), Lockett and Ahmed (1983) and Dribika (1986) find that it varies with changing mixture compositions on the trays. This effect is more pronounced in batch distillation where conditions are continually changing unlike in continuous distillation which is run at steady state. This highlights the dangers of modelling batch distillation using a fixed efficiency value for all the trays (column efficiency).

The work reported here investigates the importance of tray efficiency to model fidelity and its effects on the performance of the model. To this end, initial work was directed at the development of a rigorous model for a pilot scale distillation unit, housed in the L3 laboratory at the University of Nottingham.

The distillation unit and its operating procedure is described in Chapter 3 and the governing equations of the model developed for this work are described in Chapter 4, along with the different modes in which the tray efficiency is represented. The results obtained from experimental work and the simulation model (for the different modes of tray efficiency representations discussed in Chapter 4) are presented and discussed in Chapters 5 to 7. In Chapter 8, the

major issues arising from the different tray efficiency representation methods are highlighted and discussed and conclusions are drawn in Chapter 9.

Recommendations for further work are presented in Chapter 10 but a review of the previous work done in this field is presented in Chapter 2.

## **CHAPTER TWO.**

### **LITERATURE REVIEW**

Distillation still remains the most important separation method in the pharmaceutical, fine chemical and petroleum industries. It is a means of separation of liquid mixtures into their various components, relying on the difference in the boiling points and volatilities of these components. Throughout the chemical industry the demand for purer products, coupled with a relentless pursuit of greater efficiency, has necessitated continued research into the techniques of distillation.

In a great number of applications, distillation columns are used to separate a continuous feed stream with a continuous withdrawal of products from the top and bottom of the column. This is the continuous distillation process. In many other instances, the process is carried out in batches (batch distillation). The liquid and vapour compositions on any tray in a batch distillation column vary with time and depend on a number of factors including the number of stages in the column, the reflux ratio policy (or value) and the thermodynamic properties of the components involved.

Since the early 1950's, batch distillation has received little attention owing to the emphasis during this period on continuous processes (Luyben (1971)). The work on batch distillation prior to 1960 has been reviewed by Archer and Rothfus (1961). However (as is reflected in the publications referenced in this work), interest in batch processing has increased more recently and the volume of literature in this field since 1980 has more than doubled the volume before 1980.

## 2.1 APPLICATION OF BATCH DISTILLATION

Batch distillation is an important unit operation frequently used in small scale, high value added chemicals and biochemicals industries. It is very useful in the separation of mixtures which become more viscous on concentration. Because of its flexibility in handling feeds of variable concentration and different mixtures, it is also used in multiproduct and multipurpose plants. In the separation of a multicomponent mixture, batch distillation is often preferred because complete separation can be achieved in a single column whereas with continuous distillation, several columns may be required.

Another area where batch distillation finds great application is in the distillation of complex systems and of systems with greater difficulty of separation. This includes the distillation of close boiling and thermodynamically complex systems (azeotropic mixtures) and distillation accompanied by a chemical reaction. The latter is termed reactive batch distillation and considers the case where reaction occurs only in the reactor vessel, which acts as the still (Wilson and Martinez (1995)), or a more complicated case where reaction occurs both in the reactor vessel and the distillation column (Albet et al (1991)).

### 2.1.1 Azeotropic Batch Distillation

The complex nature of the vapour-liquid equilibrium of azeotropic mixtures makes the direct separation, by distillation, of such mixtures into its pure components impossible. Figure 2.1 shows the shape of the equilibrium curve for a binary azeotropic mixture. Most of the simulation work on azeotropic mixtures deal with the composition changes during distillation and is often based on extensive experimental data as reported by Malenko (1970).

Many shortcut and rigorous/semi-rigorous simulation models for batch distillation are based on the assumption of constant relative volatility throughout the column, updated at each time step. In the case of azeotropic

systems, this assumption is no longer valid because of the distillation boundaries and azeotropic point (where the relative volatility becomes unity).

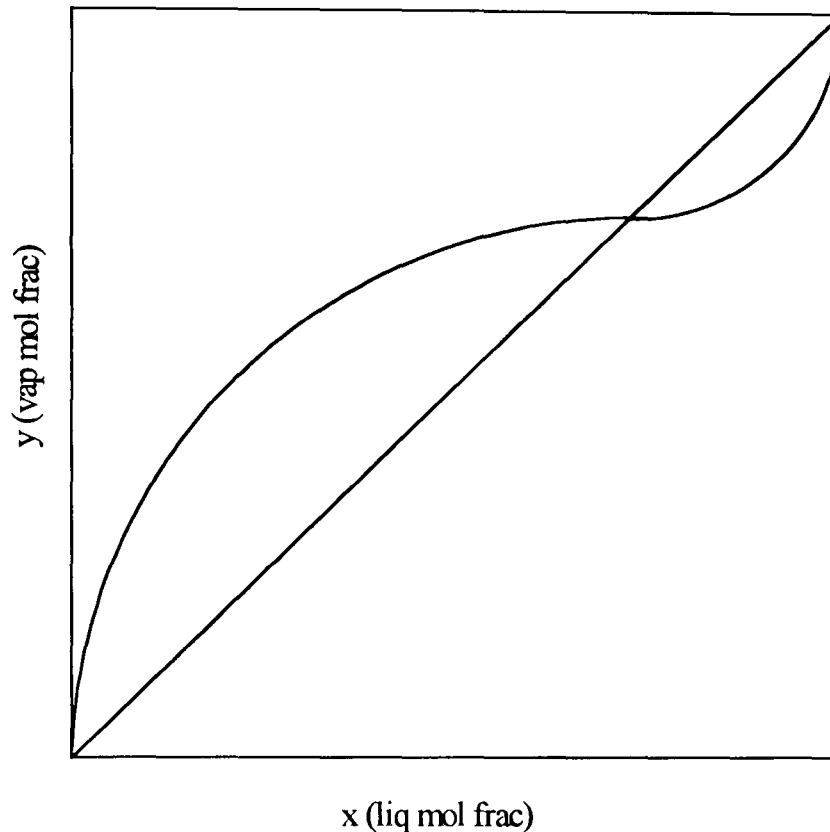


**Figure 2.1:** Equilibrium Curve for an Azeotropic Mixture.

The azeotropic points and distillation boundaries offer an impassable barrier or barriers. For binary azeotropic distillation, Anderson and Doherty (1984) transformed the variables of binary vapour-liquid equilibria calculations by splitting the equilibrium curve into two regions; one above and one below the azeotropic composition.

Azeotropic distillation is an important and widely used separation technique due to the great industrial importance of a large number of azeotropic mixtures yet, azeotropic distillation techniques remain poorly understood from a design standpoint. This is because of the complex thermodynamic behaviour of the system (Diwekar 1996). Theoretical studies on azeotropic distillation have mainly centred around methods for predicting the vapour-liquid equilibrium data from liquid solution models and their application to distillation design

(Van Dongen and Doherty (1985)). However, only during the past decade has there been a concerted effort to understand the nature of the composition region boundaries.

The use of ternary diagrams and residue curve maps in the design and synthesis of azeotropic continuous distillation columns has been established by Bernot et al (1990, 1991) and other researchers. In batch distillation they have outlined a synthesis procedure based on these residue curve maps. They defined a concept called “batch distillation region” where any initial condition taken in that region leads to the same sequence of cuts (a synthesis problem which finds ready application in azeotropic distillation). Van Dongen and Doherty (1985) presented a model which explains the behaviour of azeotropic batch distillation. Their analysis shows how it is possible to draw the exact trajectory followed by the liquid composition in a batch still and predict the exact sequence of constant boiling vapour distillates which appear overhead without solving a single equation, provided the distillation residue curve map is known.

Foucher et al. (1991) provide an automatic procedure for the determination of the structure of simple distillation residue curve maps for ternary mixtures. They assume a knowledge of the boiling points and compositions at the azeotropic points and use rules to classify the azeotropes as nodes or saddles (depending on the behaviour of the equilibrium points). Bossen et al (1993) present the computational tool needed for the simulation, design and analysis of azeotropic distillation columns in general by simulating the equilibrium point trajectories directly. Kalagnanam and Diwekar (1993) used the mathematical definition of saddles and nodes to obtain the information about the nature of the azeotropic (equilibrium) points and generate the equilibrium point trajectories, based on the linearisation information along specific directions.

Bernot et al (1993) have presented a method for estimating batch sizes, operating times, equipment sizes, utility loads and costs for the batch distillation of multicomponent mixtures. They applied their method to the separation of a quaternary azeotropic mixture arising from the

transesterification of ethyl acetate with methanol to produce ethanol and methyl acetate.

### 2.1.2 Reactive Batch Distillation

Modelling and simulation of reactive batch distillation have been investigated by a number of researchers recently. Egly et al (1979) presented a method for the optimisation of reactive batch distillation based upon models, which include the non-ideal multicomponent mixture behaviour and the kinetics of chemical reactions. Cuille and Reklaitis (1986) developed a model and solution strategies for the simulation of a staged batch distillation column with chemical reaction in the liquid phase. Wilson (1987) studied the simulation and economic optimisation of reactive batch distillation using a simple model based on Smoker's equation for the rectifying section of the distillation column. Albet et al (1991) presented a method for the development of operational policies based on simulation strategies for multicomponent batch distillation applied to reactive and non-reactive systems. They also, in Albet et al (1994), considered a complex model including mass and energy balances on each plate, a rigorous equilibrium relationship, variable liquid holdups and provision to add a pressure equation on each plate to study operational policies for the start-up of these columns.

Reuter et al (1989) incorporated the simulation of a PI controller in their model of a batch column with reaction in the reboiler alone. The controller was used to control the top tray temperature with the distillate flow as the manipulated variable. They stated that their model could be run using a variable time step integration and could also be used for the investigation of control structures with the aid of relative gain array (RGA) analysis, but no details were given.

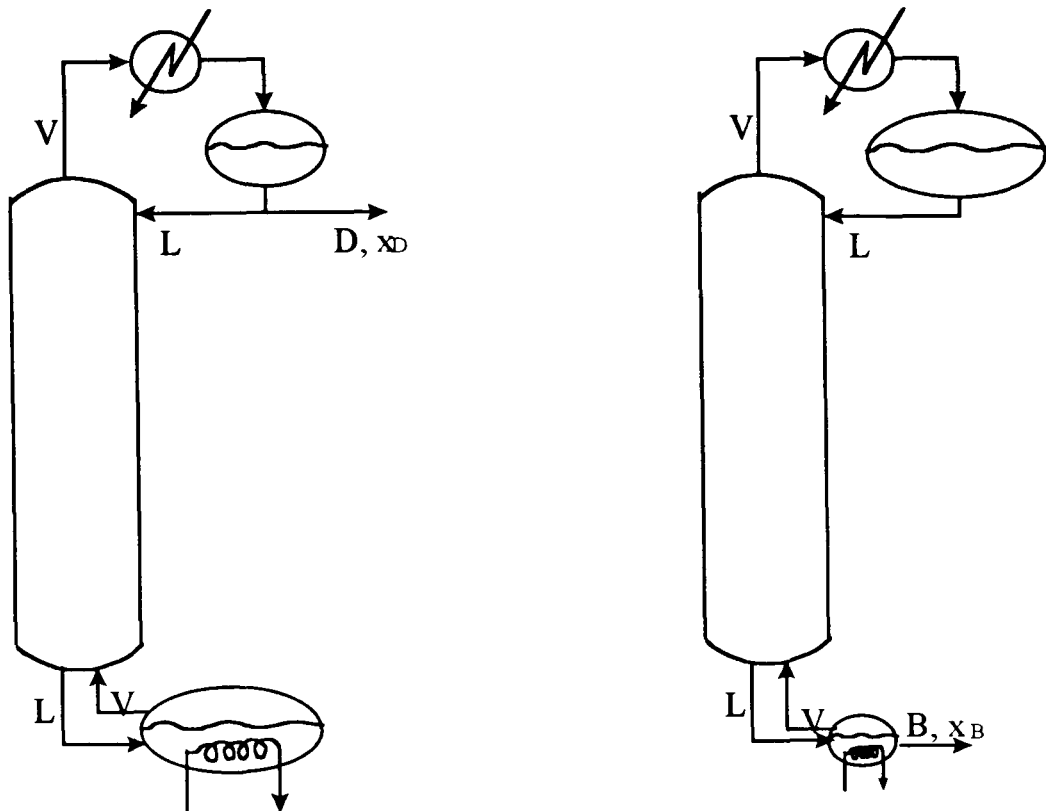
Wilson and Martinez (1995) also studied the control of distillate composition in a batch reactive distillation column. Because batch reactive distillation calls for a higher than normal degree of co-ordination in its control, they used state

estimation methods to infer compositions from temperature measurements. They investigated the performance of the Extended Luenberger Observer (ELO) and the Extended Kalman Filter (EKF) state estimation strategies in a case involving reaction in the still alone and found the Extended Kalman Filter to have superior estimation accuracy.

Sorensen and Skogestad (1994b) studied optimal control and on-line operation aspects of reactive batch distillation using a simple model for the open loop optimisation of the process, and a more complex model including linear tray hydraulics for simulation and control studies.

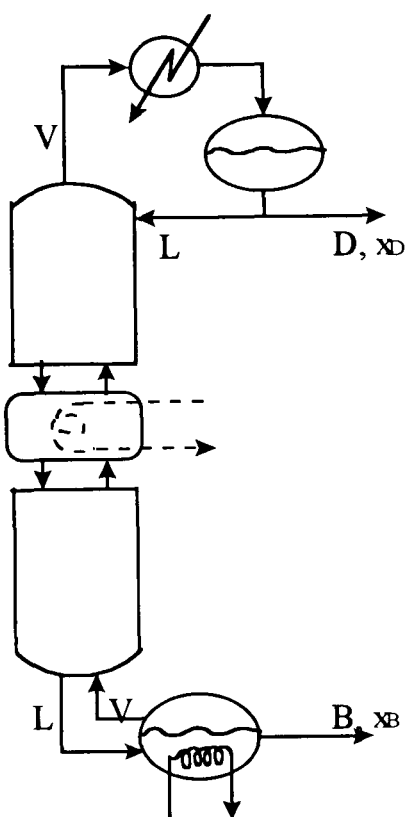
## 2.2 COLUMN CONFIGURATIONS

A continuous distillation column consists of a stripping and a rectifying section. In the batch case however, the column may be configured either as a batch stripper or a batch rectifier as shown in Figure 2.2. In the batch rectifier, the feed to the column is charged at the bottom (in the reboiler) and products are withdrawn at the top (Figure 2.2a). In the batch stripper, the batch is charged at the top of the column (in the condenser or overhead receiver) and products are withdrawn at the bottom (Figure 2.2b). The latter is a less common arrangement, but one which offers some important advantages in the separation of azeotropic mixtures (Bernot et. al. (1991)). Recently, research has been carried out by Barolo et al (1996a, 1996b), Skogestad et al (1997) and Davidyan et. al. (1994) on a third and even less common configuration, which consists of an additional vessel in the middle of the column as is shown in Figure 2.2c. Here, the feed is charged to the vessel in the middle of the column and the column is run either as a stripper or rectifier by withdrawing product from either the top or bottom, or as a stripper and rectifier when products are simultaneously withdrawn from the top and bottom of the column. The work reported here considered the batch rectification configuration only.



(a) Conventional "rectifier" configuration

(b) Inverted "stripper" configuration



(c) Column with a middle vessel

**Figure 2.2:** Different Configurations of Batch Distillation Columns (Davidyan et. al. (1994)).

## 2.3 OPERATION OF BATCH DISTILLATION COLUMNS

Conventionally during start-up, the batch (rectifying) column is usually on total reflux and the top composition will get relatively richer in the more volatile component. Because no product is withdrawn, the column may achieve steady state during the start-up period. When the purity of the material in the column overhead reaches its maximum (or specified) level, distillate flow can be begun at some appropriate flow rate. This reduces the reflux ratio from infinity to a finite value and the liquid remaining in the still will become steadily weaker in this component as it is being withdrawn. As a result, the purity of the top product will also fall at a rate, contingent upon the value of the reflux ratio and vapour flow (a function of the heat input). Depending on the required product purity and column specifications, the reflux ratio may be specified in one of three ways:

- Constant Reflux Ratio
- Variable Reflux Ratio
- Optimum Reflux Ratio

### 2.3.1 Constant Reflux Ratio Operation

This is usually the more commonly used reflux ratio policy because of its operational simplicity. If the column is operated at a constant reflux ratio, the liquid and distillate flow rates are constant, provided the vapour rate is constant. The composition of the more volatile component in the top product will fall with time but the exact composition of the product withdrawn is not accurately known. In the separation of a binary mixture, product withdrawal of the more volatile component is begun (at a fixed reflux ratio) when the top composition reaches the specified level. The composition may rise further and then begin to fall. The distillate is stored in a product tank until its average composition drops to the specified level again. Beyond this point, any distillate (slop) withdrawn will not meet the required specification and will have to be

diverted to another receiver (slop receiver). When the composition of the material within the column and the still pot reaches the required purity for the heavy product, the batch cycle is stopped.

When separating a ternary mixture, the same batch cycle is followed except that in this case there will be two overhead products and possibly two slop cuts, depending on the product specifications. If the specification for the heavy product is reached as soon as intermediate product withdrawal is stopped, then the cycle is stopped and there is no second slop cut. The same applies to other multicomponent mixtures of more than three components.

### **2.3.2 Variable Reflux Ratio Operation**

In the variable reflux ratio case, the reflux ratio is made to follow a trajectory over time, which keeps the overhead product composition constant. This reflux ratio will vary over time with respect to the distillate composition. The distillate is diverted to the slop receiver when a change in the reflux ratio will not keep overhead composition at the specified level. For multicomponent mixtures, the reflux ratio trajectories may be different for different product cuts.

Economic considerations (due to energy consumption) put a ceiling on the reflux ratio because at large reflux ratio values, very little distillate is being collected and much of the energy spent on heating up the still contents is wasted.

### **2.3.3 Optimum Reflux Ratio Operation**

In this case, the reflux ratio is set by optimising an objective function, usually related to profit. The optimal reflux ratio (optimal control) policy is essentially a trade off between the fixed reflux and fixed distillate composition policies and is based on the ability to yield the most profitable operation of the unit. Usually,

the sequence of overhead fractions during distillation, the cut location and available equipment are also decision variables in the optimisation formulation. The optimal strategy can be one which meets one of several objectives: maximum profit, minimum costs, maximum production rate/amount, or minimum time. The choice of objective function will depend on the specific requirements of the unit.

### **2.3.4 Other Operating Strategies**

Luyben and Quintero-Marmol (1990) have investigated other operating strategies that involve the recycle of the out-of-specification (slop) distillate material. These are

- Accumulated Product Strategy
- Intermittent Distillate Policy

#### **2.3.4.1 Accumulated Product Strategy**

In the Accumulate Product Strategy, the total amount of each product or slop cut is collected in the reflux drum before being discharged to the storage tanks. This reduces to a minimum, the number of samples that need to be taken to determine whether the contents of the reflux drum meet the specification.

This operating strategy requires that the reflux drum is large enough to hold the largest amount of product or slop cut expected. During product withdrawal in the application of this strategy, the reflux drum holdup varies from zero (or a fixed value) to the total amount of product or slop cut to be collected for each cut. The beginning of product accumulation or the end of slop cut collection is reached when the overhead vapour composition meets the specified product purity.

#### 2.3.4.2 Intermittent Distillate Scheme

This involves running the column at total reflux until product specification is reached, dumping the contents of the reflux drum and then running at a fixed reflux ratio to recharge the reflux drum and repeating the cycle.

The intermittent distillate scheme is similar to the cyclic operating policy described by Sorensen and Skogestad (1994a) and Sorensen and Prenzler (1997). The main difference lies in the fact that the reflux drum in the cyclic policy is refilled at total reflux, rather than at a fixed partial reflux ratio as in the intermittent distillate scheme. Sorensen and Skogestad (1994a) studied the optimal operation of this cyclic policy and compared it to conventional operating policies (constant reflux ratio, constant distillate composition and optimal reflux ratio) for a number of simulation examples. They found that the cyclic policy was favourable for difficult separations where a small amount of light product is to be recovered. In some cases, the reduction in operating time was more than 30%.

They also found the optimisation of this policy to be very time consuming and proposed a single optimisation parameter to avoid optimising the reflux drum holdup as well as the total reflux time for each cycle. Sorensen and Prenzler (1997) found the practical implementation of this cyclic policy to be very straightforward with minimal need for operator intervention and control, as it is less sensitive to disturbance. Because the reflux drum holdup is calculated based on the feed composition however, the feed composition must be known to a reasonable degree of accuracy.

#### 2.3.4.3 Slop Handling Strategies

In a batch distillation operation, off-specification material is produced in a binary system when the distillate composition falls below the required level but the still contents are still below the required concentration of the non-volatile

component. Off-specification (slop) material is also produced in multicomponent systems when distillate composition falls below the required level for the most volatile component but is not rich enough in the next volatile component. This off-specification product is usually called 'slop cut'. In general, we obtain at most, NC-1 slop cuts in the distillation of a given mixture, where NC is the number of components in the mixture.

These slop cuts contain the materials that are being distilled, but not in the right concentration and as such, can be collected between batches and fed back as a single batch when a large enough quantity is accumulated. The operation and optimisation of batch distillation of mixtures with slop cuts have been investigated by Luyben and Quintero-Marmol (1990) and Mujtaba and Macchietto (1992, 1993). Using a ternary mixture, Luyben and Quintero-Marmol (1990) explored alternative slop handling policies for multicomponent batch distillation, comparing the performance of different operating and slop handling schemes:

- Total Slop Recycle: All slop cuts of the previous batch are combined with fresh feed in the initial charge to the still for the next batch.
- Multicomponent-Binary Component: Slop cuts from different runs are saved in segregated tankage and when enough material has accumulated, each slop-cut (now a binary mixture) is distilled.
- Fed-Batch Recycle: The slop cuts are fed into the column at an appropriate time and tray during the next batch when the composition on that tray is similar to that of the slop cut.
- Segregated Initial Charge: The second slop cut is fed to the column while the first is used to fill the reflux drum and the column. This makes the column richer in the more volatile component contained in the first slop cut, right from the start of the batch.

Using 'Capacity Factor' (the total specification product, averaged over a complete batch, produced per unit time) as a performance index, Luyben and

Quintero-Marmol (1990) found that in general, mixing of already separated waste cuts with fresh feed has a detrimental effect on the performance of the distillation system. Their results show that of all the slop handling schemes, the multicomponent-binary component scheme showed an improvement of up to 38% over the slop recycle scheme which is the most commonly used in practice. The intermittent distillate scheme (discussed in section 2.3.4.2) was found to perform almost as well, but required optimisation of the reflux ratio.

### 2.3.5 Optimisation

Recently, some researchers have investigated batch distillation as an optimisation problem for binary and multicomponent systems. The optimal control problem in batch distillation can be formulated in three ways:

- The “minimum time problem” which defines the optimal operating policy to be that which produces the required quantity of distillate, of specified purity in the shortest possible time.
- The “maximum distillate problem” which defines the optimal operating policy to be that which produces the maximum amount of distillate of a given purity in a prescribed duration of time.
- The “maximum profit problem” which maximises a profit function for a specified concentration of distillate.

The optimal control variable is usually the reflux ratio since the optimal boilup rate frequently remains at its upper bounds as shown by Logsdon and Biegler (1993). Diwekar et al. (1987) used shortcut models along with Pontryagin’s maximum principle to obtain control policies for the maximum profit problem. Logsdon et al. (1990) also used a shortcut model to simultaneously optimise the design of a column and obtain the optimal reflux policy to maximise a profit function which includes capital costs along with operating costs.

Mujtaba and Macchietto (1988) solved the maximum distillate problem using a detailed model, which included tray-to-tray dynamics (material and energy balances), finite plate holdup and detailed phase equilibrium. They also (in Mujtaba and Macchietto (1992)) solved the minimum time problem for a multicomponent mixture using a full dynamic model with general thermodynamics and finite holdup. Their method decomposes the multiperiod problem to a sequence of pseudo-binary optimal control problems and results in overall batch-time saving of more than 45%, using the proposed optimal recycling strategy. They further extended the work (in Mujtaba and Macchietto (1993)) by proposing a method for determining optimal operation policies by maximising a general profit function over the whole multiperiod operation. This method relaxes the restrictions derived from the need to use predefined reflux policies and fixed periods of operation for a multicomponent batch distillation. This involved the formulation and solution of a multiperiod optimisation problem as opposed to the optimisation of the amount or the batch time of a single product cut

Sundaram and Evans (1993a) presented a mathematical programming approach to solving the synthesis problem for batch distillation columns. They proposed a method which consists of a superstructure which has embedded in it, all possible combinations of conducting the proposed separation, formulating the superstructure as an optimisation problem and solving the resulting non-linear program as an optimisation problem. Bonny et al. (1994) also propose a general model, based on a superstructure, for the calculation of the proportion of each slop cut to be added to each initial load and to each new batch in order to optimise the global distillation operation.

## 2.4 MODELLING & SIMULATION

Batch distillation is a dynamic process and the equations that describe the operation are non-linear differential in form, including mass and energy balances, Vapour-Liquid equilibrium (VLE) relationships and liquid hydraulics

correlation, depending on the degree of complexity of the model. Simulation requires integration of these equations, which are usually also stiff as a result of the large difference in the time constants of the still and the trays in the column. Thus, the model for batch distillation is usually complex. The more rigorous the model, the more computationally expensive it is. Therefore, there is always a trade-off between model complexity and model speed and in practice, a balance has to be struck to meet the specific requirements of the user. Simplified models are generally used for preliminary design and optimisation studies but more complex models are required for advanced operational studies.

Dynamic models, as opposed to steady state models, are characterised by non-zero derivatives for tray composition and often, for holdup and specific energy. Early work concentrated on the development of approximate methods for dynamic simulation of distillation columns. Whilst models have long been recognised as useful tools in the design and operation of distillation columns, the level of detail in early models was very much constrained by the tedious computations involved, especially before the advent of the modern computer.

Dynamic simulation models are of particular benefit in areas such as:

- Design: cheap, fast and safe investigation of new processes, especially potentially hazardous operations. This is especially important in batch processes because of the high degree of manual intervention.
- Operation: optimisation studies and the investigation of advanced operation schemes and control strategies.
- Predicting plant behaviour as part of a state estimation scheme when reliable on-line measuring techniques to monitor key variables of the process are not available or not easily applicable.

Generally, distillation column models are based on the basic continuity equations for mass and energy. Appropriate equations are used to represent the vapour-liquid equilibrium depending on the nature of the components of the

mixture. Iterative bubble point calculations are used to obtain the vapour compositions given liquid compositions. Because distillation trays are not perfect, it may be necessary to introduce a performance factor for the tray or the column, usually in the form of an efficiency factor (overall, Murphree, local, Standart, vaporisation efficiency, etc.).

Lord Rayleigh (1902) was the first to develop a mathematical relationship between the initial charge to the still pot, the liquid left in the pot at any time, the liquid composition in the pot and the vapour composition. Bogart (1937) developed a design method for the case of constant overhead composition for distillation with a mounted column while Smoker and Rose (1940) presented the design method for a constant reflux ratio operation. Most of the design methods derive from the classical McCabe-Thiele method which, in the batch distillation case, calls for an iterative solution.

Huckaba and Danly (1960) presented the first comprehensive model of a batch distillation column in that it employed enthalpy balances as well as material balances for a constant holdup, adiabatic rectification of a binary mixture. Meadows (1963) however, presented the first model of multicomponent batch distillation using finite differences to solve the set of differential equations. The model employed heat and material balances as well as volume balances and was limited only by the assumptions of ideal plates, constant volume plate holdup, adiabatic operation and negligible vapour holdup. Distefano (1968) extended Meadows' model and conducted a study on the degree of stiffness of the differential equations. However, no experimental verification of the mathematical model was provided. Stewart et al (1973) went further by extending the model to include non-ideal plates (with plate efficiencies obtained experimentally) and various holdup assumptions, and also verifying the model by comparing with experimental results.

Boston (1980) and Boston et al (1981) developed an efficient method to solve the set of differential equations arising from Meadows' model, using an "inside-out" algorithm. This proved to be a robust and efficient method, which could

cope with the stiff non-linear equations produced by the integration formula. Cuille and Reklaitis (1986) further extended Meadows' model to account for chemical reactions.

The use of rigorous models to simulate batch distillation involves the solution of a number of stiff differential equations. The dimensionality of the problem increases with an increase in the number of stages and components. This imposes limitations on the use of rigorous models. In addition, problems in design, optimisation and control involve iterative procedures and considerable computational effort would be required to solve them rigorously.

#### **2.4.1 Simplified / Shortcut Models**

A lot of research has been carried out on simplifying models without sacrificing accuracy (Diwekar & Madhavan (1991a), Sundaram & Evans, (1993b) etc.). Diwekar (1994), on the other hand, worked on the concept of "optimal model reduction" where the trade-offs between model accuracy and model speed are decided using non-linear optimisation techniques.

An example of a simplified model is that proposed by Kumana (1990) which he ran on spreadsheet software. His model incorporates many simplifying assumptions and is based on the McCabe-Thiele method for binary mixtures, with integration performed by a difference method (trapezoidal rule). He used the model to determine the optimum batch times for each cut in a multicomponent distillation, based on net profit maximisation.

Diwekar and Madhavan (1991a) presented a shortcut simulation method based on the Fenske-Underwood-Gilliland (FUG) method for continuous distillation design, assuming negligible holdup and equimolar overflow. The basic assumption in applying the FUG method to batch distillation is that at any given time, the batch column is identical to the rectifying section of a continuous column, with changing feed. This means that the bottom product from one time

step forms the feed of the next time step. The pseudo-continuous distillation model thus obtained is then solved using the FUG equations, with no plate-to-plate calculations.

Diwekar and Madhavan (1991a), as well as comparing the simulation results with that from a rigorous model, also compared it with experimental data. In many cases, the shortcut model was seen to compare quite well with the experimental and rigorous models and thus lead to savings in computational effort.

Sundaram and Evans (1993b) presented a similar simplified model for batch distillation, also based on the FUG shortcut method for continuous distillation design. Their model was run at constant overhead composition and constant reflux ratio and were shown to be in excellent agreement with rigorous simulations under the assumption of constant molal overflow and zero liquid and vapour holdup. The main difference between the models of Diwekar and Sundaram is in their input data. The model input data required makes Diwekar's model suited to design while Sundaram's model is applicable also to rating studies on an existing column.

Diwekar's shortcut method requires specification of the mole fraction of all components in each product cut in addition to that of the key component recovered in that cut. In practice it is very difficult to achieve a specification of this type with a multicomponent mixture and considerable differences in the results may be noticed compared with the case of variable non-key product composition. This method is also limited to columns with a large number of trays and negligible tray holdup.

Although shortcut models have advantages over rigorous methods in terms of computation time, their use is very much restricted to an initial trial design or to finding initial trial operating policies and in optimisation studies. These simplified models involve the integration of far fewer system equations (as a result of the simplifying assumptions made) thus resulting in faster models

albeit less robust in their application. Their results must still be verified and refined (by repeated simulations) using rigorous dynamic models, accurate physical property data and rigorous integration methods, particularly with non-ideal mixtures and when holdup is significant.

### 2.4.2 Rigorous Models

Rigorous dynamic models of batch distillation columns differ from the shortcut models in the level of detail incorporated in the model. While plate-to-plate calculations are not carried out in some shortcut models, it is performed in rigorous models. The level of rigour between rigorous models also differ, depending on the requirements of the user. Most rigorous batch distillation models use finite tray holdup and incorporate energy balances on each stage. Some include hydraulic correlations for the calculation of plate pressure drops and liquid flows (Wittgens and Skogestad (1995)). Some rigorous models incorporate various VLE prediction methods (Galindez and Fredenslund (1988)) and some account for the non-ideal behaviour of a tray either by using a tray efficiency factor or employing a non-equilibrium stage model (Pescarini et al (1996)).

Currently, there exist numerous sophisticated tools for the simulation of batch distillation columns (rigorous and simplified) given the feed conditions, column configuration and operating policy of the column. One such tool is BATCH-DIST (Diwekar and Madhavan (1991b)). BATCH-DIST is a general-purpose simulation package for batch distillation columns, incorporating models of varying degrees of complexity and rigor. Model complexities in this package vary from the simplified model based on the FUG calculation procedure, the semi-rigorous model which includes holdup effects and plate-to-plate computations, to the rigorous dynamic model which also includes energy balances and heat effects and can handle non-ideal systems.

Domench and Enjalbert (1981) also presented a modular program for simulating batch distillation to allow for different levels of complexity. The modularity of their program however only allowed for zero and finite holdup models with plate to plate calculations, employing ideal or constant efficiency trays.

Pescarini et al (1996) developed a program for multicomponent distillation, which solves the component material and energy balance relationships for each phase together with mass and energy transfer rate equations and equilibrium equations for the interface. The profiles predicted by their program were compared with those obtained from the simulation of a conventional equilibrium stage model and showed good agreement.

Galindez and Fredenslund (1988) proposed a method for rigorous simulation of batch columns, which assumes quasi-steady-state approximation at each time step. Their model considers three liquid holdup situations: when the trays and condenser are initially dry but later contain given amounts of holdup, when they are initially filled with liquid at appropriate concentrations and when holdup is neglected. Their method is very efficient and is based on a model corresponding to continuous distillation, but the accuracy of the results depend upon the proper choice of integration step size.

Non-linear Programming codes have been proposed which avoid the nested iterative procedure involved in rigorous numerical integration of distillation equations and optimisation by Chiotti and Iribarren (1991). Their model can be run either as batch rectifier or stripper, based on a zero holdup model and constant molal overflow.

Most of the simulation and research work on batch distillation have considered only plate columns. The problem of poor convergence characteristics when dealing with anything but the simplest physical systems in packed column simulation is one of the reasons for this. However, Hitch and Rousseau (1988) simulated multicomponent batch distillation in a continuous contact (packed)

column. They formulated a method, which uses a relaxation procedure to simulate both the startup and product withdrawal periods of the column operation. The program thus obtained was used to show the effects of varying packing height, boilup rates, reflux ratio and condenser holdup for the distillation of a ternary mixture. This also demonstrated the stability of their computational procedure.

### **2.4.3 State Estimation**

The control of product composition is the focus of most control studies but on-line composition measurement using composition analysers is usually very expensive, the equipment is difficult to maintain and could also introduce time delays in control loops. These problems associated with on-line analysers can be circumvented by inferring composition from secondary process measurement, usually temperature. In a binary system, the temperature at any point in the column is fixed for a given composition, at a given pressure. In a multicomponent system however, the composition is more difficult to infer from temperature and pressure alone due to the additional degrees of freedom.

Choo and Saxena (1987) presented a review of literature on state estimation methods, which use temperature as the primary measurement for composition estimation. These estimators are used in inferential control systems where measurement of secondary outputs are used to infer the effect of unmeasurable disturbances on the primary process outputs. Choo and Sexena (1987) reported significant improvement in the variability of the overhead composition when inferential control was applied to an extractive distillation column (continuous).

## **2.5 FACTORS AFFECTING BATCH DISTILLATION**

Most batch distillation studies consider the operating problem (i.e. choice of reflux ratio, vapour boil-up rate or start-up policy) for a given column but some

have also examined the influence of design variables (e.g. number of stages, column size, holdup). A number of these studies on batch distillation design and operation have been focused on ideal or constant-volatility binary and ternary mixtures (Bernot et. al. (1990)).

Bernot et al (1989) described a procedure for the selection of equipment, batch sizes, cycle times and operating policies in multicomponent batch distillation. Their approach is suitable for ideal and non-ideal mixtures, including those with distillation boundaries and azeotropes. Houtman & Husain (1956) have used an equation, which relates sharpness of separation to the number of theoretical trays, reflux ratio and holdup of the column, to suggest a method for choosing the most beneficial combination of these three factors.

A number of factors affect a batch distillation process but the effects of tray holdup and reflux ratio as well as tray efficiency have generally received more attention from researchers and are discussed in more detail here.

### 2.5.1 Tray Holdup

The effect of tray holdup on batch distillation has been investigated by a number of researchers. Luyben (1971, 1988) studied the influence of design variables such as number of trays, reflux ratio, amount of initial charge and holdup on the separation of ideal binary mixtures. He uses “Capacity Factor” (total product produced per unit time, averaged over a batch) as a performance index, to determine an optimum number of stages and fixed reflux ratio for the separation of a binary mixture.

From his investigation using a binary mixture, Luyben (1971) concluded that while it is advisable to minimise reflux drum holdup, some tray holdup might be beneficial as a result of the “flywheel” (or inertia) effect. He extends the work further (Luyben (1988)) to include multicomponent mixtures.

Holdup affects the column in two basic ways namely, the dynamic “flywheel” effect and the steady state “capacitance” effect (Diwekar (1994)). The tray holdup affects the overall column composition profile and the dynamic time constants of the trays. The flywheel effect can be characterised by the column time constant,  $\tau$  :

$$\tau = \frac{\text{column holdup}}{\text{reflux ratio} \times \text{distillate rate}} \quad 2.1$$

For large values of  $\tau$ , the initial composition profile predicted by a zero holdup model departs significantly from the results from a finite holdup model (Diwekar (1994)). The flywheel effect hinders the quick adjustment of concentrations on the tray when conditions in the column change.

The capacitance effect is observed at the end of the initial total reflux operation when the given charge distributes itself through the column, associated with the equilibration time (i.e. time taken to reach equilibrium at total reflux). It accounts for the steady state difference in the composition of the mixture on a tray when the holdup of liquid on the tray changes.

Pigford et al (1951) and Rose and O’Brien (1952) also investigated the effect of holdup on batch distillation. The work of Pigford et al showed a general tendency for a decrease in the sharpness of separation with increasing tray holdup. Some other investigators including Luyben however, found holdup either to have no effect on the degree of separation or to have a beneficial effect (for small holdup). Rose and O’Brien (1952) investigated holdup effects on ternary distillation in a packed column and found it to depend on the reflux ratio. They found, using an n-heptane-methylcyclohexane-toluene mixture, that when the column was initially run at total reflux, increasing percentage holdup was beneficial to the sharpness of separation. However, when the column is started at fixed reflux, holdup was found to be either beneficial, detrimental or to have no effect depending on the reflux ratio used. A ‘critical reflux ratio’

was found at which increasing holdup had very little effect on the sharpness of separation. Below this critical reflux ratio, they found increasing holdup to be beneficial and above it, detrimental to the separation.

### 2.5.2 Reflux Ratio

Investigations into the effect of reflux ratio on the degree of separation are generally linked with the effect of holdup. Also, most of the published work (Pigford et al (1951), Rose and O'Brien (1952), Luyben (1971, 1988)) investigates the effect of reflux ratio as a design parameter.

Investigation of the performance of the fixed reflux operation compared to a variable reflux operation by Luyben (1988) showed very little difference, with a reduction in batch time (or energy consumption) of less than 5% for the variable reflux operation. This is in agreement with the findings of Converse and Gross (1963), Coward (1967) and Stewart et al (1973). Converse and Gross (1963) also found that the optimal reflux policy results in an improvement in product yield of only 4-5%, compared with the constant and the variable reflux ratio policies. Some other investigators including Robinson (1970) however, have found a significant improvement of up to 13.5% in batch time using the variable reflux policy, compared with the constant reflux policy, but no significant difference between the variable and optimal reflux policies.

Stewart et al (1973) presented a mathematical model which was used to investigate the effect of holdup, reflux ratio and number of trays on the degree of separation obtainable in a multicomponent batch distillation. Their model included both material and energy balances and also accounted for tray efficiencies. It was run at constant distillate rate (variable reboiler heat input) and constant heat input rate (variable distillate rate) and they found that the degree of separation (measured by the average product concentration) was not affected by whichever mode was used, other factors held constant. Pigford et al

(1951) found operation at lower reflux ratios to enhance the sharpness of separation when the column holdup is small.

### 2.5.3 Tray Efficiency

The distribution of components as well as the instantaneous distillate composition is affected by the efficiency. Numerous simulation models and packages exist for batch distillation but many of these employ theoretical stage models. Some of these models allow for tray efficiency but only as a tuning parameter, obtained by a trial and error process, for matching simulation results with actual experimental data.

The better known definitions of efficiency include:

- *Overall Column Efficiency* - Here, a single value is used to define the efficiency of the entire column, based on the degree of separation achieved. The implication is that the actual and ideal column will have different number of trays, thus we may assume equal reflux rates and product concentrations even when number of trays differ (Standart (1965)). This overall column efficiency can be safely applied to continuous distillation but leads to difficulties for batch distillation, where conditions are continually changing throughout the column.
- *Murphree Tray Efficiency* - This is the ratio of the actual enrichment observed on a tray to that which would be obtained assuming the tray was ideal. This definition assumes constant molal flows in the column, which is a reasonable assumption, but does not address the issue of saturation
- *Carey (Thermal) Efficiency* - This is analogous to the Murphree efficiency but assumes thermal equilibrium as opposed to phase equilibrium. It therefore suffers the same drawbacks with regards to the issue of saturation (phase equilibrium in this case).
- *Vaporisation Efficiency* - This is the ratio of the actual composition of the vapour leaving the tray to the composition of the vapour in equilibrium

with the liquid (saturated or not) on that tray. This definition was proposed by Holland (1963) who in Holland and McMahon (1970) attempted to show that under certain conditions in a multicomponent distillation, Murphree efficiency values of zero or infinity could be obtained while vaporisation efficiencies had finite, bounded values. This claim was criticised by Standart (1971).

- *Hausen Efficiency* - This definition of efficiency is in effect analogous to Murphree's definition but is developed in terms of rates of mass transfer, thus circumventing the issue of saturation and thermal equilibrium. However, the determination of the efficiency using this definition requires experimental measurements of stream compositions and enthalpies, condenser heat duty and heat losses from the column, per unit amount of distillate produced (Standart (1965)).

Standart (1965) reviewed, discussed and criticised the overall tray efficiency as well as the Murphree, Carey and Hausen tray efficiencies, pointing out their limitations. He also defined a new efficiency term, which is a generalisation of the Hausen efficiency, that is applicable to multicomponent mixtures with unsaturated phases. Similarly, Medina et al (1978) made a quantitative comparison between Murphree and vaporisation efficiencies based on distillation data for the ternary mixtures of acetone/methanol/ethanol, acetone/benzene/chlorobenzene, benzene/toluene/m-xylene and also for a hexane/methylcyclopentane/benzene mixture. They came to the conclusion that the murphree efficiency model gives a more useful representation of the behaviour of distillation columns than does the vaporisation efficiency model.

Another common way in which efficiency is represented in operational studies is in the use of actual number of trays. Here, the column is modelled using the number of trays that produces the required specification product, without the need to apply an efficiency factor. This 'actual number of trays' is usually different from the ideal number of trays.

### 2.5.3.1 Non-Equilibrium Stage Models

Tray efficiency is a function of physical properties, geometric characteristics and operating condition (Pescarini et al (1996)). Because tray efficiencies do not have a simple explanation and must be measured, several researchers including Kraishnamurthy & Taylor (1985a,b,c), Pescarini et al (1996) and Mehlhorn et al (1996) have tried to avoid its use. Instead, they have developed non-equilibrium stage models where the conservation equations are written for each phase independently and solved together with the transport equations that describe the mass and energy transfer rates in multicomponent mixtures. They have shown that this non-equilibrium stage model is capable of predicting the actual performance of a distillation process unit. One of the assumptions made for the non-equilibrium model however is that the vapour phase is continuous. This is valid for packed columns but in plate columns, the vapour phase is represented by bubbles, introducing possible errors in the model prediction.

Mehlhorn et al (1996) also developed a model for batch distillation in columns with perforated plates using both equilibrium and non-equilibrium models together. Their model did not involve detailed plate hydraulics modelling but uses a two- vapour phase model. The basis for this was that their investigation into the hydraulics of sieve trays showed a distribution of bubble sizes in the vapour phase, of mainly two different sizes: large and small bubbles. The small bubbles have a higher interface to volume ratio than the larger bubbles and a higher contact time in the bubbling zone. Therefore, the small bubbles represent the equilibrium part and the large bubbles, the non-equilibrium part of the model. With such models however, a distribution factor in the vapour phase between the large and small bubbles is essential for the correct response of the model and this, in effect, is synonymous to an efficiency value.

Despite the successful application of these non-equilibrium models, which avoid the use of efficiency values, an efficiency parameter still remains the more acceptable and much easier way of representing the non-achievement of phase

equilibrium on the tray. Also, of all the different definitions of efficiency available, Murphree's tray efficiency is often the preferred mode of efficiency representation.

### 2.5.3.2 Murphree Vapour Phase Tray Efficiency

Murphree (1925) defining rectification as a special case of absorption, described a method for calculating actual plates in a column. The resulting equation was derived from the general equation for the rate of mass transfer between a liquid and vapour phase, for the case when liquid film resistance is negligible in comparison with the vapour film resistance or when the partial pressure is a linear function of concentration. The equation derived by Murphree is

$$y_n = y_n^* - M (y_n^* - y_{n-1}) \quad 2.2$$

or in it's more familiar form,

$$E_{MV} = \frac{y_{n,i} - y_{n-1,i}}{y_{n,i}^* - y_{n-1,i}} \quad 2.3$$

where  $E_{MV} = (1-M)$  is the Murphree vapour phase efficiency,

$y$  = vapour phase composition of the volatile component

$n$  = tray number

$i$  = component number

He also showed that this equation is easily applied to the case where the vapour film resistance is negligible in comparison with the liquid film resistance. An equivalent equation for the liquid phase is easily obtained.

This definition of efficiency assumes that the liquid stream from a tray is saturated (in thermal equilibrium with the vapour) so that a saturated vapour phase can exist in equilibrium with it. Although this might pose a problem when

handling complex systems, the deviation from saturation in most systems is usually small (Standart (1965)). Taylor (1962) extended Murphree's equation to handle unsaturated liquid and vapour streams.

### 2.5.3.3 Tray Efficiency Variation

Although most distillation processes in the chemical and petrochemical industries often involve multicomponent mixtures, there is very limited information on the efficiencies of multicomponent systems compared with binary systems. This lack of data has resulted in the usual assumption of equal component tray efficiencies. This is true for thermodynamically ideal systems if complete liquid mixing is achieved on the tray. However, for thermodynamically non-ideal systems made up of components of different molecular size and nature, significant differences exist between the efficiencies of the different components (Bidulph (1975)).

Quereshi and Smith (1958) were among the first investigators to point out that in multicomponent systems, individual components may operate with different efficiencies. Toor (1957) showed theoretically that for thermodynamically non-ideal multicomponent systems, there are marked differences between binary and ternary mass transfer arising out of interactions between the diffusing species. These interactions were designated firstly as diffusion barriers (no mass transfer occurs despite the presence of a driving force), secondly as osmotic diffusion (mass transfer in the absence of a driving force) and thirdly as reverse diffusion (mass transfer against the direction of the driving force).

Toor and Burchard (1960) studied the mass transfer behaviour of the non-ideal system methanol/isopropanol/water to demonstrate these effects and computed different point efficiencies in the system. Dribika (1986) using the system methanol/ethanol/n-propanol measured equal point efficiencies on a tray as expected, this being a thermodynamically ideal system. Despite the existence of

equal component point efficiencies in this system however, Dribika measured different component tray efficiencies.

Bosley and Edgar (1994) have reviewed some of the work done in batch distillation modelling and present experimental results using an ethanol/water mixture in a pilot scale batch distillation column. They presented a model which takes into account tray hydraulics, stage efficiencies and energy balances and they compare the results with experimental data and other rigorous simulators. They show that the tray efficiencies are not constant, but vary as the state of the column varies.

Dribika (1986) also showed, using a methanol/ethanol/n-propanol mixture, that not only did the efficiencies vary from tray to tray, but that they also depended on the composition of the mixture on the tray. This corroborated the findings of Bidulph and Ashton (1977) whose investigation was based on data from an industrial size continuous distillation column with a multicomponent feed. They found the efficiencies of each component to vary widely throughout the column. They observed, as did Dribika (1986), that in the distillation of a ternary mixture, the Murphree tray efficiency of the intermediate component took on strange values (sometimes going above 100% or taking on a negative value) when a maximum occurs in its composition. The occurrence of these high murphree tray efficiencies is not restricted to ternary mixtures as was found by Shilling et al (1953), Lockett and Ahmed (1983) and Dribika (1986), but also binary mixtures (Mostafa (1979), Bidulph (1975)).

These large variations in tray efficiency from tray to tray and component to component highlight the possible dangers of designing batch distillation columns using constant and equal tray efficiencies for the components. This is of particular significance in batch distillation simulation and modelling because of the dynamic nature of the process, which means that conditions are continually changing throughout the column. The implication is that errors, which may be significant, are introduced into the model if a single, constant tray efficiency value is used. An accurate model of batch distillation must

therefore take into account, these variations in tray efficiency – the motivating case for this study.

#### **2.5.3.4 Estimating Tray Efficiency**

The problem of predicting distillation tray efficiency with a large degree of confidence still exists. The usual practice is to choose an arbitrary efficiency value with which to carry out simulations. In some sensitive columns such as absorption and stripping columns which often have low tray efficiencies, a difference of a few percentage points between the predicted and actual efficiencies can have a large influence on the number of trays required for a separation. Vital et al (1984) presents an extensive review of empirical and theoretical efficiency estimation methods for tray columns. The prediction problem can be divided into two parts; that of predicting the point efficiency and that of relating the point efficiency to the tray efficiency, taking into account such factors as liquid mixing, liquid residence time, entrainment, and weeping (Lockett and Ahmed (1983)).

Considerable success has been achieved in the latter part but actual accurate point efficiency prediction still remains a difficult task. Most efficiency estimation methods involve using the Maxwell-Stefan diffusion equations to calculate individual component point efficiencies, taking into account diffusional interactions (Kalbassi (1987)). These have certain limitations in that they incorporate a large number of assumptions and can only be used for ternary systems. Medina et al (1979) applied these Maxwell-Stefan equations and their results were shown to compare very well with experimental data while Lockett (1986) used the theory from first principles, to calculate efficiencies for the system methanol/ethanol/water. The estimated efficiencies were different for each component and similar to industrial data.

The AIChE method devised by Gerster et al (1951) and summarised in the AIChE Bubble Tray Design Manual (1958) has come to be the accepted

framework on which most currently used efficiency prediction methods are based. This method however has a few drawbacks including the fact that the correlations for  $N_G$  and  $N_L$  (vapour and liquid phase transfer units) assume that resistance is either entirely in the liquid or in the vapour phase and not a mixed resistance system, as is usually encountered in distillation.

This shortcoming was overcome by Lockett and Ahmed (1983) who carried out experiments using a methanol/water mixture and estimated vapour phase point efficiencies from the measured concentration profile across the tray. They determined individual values of  $N_G$  and  $N_L$  from the variation of the number of overall transfer units with composition. An interesting feature of the results of their work is some very high tray efficiencies obtained at low liquid concentrations. This was attributed to the large enhancement of tray efficiency over point efficiency, because of the large value of the slope of the equilibrium line at these low concentrations. These high efficiency values were not obtained at high column F factors (vapour loads). This is consistent with the increased liquid mixing at high vapour velocities, which reduces the enhancement of tray efficiency over point efficiency.

More recently, Rao et al (1995) presented a method for estimating tray efficiencies from point efficiencies for dispersed and plug flow of the liquid phase, accounting for liquid entrainment. They use the Maxwell-Stefan approach to develop a component point efficiency matrix which does not suffer the general drawbacks that applies to most other models that do not account for the effect of flow patterns and liquid mixing on the tray. They also demonstrated the superiority of their model, using two ideal and two non-ideal mixtures.

Because of the shortcoming of these prediction methods, small columns especially sieve-tray Oldershaw columns, have been used to experimentally obtain efficiency data which is then scaled up for large industrial trays. However, the use of efficiencies measured in small columns to design large tray columns is difficult because the dispersion stability, holdup and character are

sufficiently different to make the translation (scale-up) to industrial scale difficult. Different investigators have found a good match between scaled up efficiencies and large column data (Fair et al (1983)) while others have not (Dribika and Bidulph (1986)).

## **2.6 FACTORS AFFECTING TRAY EFFICIENCY**

Many factors may affect the efficiency of a tray including mechanical design factors (tray type and size, hole size, weir height), operating conditions (liquid and vapour rates) and the characteristics of the mixture on the tray. Some of these factors which have received attention (Langdon and Keyes (1943), Fane and Sawistowki (1969), Lockett and Uddin (1980)) include outlet weir height, hole size, liquid mixing, entrainment, flow patterns, flow regimes (i.e. froth or spray regimes), reflux ratio, composition and surface tension of the components of the mixture.

### **2.6.1 Hole Size and Outlet Weir Height**

The effect of hole size in sieve trays and weir height (in other trays) on the tray efficiency is usually associated with its holdup characteristics. Investigation into the effect of hole size in sieve trays on tray efficiency by Lockett and Uddin (1980) showed that smaller holes exhibited higher efficiencies at low vapour rates but at higher vapour rates, hole size was not seen to have any effect. They suggested that smaller holes at low vapour rates prevented liquid being dumped due to the capillary surface tension effects, thus increasing the tray liquid holdup and efficiencies. Smaller jets are issued from smaller holes thus increasing the mass transfer process.

Likewise, outlet weir height is used to maintain an appropriate liquid depth (holdup) on the tray and as is expected, tray efficiency increases with increasing

outlet weir height. Deeper liquid levels on the tray means the residence time and mass transfer time of the vapour bubble through the liquid is increased.

### 2.6.2 Reflux Ratio and Tray Holdup

Investigating the effect of reflux ratio, Pigford et al (1951) showed that in the presence of appreciable holdup, the effect of reflux ratio on the sharpness of separation was less pronounced than in a column with negligible holdup. Langdon and Keyes (1943) however, concluded based on results obtained from experimental data using an isopropyl-water mixture that changes in reflux ratio had a negligible effect on the tray efficiency. Other researchers including Ellis and Hardwick (1969) and Gerster et al (1949) have however found plate efficiency to vary appreciably with reflux ratio. Ellis and Hardwick's results were based on results obtained from the distillation of a methylcyclohexane-toluene mixture and their deductions did not take into account the effect of concentration on the tray efficiency.

The effect of holdup on actual tray efficiency is not reported but its effect on the sharpness of separation gives an indication of how it affects the distillation operation. However, Fane and Sawistowski (1969) found that in surface tension positive systems at low vapour velocities, holdup is strongly concentration dependent and passes through a minimum which corresponds roughly to the concentration where a maximum is observed for the tray efficiency.

In a different vein, Chen et al (1990) investigated the performance of a combined mesh packing and sieve tray in the distillation of a methanol-water system, for a wide range of feed concentrations. They found that the presence of the packing on the tray increased the Murphree efficiency of the tray by up to 50% in some cases. They attributed this increase in tray efficiency to a much smaller and more uniform bubble formation on the packed tray.

### 2.6.3 Fluid Flow Regime

Fane and Sawistowski (1969) conducted research into how operating the column in the foam (liquid-phase continuous) or spray (vapour-phase continuous) regimes affected plate efficiencies for surface tension positive and negative systems. They showed that in the spray regime, plate efficiency decreases with increasing concentration of the more volatile component (higher surface tension) for negative systems, but increases in the same direction for the positive system. They also concluded that under foam conditions, positive systems tend to give higher tray efficiencies than negative systems as a result of greater interfacial area presented by the cellular foam of the former compared with the mobile foam or froth of the latter.

At high vapour rates (spray regime), the liquid phase becomes the dispersed phase and they found that negative systems then give higher efficiencies than positive systems. This was explained by the influence of the Marangoni effect on the stability of the liquid sheets and ligaments and it results in finer dispersion and hence greater interfacial area for the negative system. They found performance in the spray regime to be strongly dependent on surface tension and almost inversely proportional to it.

Their deductions were confirmed with experimental results using three different systems: a strongly positive heptane-toluene system, a strongly negative benzene-heptane system and a third system of benzene-cyclohexane which formed an azeotrope and the mixture was either weakly positive at high benzene concentrations or weakly negative at low benzene concentrations.

### 2.6.4 Liquid Viscosity

Barker and Choudhury (1959) studied the effect of liquid viscosity on mass transfer and plate efficiency correlations. With increasing liquid viscosity, a reduction in interfacial area occurs thus leading to a reduction in gas-film

efficiency. Also, viscosity can increase the size of a bubble at bubble formation at the slot or orifice by retarding the rate of closure of the neck of the bubble. This change in bubble size could be detected by liquid holdup measurements for the tray. Liquid holdup decreases with increasing liquid viscosity.

The beneficial effect of liquid viscosity will be to retard the rate of bubble rise through the liquid on the plate, leading to increased mass transfer. This effect, however does not appear to be sufficient to balance the decrease in surface area obtained at higher liquid viscosities.

### 2.6.5 Surface Tension Effects

Early studies of surface tension effects on distillation resulted in a classification of systems (mixtures) according to their surface tension characteristics. The systems are defined as:

- *Positive*: if the surface tension of the reflux increases down the column and is characterised by stabilised foam on each tray.
- *Negative*: if the surface tension decreases down the column and the liquid films break up into rivulets or droplets.
- *Neutral*: if the surface tension remains unchanged.

Surface tension neutral systems are encountered when the pure components have similar surface tensions or if the mass transfer driving force is insufficient to cause a major surface tension change. Figure 2.3 illustrates the difference in liquid structure between positive and negative systems on an Oldershaw column tray as was reported by Ellis and Legg (1962).

The work of Zuiderweg and Harmens (1958) with packed and sieve tray columns revealed higher efficiencies for the positive systems. This was explained in terms of Marangoni effects on the stabilisation of the liquid films or froth in the positive system. Similar conclusions were made by other

investigators including Medina et al (1978) but Bainbridge and Sawistowski (1964) observed the reverse. They operated their column in the spray regime and their higher efficiencies for the negative systems were explained in terms of Marangoni effects on droplet formation. Sawistowski (1973) stated that these Marangoni effects affect both the mass transfer coefficient and the effective interfacial area and Dribika (1986) corroborates this statement.

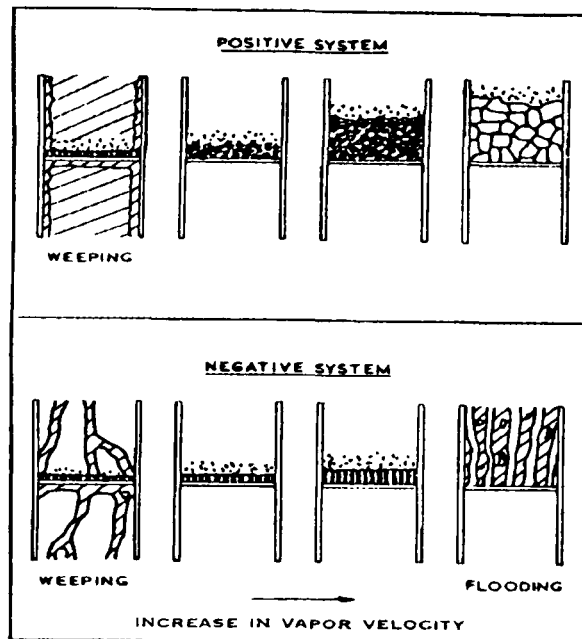


**Figure 2.3:** Interfacial Contacting on a Perforated Plate for a Positive and a Negative System (from Ellis & Legg (1962)).

Hart and Haselden (1969) used four different mixtures in their investigations. They employed benzene/ethanol and carbon tetrachloride/methanol mixtures, which form azeotropes and can exhibit surface tension positive or negative characteristics depending on their composition. They also employed a benzene/n-hexane system, which is surface tension positive and acetone/methanol system which is neutral. Their experimental work was carried out on a small, sieve tray, representative of a small region of a large operating tray, thus ensuring complete mixing on the tray. The resulting observation was that there was no significant difference between experimental values of point efficiency obtained, and tray efficiency.

They observed with positive systems, that foam height on the tray passes through a maximum as predicted by Zuiderweg and Harmens (1958), and that the magnitude of this maximum is not related directly to the difference in surface tension of the pure components. The composition at which the maximum occurred, but not its magnitude, was found to be independent of the fluid flow-rates. For negative systems, they observed an appreciable foam height at pure alcohol compositions and at the azeotropic compositions of the relevant systems. They noted also a slight displacement between predicted and observed compositions of the maximum foam heights (and maximum tray efficiency).

Fane and Sawistowski (1969) defined a foam and a spray regime within the column and showed that in the spray regime, Bainbridge and Sawistowski's (1964) observation was repeated for negative systems and in the froth regime, Zuiderweg and Harmens' (1958) observations were repeated. Their results also confirmed the effect of Marangoni instabilities on droplet sizes. They demonstrated that tray holdup in the spray regime is independent of the type of system but higher plate efficiencies were observed for negative systems than for positive systems at approximately equal values of other physical properties. This observation could only be attributed to larger interfacial area, hence smaller drop sizes in negative systems. This means that in a column with close tray spacing, liquid entrainment rates for negative systems are expected to be higher compared with positive systems.

Experimental work by Ellis and Legg (1962) with negative systems showed that maximum efficiency occurred at low vapour boilup rates (or F factor) especially when the plates are weeping. However, the difference in surface tension between different negative systems was not seen to have any significant effect on the tray efficiency.

In general, Fane and Sawistowski concluded that for practical purposes, one can assume that tray efficiency (which they expressed in terms of number of

transfer units) is inversely proportional to surface tension. They also inferred from their findings that enhanced interfacial area is obtained for surface tension positive systems in the froth regime and for surface tension negative systems in the spray regime. Fell and Pinczewski (1977) have suggested taking advantage of this effect by designing surface tension positive and negative systems to operate in the froth and spray regimes respectively.

### 2.6.6 Concentration Effects

The effect of concentration on tray efficiency is demonstrated by Fane and Sawistowski (1969) where they showed a composition dependence for a benzene-cyclohexane (surface tension positive) system, with the efficiency passing through a maximum. This composition dependence was found to be strong at medium weir height and low vapour velocity. These are the conditions under which the results of Zuiderweg and Harmens (1958) of higher tray efficiencies for positive systems compared with negative systems apply. For a negative system, Fane and Sawistowski (1969) found tray efficiency, under spray conditions, to decrease with increasing composition of the more volatile component using a benzene-heptane system.

They found from their investigation that under spray conditions with the surface tension positive system, the efficiency maximum disappears and there is a gradual increase in efficiency towards higher concentration of heptane in a benzene-heptane system. In this concentration region, the efficiency also tends to become independent of flow rate.

Many other investigators, including Langdon and Keyes (1943) and Mostafa (1979), have looked at the influence of concentration on the tray efficiency of a distillation column for various tray types and column configurations. Langdon and Keyes (1943) investigation showed a strong variation in Murphree efficiency with composition for an isopropyl-water system.

In his study, Mostafa (1979) used 2 systems, one near ideal system (benzene/toluene) and one non-ideal system (ethanol/water), with the Kirschbaum cell model as a model of a cross-flow plate. He suggests various reasons for the variation in plate efficiency with concentration, including variations in the sign and magnitude of the surface tension gradient, the interfacial area, the mass transfer coefficient, physical properties, the slope of the equilibrium curve and thermal effects. These parameters in turn influence the mass transfer between phases, the plate hydrodynamics, the slope of the operating line and the value of the driving force.

Mostafa observed in his work that the plate efficiencies in the near ideal system were more or less constant with concentration. With the more non-ideal system however, considerable variations in plate efficiency were observed with changing concentration. This effect was found to be more significant at concentration ends, near azeotropic points and where the driving force is very small. Hart and Haselden (1969) have also investigated these concentration effects. They suggest that while none of the reasons proposed for the variation of tray efficiency with the composition of the mixture on the tray provides a complete explanation, a major factor for this variation is the development of surface tension gradients within the dispersion, the magnitude and sign of which depends on the concentration of the mixture. This surface tension gradient influences both the interfacial area and the rate of mass transfer.

Shilling et al (1953) obtained tray efficiency data for the distillation of an ethanol/water mixture, at mixture concentrations between 0 and 70 mole percent ethanol. They observed an efficiency maximum in the composition range 35 to 60 mole percent ethanol with efficiency falling more sharply in the lower ethanol composition range. At very low ethanol concentrations, Murphree efficiency values were observed to exceed 100%, which they suggested was erroneous.

The concentration effect on tray efficiency was also studied by Lockett and Ahmed (1983) with experimental data obtained from a 0.6m diameter column

and using a methanol-water system. The column contained 4 sieve trays, and data (i.e. liquid and vapour samples) was collected with the column operating at total reflux. Murphree vapour phase tray and point efficiencies were estimated from the experimental data and they observed that the tray efficiency goes through a slight minimum while point efficiency increases monotonically with methanol liquid concentration. The results also show a small but inconclusive variation of the tray efficiency with F factor over the range of F factors used. All the runs carried out in their experiments were in the froth regime implying low level of entrainment which will therefore have a negligible effect on the tray efficiency.

Lockett and Ahmed (1983) in their experiments, obtained very high tray efficiencies at very low methanol concentration in the liquid. A similar observation was made by Shilling et al (1953), using an ethanol/water mixture in his study. Langdon and Keyes (1943) using an iso-propanol/water mixture in a 4 tray bubble cap distillation column also observed this variation of Murphree Tray efficiency with composition. A sharper decrease in efficiency with concentration was observed as the azeotropic composition was approached from either side.

Results of research by Bidulph and Ashton (1977) and Dribika (1986) with ternary mixtures of benzene/toluene/m-xylene and methanol/ethanol/propanol respectively, also establishes a relationship between tray efficiency and the composition of the mixture on the tray even when point efficiencies were constant. Equally interestingly, they observed that the tray efficiency for the intermediate component went through a maximum when its composition peaks and, in some instances, efficiencies of over 100% were observed. This, they suggest, typifies the behaviour of conventional Murphree tray efficiency when a maximum occurs in the composition of an intermediate component and/or when the driving force difference approaches zero. This also reinforces the inaccuracy of the constant tray efficiency model

## 2.7 SUMMARY

Simulation methods and programs for batch distillation of varying degrees of complexity and detail are currently available. Shortcut models incorporate numerous simplifying assumptions and are largely used for initial trial designs and preliminary studies while rigorous models include more detail as well as energy balances and are therefore, able to handle more complex, non-ideal systems. However, the majority of these rigorous models are based on equilibrium stage simulations. Those that account for the non-attainment of phase equilibrium on the tray usually apply a single tray efficiency value throughout the column (column efficiency). Tray efficiency estimation methods exist which use either direct tray efficiency calculation methods or point efficiency estimation procedures, which are then related to tray efficiency by mixing characteristics. Many researchers and column designers also still infer tray efficiencies from data taken from operating columns as has been done for many years. In many simulation instances also, it is used as a tuning parameter to match model predictions with experimental results.

Research has shown that a large variation in tray efficiency from tray to tray as well as between the components on a tray is not uncommon and this highlights the possible dangers of designing columns using constant and equal tray efficiencies. Furthermore, investigations reveal that on large industrial sized trays where complete mixing is not achieved on the tray, a concentration gradient, hence an efficiency gradient exists on the tray.

Explanations have been forwarded as to why tray efficiency is affected by mixture composition. These include the slope of the equilibrium curve, mass transfer coefficients, interfacial area, surface tension gradients, physical properties and thermal distillation effects. While none of these factors alone can fully explain this efficiency variation, Hart and Haselden (1969) suggest that the development of surface tension gradients within the dispersion constitutes a major factor, the magnitude and sign of these gradients being a function of the

mixture composition. These surface tension gradients in turn influence the interfacial area and the rate of mass transfer between the phases.

These factors would have a more significant effect in a batch distillation unit than they would in a continuous distillation. This is because in a batch distillation unit, the composition on a tray will change greatly during a single batch run while composition variations on a tray in a continuous column are usually very small.

The lack of appreciation of the implication of these varying efficiencies and their composition dependence may well explain the fact that many columns do not achieve their expected performance and why over-design is still so widely used. It may also be an important factor affecting model accuracy. This necessitates the investigation of the performance and behaviour of a batch distillation model, which includes a tray efficiency-composition dependence. This is as opposed to the common practice where an overall column efficiency is used in the simulation model.

## **CHAPTER THREE.**

### **THE KESTNER COLUMN**

The experimental column used for in this work was designed and constructed by Kestner Evaporator and Engineering Co. Ltd. and had been used previously for dynamics and control studies within this Chemical Engineering department. Dribika (1986) has also used it in other studies on distillation efficiencies. It can be operated either batchwise or continuously but is run as a batch distillation column in this study. The column has the advantage that the trays are small in size so that complete liquid mixing is achieved (Dribika (1986)).

The column is made of stainless steel with an elliptical cross section and contains 10 bubble cap trays, with each tray carrying 7 bubble caps. The column is assembled in flanged sections, each section containing a tray and equipped with a sight glass for visual observation of the fluid behaviour above the tray. A diagram of the column is shown in Figure 3.1, while Figure 3.2 shows details of the bubble cap tray, with dimensions given in Table 3.1.

#### **3.1 THE STILL / BOILER**

The column still, A, in Figure 3.1 is a 40-litre stainless steel vessel provided with an external steam jacket and an internal heating coil. This arrangement permits steam pressures of up to 4 bar to be attained in the jacket. It is fitted with a sight glass (for visual observation and measurement of liquid level) and pressure gauges on both the jacket and vessel side of the still. The jacket pressure gauge gives readings of the steam pressure in the jacket side of the still and the vessel side pressure gauge gives the actual reboiler pressure. Two valves are located across a T-junction in the steam condensate return line from

the still so that condensate can be diverted to a collection vessel for a short period, for flow rate and temperature measurement.

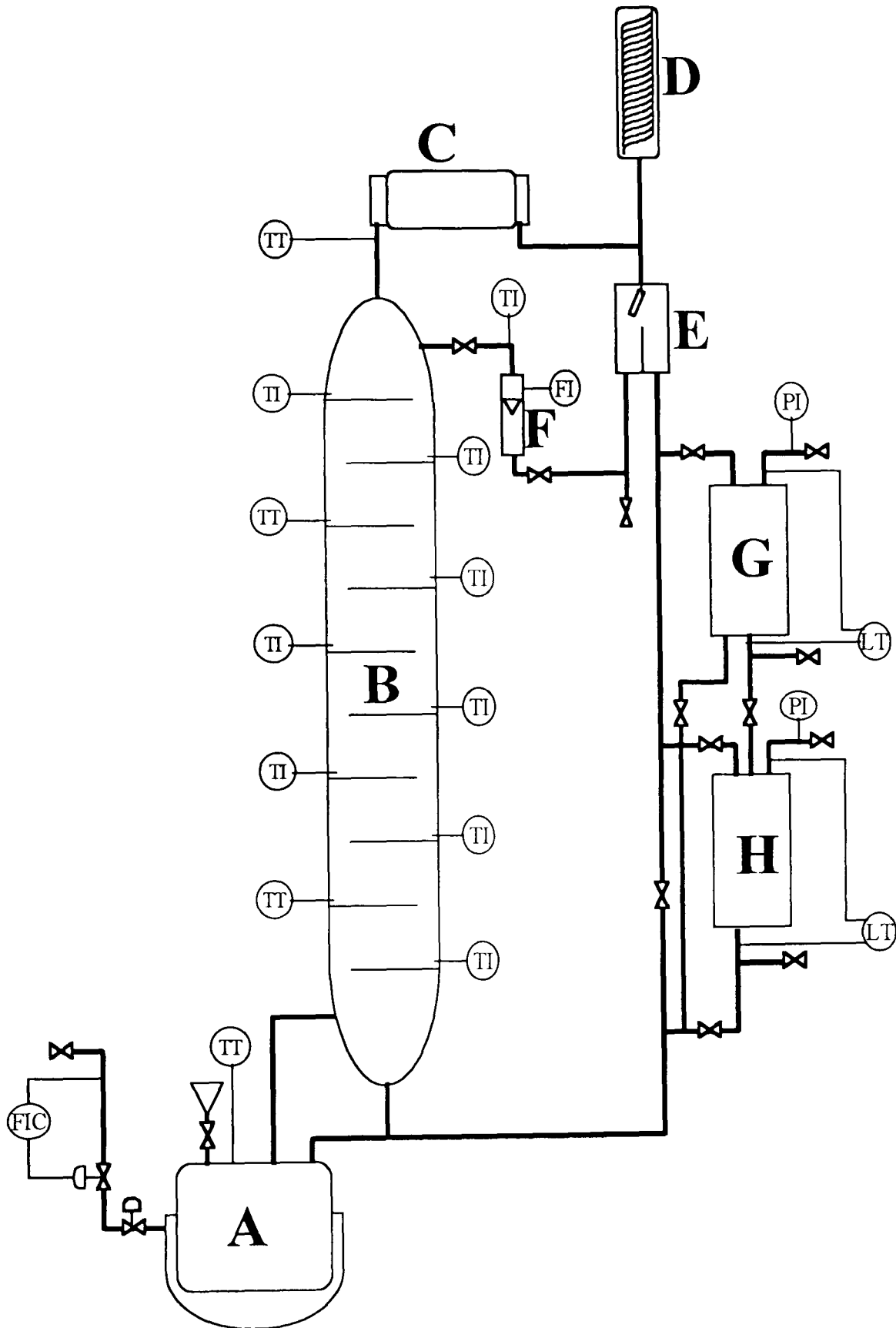
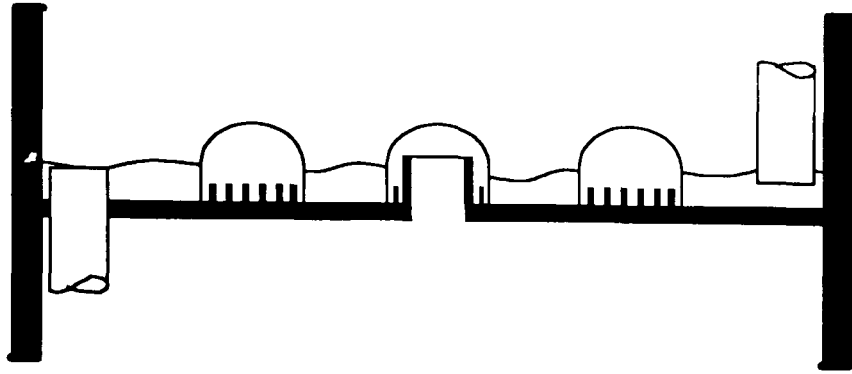
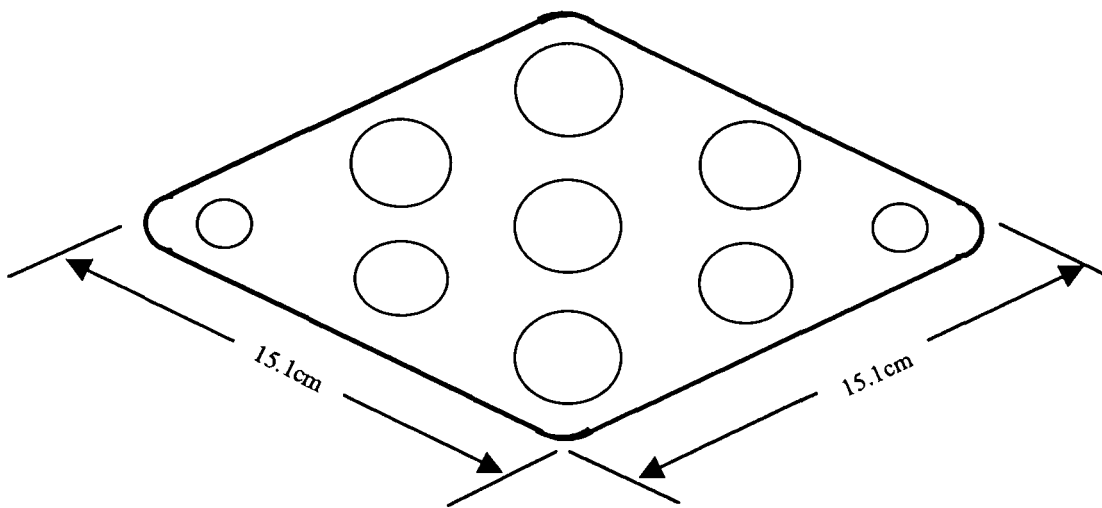


Figure 3.1: The Kestner Distillation Column.



a) Sectional view of The Tray including Bubble Caps and Downcomers



b) Plan View of Tray including the Bubble Caps and Downcomers

**Figure 3.2:** Bubble Cap Tray Details.

**Table 3.1:** Dimensions of Tray Details

Item	Size
Total Plate Area	197.40 cm <sup>2</sup>
Tray Spacing	20.50 cm
Weir Height	2.54 cm
Downcomer Area	7.80 cm <sup>2</sup>
Riser Diameter	3.10 cm
Total Riser Area	52.83 cm <sup>2</sup>

Steam is supplied as low-pressure steam from a central boiler through insulated piping. Constant heat input is required during the experimental runs as this gives a close approximation to constant vapour boilup, provided the still content is not greatly depleted. Constant heat input was achieved by controlling the steam flow to the still using a Eurotherm T640 controller unit. Flow measurements are taken from an orifice plate in the steam line using a differential pressure (DP) cell to sense the pressure drop. This information is transmitted to the controller, which outputs a 4/20 mA signal to a pressure transducer which in turn links to a pneumatically activated control valve, thereby regulating the steam flow.

### 3.2 THE COLUMN

The column (B, in Figure 3.1) consists of 10 bubble cap trays. Each tray is fitted with a thermocouple pocket and a liquid sample point, located just above the floor of the tray. This permits temperature measurement of the liquid on the tray as well as the withdrawal of liquid samples from the tray for analysis. It also has flow lines entering every tray so that feed can be introduced into the column at any tray if run in continuous distillation mode and material can be returned from the receivers to the column at any tray for slop recycle studies. The column is also insulated with glass wool to minimise heat loss to the environment.

The column is assembled in flanged sections, each section containing a tray. This makes column modification less tedious in terms of changing the number of trays in the column. Each section of the column is fitted with a sight glass just above the tray. This permits visual observation of the bi-phase within the column.

The liquid returned to the column from the condenser passes through a reflux splitter (labelled E in Figure 3.1) where product may be withdrawn and the rest of the condensate is returned to the top tray in the column via a rotameter

(labelled F). The reflux splitter is a swinging-bucket type and is divided into a product withdrawal section and a reflux return section by a baffle. The swinging bucket is located directly above the baffle and swings between either section depending on whether or not product is being withdrawn or the column is being run at total reflux. A sample point is also fitted along the return line from the reflux splitter to the reflux rotameter permitting distillate sampling and analysis. At total reflux, the reflux rotameter gives measurement of the amount of vapour that is cooled in the condenser, thus giving an indication of the vapour boil-up rate. A valve is located along the return line from the reflux rotameter to the column, which permits the manipulation of the amount of liquid holdup in the reflux splitter.

Distillate can be collected in either of the two product receivers, G and H, shown in Figure 3.1. They are both fitted with DP cells for liquid level measurement. Also, a vacuum pump is connected to the distillate receivers so that the column can be run under vacuum conditions if so desired. However, only runs at atmospheric conditions were required for the work reported here.

Fluid flow and liquid level information from the DP cells and temperature measurements from the thermocouple are logged on a PC (286 processor, DOS operating system) which is linked directly to the instrument panel using RS422 serial communication. Software developed by Rance (1993) communicates with the Metrabyte "DAS 16" analogue-to-digital converter card in the computer to serve as a data logging and display software. The software is also capable of controlling flow rates (steam flow rate in this work) and the reflux ratio. Reflux ratio setting is achieved by a keyboard operation, which causes signals to be sent to a pressure transducer. This then causes the swinging bucket reflux divider to swing between the reflux return and the product withdrawal sections of the reflux divider based on a prescribed time-base. Data is logged and displayed on the display unit every 10 seconds.

### 3.3 THE CONDENSER

The column has two condensers attached to it, together providing a total condensing area of  $2\text{m}^2$ . It is operated as a total condenser with one main condenser, C and the second one, D (in Figure 3.1) serving only as an overload condenser to ensure (for safety reasons) that all the vapour is totally condensed. The main condenser is a stainless steel type shell and tube heat exchanger with the process fluid as the tube side fluid and the cooling utility as the shell side fluid. During the experimental runs, this condenser provided sufficient cooling duty to condense all the vapour produced. Water is used as the cooling utility and is supplied to the condenser at about  $10\text{-}16^\circ\text{C}$ . A rotameter in the cooling water line, and thermocouple pockets at the inlet and outlet of the condenser on the utility lines, are also provided to assist in condenser duty estimation.

The second, guard condenser is smaller in size and is made of glass. This allows visual observation of the operation of this backup condenser when the capacity of the main condenser is exceeded. During some of the initial dummy runs when the column integrity and limits of operation were being tested, some condensate was detected in this second condenser at very high steam flow and low cooling water rates. The column is vented to atmosphere above this second condenser to ensure that all operations are at atmospheric pressure.

### 3.4 EXPERIMENTAL PROCEDURE

Prior to the startup of the column, precautionary safety checks are carried out to ensure that there are no electrical or ignition sources in close proximity to the column. The valves on the distillate withdrawal line from the condenser and the return line from the product receivers to the still are shut because the column is always started up on total reflux. The valves on the vapour line between the still and the column, the distillate return line from the condenser to

the column and the liquid line from the column to the still, are opened. The cooling water supply to the condenser is then started.

The feed material is prepared and charged to the still via a funnel located on top of the still and the charge valve is shut. The reflux divider is set to return all condensed vapour to the column (total reflux startup) and the steam supply valve is slowly opened to let steam into the still jacket. Steam flow rate is fixed by the setpoint on the controller. The setpoint is initially set to a low value and gradually increased, step-wise to the required flow rate in order to avoid a high vapour velocity within the column, which could unseat the bubble caps on the trays. The bubble caps are not fixed to the plate or riser but remain in place by virtue of their weight. This sets an upper limit on the vapour rates permissible for the column.

At startup, the trays and reflux receiver are dry, and their liquid holdup is built up as the vapour rises through the column. Data logging is started immediately heat is supplied to the still and the column is run at total reflux until steady state is achieved. Using pure water as a test fluid, steady state is indicated by a flat temperature profile in the column, of values close or equal to 100°C.

Condenser holdup was kept as small as possible by keeping the reflux return valve almost fully open, to minimise time lags in the response of the column, especially in the distillate composition. Because of the way the reflux divider functions however, a reasonable amount of holdup has to be maintained in the reflux divider to minimise fluctuation in the flow rate of the refluxed liquid returning to the column.

For proper testing and calibration purposes, the runs with pure water as process fluid were performed at various steam rates (hence different vapour boilup rates and velocities) and data was collected at steady state conditions. The results of these runs are presented and discussed in Appendix A along with initial methanol/water test runs.

### 3.4.1 Sampling Procedure

Only liquid samples are withdrawn and analysed in the experimental work carried out. A 10ml sample of the liquid on the tray is withdrawn using a hypodermic syringe, from the sample port on each tray, through a septum cap.

The samples are immediately transferred into a vial and quenched in an ice bucket to prevent evaporation of volatile components. At every sample time, two samples are withdrawn from each sample point. The first sample, serves to purge the line and is set aside and later returned to the still together with the analysed portions. Samples of distillate are taken from the reflux return line sample valve, and the still sample from a sample valve at the base of the still.

Samples are analysed in a Perkin Elmer model 452 gas chromatograph, which uses Nitrogen as the carrier gas. The chromatograph was calibrated using 21 samples of known composition in the range 0.0 to 1.0 mole fraction of methanol in steps of 0.05. Two injections were made for each sample and the area readings for the methanol and water peaks are output directly onto a printer. A graph of composition against area is plotted and using the least-squares method, the best correlating equation, which describes the relationship between methanol weight fraction and area peaks is found to be

$$w = 3 * 10^{-6} a^4 - 0.0007a^3 + 0.0416a^2 + 0.6526a - 0.2917 \quad 3.1$$

where  $w$  = methanol composition (weight %) and 'a' is the percentage of the total area from chromatograph readings that represents methanol peaks

This equation is used to interpolate for actual mixture compositions from sample analyses during the main rig runs and mole fractions are obtained from weight fraction values.

## **CHAPTER FOUR.**

### **THE SIMULATION MODEL**

In general practical situations, a process model is not usually available and even when it is, the model does not always exactly matches the process and uncertainties involved. As the amount of available information and the overall objective vary from one problem to another, no best or unique modelling method exists. As a result, many current industrial batch processes are not formally modelled, but are operated using heuristic process understanding. Models must therefore be developed which give a better representation of the process, resulting in a more accurate prediction its performance. The approach for a particular problem will depend on factors such as available data, physical insight, constraints and overall economic process objectives (Terwiesch et al (1994)).

The mathematical model developed for use in this work was designed from first principles, based on material balance equations, to mimic the behaviour of the Kestner distillation column described in Chapter 3.

#### **4.1 MODEL SPECIFICATIONS**

Four scenarios can be considered for the initialisation (i.e. time,  $t = 0$ ) of a distillation simulation. These are:

1. the initial state of the column could be taken as the time heat is first applied to the reboiler. In this case, the model must account for the thermal dynamics of the reboiler and column, as well as the filling of the trays (dry startup).

2. the reboiler content starts at its bubble point temperature and that the trays are dry. In this case, the reboiler dynamics are not modelled but the model must also account for the filling of the trays
3. the reboiler content is at its bubble point temperature and that the trays contain some of the feed charge material also at its bubble point temperature.
4. the column is at steady state under total reflux and product withdrawal can commence. The initial condition for this option is the result of a steady state, total reflux calculation.

The third option is chosen for this simulation model. The trays are assumed to initially contain the same material as the charge mixture at its bubble point temperature at the start of the simulation. This implies a flat temperature profile in the column at the start of the simulation after which tray temperatures and compositions progress towards steady state.

## 4.2 MODEL ASSUMPTIONS

As with almost all computer modelling processes, certain assumptions were made in the development of this model, some of which deserve particular mention :

- **Holdup:** The liquid holdup in the column is a function of the geometry and type of contacting device. For a given column, the volumetric holdup is often constant. If the overall liquid density does not change very much during the process, we can assume that the mass holdup remains constant. Also, if the variation in the molar mass of the mixtures over the period of time is not large, we can assume a fixed molar density, hence constant molar tray holdup. To make the model slightly more robust in the handling of different mixtures, the constant volume holdup model is adopted to allow for any variations in molar mass and mixture compositions. This is not unreasonable as severe composition swings are expected to occur on each

tray during the batch. Tomazi (1997) investigated the effect of using a model that accounts for this holdup variation in the tray hydraulics and compared it to one which doesn't and reports a significant improvement.

- **Constant Molal Overflow:** This is assumed, eliminating the need for energy balances giving instantaneous equal vapour flows.
- **Liquid Hydraulics:** These are assumed instantaneous, with liquid imbalances on each tray transferred to the still. This is a conservative approach.
- **No Heat Losses:** This assumption is confirmed by the water test results presented in Appendix A.
- **Negligible Vapour Holdup:** The most common simplification is the negligence of vapour holdup. This is usually a valid assumption in low-pressure systems, away from the critical point of the mixture components.
- **Constant Pressures:** Another common simplification, also employed here, is the assumption of constant pressure on all trays, which is often justified when columns are vented to atmosphere and because pressure drop through the column is usually small, compared with the absolute pressure values. This model assumes constant pressure on each tray, though pressure is allowed to vary linearly from tray to tray, up the column. Obviously, for dynamic models to be used over a wide pressure range such as during some startup and shutdown simulations (which is not required of the model used in this work), such constant pressure assumptions cannot be used. Such cases require tray pressures and pressure drops to be estimated accurately in order to obtain a realistic behaviour. Wittgens and Skogestad (1995) carried out dynamic simulations based on a model which included tray hydraulic and pressure drop calculations. They found that this model gave good agreement

with experimental responses during startup while simpler models based on linear tray hydraulics and constant molar flows gave quite large deviations.

### 4.3 MODEL EQUATIONS

The model used here was designed in a modular form. The modularity allowed for easier debugging and upgrading or amendment for use under different operating conditions and column specifications. A complete listing of the program is given in Appendix B and the component sections are described below.

#### 4.3.1 Main Column Equations

Based on the diagram shown in Figure 4.1, a component material balance around an arbitrary tray,  $n$  (envelope 1) is given by

$$\frac{dH_n x_{n,i}}{dt} = Vy_{n-1,i} + Lx_{n+1,i} - Vy_{n,i} - Lx_{n,i} \quad 4.1$$

where  $D$  = Distillate flow rate (kmol/hr)

$L$  = Liquid flow rate (kmol/hr)

$V$  = Vapour flow rate (kmol/hr)

$H_n$  = tray holdup on tray  $n$  (kmol)

$x_{n,i}$  = liquid phase mole fraction of component  $i$  on tray  $n$

$y_{n,i}$  = vapour phase mole fraction of component  $i$  on tray  $n$

$t$  = time (hrs)

Tray numbering starts from the bottom of the column upwards. For the still, top tray and the condenser holdups, the equivalent equations are respectively

$$\frac{dH_B x_{B,i}}{dt} = Lx_{1,i} - Vy_{B,i} \quad 4.2$$

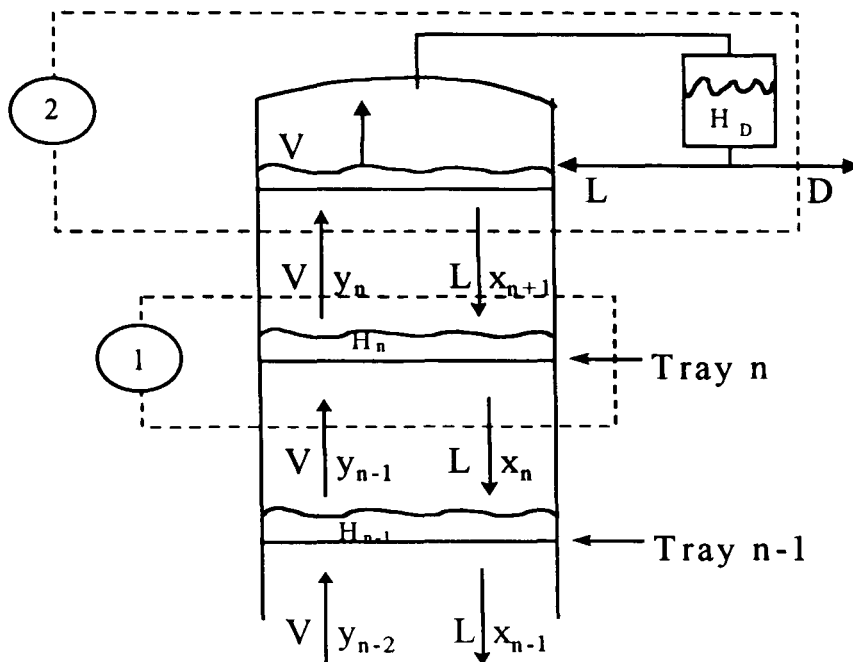


**Figure 4.1:** Column Section for Arbitrary Trays,  $n$ ,  $n-1$  and Top of Column.

$$\frac{dH_{NT}x_{NT,i}}{dt} = Vy_{NT-1,i} + Lx_{D,i} - Vy_{NT,i} - Lx_{NT,i} \quad 4.3$$

and

$$\frac{dH_D x_{D,i}}{dt} = Vy_{NT,i} - (L + D)x_{D,i} \quad 4.4$$

where subscript B denotes the still, D the distillate and NT, the top tray. Constant molal overflow is assumed so, the liquid and vapour flow rates are the same on all trays. An overall material balance around the top of the column (envelope 2 in Figure 4.1) gives

$$\frac{dH_D}{dt} = V - (L + D) \quad 4.5$$

In Equations 4.1 to 4.4, a constant molar holdup  $H_n$  is not used. Rather, a constant volume holdup  $v$ , is used and molar holdup is allowed to vary with the concentration of the mixture on the tray according to the equation

$$H_n = \frac{v_n \sum \rho_i w_i}{RMM_{av}} \quad 4.6$$

where  $\rho_i$  = the liquid density of component  $i$  ( $\text{kg/m}^3$ )

$v_n$  = volume holdup ( $\text{m}^3$ )

$w_i$  = weight fraction of component  $i$ .

$RMM_{av} = x_1 RMM_1 + (1 - x_1) RMM_2$ , average molecular mass.

Equation 4.6 applies to all the trays as well as the reflux splitter holdup and allows calculation of the molar holdup as composition varies. For a binary mixture therefore, the rate of change of molar liquid holdup on any tray is

$$\frac{dH_n}{dt} = \frac{v_n (\rho_1 RMM_1 - \rho_2 RMM_2)}{RMM_{av}^2} \frac{dx_1}{dt} \quad 4.7$$

The still content  $H_B$ , at any time is calculated from an overall material balance on the initial charge, the holdup in the column and the material removed from the column, as

$$H_B = H_B^o - \sum_{n=1}^{NT} H_n - H_D - \Delta D_{Total} \quad 4.8$$

$H_B^o$  is the initial charge to the still and  $\Delta D_{Total}$  is the total amount of distillate (products and slop cuts) collected, given by

$$\Delta D_{Total} = \int_0^t D \, dt \quad 4.9$$

The average composition of distillate (product or slop cut) collected is given by

$$x_{P,i} = \frac{\int_{ts}^{tf} D x_{D,i} dt}{\int_{ts}^{tf} D dt} \quad 4.10$$

where  $x_{P,i}$  = composition of component i in product (or slop) cut

ts = start time for product (or slop) withdrawal

tf = stop time for product (or slop) withdrawal

Equations 4.7 and 4.9 are integrated numerically for holdup and amount of distillate collected. Holdup values are substituted into Equations 4.1 to 4.4, which are also integrated numerically for liquid compositions. Integration is carried out using the Euler method with typically a time step of 0.001hrs. Depending on the operating conditions of the simulation, the time-step size can be varied during the course of the simulation.

### 4.3.2 Vapour Liquid Equilibrium

The vapour-liquid equilibrium is represented here by Raoult's law, with liquid phase non-ideality accounted for by the activity coefficient,  $\gamma$

$$y_{n,i}^* P_n = \gamma_{n,i} x_{n,i} P_{n,i}^o \quad 4.11$$

where  $P_n$  = Pressure on tray n

$P_{n,i}^o$  = saturated vapour pressure for component i on tray n.

$\gamma_{n,i}$  = activity coefficient of component i on tray n.

$y_{n,i}^*$  = vapour composition of i in equilibrium with liquid on tray n

Liquid compositions are obtained for every time step from the material balance Equations 4.1 to 4.4 and the equivalent vapour compositions are calculated using Equation 4.11. The activity coefficient for each component i, is estimated using the Wilson equation (Coulson and Richardson (1993))

$$\ln \gamma_i = 1.0 - \ln \left[ \sum_{j=1}^{nc} (x_j \Lambda_{ij}) \right] - \sum_{k=1}^{nc} \left[ \frac{x_k \Lambda_{ki}}{\sum_{j=1}^{nc} x_j \Lambda_{kj}} \right] \quad 4.12$$

where  $\Lambda_{ij}, \Lambda_{ji}$  = Wilson coefficients for the binary pair  $i,j$  and

$nc$  = number of components

The pure component vapour pressure,  $P_i^\circ$  for each component  $i$ , is modelled by the Antoine equation (Coulson and Richardson (1993),

$$\ln P_i^\circ = A_i - \frac{B_i}{(T + 273) + C_i} \quad 4.13$$

which is solved iteratively on  $T$  (the bubble point temperature ( $^\circ\text{C}$ ) of the liquid mixture) for a value of  $P_n$  in Equation 4.11 that satisfies the condition

$$\sum_{i=1}^{NC} y_{n,i}^* = 1.0 \quad 4.14$$

on each tray,  $n$ . The form of Equation 4.13 and the coefficients used, result in pure component vapour pressures in mmHg but this is converted to atmospheres to ensure uniformity of units in the model. Wilson coefficients were used, from data published by Hirata et al (1975) and Antoine coefficients  $A$ ,  $B$  and  $C$  for Equation 4.13 were used, from data published Coulson and Richardson (1993). The data used is listed in Appendix C.

Because non-ideal tray simulation is being employed, a vapour phase Murphree tray efficiency is applied to the equilibrium vapour composition obtained. This Murphree efficiency is applied to each tray in the form

$$y_{n,i} = E_{MVn,i} y_{n,i}^* + (1 - E_{MVn,i}) y_{n-1,i} \quad 4.15$$

to obtain the actual composition of the vapour leaving the tray.

Tray efficiency is not applied to the still because the vapour leaving the still is assumed to be in equilibrium with its liquid contents,  $y_{B,i} = y_{B,i}^*$ . Substitution into Equation 4.15 (with  $y_{B-1,i} = 0$ ) therefore gives, for all components,

$$E_{MV,B} = 1.0 \quad 4.16$$

### 4.3.3 The Heat Input and Fluid Flow Rates.

The heat duty to the column is estimated using the measured steam flow rate to the still. The pressure of the condensing steam in the reboiler jacket is known and hence, so is its temperature and heat of vaporisation,  $\lambda_{st}$ . Assuming heat losses to the environment are negligible, the heat gained by the still contents is the heat lost by the condensing steam so that the vapour rate from the still to the column is given by

$$V = \frac{V_{st} \times \lambda_{st}}{\lambda_m} \quad 4.17$$

where  $V_{st}$  = steam flow rate (kmol/hr)

$\lambda$  = latent heat of vaporisation (kJ/kmol) and subscripts *st* and *m* refer to the steam and the still mixture respectively.

The reflux ratio is specified as either constant or variable. The variable reflux ratio option is chosen when the column is run under the fixed distillate composition policy. The reflux liquid rate is specified depending on the operating procedure chosen. For the constant reflux ratio operation, the liquid rate is calculated from the equation

$$L = V \times \frac{R}{R + 1} \quad 4.18$$

where  $R = \text{fixed reflux ratio value}$

and the distillate flow rate,  $D$  is obtained from Equation 4.5. When the column is set to total reflux in order to achieve steady state,  $D=0$ , thus making the liquid rate equal to the vapour rate (i.e.  $L = V$ ).

In the simulation of the constant distillate composition operation (variable reflux ratio), the distillate rate is again given by Equation 4.5, while liquid rate is specified such that it varies to keep the distillate composition constant. This could be achieved in simulation by controlling distillate composition using a PID control algorithm with the reflux ratio as the manipulated variable. Here however, a more direct approach of actually estimating the liquid split of the condensed vapour that gives the desired distillate composition at the top of the column is employed.

Keeping the distillate composition constant involves keeping the composition of the vapour leaving the top tray of the column,  $y_{NT}$  constant. This in turn requires top tray liquid composition,  $x_{NT}$  to remain constant. Substituting Equation 4.7 into Equation 4.3 gives the equation for the rate of change of top tray composition as

$$\frac{dx_{NT}}{dt} = \frac{V(y_{NT-1} - y_{NT}) + L(x_D - x_{NT})}{H_{NT} + x_{NT}v_{NT}(\rho_1 - \rho_2)} \quad 4.19$$

Equations 4.7 and the denominator of Equation 4.19 are only valid for binary mixtures but can be extended to include multicomponent mixtures. None the less, a constant composition on the top tray is the aim and Equation 4.19 is therefore equated to zero resulting in an equation for reflux liquid flow rate of the form

$$L = \frac{V (y_{NT} - y_{NT-1})}{x_D - x_{NT}} \quad 4.20$$

Equation 4.5 is then used to obtain the distillate flow rate and the reflux ratio is calculated as the ratio of reflux rate to distillate rate

$$R = L / D \quad 4.21$$

In the methanol water system for example, the density increases and the average molecular weight decreases as the methanol composition is depleted. Since the molar latent heats of both chemicals are about equal, the constant heat input results in a consistently decreasing volumetric flow of liquid condensate at the top of the column as the batch proceeds. Therefore if the distillate draw is held constant, the liquid reflux ratio falls. This gives a decreasing reflux ratio. This is why for the fixed reflux ratio policy operation, liquid rates are calculated based on the value of the chosen reflux ratio as shown in Equation 4.18, rather than deriving an expression similar to Equation 4.20.

#### 4.3.4 Variable Tray Efficiency

Variable tray efficiency simulation constitutes a major part of the novelty of this model. The simulation can be run either with a single value tray efficiency for all the trays (Overall Column Efficiency Model) or a constant but different value for each tray (Constant Efficiency Model). It may also be run such that the tray efficiency varies with time, according to the mixture composition on the tray, thus giving the Variable Efficiency Model.

The concentration-efficiency relationship is determined experimentally by plotting the Murphree tray efficiencies obtained from sample composition readings against the liquid (sample) composition on that tray. Data at low methanol concentrations is sparse and so, the concentration-efficiency data is

input into the simulation in a tabular manner, permitting linear interpolation for the deduction of the Murphree tray efficiencies for any liquid concentration.

#### 4.4 SIMULATION USING THE MODEL

A flowchart of the program algorithm is given in Figure 4. 2. The model input data includes total number of moles and the component mole fractions of the feed charged to the column. Component names and physical properties (density, heats of vaporisation, molecular weight), number of trays in the column, operating conditions (constant or variable reflux ratio), steam flow rate. are also input data. Furthermore, the equation of the curve describing the relationship between the mixture composition and the vapour phase Murphree tray efficiency (or its tabular form) constitutes a part of the input data.

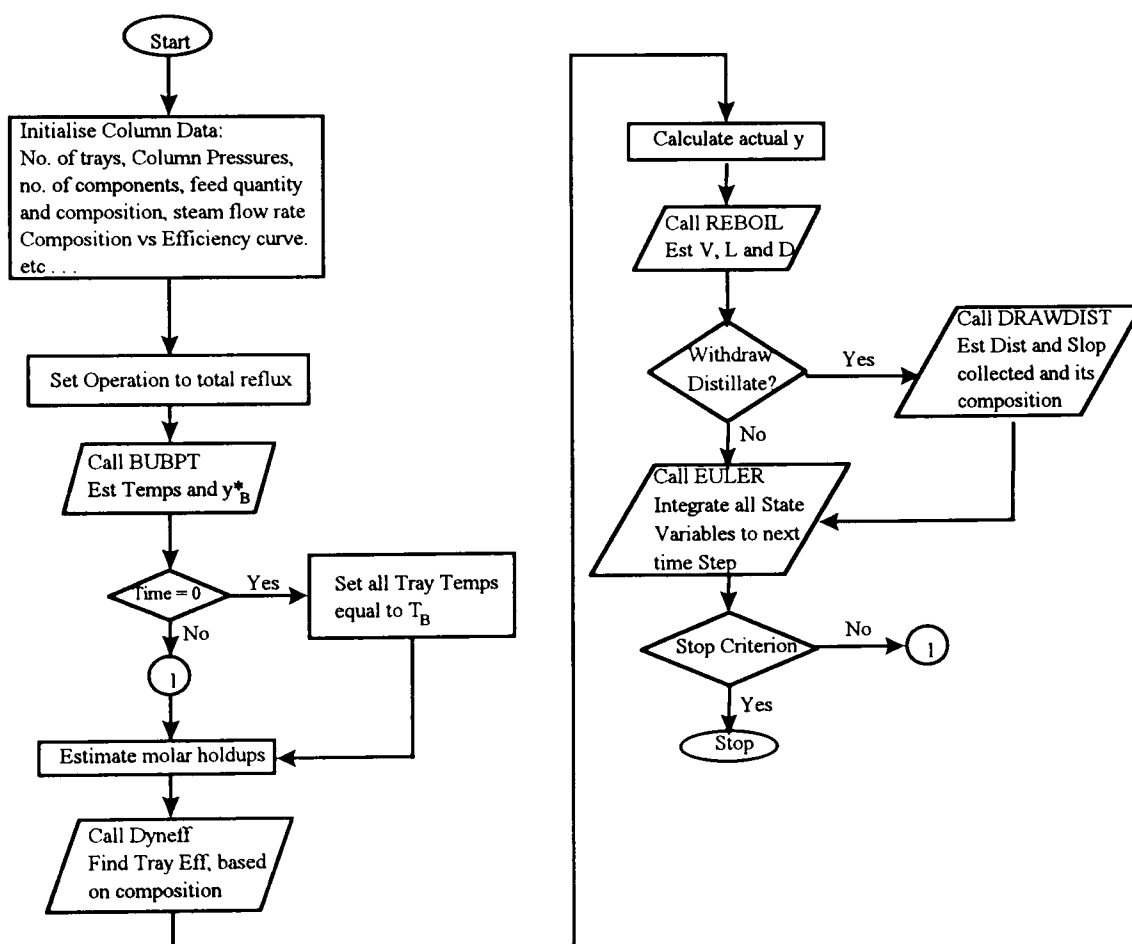


Figure 4. 2: Flowchart of Program Algorithm

This information is used to run the simulation to produce results for a constant or variable efficiency system, depending on which model option is chosen. All the derivatives are evaluated at the current values of all the variables before integrating any of the equations. All the simulation results are printed to file at 0.01 hour intervals from which they can be retrieved and analysed.

The simulation starts with a bubble point temperature estimation of the feed charged to the still, and the entire column is then assumed to contain the same mixture composition at the same temperature. The actual amount of the feed in the still at startup is assumed to be equal to the total amount charged, less the amount required to establish the holdup on all the trays and the reflux receiver. The rate of steam flow gives the vapour boilup rate and the simulation is run at total reflux by setting  $D=0$ , until steady state is achieved. Steady state is achieved when the tray, still and reflux receiver compositions, estimated for five consecutive integration time steps, are constant.

Distillate withdrawal is begun either at a prescribed time (for constant reflux ratio operation) after steady state has been reached or when the overhead composition reaches the specified value (for the variable reflux operation). This means that steady state may not be achieved during the variable reflux operation. The amount and average composition (calculated as an integral of the distillate collected in the given time (Equation 4.10)) of distillate withdrawn, either as product or slop cut, is calculated until product withdrawal is stopped (column is returned to total reflux) or the defined stop criterion is reached. The stop criterion could be the elapsed batch time, still completely empty or the composition threshold on distillate or still contents is reached.

#### **4.5 LIMITATIONS OF THE MODEL**

The major limitations of the model arise from the assumptions made during its development, most of which have been addressed in the previous sections. This

model assumes complete mixing on the tray because of the small column diameter modelled. It can not therefore, necessarily be used to simulate a large industrial column without the possible introduction of errors, albeit minor in some cases unless complete mixing can also be assumed on the tray. Tray hydraulics correlations will have to be taken into account when applying this model to a large column where perfect mixing can not be assumed.

The model cannot be used with systems where pressure effects on the tray are significant. As a result, the model will need to be extended for use in startup and shutdown simulations, which involves a large range of operating pressures and different holdup characteristics, including starting from dry trays. It cannot also be used for zero tray holdup simulations, as this would cause the program to crash. A zero tray holdup simulation can be approximated by using a very small value of volume holdup.

The model is also subject to the limitations of the integration method used, the Euler method. Care must be taken in selecting an integration time step size as accuracy is sacrificed for speed when large step sizes are used and the system also becomes unstable for large step sizes. Systems with fast dynamics require a small time step size and vice versa. Other numerical integration methods such as the 4<sup>th</sup> order Runge-Kutta method can be used when accuracy is of great importance. The modular nature of the program (in Appendix B) allows easy substitution of the integration subroutine.

In the following chapters, the results obtained from the use of this model in constant and variable efficiency simulations are presented, discussed and compared with experimental data.

## **CHAPTER FIVE.**

### **THE CONSTANT EFFICIENCY MODEL**

The Constant Efficiency Model as defined in this work, is taken to mean the model which permits the use of different Murphree tray efficiency on each tray within the column but these efficiency values remain constant for each run.

Before the methanol/water experimental runs used to verify the simulations of the Constant Efficiency Model, the column integrity was tested using a water charge to the still. The results of the water test runs are presented in Appendix A and they verify the assumption of negligible heat losses from the column made during the development of the model. Appendix A also contains results of the initial methanol/water mixture experimental runs, which were used to verify the model using a fixed column efficiency value (overall column efficiency).

The results from experimental runs and from simulation using the Constant Efficiency Model are presented in this chapter for different feed compositions and operating conditions for the distillation of a methanol/water mixture. Results of steady state temperature and composition profiles as well as temperature and composition movements during transient periods are presented and analysed.

#### **5.1 METHANOL/WATER MIXTURE DISTILLATION**

##### **5.1.1 Runs 1 and 2**

The initial test runs presented in Appendix A show a good agreement between experimental and simulation temperatures and compositions but only three

sample points were used to verify composition results. This is obviously not sufficient to base any conclusions upon, if entire column profiles are to be compared so the sample points on all the other trays were unblocked to permit sampling throughout the column. Two separate runs were then carried out at total reflux to compare steady state profiles obtained experimentally with that from the Constant Efficiency Model simulation.

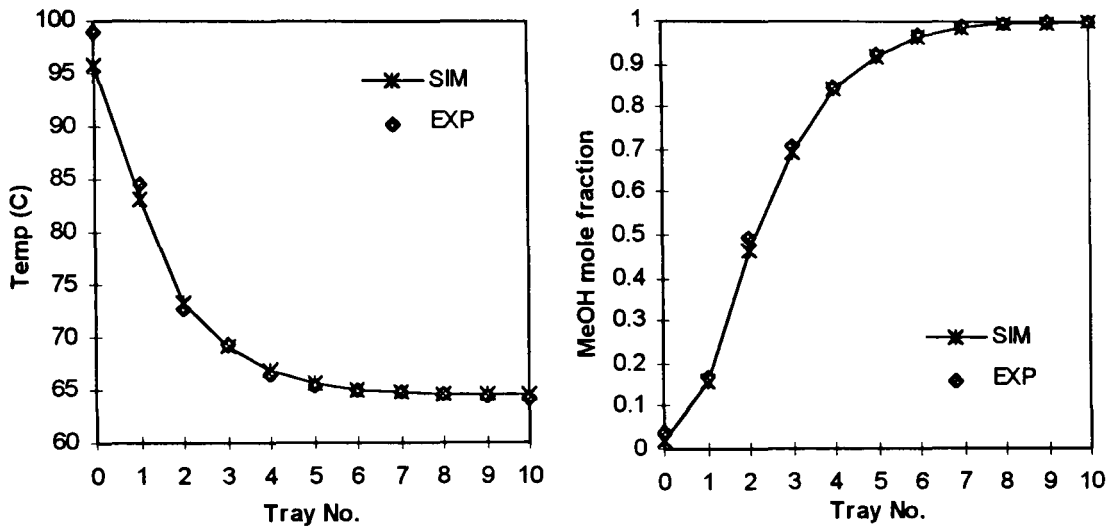
Run 1 used a 1.54 kmol charge of 0.0639 methanol mole fraction concentration, and Run 2 used a 1.58 kmol charge of 0.0452 methanol mole fraction concentration. The steady state profiles obtained experimentally are compared with the corresponding simulation results in Figure 5.1a for Run 1 and in Figure 5.1b for Run 2. Efficiency values used in the simulation for the results in Figure 5.1 were estimated experimentally. Liquid samples only were collected but the column was run at steady state on total reflux therefore, the operating line lies along the  $y = x$  line on an  $x$ - $y$  diagram (McCabe-Thiele plot). Therefore, on any tray  $n$ ,

$$y_{n,i} = x_{n+1,i} \quad 5.1$$

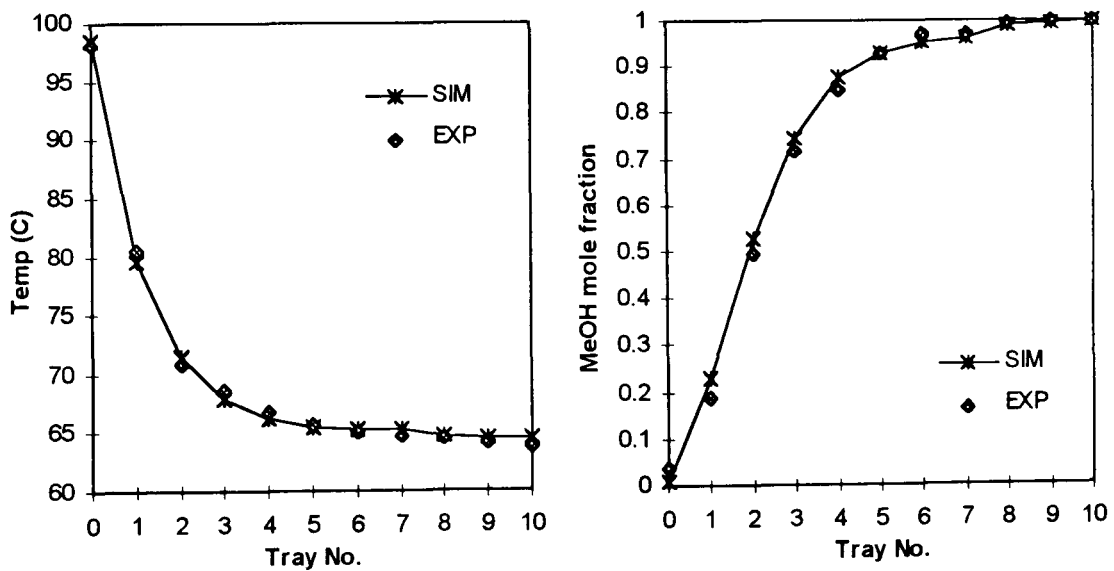
This is substituted into the expression for Murphree tray efficiency given in Equation 2.3, resulting in the equation

$$E_{MVn,i} = \frac{y_{n,i}^* - x_{n,i}}{x_{n+1,i} - x_{n,i}} \quad 5.2$$

which gives the vapour phase efficiencies for the trays. The still is assumed to be an equilibrium stage so, a tray efficiency of 1.0 is always used for the still. The values of tray efficiency obtained for the methanol are given in Table 5.1. These are the values used in the simulation which gives an even better match between experimental and simulation results than was observed when a single overall column efficiency value was used.



a) Steady State Profile for Run 1 After Total Reflux Startup



b) Steady State Profile for Run 2 After Total Reflux Startup

**Figure 5.1:** Steady State Temperature and Composition Profiles for Run 1 and Run 2

**Table 5.1: Murphree Tray Efficiencies for Methanol in Run 1 and Run2**

	Run 1 Efficiency (%)	Run 2 Efficiency (%)
Still	1.000	1.000
Tray 1	0.726	0.875
Tray 2	0.858	0.805
Tray 3	0.744	0.768
Tray 4	0.832	0.824
Tray 5	0.865	0.900
Tray 6	0.969	0.947
Tray 7	0.985	0.722
Tray 8	1.081	0.999
Tray 9	1.050	1.048
Tray 10	0.980	0.891

### 5.1.2 Run 3

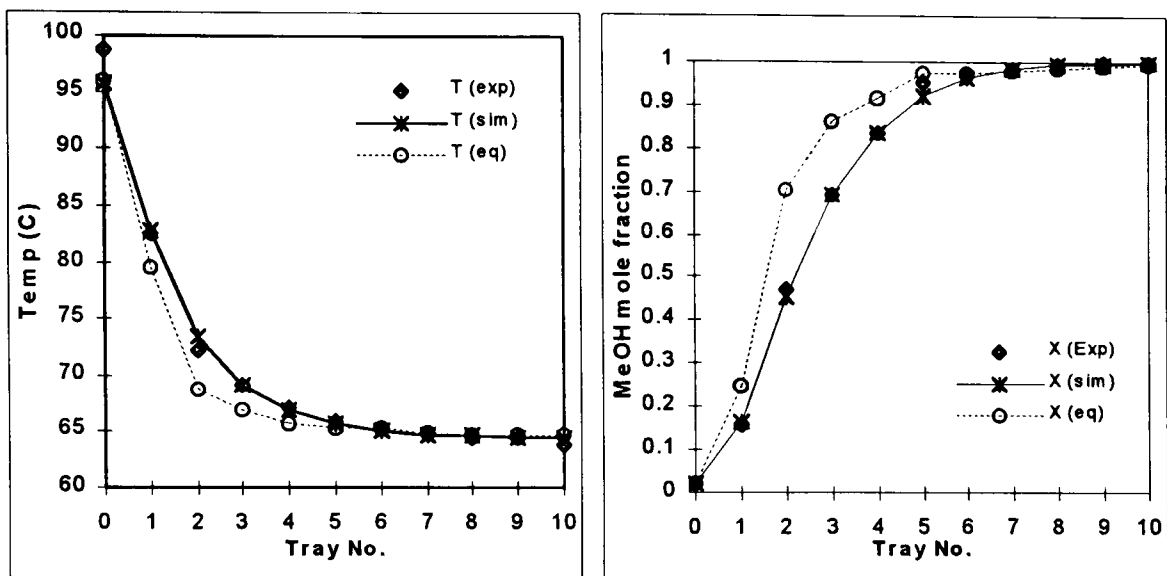
Up to this point, only steady state profiles have been used in the model verification process. Further experimental runs were therefore designed to include the investigation of the dynamic behaviour of the column and comparing with simulation results. Tray temperatures were recorded in the transient period during product withdrawal and compared to the results obtained from the simulation when it is set to run under the same conditions and specifications as the column. For Run 3, the charge was a 1.54 kmol methanol/water feed of 0.0639 methanol mole fraction concentration. Tray efficiencies used in simulating this run were estimated using Equation 5.2, with experimental data from samples collected when the column is at steady state. The tray efficiencies used for this run is given in Table 5.2 and the steady state

profiles in Figure 5.2. The profiles are also compared with the profile obtained, assuming the trays were equilibrium stages - i.e. tray efficiency of 1.0 (subscript “eq” in Figure 5.2). As in the previous runs, the column was run at total reflux until steady state was achieved and then set to partial offtake at a reflux ratio of 8:1 for 20 minutes, then returned to total reflux and allowed to reach a new steady state. Figure 5.2b indicates a temperature reading on tray 3 which can be considered spurious as it is in contrast with the measured composition of the liquid sample obtained from that tray.

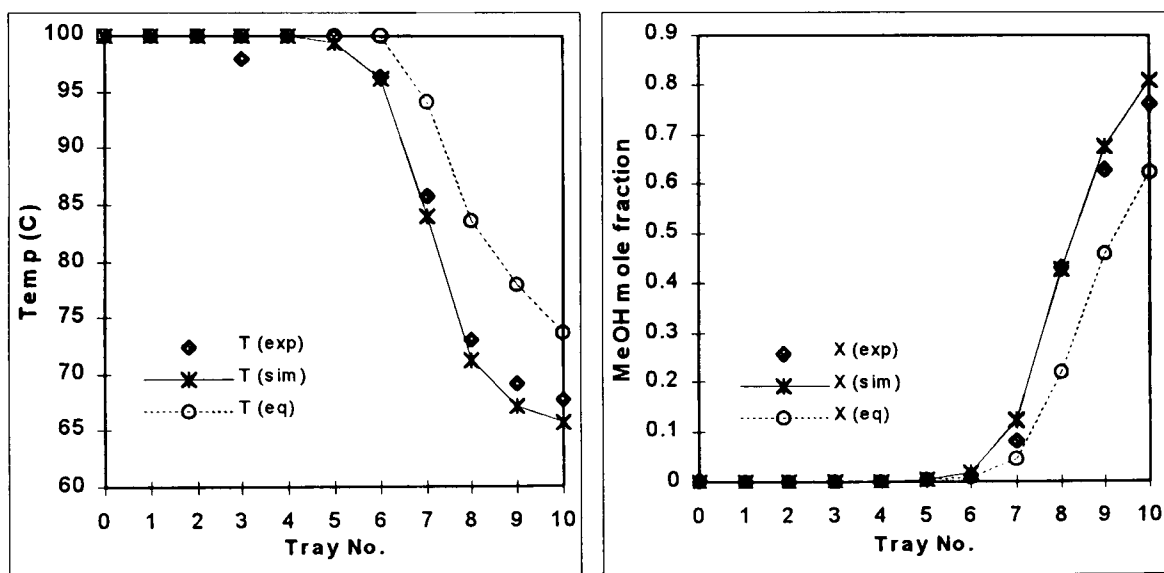
**Table 5.2: Murphree Tray Efficiency Values for Run 3**

Location	Run 3 Efficiency (%)
Still	1.000
Tray 1	0.826
Tray 2	0.755
Tray 3	0.811
Tray 4	0.896
Tray 5	0.935
Tray 6	0.979
Tray 7	1.138
Tray 8	1.036
Tray 9	0.980
Tray 10	0.980

Due to limitations on the ancillary devices, only 4 temperature measurements are logged directly to the computer. These are the temperatures measured by the thermocouples located on trays 2, 3, 4 and 5. They are compared with the equivalent temperatures predicted by the Constant Efficiency Model in the transient process in Figure 5.3

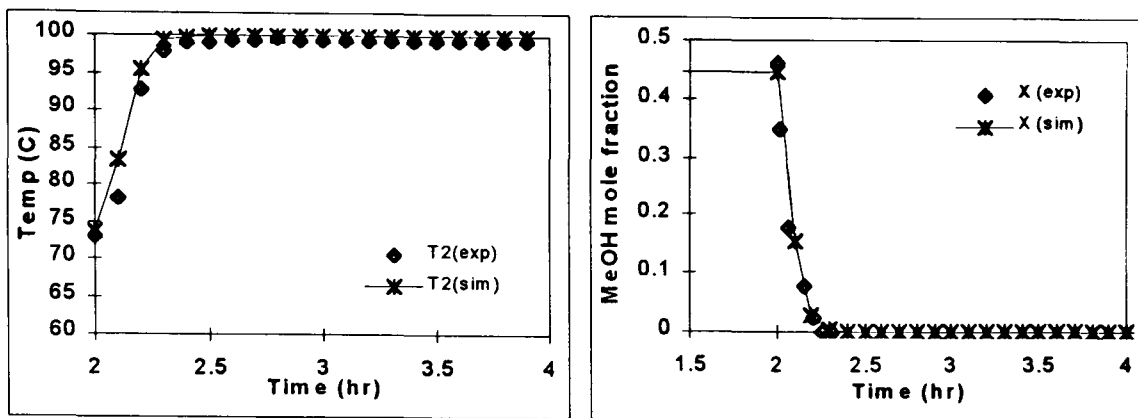


a) Initial Steady State Profile of The Column After Startup

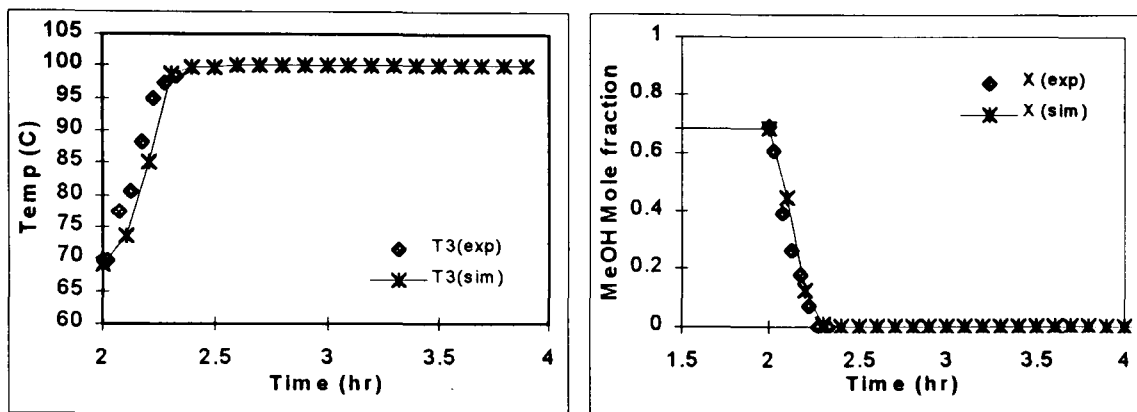


b) Final Steady State Profile of Column After Distillate Withdrawal.

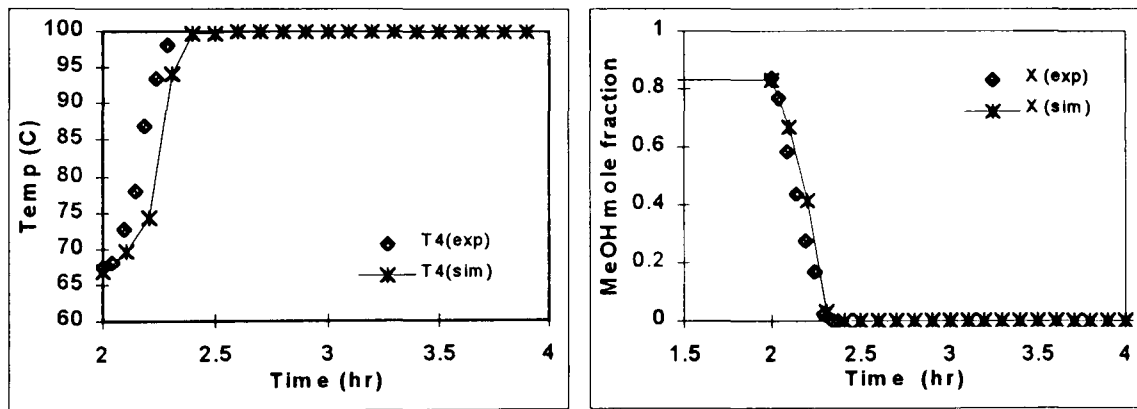
**Figure 5.2:** Column Steady State Profiles for Run 3 after Initial Total Reflux Startup and after Timed Product Withdrawal.



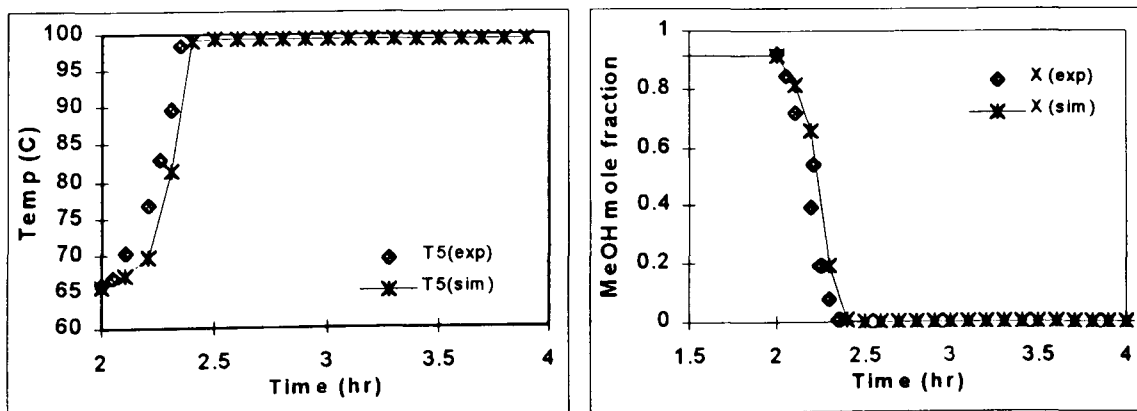
a) Tray 2 Temperature and Composition Profile



b) Tray 3 Temperature and Composition Profile



c) Tray 4 Temperature and Composition Profile



d) Tray 5 Temperature and Composition Profile

Figure 5.3: Temperature and Composition Movements in the Column during Product Withdrawal for Run 3

The temperature in the column from trays 2 to 5 were monitored for their transient behaviour because previous runs show that the largest movement in concentration between steady states, occurred in this section (see Figure 5.2) for the feed compositions employed. The methanol concentrations on these trays were seen to swing from a very high to a very low value in the process of a single batch run. If the column is run at partial offtake until the entire methanol in the feed mixture is withdrawn, any concentration swings observed in the lower section of the column will traverse the entire column in the course of the distillation. In such a case, the choice of trays to monitor in the transient period would not arise as the temperature and composition movements would occur on all the trays, albeit at different times.

The graphs shown in Figure 5.3 indicate that the model is able to track, very closely, the transient behaviour of the column as well as its steady state profiles.

### 5.1.3 Run 4

For an even better observation of the transient behaviour of the column, it was decided to run the column with an even lower methanol concentration feed. The methanol mole fraction of the charge for Run 4 was 0.01 and the batch size was 1.375 kmols. During distillate withdrawal, a slower transient was also desired so the reflux ratio is set to a higher value of 18:1. Practically, this does not make any thermodynamic sense as returning a large portion of the condensed vapours to the column is a waste of the separation energy but this is carried out strictly for model verification purposes.

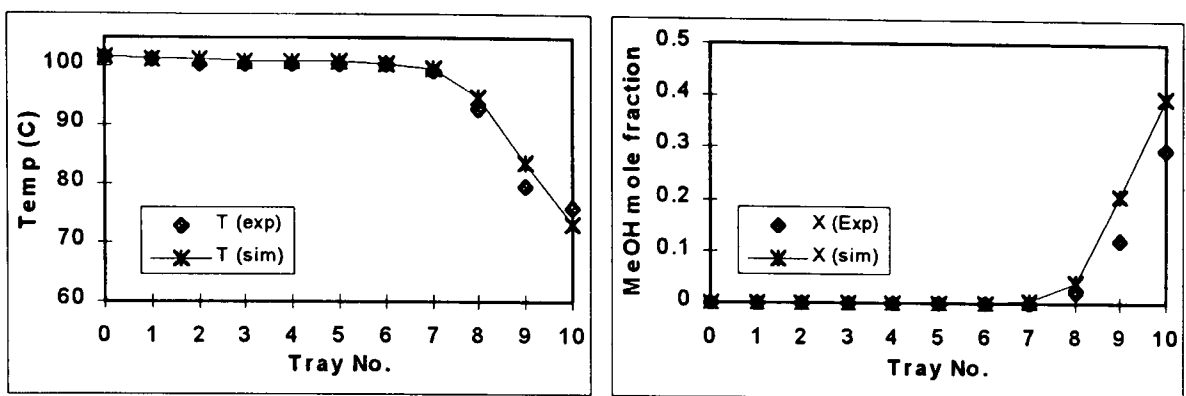
The column was run at this reflux ratio for 28 minutes and then returned to total reflux and allowed to reach a new steady state. Using liquid samples collected at steady state, the tray efficiency values used in the simulation runs

were calculated using Equation 5.2. With the lower methanol concentration in the feed, it is expected that the methanol will accumulate towards the top of the column at steady state. This is evident from the steady state temperature profile shown in Figure 5.4a. Consequently, trays 7,8,9 and 10 transient temperatures are recorded and compared with the simulation results.

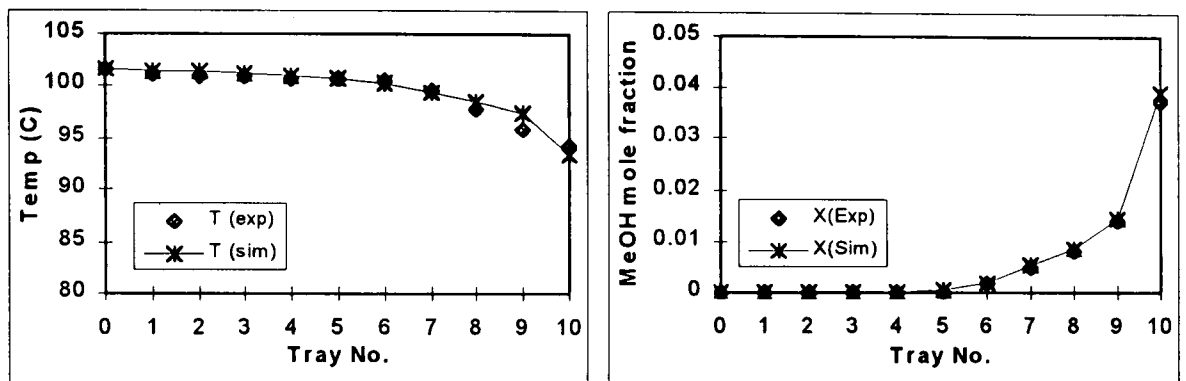
The quantity and concentration of the product taken off during the distillate withdrawal stage of Run 4 is shown in Table 5.3 for the experiment and simulation.

**Table 5.3:** Product Withdrawn From The Column For Run 4

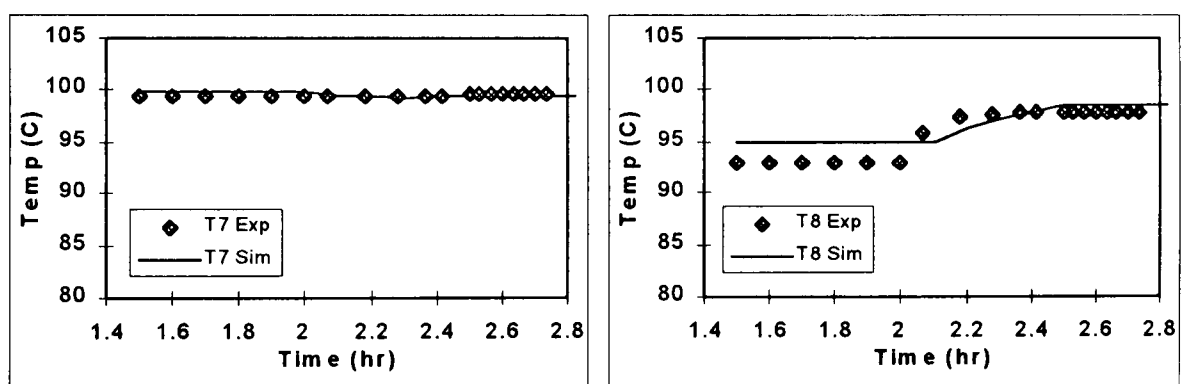
	<b>Product Withdrawn (kmols)</b>	<b>Methanol Conc. (mole fraction)</b>
<b>Experiment</b>	0.02760	0.5244
<b>Simulation</b>	0.02759	0.4476



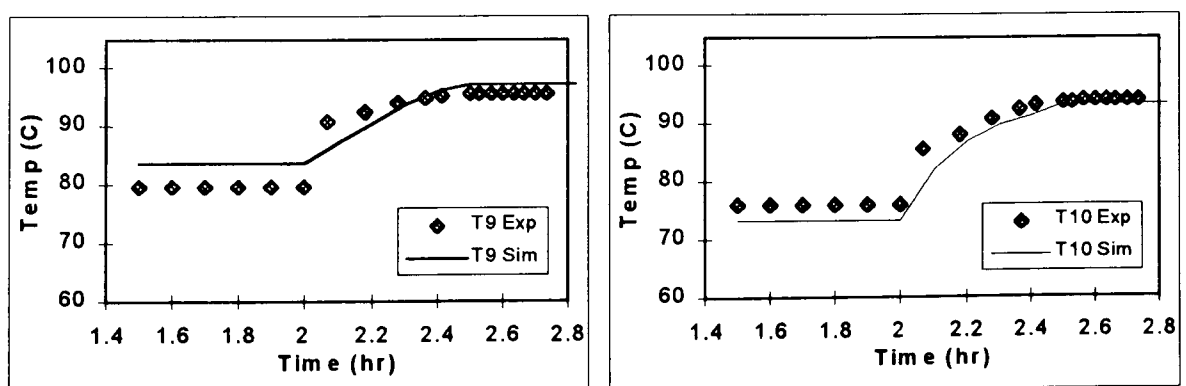
a) Column Initial Steady State Profiles



b) Column Final Steady State Profiles



c) Trays 7 and 8 Transient Temperature Profiles



d) Trays 9 and 10 Transient Temperature Profiles

**Figure 5.4:** Column Steady State Profiles and Temperature Movements during Product Withdrawal for Run 4.

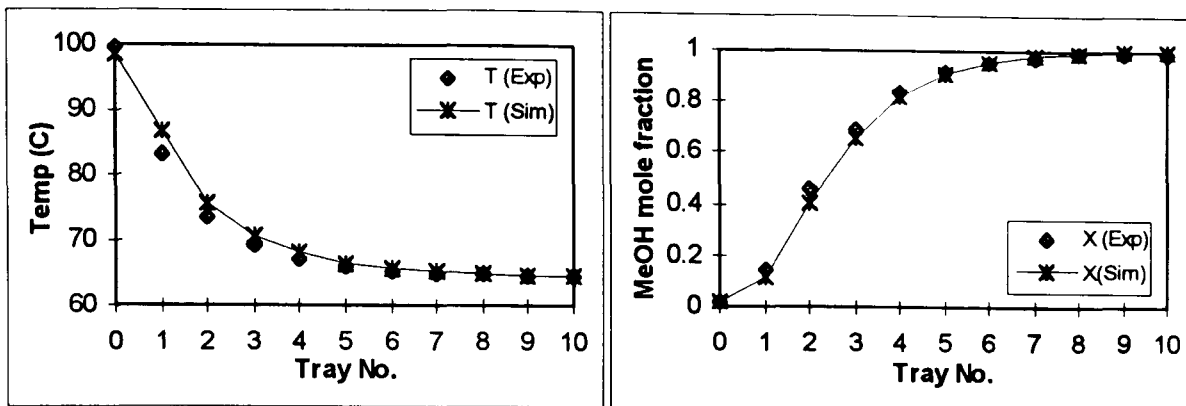
#### 5.1.4 Runs 5, 6 and 7

Three further runs were carried out with different feed charges and for decreasing methanol composition in the feed charge (Runs 5, 6 and 7). The column feeds used for all the runs are summarised in Table 5.4. In each run, the column was run at total reflux until steady state was achieved and then set to partial offtake. During Run 5, product was withdrawn for 31 minutes at a reflux ratio of 6.9 and returned to total reflux until a new steady state was attained. Tray temperature movements were monitored between the steady states on trays 3 to 6. The steady state and transient profiles thus obtained experimentally and from the simulation are presented in Figure 5.5.

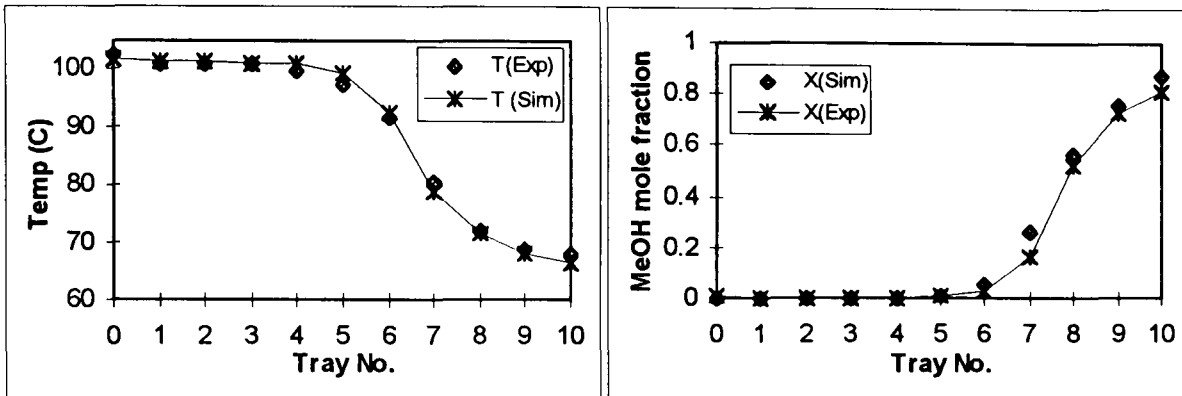
For Runs 6 and 7, product was withdrawn for 25 minutes during both runs but at a reflux ratio of 4.5 and 5.6 respectively. Temperature movements were also monitored between the steady states on the relevant trays where temperature swings indicated a composition movement from almost pure methanol to almost pure water during the run. The experimental results are compared with simulation results in Figure 5.6 and Figure 5.7.

**Table 5.4:** Size and Concentration of Charge for Rig Runs.

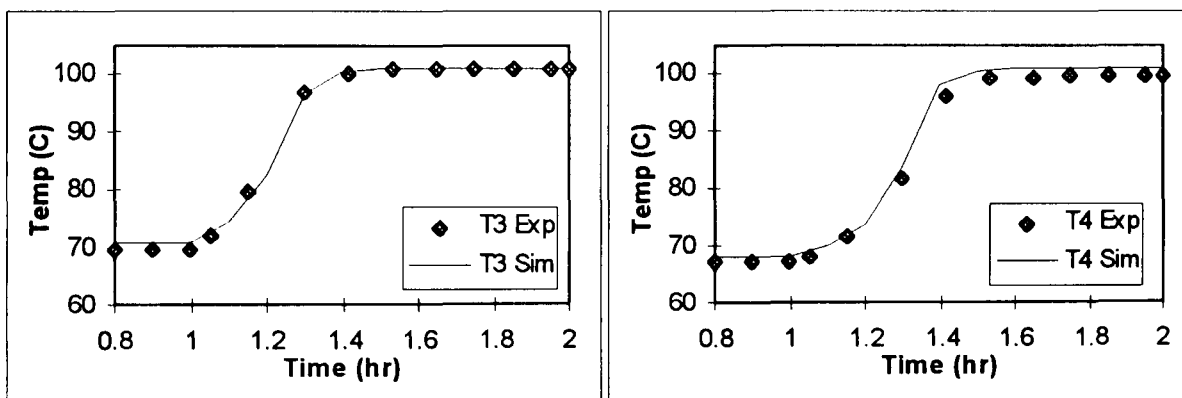
	<b>Column Feed (kmols)</b>	<b>Methanol Conc. (mole fraction)</b>
<b>Run 5</b>	1.148	0.1079
<b>Run 6</b>	1.168	0.0925
<b>Run 7</b>	1.206	0.0660



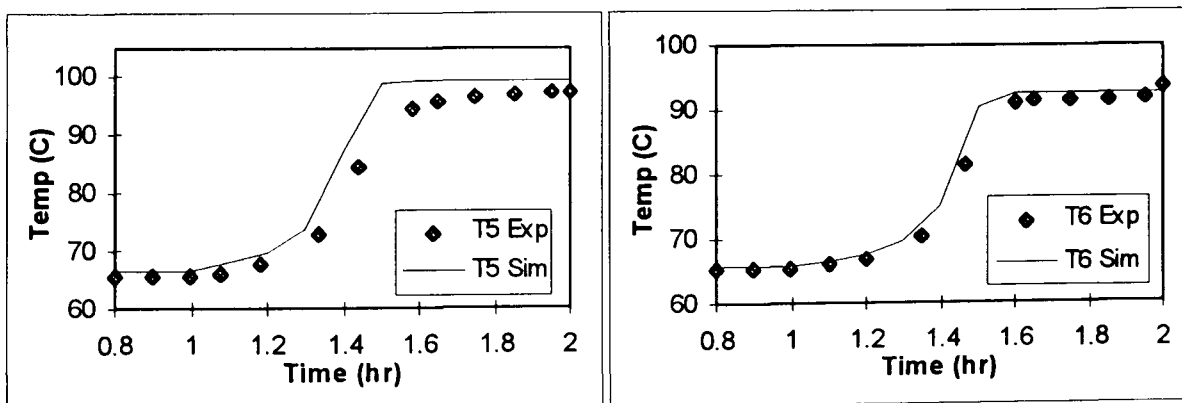
a) Column Initial Steady State Profiles



b) Column Final Steady State Profiles

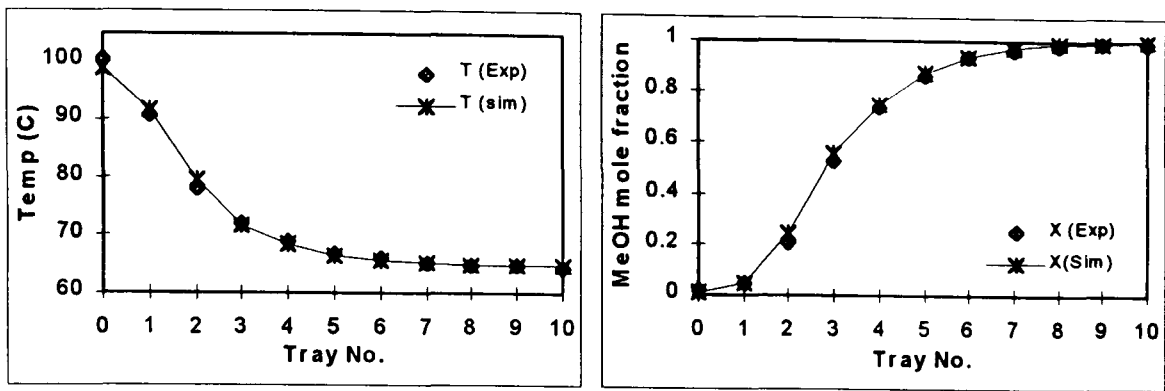


c) Trays 3 and 4 Transient Temperature Profiles

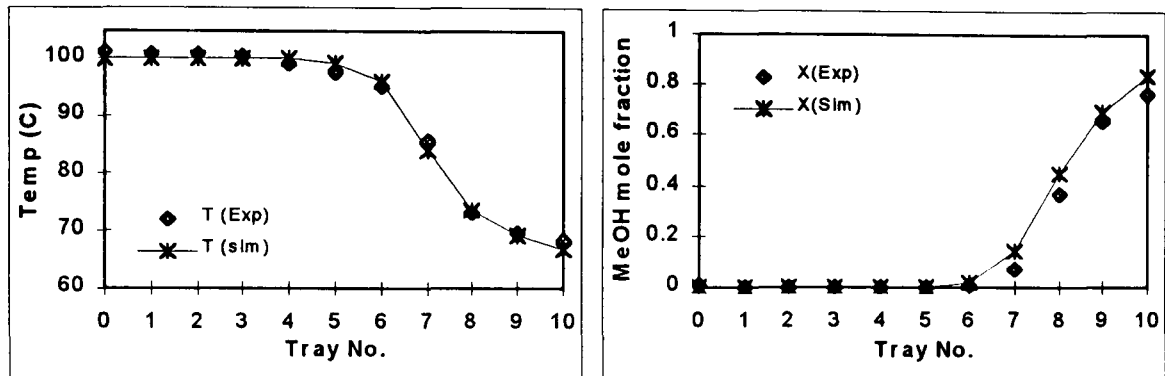


d) Trays 5 and 6 Transient Temperature Profiles

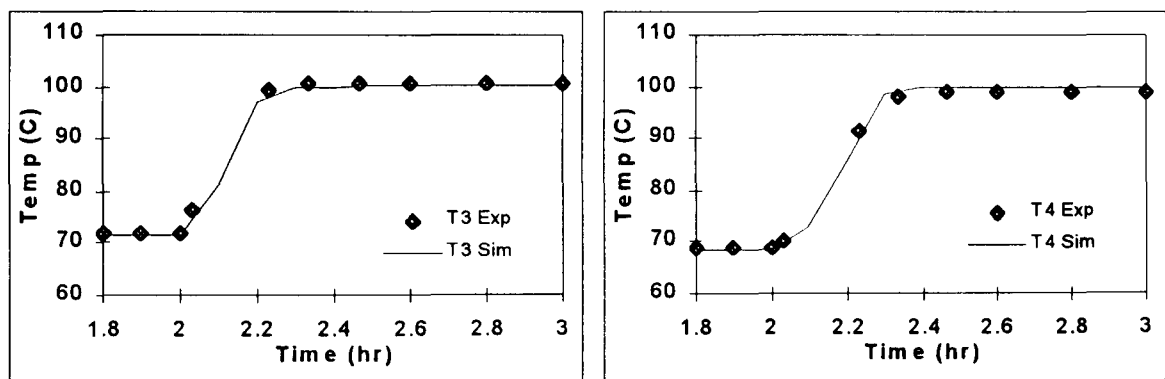
Figure 5.5: Column Steady State Profiles and Temperature Movements during Product Withdrawal for Run 5



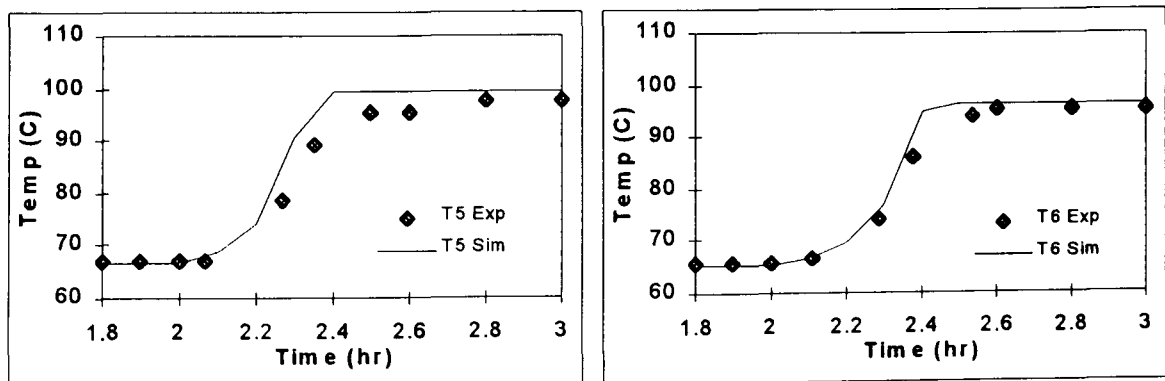
a) Column Initial Steady State Profiles



b) Column Final Steady State Profiles

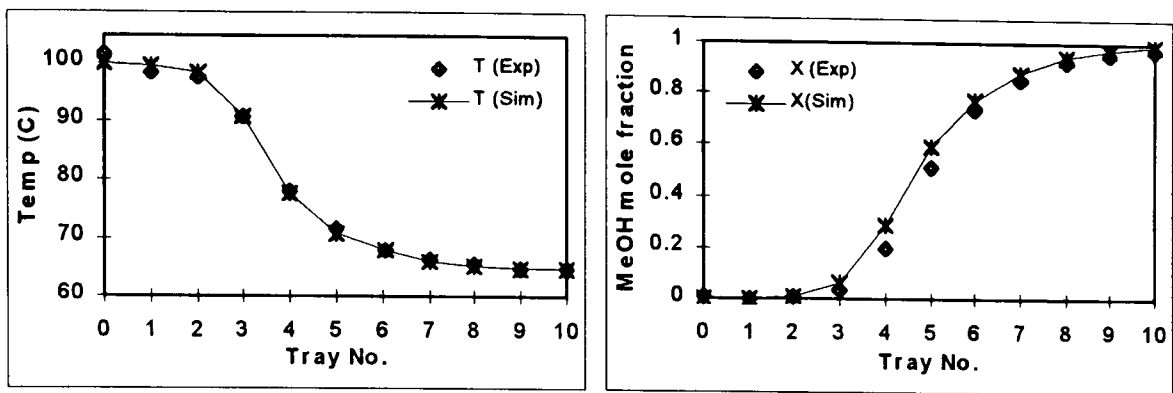


c) Trays 3 and 4 Transient Temperature Profiles

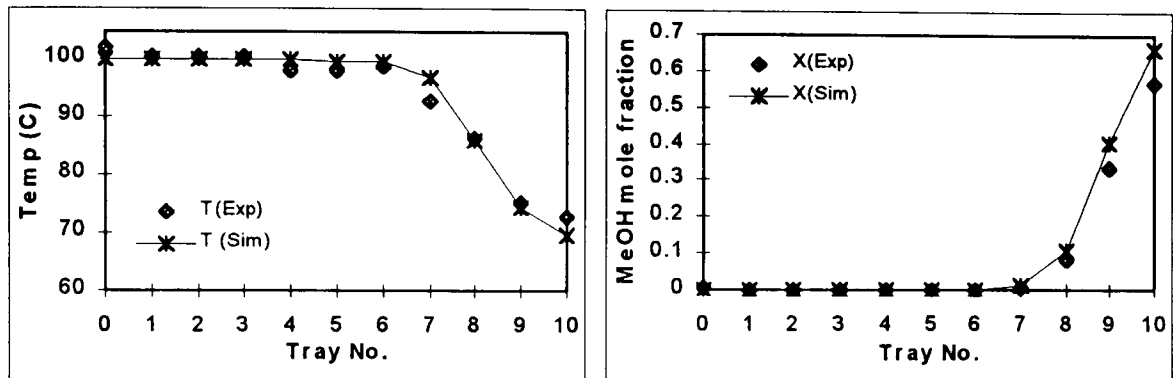


d) Trays 5 and 6 Transient Temperature Profiles

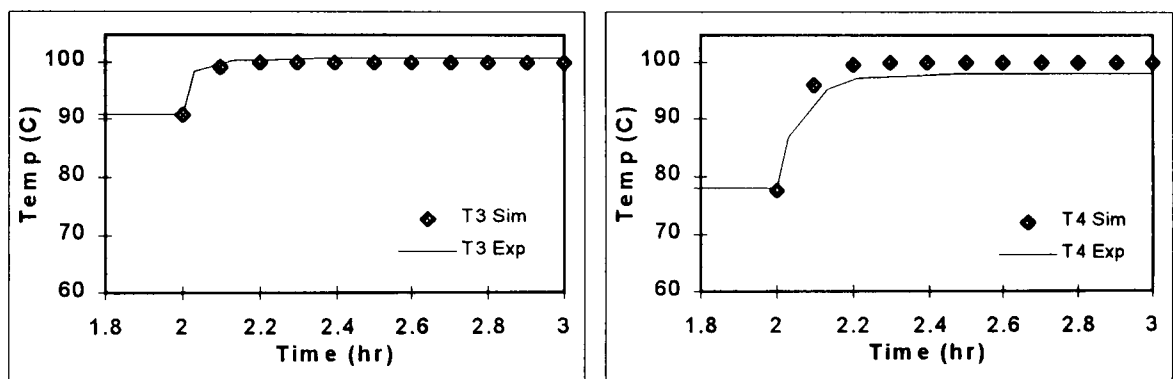
**Figure 5.6:** Column Steady State Profiles and Temperature Movements during Product Withdrawal for Run 6



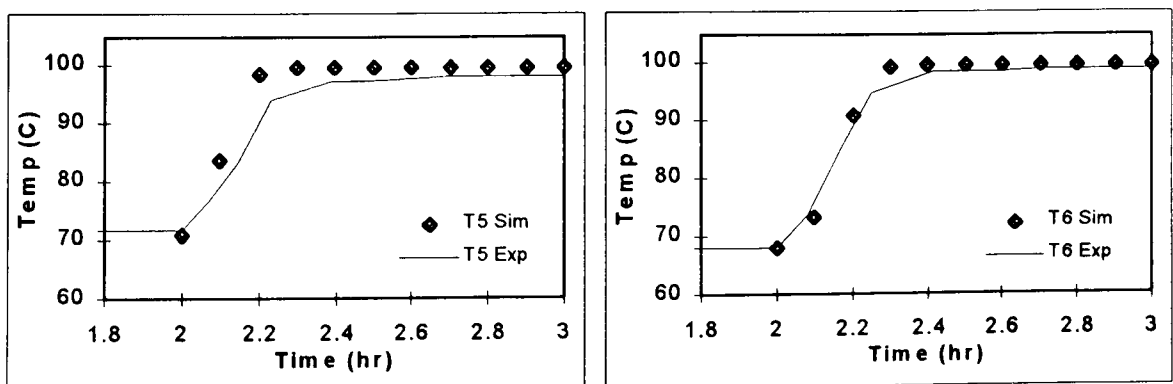
a) Column Initial Steady State Profiles



b) Column Final Steady State Profiles



c) Trays 3 and 4 Transient Temperature Profiles



d) Trays 5 and 6 Transient Temperature Profiles

**Figure 5.7:** Column Steady State Profiles and Temperature Movements during Product Withdrawal for Run 7

The steady state and transient profiles predicted by the Constant Efficiency Model have been compared with the experimental results in Figure 5.5 to Figure 5.7 for different feed charges and boilup rates. In all the cases considered, the initial and final steady state profiles predicted by the Constant Efficiency Model after the initial total reflux and after product withdrawal gave a very good agreement with the experimental profiles. Similarly, the transient temperature trajectories, predicted by the model on the relevant trays where large composition swings are observed during distillate withdrawal, match the experimental trajectories.

These observations, in conjunction with the results of Figure 5.2 to Figure 5.4, verify the ability of the Constant Efficiency Model to accurately simulate the batch distillation of a methanol-water mixture. The superiority of the Constant Efficiency Model predictions to the Overall Column Efficiency Model predictions is demonstrated in Appendix A.

## 5.2 MODEL VERIFICATION USING OTHER FEED MIXTURES

Any accurate process model must be able to handle a variety of mixtures under different operating conditions. Because only a methanol-water mixture was used in the experiments described in Section 5.1.1 to 5.1.4 to verify the model predictions, experimental results reported by Dribika (1986) and Domench et al (1974) are now simulated and the simulation results obtained are compared with their reported experimental results.

They report results obtained from the batch distillation of different quantities of other feed mixtures at different operating conditions and number of stages. Dribika (1986) distilled a ternary mixture in a batch column at total reflux and obtained composition data at steady state. Domench et al (1974) on the other hand, distilled a non-ideal binary mixture (as compared with the almost-ideal

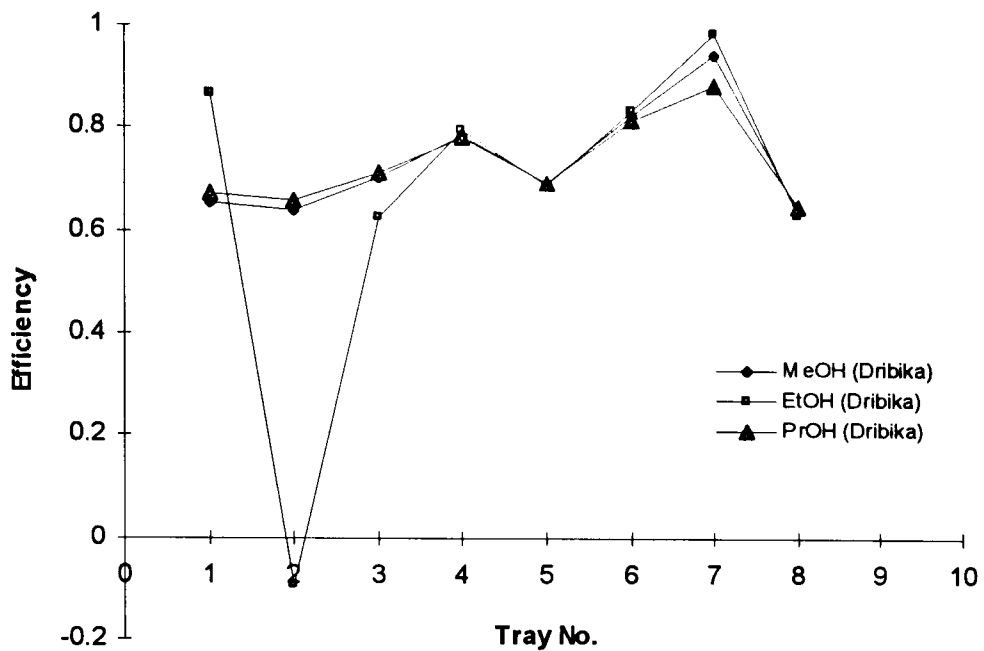
methanol/water mixture) and also ran their column at partial offtake for distillate withdrawal.

### 5.2.1 Simulating the Experimental Work of Dribika (1986)

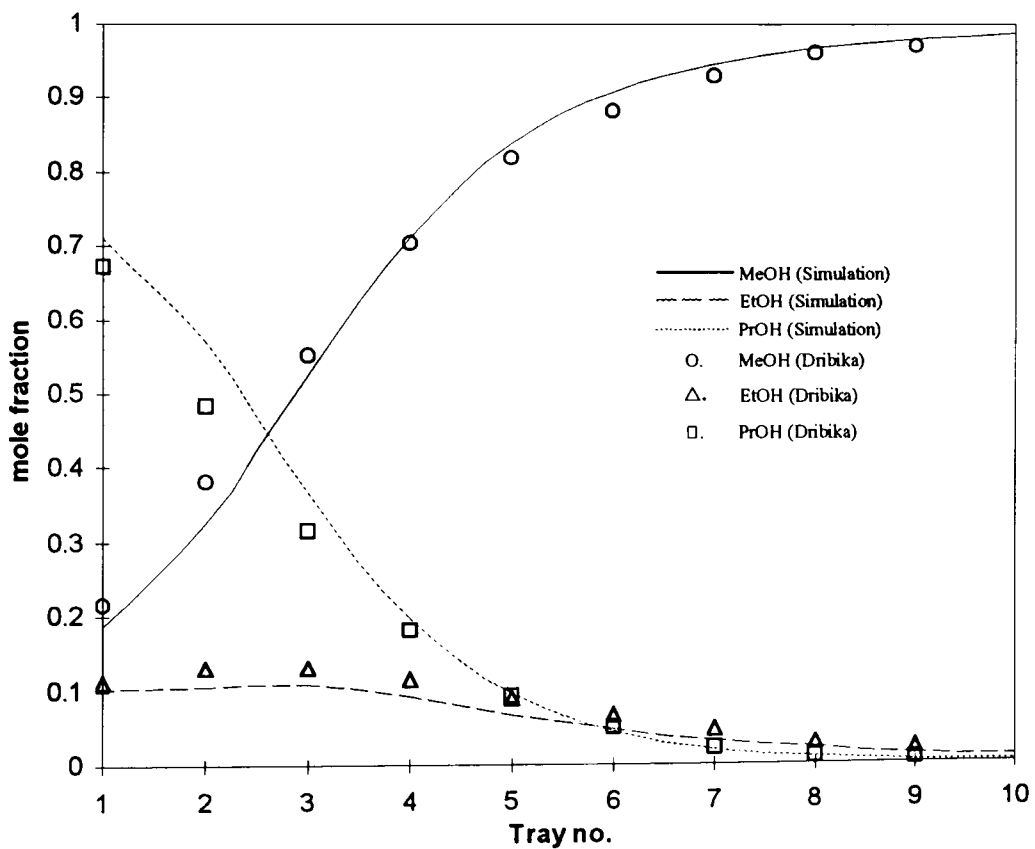
Dribika's data was based on the distillation of a ternary mixture of methanol/ethanol/propanol in a 10-tray batch distillation column. He ran the column at total reflux with different charge compositions, until steady state was achieved and collected liquid samples from each tray. This data was used to obtain Murphree efficiency values for the trays, which is now used in the Constant Efficiency Model to simulate the experimental work reported by Dribika (1986). The feed and operating conditions used by Dribika are presented in Table 5.5. No tray efficiencies were reported for trays 9 and 10 so, for simulation purposes, a tray efficiency of 1.0 was assumed for these trays. In Figure 5.8 to Figure 5.10, the tray efficiencies for each component reported by Dribika are presented and Dribika's experimental results are compared with the steady state composition profiles predicted by the Constant Efficiency Model for the examples chosen.

**Table 5.5:** Sample Experimental Run Details From Dribika (1986)

Example	Vol. of Charge (litres)	Charge Concentration			F-factor
		Methanol	Ethanol	Propanol	
Drib -1	25.0	0.08	0.07	0.85	0.2
Drib -2	25.0	0.0095	0.0950	0.8955	0.2
Drib -3	25.0	0.0013	0.1100	0.8887	0.2

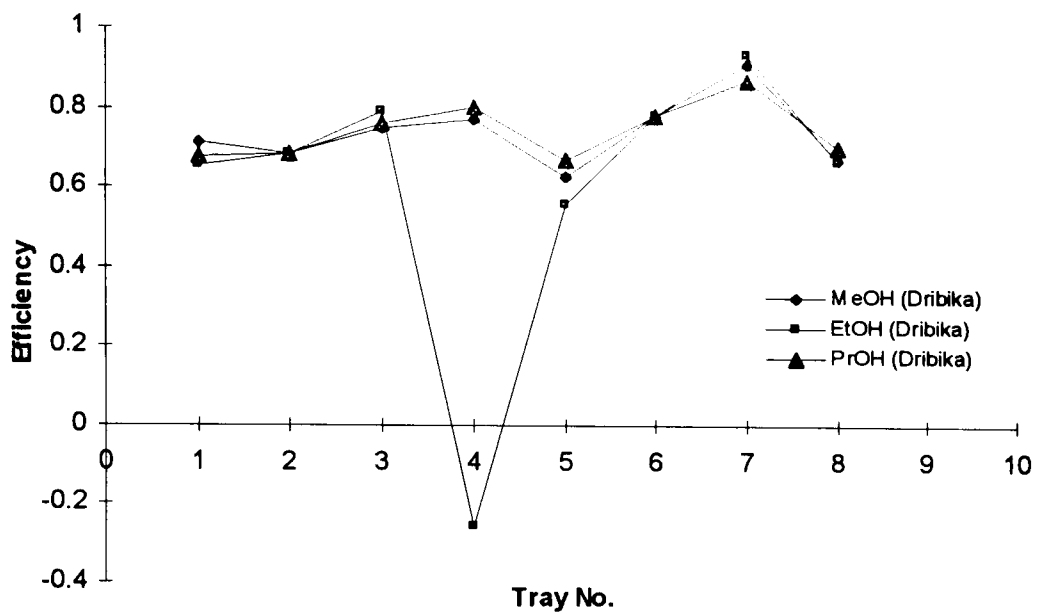


a) Tray Efficiencies for Methanol, Ethanol and Propanol in a Ternary Batch Distillation (Dribika (1986))

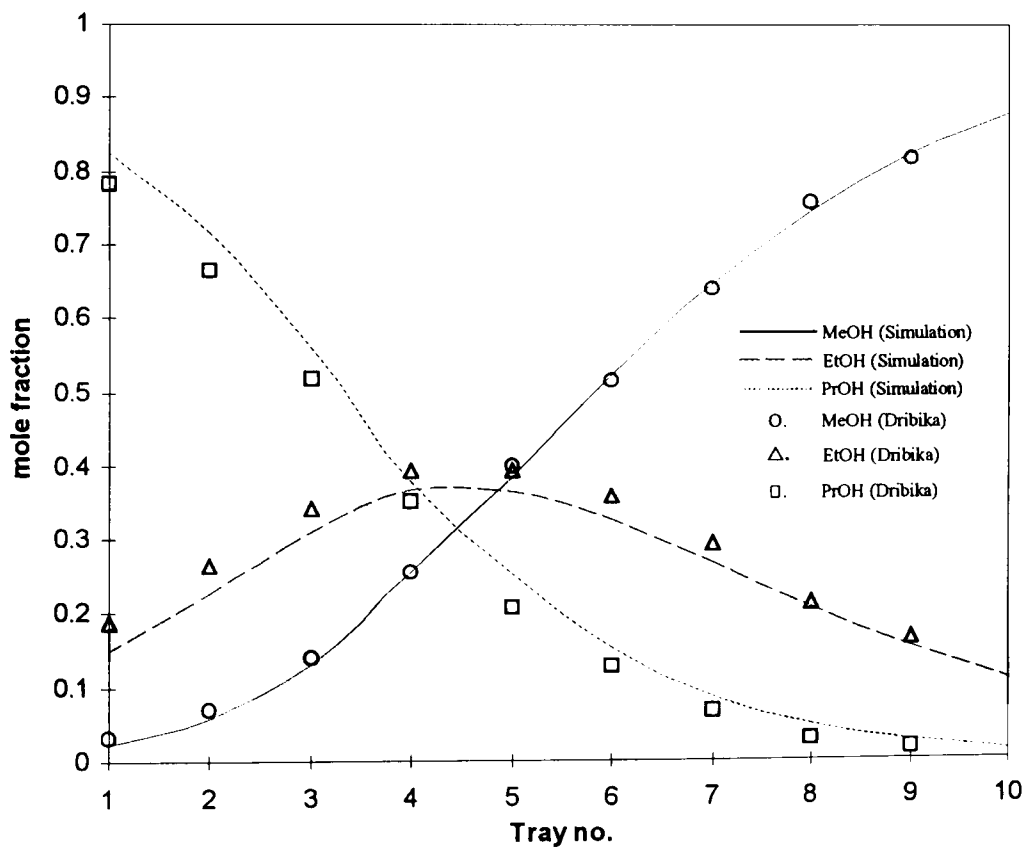


b) Constant Efficiency Model vs. Dribika's Experimental Composition Profiles

**Figure 5.8:** Constant Efficiency Model Profiles at Steady State Compared with Profiles from Dribika (1986) for the Drib -1 example

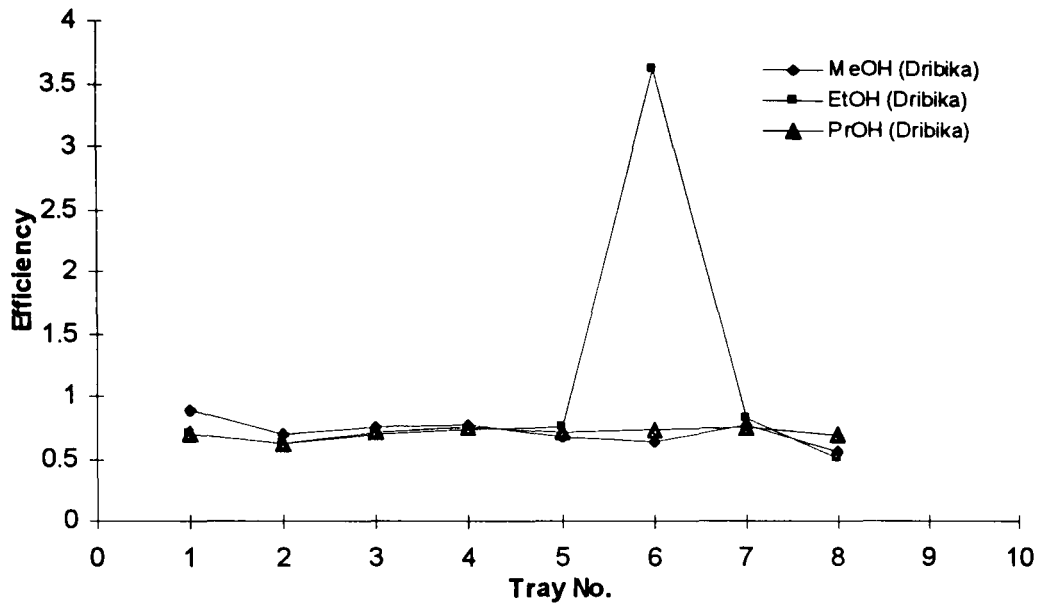


a) Tray Efficiencies for Methanol, Ethanol and Propanol in a Ternary Batch Distillation (Dribika (1986))

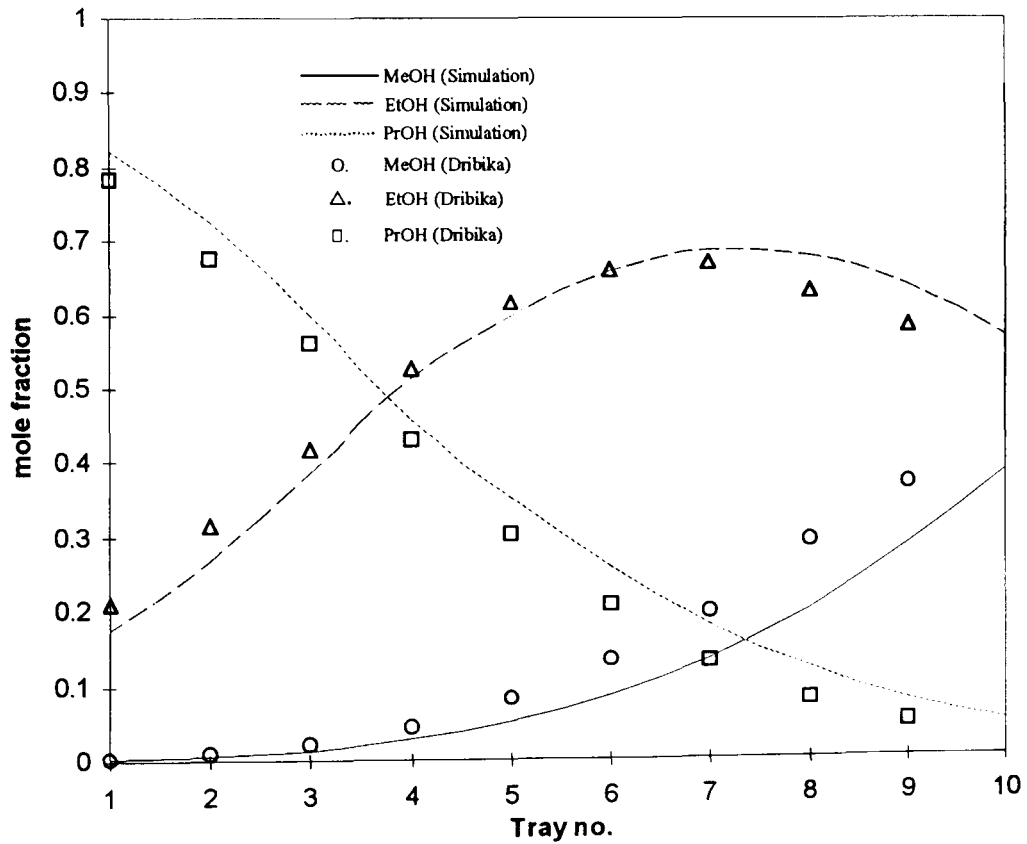


b) Constant Efficiency Model vs. Dribika's Experimental Composition Profiles

**Figure 5.9:** Constant Efficiency Model Profiles at Steady State Compared with Profiles from Dribika (1986) for the Drib -2 example



a) Tray Efficiencies for Methanol, Ethanol and Propanol in a Ternary Batch Distillation (Dribika (1986))



b) Constant Efficiency Model vs. Dribika's Experimental Composition Profiles

**Figure 5.10:** Constant Efficiency Model Profiles at Steady State Compared with Profiles from Dribika (1986) for the Drib -3 example

Figure 5.8 to Figure 5.10 show that the Constant Efficiency Model (as described in Chapter 4) is able to model not only the distillation of a binary mixture, but also a ternary mixture. The efficiency values on some of the trays are seen to exhibit strange values for the intermediate component, ethanol, when there is a peak in its concentration. They tend to take up values either above 1.0 or they take up negative values. For each of these examples, the steady state profiles predicted using the Constant Efficiency Model closely matches the actual experimental composition profile reported by Dribika. The Constant Efficiency Model also predicts the concentration maximum for the intermediate component, which Dribika observed experimentally, as well as the tray on which this maximum occurs.

### 5.2.2 Simulating the Experimental Work of Domench et al (1974)

Domench et al (1974) carried out a series of experimental tests on a pilot installation to prove the validity of their simulation model and to investigate the effect of parameters such as heat loss, tray holdup, and tray efficiencies. They reported results from the distillation of a non-ideal cyclohexane/toluene mixture in a 4-tray batch distillation column at atmospheric pressure and a heat input of 3kW to the reboiler.

In some of their experiments, the column was charged with 200 moles of the feed mixture of 0.3 mole fraction cyclohexane. Figure 5.11 shows the result of one of such runs where the column was run at total reflux until steady state and product was withdrawn at a reflux ratio of 5:1. The mole fraction of cyclohexane in the distillate is plotted against the amount of distillate collected.

These feed and operating conditions are simulated using the Constant Efficiency Model with an average, constant tray efficiency of 0.8 (value assigned by Domench et al) for all trays and negligible tray holdup. The

simulation result is seen to compare very well with the published results of Domench et al (1974) as shown in Figure 5.11.

Another example reported by Domench et al (1974) was the batch distillation of a 0.55 cyclohexane mole fraction, 200 mole cyclohexane/toluene feed charge to the column. The top product was withdrawn in this example, at a reflux ratio of 4:1 and the tray holdup was approximately 2.0 moles. This experimental condition and feed specification was also simulated (using an average tray efficiency of 0.8 again) and the rate of change of distillate composition is once more compared with the experimental results of Domench et al in Figure 5.12.

Figure 5.11 and Figure 5.12 show a very close agreement between the distillate composition profiles reported by Domench et al and that obtained from simulation using the Constant Efficiency Model with a single value of tray efficiency on all trays. Only the distillate compositions were reported by Domench et al as opposed to the entire column profile. As such, the column composition profile under these conditions and using this mixture could not be compared with the results obtained from the Constant Efficiency Model. However, we can assume that it must agree with the experimental results because the model fairly accurately predicts the distillate composition profiles during product withdrawal.

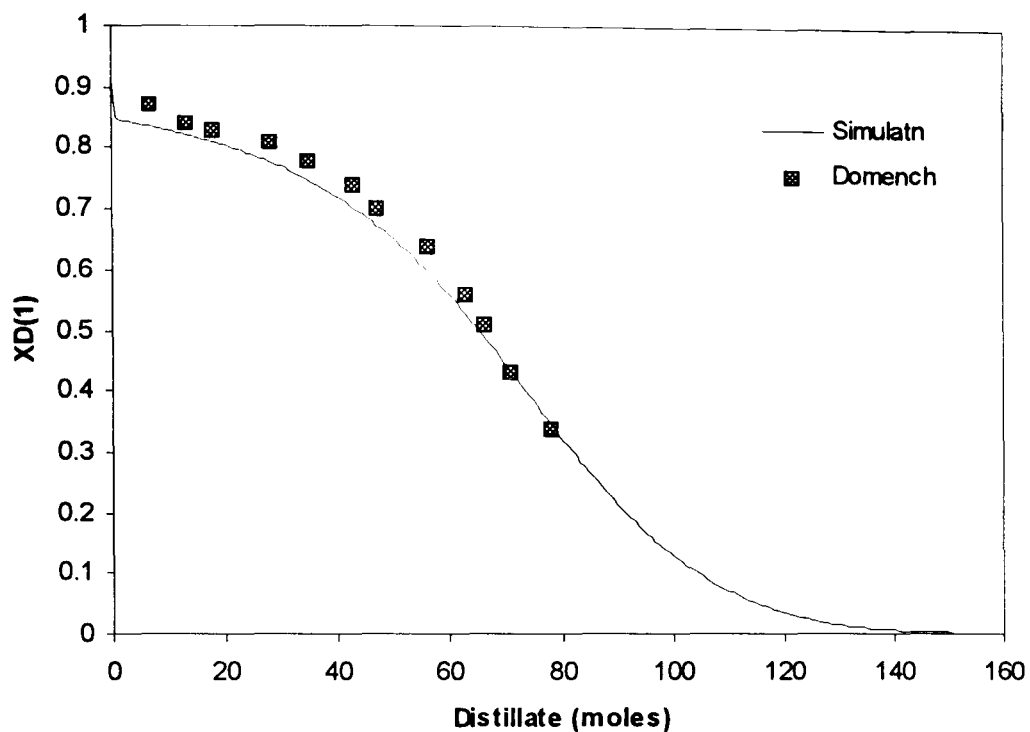


Figure 5.11: Cyclohexane-Toluene Distillation results - Example 1 (Domench et al (1974)).

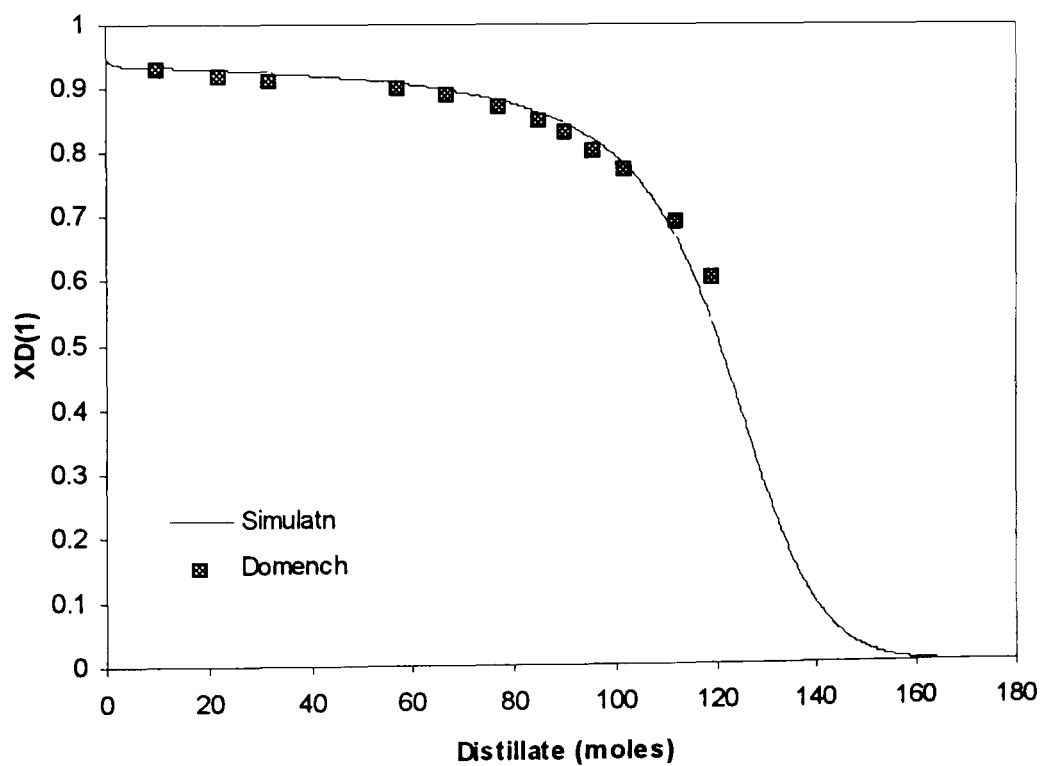


Figure 5.12: Cyclohexane-Toluene Distillation results - Example 2 (Domench et al (1974)).

### 5.3 SUMMARY

The model developed for this study has been extensively tested to verify its performance at steady state (total reflux) and during the transient period of product withdrawal under various operating conditions. It has also been tested using both ideal and non-ideal mixtures.

Experimental data used for the verification of the model include not only data collected during the distillation runs reported in this work. It also includes experimental data reported by other researchers using ternary mixtures (Dribika 1986)) as well as data from the distillation from other more non-ideal binary mixtures (Domench et al (1974)).

Unlike models used elsewhere in the literature, tray efficiency here was not assigned, based on a trial and error process to match simulation results to experimental data. Instead, the efficiencies used were obtained experimentally and are therefore reflective of the actual performance of the tray. The simulation results are seen to compare very well at steady state and in the transient period during product withdrawal, with the reported experimental results for the distillation of different methanol/water mixtures. Experimental and simulation result comparison is made, not only of the top product composition, but the entire column profile.

Model predictions were also verified using experimental results of the steady state profiles for different compositions of a methanol-ethanol-propanol mixture reported by Dribika (1986) and distillate composition as a function of quantity distilled reported by Domench et al (1974). In both cases, a good agreement is observed between the reported experimental composition profiles and the profiles predicted by the Constant Efficiency Model.

The model, using the Constant Efficiency Model simulation, produces results that very closely match those obtained experimentally. For the methanol/water

mixture separations considered however, a closer match is observed at the initial column steady state after the total reflux startup, compared with the steady state match after the timed product withdrawal. Improved model accuracy at all stages of the distillation is expected if the tray efficiencies are allowed to vary with the mixture composition on the tray and this is investigated using the Variable Efficiency Model.

## **CHAPTER SIX.**

### **THE VARIABLE EFFICIENCY MODEL**

In the previous chapter, the model tested was the Constant Efficiency Model. The Murphree tray efficiency for each individual tray is constant for the simulation run but values may differ from one tray to another. The Variable Efficiency Model on the other hand, does not have a fixed efficiency value for the tray, but allows the efficiency to vary at each point in time as a function of the concentration of the mixture on the tray.

Medina et al (1979), Lockett (1986) and Rao et al (1995) have investigated tray efficiency estimation methods. However, most researchers and engineers still prefer to use efficiencies taken from experimental work and existing operating columns. In this work, the tray efficiencies used were calculated from experimental data obtained from the distillation of the methanol/water mixtures described in Chapter 5. The results of the Variable Efficiency Model are analysed and the accuracy of its predicted column temperature profiles and temperature movements is compared with the Constant Efficiency Model predictions.

#### **6.1 TRAY EFFICIENCY VS CONCENTRATION CURVES**

The tray efficiencies calculated for each tray in Runs 3 to 7, as described in Chapter 5, are plotted in Figure 6.1 as a function of the methanol compositions on the trays. A simple polynomial curve is used to represent all these curves as shown in Figure 6.2 and this gives the tray efficiency (for methanol) as a function of the methanol concentration. Efficiency values at the ends of the concentration range must be carefully handled because compositions in these regions cannot be accurately measured (due to limitations in accuracy of the

measuring device). In this concentration region, the equilibrium line is close to the operating line and very little enrichment is achieved on the trays.

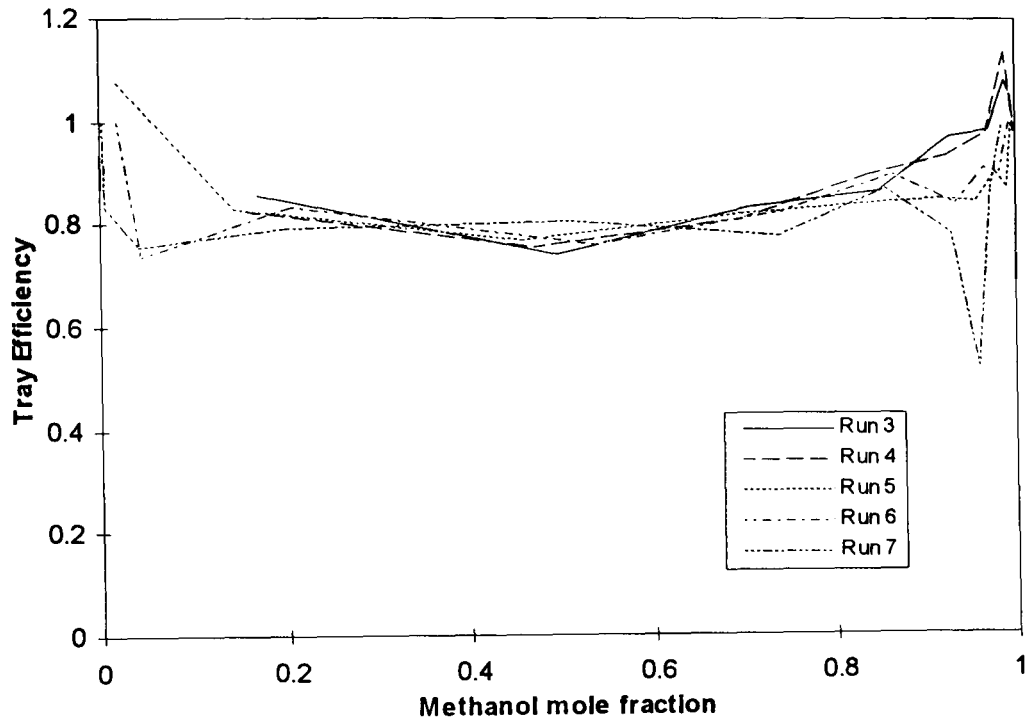


Figure 6.1: Tray Efficiency vs. Concentration for Runs 3 to 7.

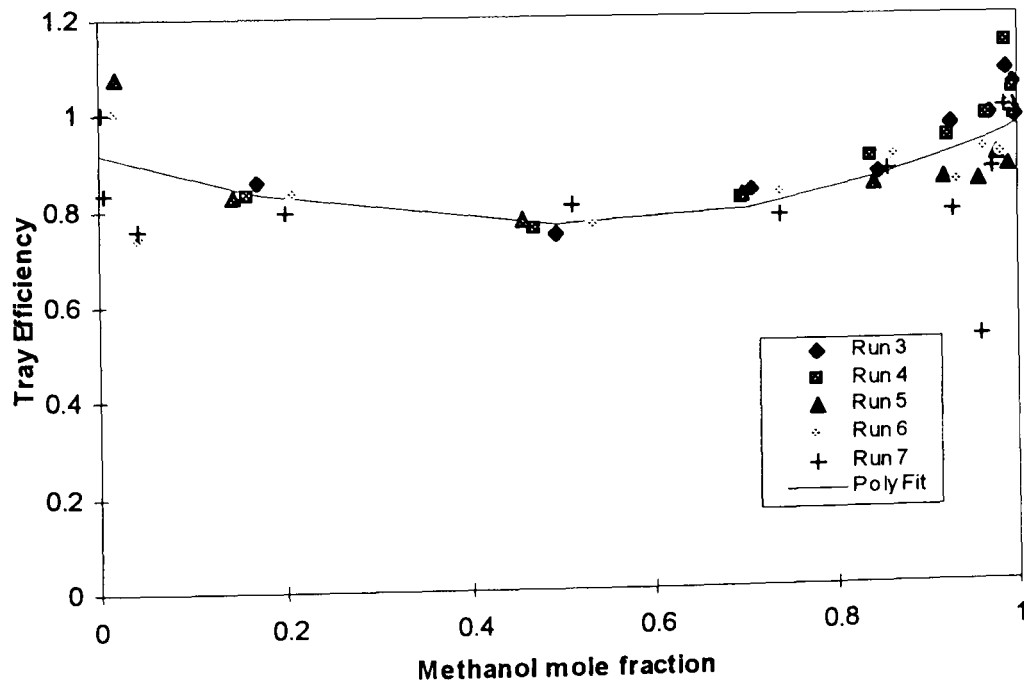


Figure 6.2: Polynomial Best-Fit Curve for Tray Efficiency as a Function of Methanol Concentration

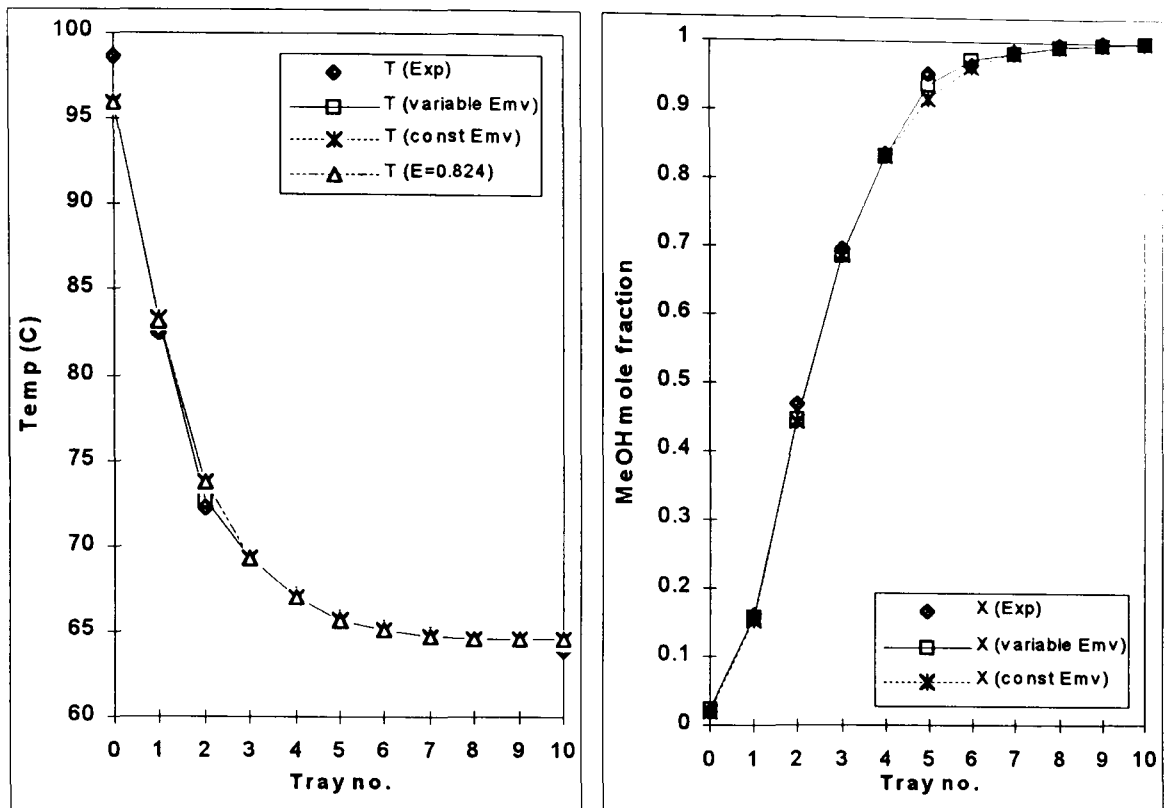
Because of the modular nature of the model, the efficiency vs. concentration data is easily incorporated. The simulation code allows efficiency data input, either in a tabular form or as an equation which describes the curve.

## 6.2 MODEL VERIFICATION

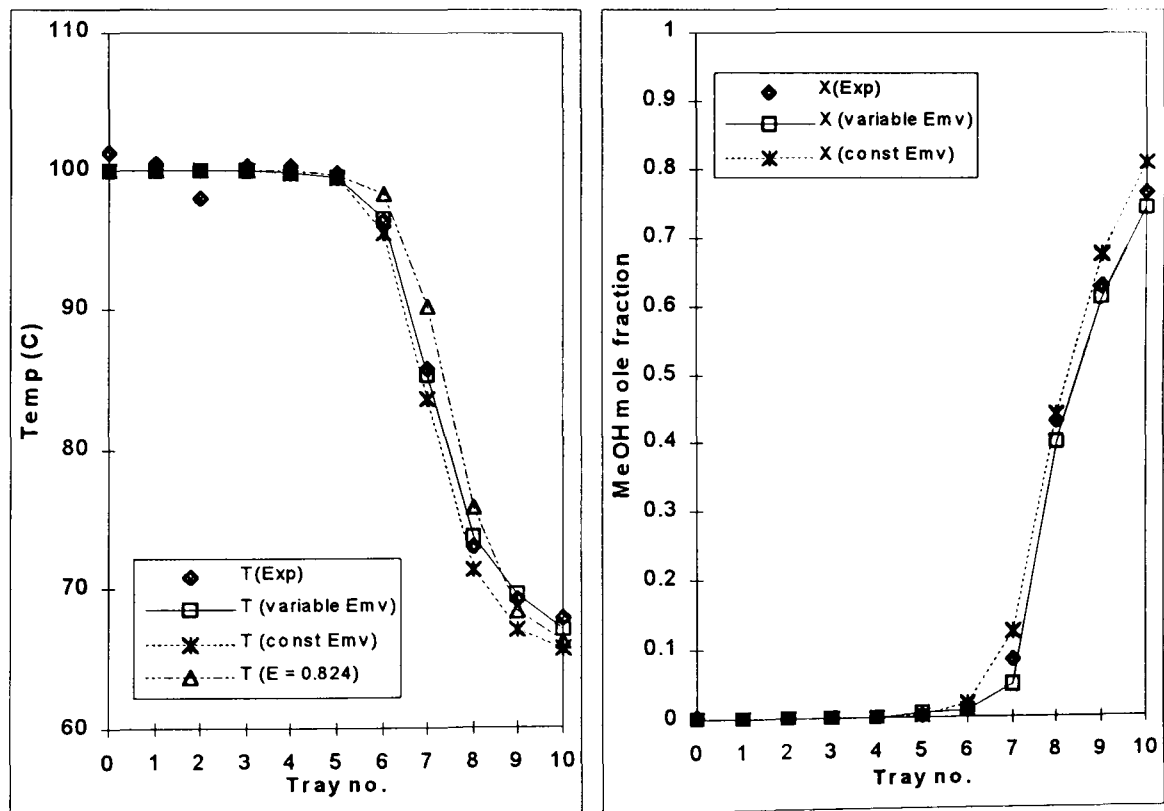
The Variable Efficiency Model simulation was run using the feed and operating conditions given in Chapter 5. The predicted steady state profiles are compared with the experimental results of Runs 3 to 7 and the simulation results of the Constant Efficiency Model in Figure 6.3 to Figure 6.6. The temperature movements during transient periods predicted by the Variable Efficiency Model are also compared with experimental data and the Constant Efficiency Model predictions on relevant trays in the column in Figure 6.7 to Figure 6.11.

The average of the efficiency values plotted in Figure 6.1 and Figure 6.2 is 0.824. The model is run with all trays having a fixed efficiency, equal to this average value (Overall Column Efficiency Model) and the resulting steady state temperature and composition profiles are also presented in Figure 6.3. These results show that the Overall Column Efficiency Model (using an efficiency of 0.824) gives a good match with experimental temperature and composition profile but the Constant Efficiency Model gives a better match and the Variable Efficiency Model gives an even better match. The greatest deviation in the results between experimental and simulation profiles is seen to occur in the intermediate composition regions and it is in this area that the Variable Efficiency Model gives a better steady state profile match than the Constant Efficiency Model.

In general, Figure 6.3 to Figure 6.6 show that for the methanol-water system under investigation, a small but evident improvement in predicted temperature profiles is achieved by using the Variable Efficiency Model over both the Constant Efficiency Model and the Overall Column Efficiency Model.

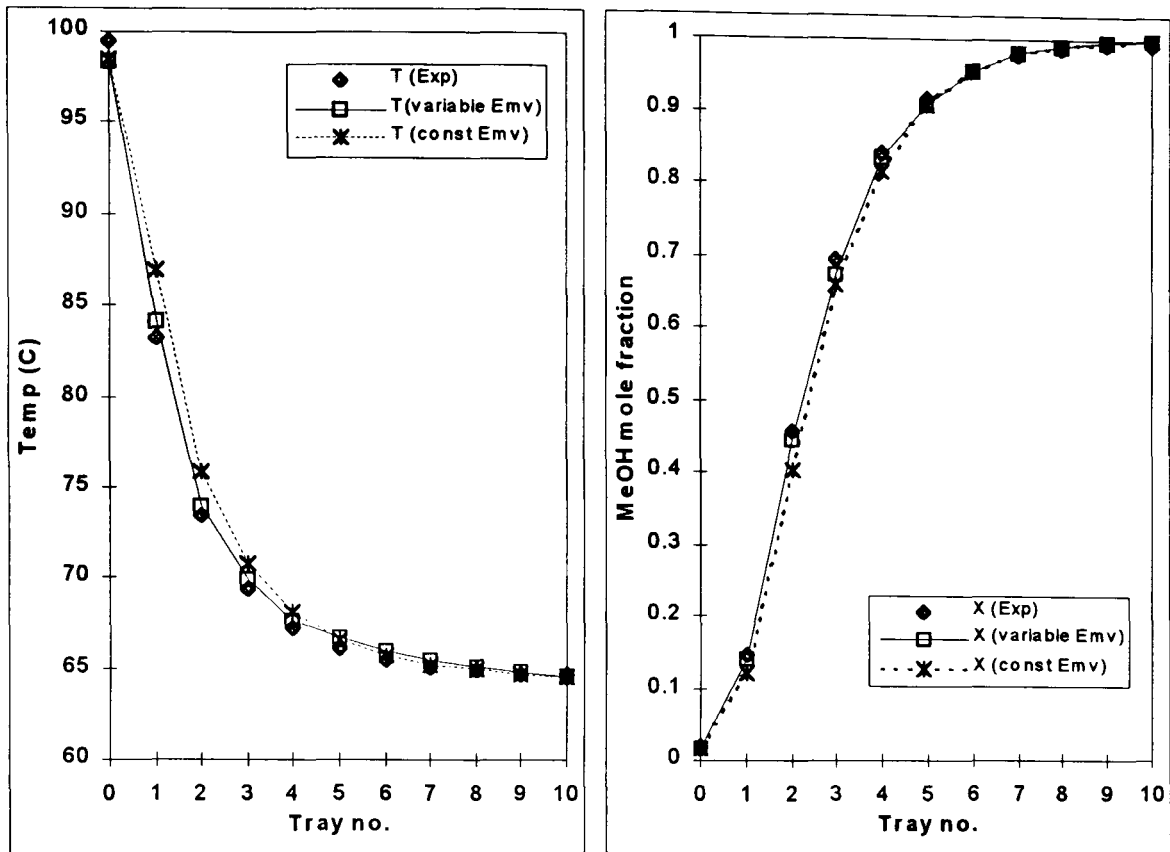


a) Initial Column Profile For Run 3

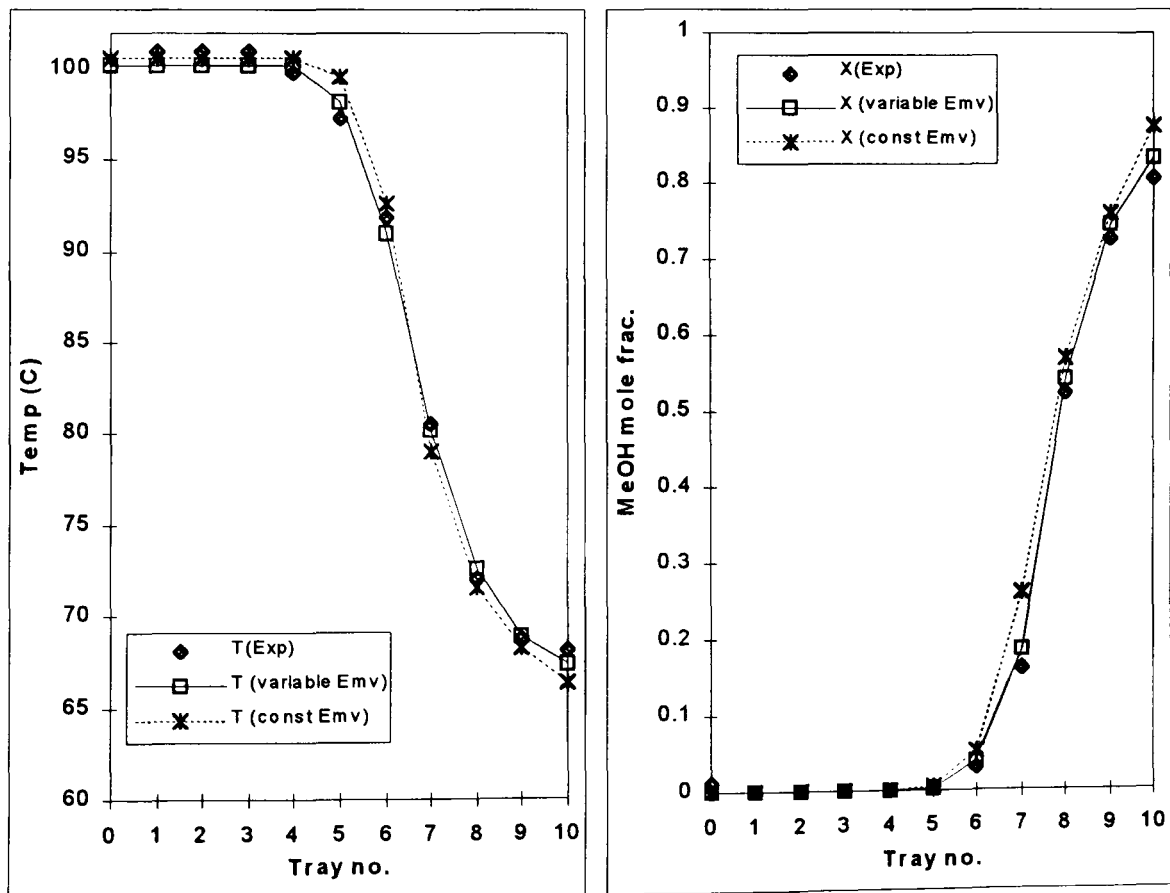


b) Final Column Profile For Run 3

**Figure 6.3:** Constant & Variable Efficiency Model Steady State Temperature and Composition Profiles for Run 3.

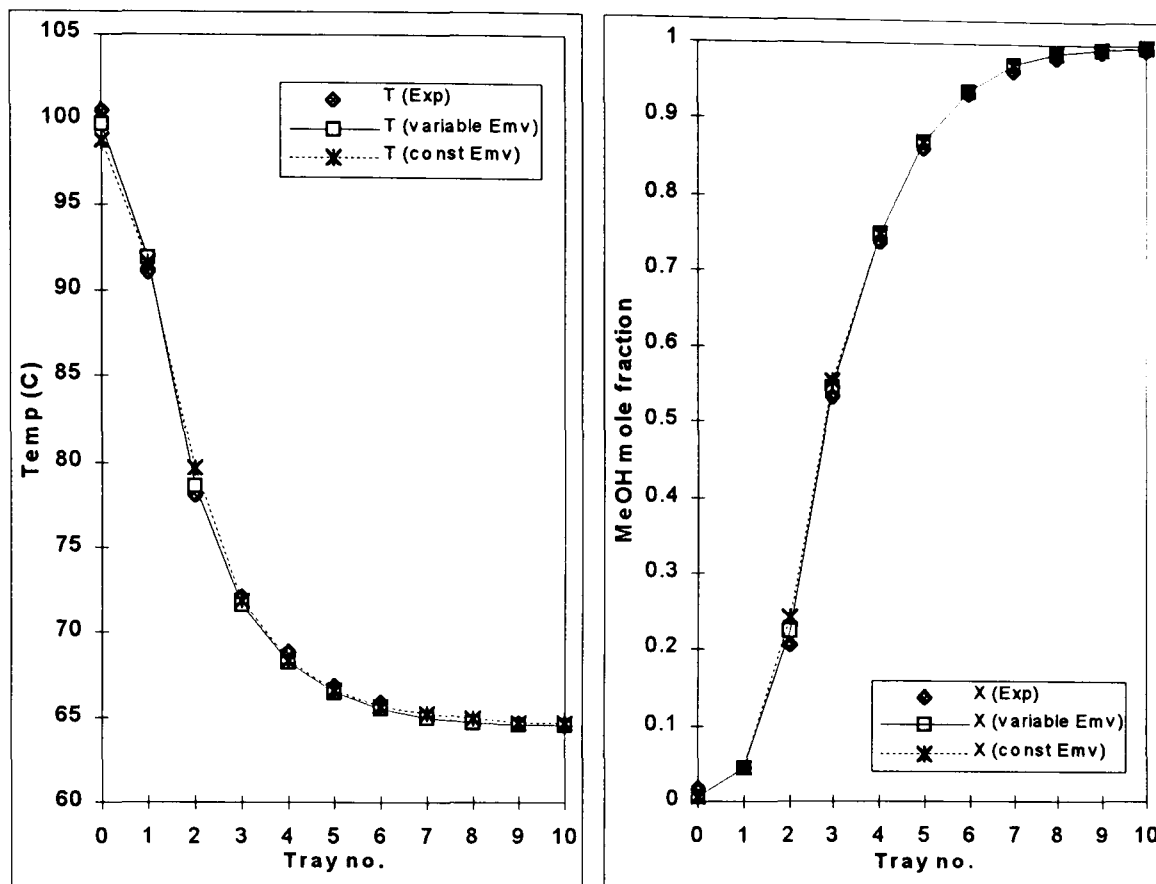


a) Initial Column Profile for Run 5

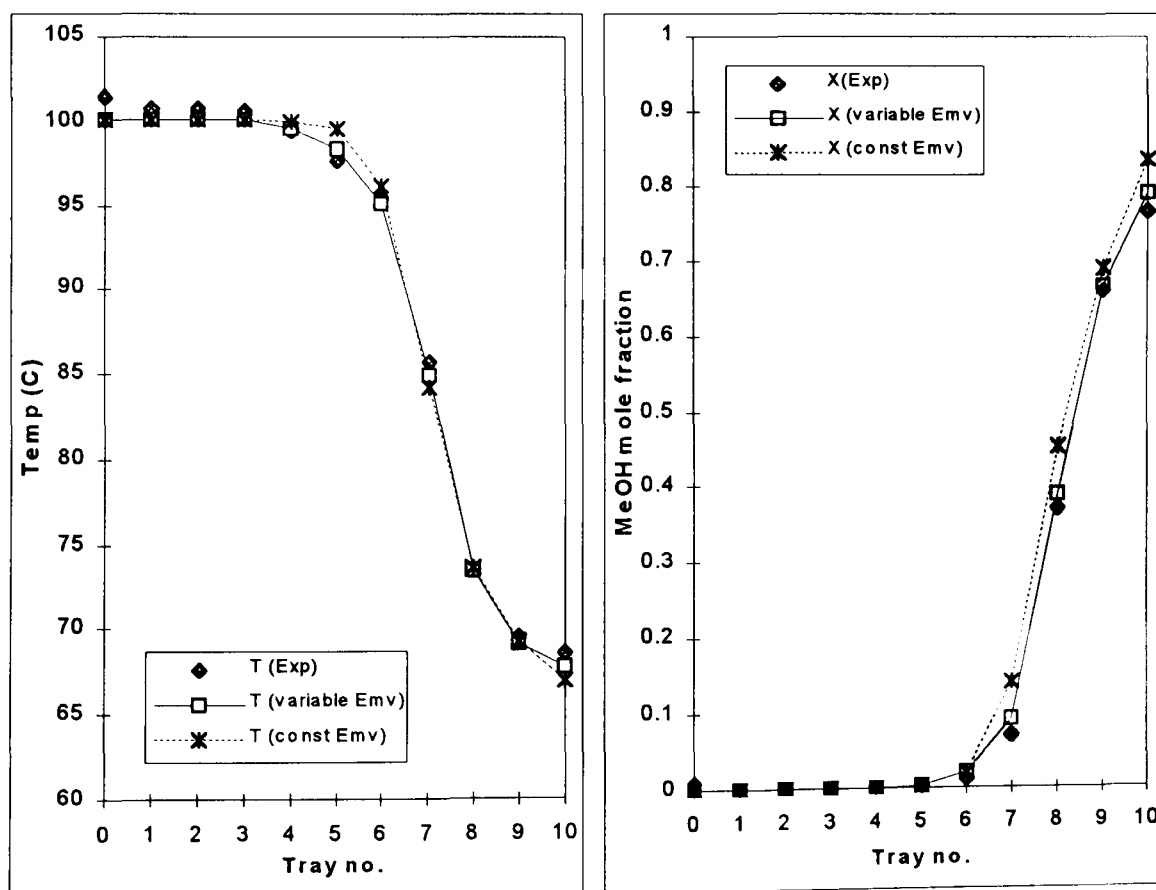


b) Final Column Profile for Run 5

Figure 6.4: Constant & Variable Efficiency Model Steady State Temperature and Composition Profiles for Run 5

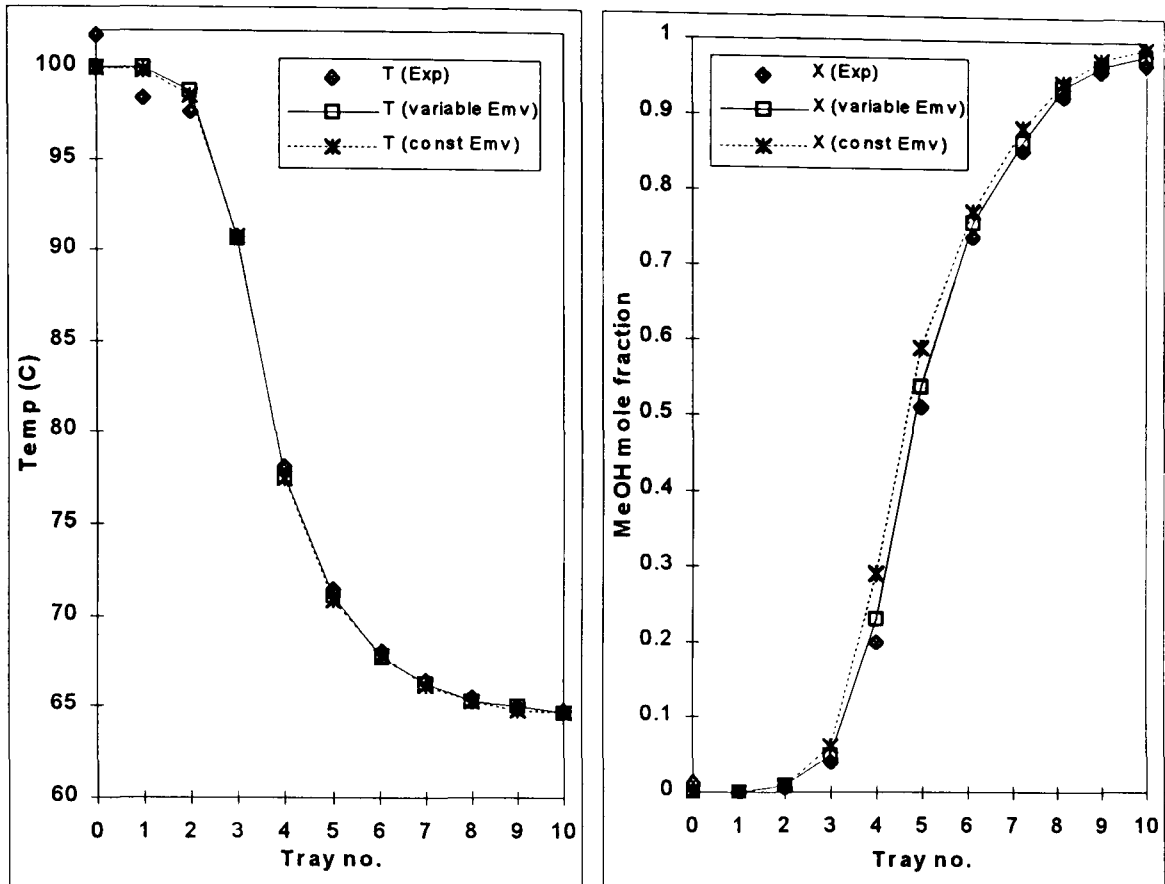


a) Initial Column Profile for Run 6

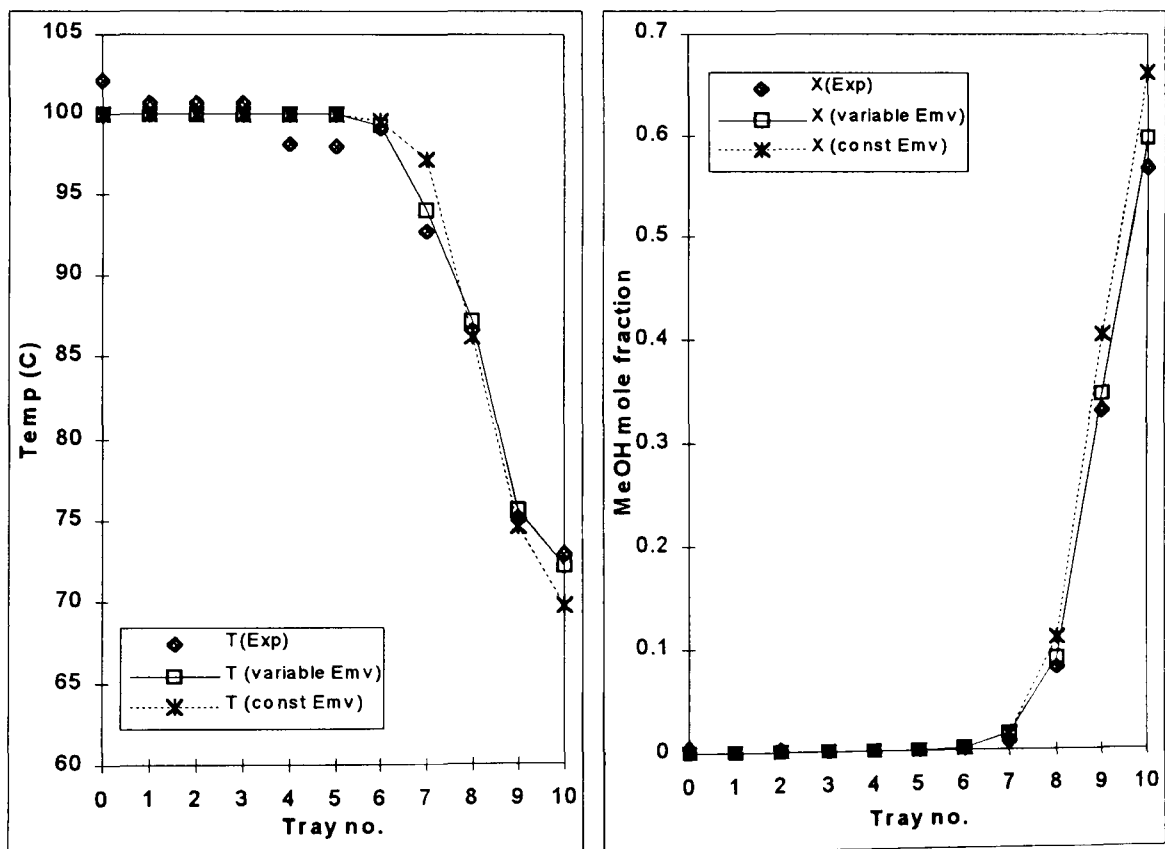


b) Final Column Profile for Run 6

**Figure 6.5: Constant & Variable Efficiency Model Steady State Temperature and Composition Profiles for Run 6**



a) Initial Column Profile for Run 7



b) Final Column Profile for Run 7

**Figure 6.6:** Constant & Variable Efficiency Model Steady State Temperature and Composition Profiles for Run 7

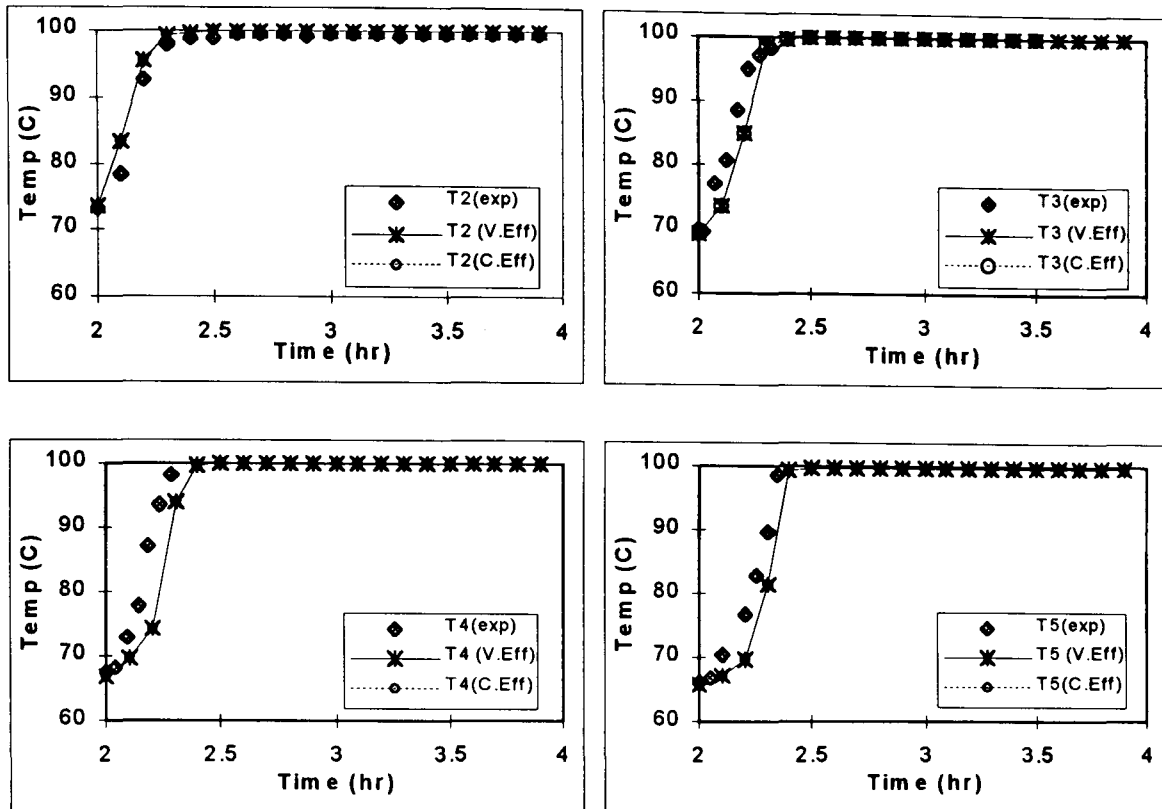


**Figure 6.7:** Experimental and Simulation (Variable and Constant Efficiency) Temperature Movements on Trays 2, 3, 4 and 5 between the Initial and Final Steady States for Run 3.

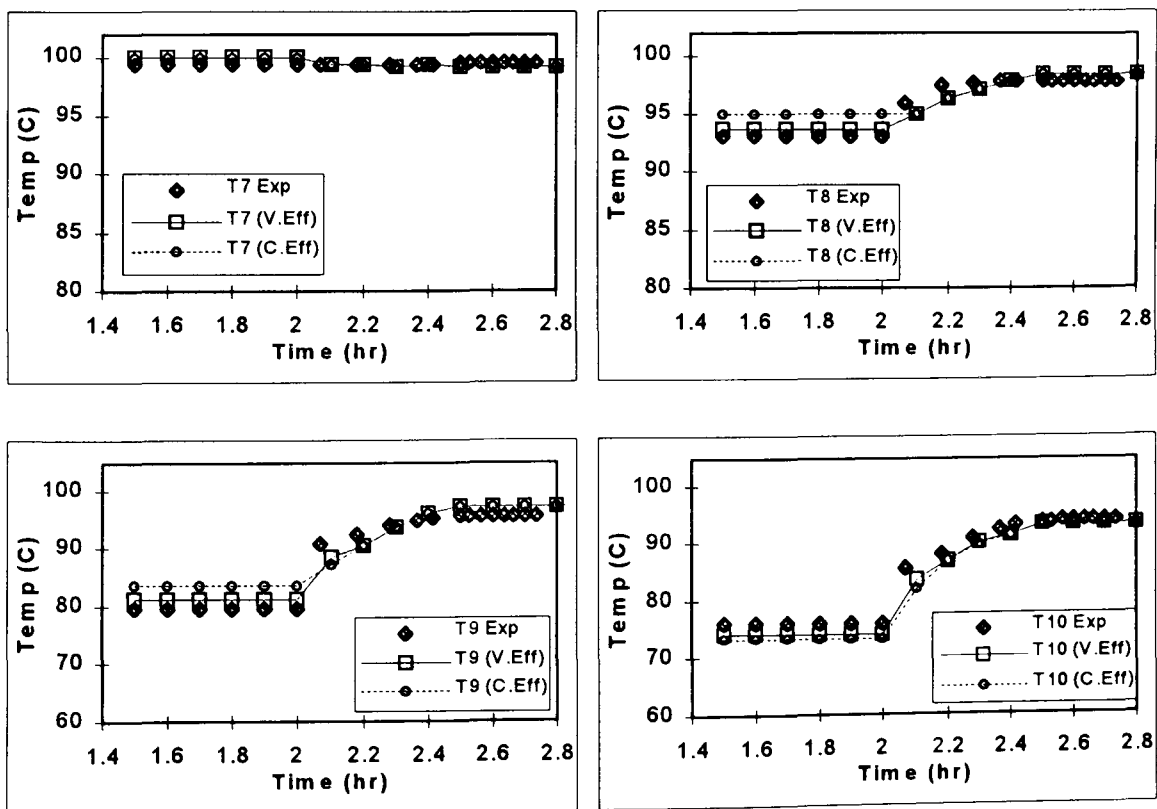


**Figure 6.8:** Experimental and Simulation (Variable and Constant Efficiency) Temperature Movements on Trays 7, 8, 9 and 10 between the Initial and Final Steady States for Run 4.

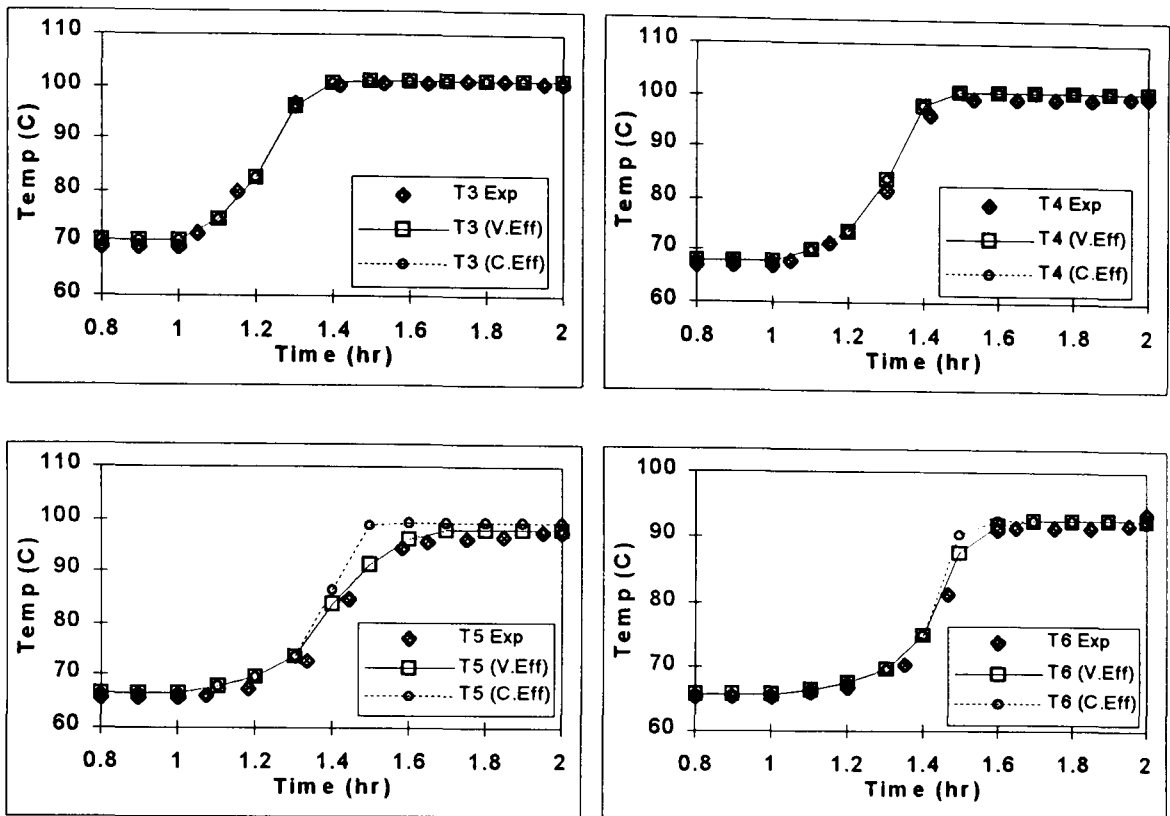


**Figure 6.9:** Experimental and Simulation (Variable and Constant Efficiency) Temperature Movements on Trays 3, 4, 5 and 6 between the Initial and Final Steady States for Run 5

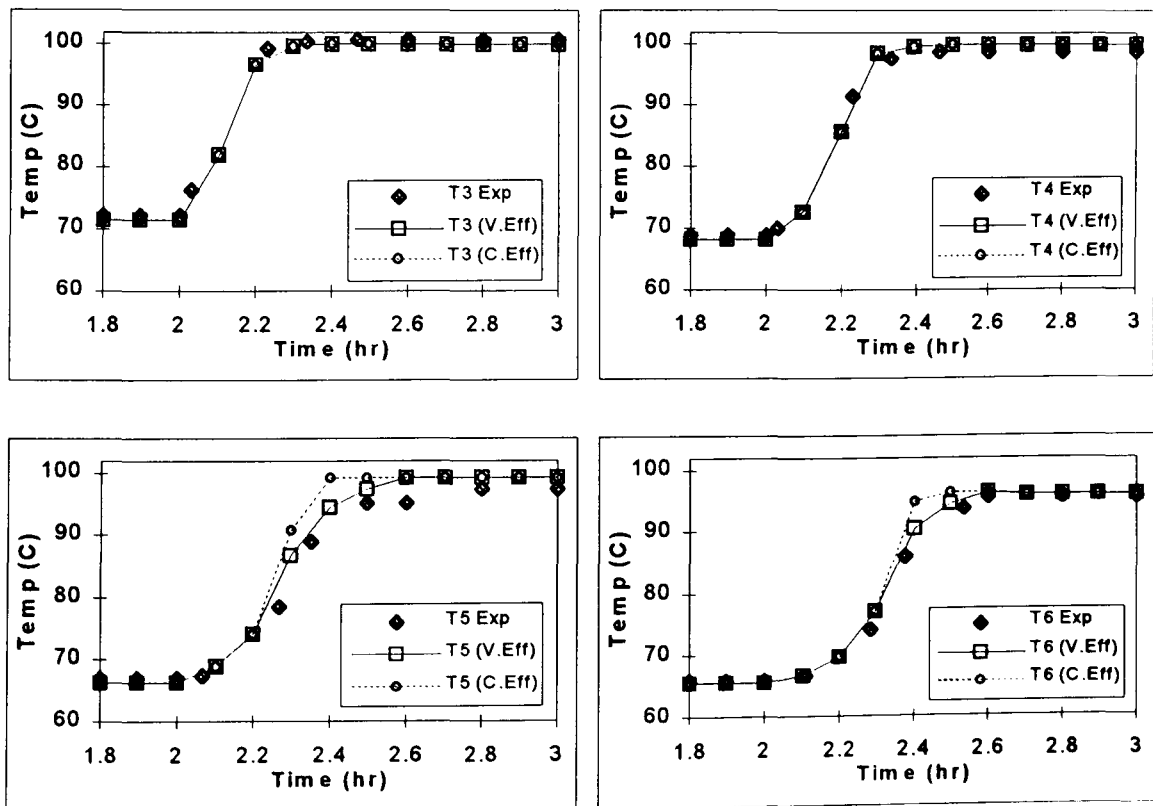


**Figure 6.10:** Experimental and Simulation (Variable and Constant Efficiency) Temperature Movements on Trays 3, 4, 5 and 6 between the Initial and Final Steady States for Run 6

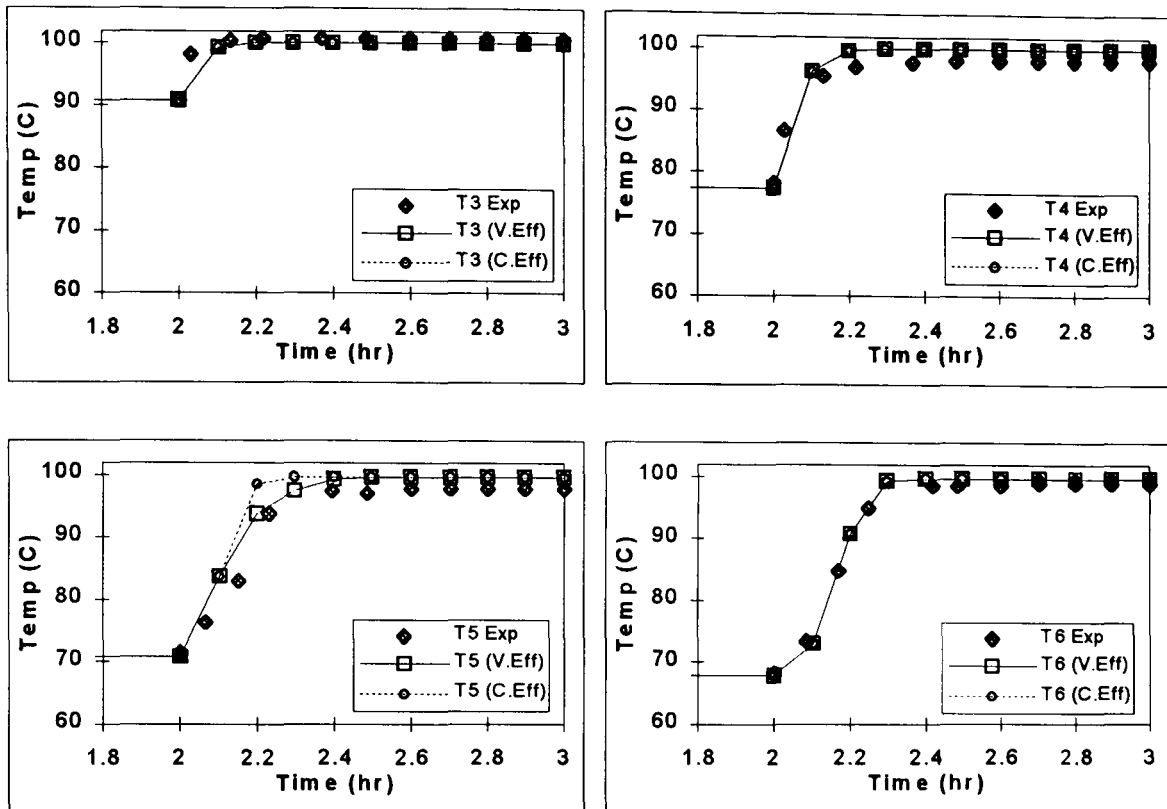


**Figure 6.11:** Experimental and Simulation (Variable and Constant Efficiency) Temperature Movements on Trays 3, 4, 5 and 6 between the Initial and Final Steady States for Run 7

The temperature movements for Runs 3 and 4 which are plotted in Figure 6.7 and Figure 6.8 show that the Variable Efficiency Model gives a slightly closer match with experimental data than the Constant Efficiency Model. In general, for the experimental runs considered, the graphs in Figure 6.7 to Figure 6.11 lead to the conclusion that for the short transient periods investigated, the Variable Efficiency Model gives a closer match with experimentally measured temperature movements during distillate withdrawal than the Constant Efficiency Model. This alongside the improved accuracy of the steady state temperature profiles predicted by the Variable Efficiency Model, shown in Figure 6.3 to Figure 6.6, proves that including the tray efficiency-composition dependence in batch distillation modelling leads to improved model accuracy. This implies that the Variable Efficiency Model gives a better representation of

the process because the predicted column behaviour under total and partial reflux ratios, more closely matches the actual column behaviour observed in experimental methanol/water distillation.

The potential effect of the tray efficiency-composition dependence on distillation and model fidelity is investigated using two hypothetical case studies with different tray efficiency-concentration relationships. The tray efficiency-concentration relationships investigated in the case studies are extensions of the relationship observed for methanol/water system in Figure 6.2. This work is presented in the next chapter.

# CHAPTER SEVEN.

## CASE STUDIES

The relationship between tray efficiency and composition for a methanol/water mixture determined in this work is shown Figure 6.2 whilst Figure 7.1 (from Mostafa (1979)) shows a similar relationship for an ethanol/water mixture.

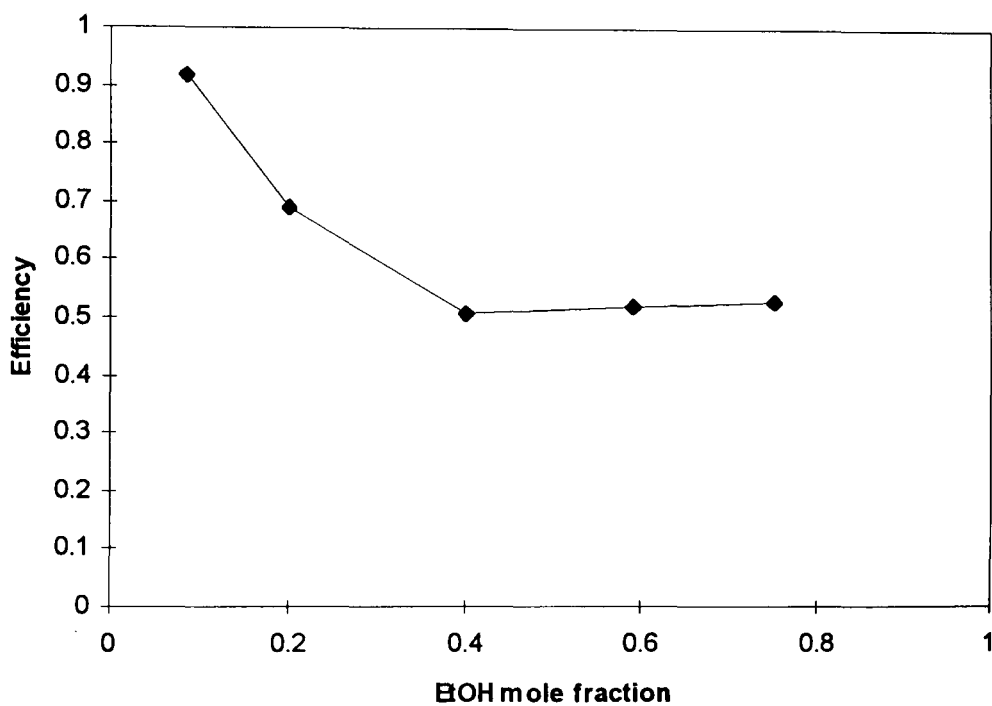


**Figure 7.1:** Efficiency-Concentration Relationship for an Ethanol-Water Mixture (Mostafa (1979)).

Figure 7.1 shows a similar trend in the Murphree tray efficiency with mixture composition to that in Figure 6.2. High tray efficiency is obtained at low ethanol (or methanol) concentrations and the efficiency passes through a minimum in the mid-range of the composition scale. Mostafa (1979) gave no efficiency data at high ethanol concentrations but the efficiency is seen to rise

gradually with composition, above the minimum value with increasing ethanol concentration.

The tray efficiencies for methanol in Figure 6.2 range from a high of 0.97 at one end of the concentration range, to a minimum of 0.78 in the mid-composition region but for ethanol in Figure 7.1, it ranges from 0.93 to a minimum of 0.5, a much steeper curve. This highlights the fact that the nature and severity of the tray efficiency-concentration relationship differs for different mixtures. The effect of the severity of the dependence of tray efficiency on composition, on the performance of a batch distillation column is therefore investigated here. To do this, two forms of relationship were assumed:

- case study 1, where the maximum tray efficiency may exceed 1.0.
- case study 2 where tray efficiency is restricted to a maximum of 1.0.

These provide a basis for the generation of hypothetical tray efficiency-concentration relationships to facilitate the study of its effects on the performance of a batch distillation column.

## 7.1 CASE STUDY –1

Because Murphree tray efficiency can exceed 1.0 (Shilling et al (1953), Dribika (1986)), Case Study –1 considers the case where the tray efficiency exceeds 1.0 at the ends of the concentration range. The curves are assumed extensions of the methanol/water concentration-efficiency curve in Figure 6.2 and as such, are generated so that the average efficiency across the concentration range equals the average of the efficiencies in Figure 6.2 (average efficiency is 0.824). The assumed efficiency curves are in the form of a simple polynomial, given by

$$E_{mv} = 1.656x^2 - 1.656x + E_{max} \quad 7.1$$

under the condition that

$$\int_0^1 E_{mv} dx = 0.824 \quad 7.2$$

Equation 7.1 closely matches the efficiency curve of Figure 6.2.  $E_{max}$  is the maximum efficiency and 0.824 in Equation 7.2 is the average efficiency, obtained from the experimental data plotted in Figure 6.2. Hypothetical efficiency curves are generated for maximum efficiency values ( $E_{max}$ ) of 1.1, 1.3, 1.5, 1.7 and 2.0 and are plotted in Figure 7.2.

Equation 7.1 gives efficiencies as low as 0.236 in the mid-composition range for an efficiency maximum of 2.0 (curve  $E_{2.0}$ ) and 0.686 for a maximum efficiency of 1.1 (curve  $E_{1.1}$ ). The efficiency maximum of 1.1 represents the relationship observed here for the methanol-water mixture while the efficiency maximum of 2.0 represents an extension of this relationship, keeping the average efficiency constant (see Figure 7.2).

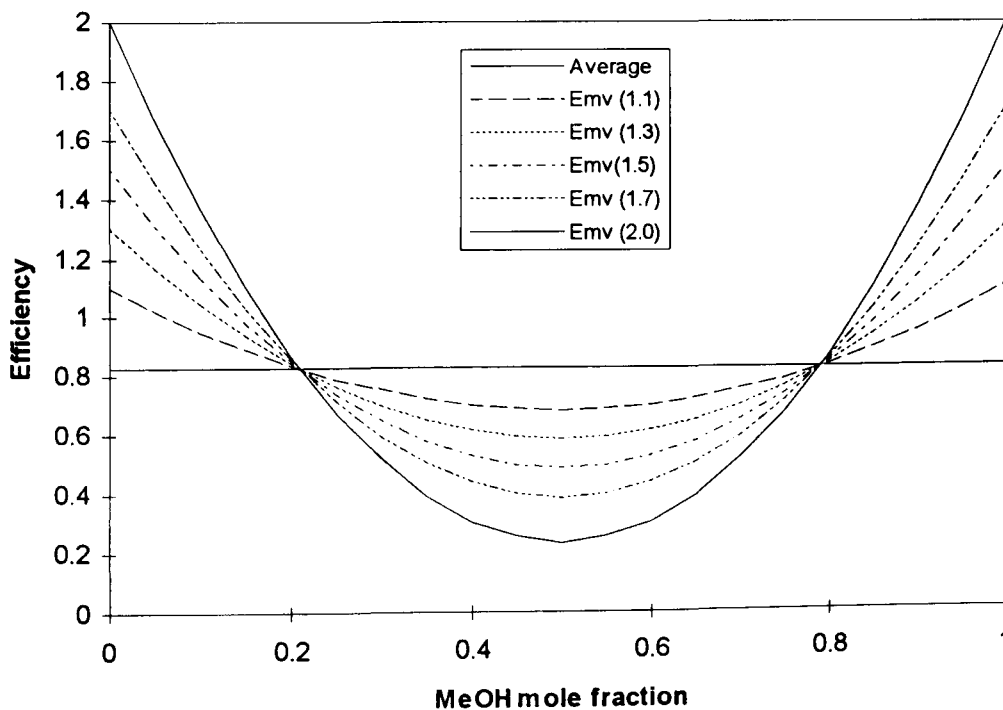


**Figure 7.2:** Assumed Tray Efficiency-Concentration Relationship used For Case Study -1. (Note: Values in legend represent the maximum efficiency values at the ends of composition range)

### 7.1.1 Case Study –1 Simulations

These hypothetical tray efficiency-concentration relationships (in Figure 7.2) are used in simulation, in the Variable Efficiency Model. The simulation is run assuming a feed of 1.168 kmols with 0.0925 mole fraction of methanol and a steam flow rate of 18 kg/hr to the still jacket at 2.2 bar. This is similar to the feed conditions described for Run 6 (Appendix A). The simulation is run at total reflux, as usual, until steady state and set to partial offtake either at a constant or varying reflux ratio. For the constant distillate composition operating policy, the attainment of steady state is not essential and product withdrawal is begun when the distillate composition reaches the specified value.

The case is also considered (for the fixed reflux ratio policy) where the column is run at total reflux until a specified distillate composition is reached and product is withdrawn at a fixed reflux ratio. This differs from the normal fixed reflux ratio operations considered here in that steady state is not necessarily achieved before product withdrawal is begun. Backed by a heuristic knowledge of the process and mixture to be distilled, this procedure is often used in practice to obtain distillate of a prescribed composition using the operationally simpler fixed reflux ratio policy. This is only permissible when strict distillate composition control is not critical

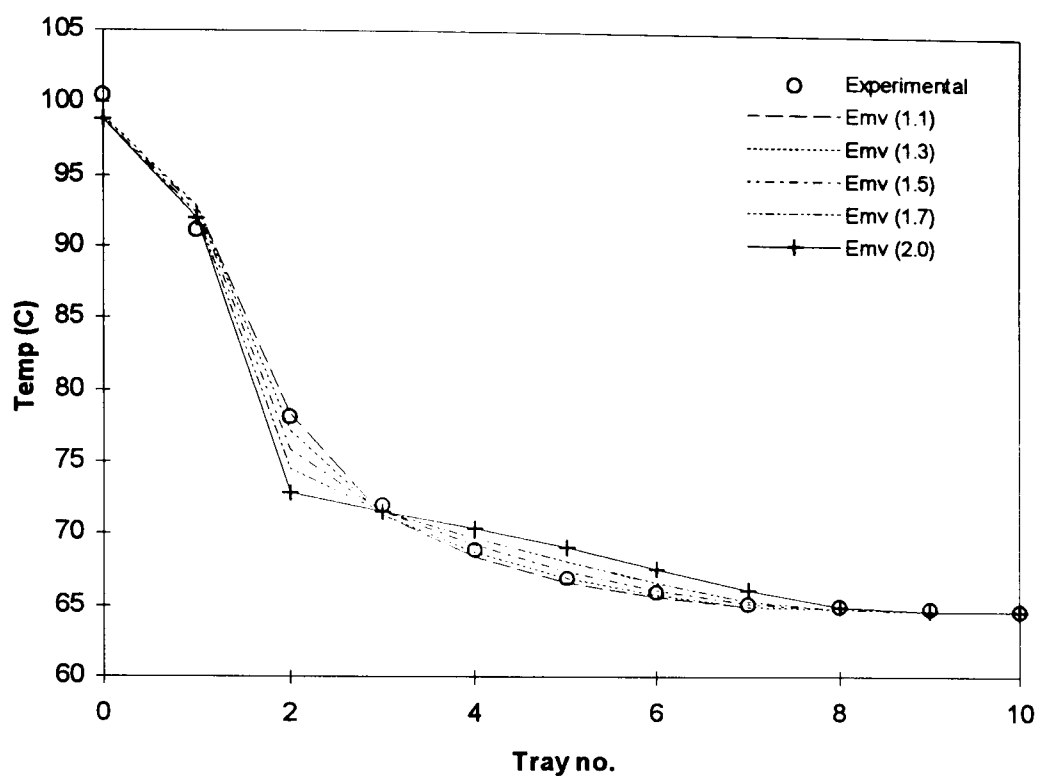
#### 7.1.1.1 Fixed Reflux Ratio Simulation For Case Study –1

The simulation is set to run using the feed and operating conditions used for Run 6. A 1.168 kmol feed (of 0.0925 methanol mole fraction) is specified and run at total reflux until steady state. After the initial total reflux operation where steady state is attained, the column is set to partial offtake at a reflux ratio of 4.5 for 25 minutes (0.417hrs) and returned to total reflux until a new

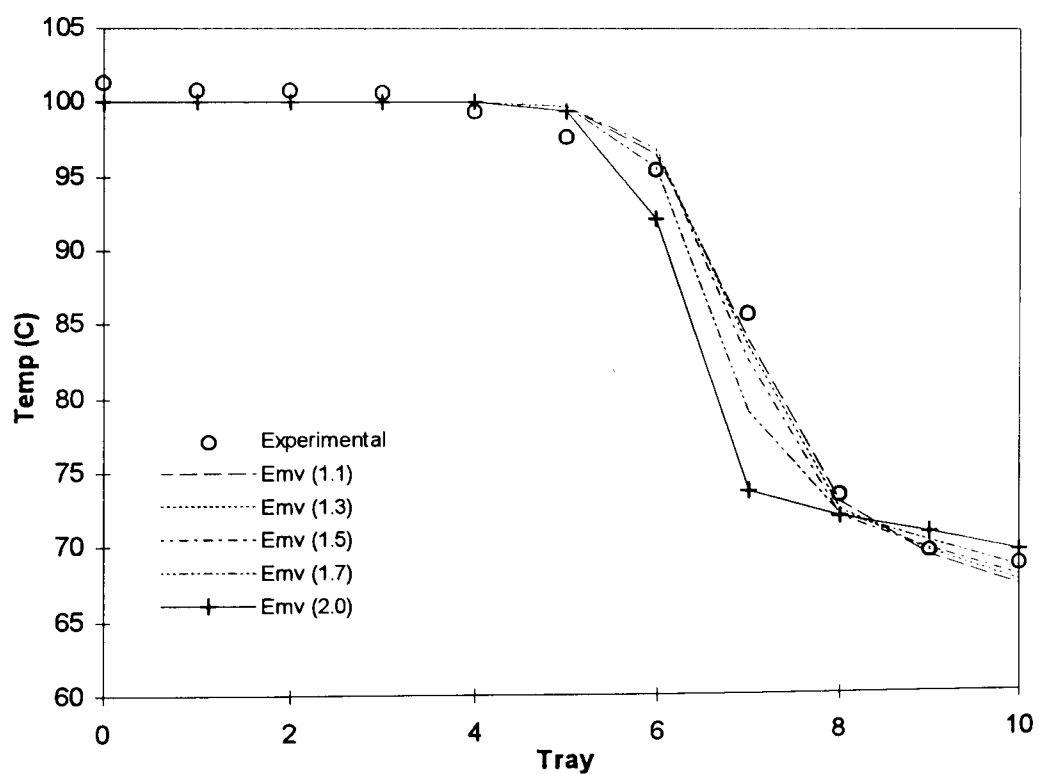
steady state is reached. The initial and final temperature profiles of the column are shown in Figure 7.3 for the different efficiency curves.

The graphs in Figure 7.3 as expected, show that the efficiency curve with a maximum value of 1.1 ( $E_{1.1}$ ) gives a trend closest to the Run 6 experimental results. Experimental results show that almost pure water and pure methanol are obtained at either end of the column and the simulation, using the different efficiency curves predicts this result. In the mid-section of the column where the trays contain a mixture of methanol and water, the profiles predicted by the simulation for the different efficiency curves deviate slightly from the experimental results. The deviation from experimental results increases as the severity of the concentration-efficiency relationship increases, as is shown in Figure 7.3a and b. The largest deviation from experimental results is observed with the efficiency curve with a maximum of 2.0 ( $E_{2.0}$ ). The tray on which the maximum deviation occurs is also seen to shift from Tray 2 in Figure 7.3a at the initial steady state after startup, to Tray 7 in Figure 7.3b for the second steady after some product withdrawal.

The composition movement of the column overhead composition is presented in Figure 7.4 for  $E_{1.1}$ ,  $E_{1.3}$ , and  $E_{1.5}$ . The simulation results for curve  $E_{1.1}$  shows that the distillate composition drops steadily until product withdrawal stops and remains at its value at the distillate withdrawal stop time. For the other curves however, the distillate composition is seen to pass through a minimum before settling at its new value. This phenomenon is investigated and discussed in more detail later.

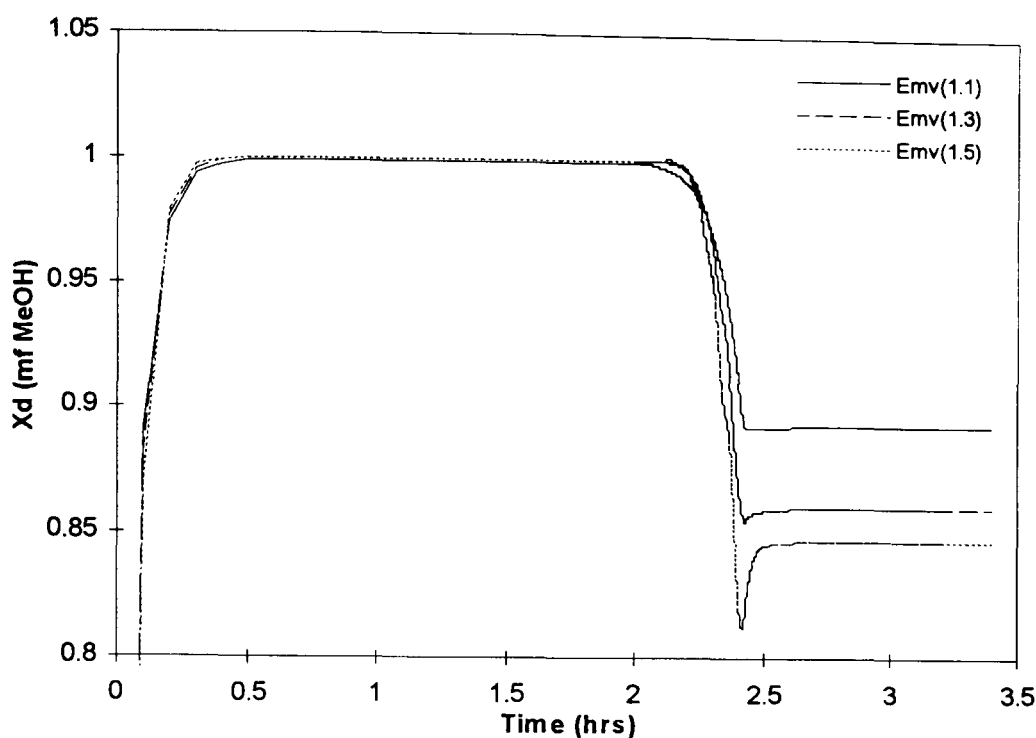


a) Initial Column Steady State Profiles after Total Reflux Startup



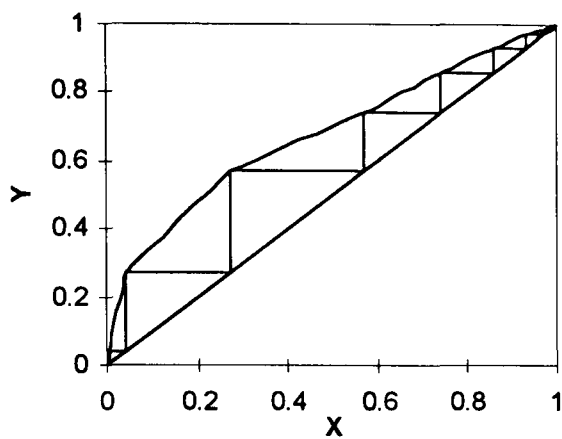
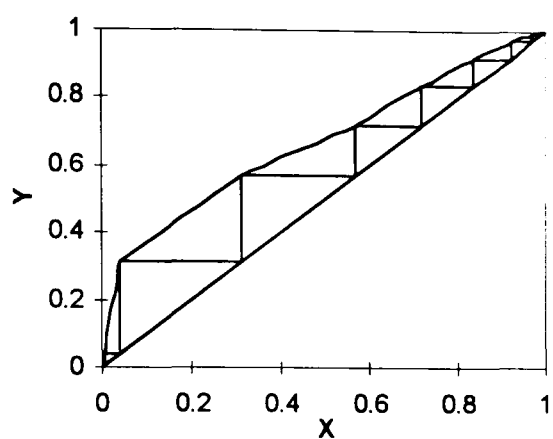
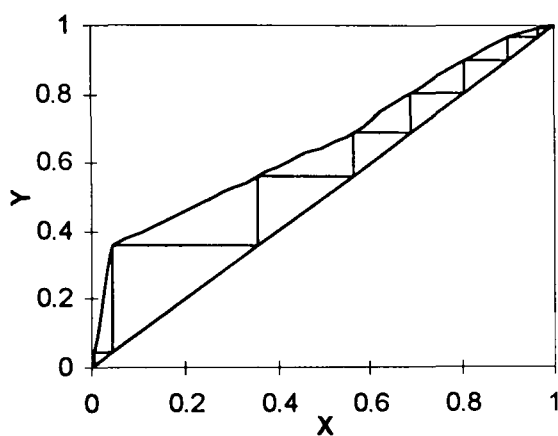
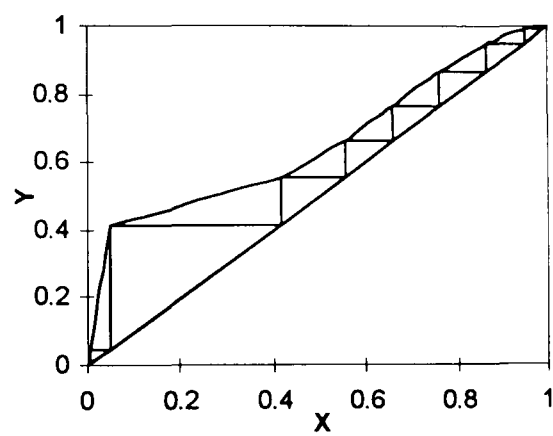
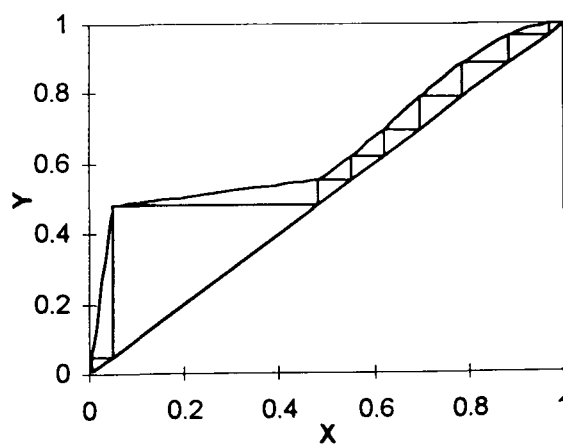
b) Final Column Steady State Profiles after Product Withdrawal for 0.417hrs

**Figure 7.3:** Initial and Final Steady State Temperature Profiles for the Case Study -1 Efficiency Curves with Different Severities of Tray Efficiency-Concentration Relationship.



**Figure 7.4:** Overhead composition profile for 25min Distillate Withdrawal from Steady State for Case Study -1 Efficiency Curves

McCabe-Thiele diagrams for the different concentration-efficiency curves are plotted in Figure 7.5 for the system at its initial steady state. At steady state in a column under total reflux with ideal stages, the operating line on a McCabe-Thiele diagram will lie along the  $45^\circ$  diagonal ( $y = x$ ) and the equilibrium line forms the other boundary where stages are stepped-off. Applying a single tray efficiency value in a McCabe-Thiele diagram introduces a “pseudo-equilibrium” line that is closer to the operating line than the true-equilibrium line. However, as is the case in this model, the efficiencies may vary continuously with liquid composition (and hence with time) and as is seen in Figure 7.5, this has the effect of distorting the shape of the equilibrium curve. The degree of distortion is proportional to the degree of severity of the concentration-efficiency relationship, almost causing a pinch for the  $E_{2.0}$  curve as is seen in Figure 7.5e.

a) McCabe-Thiele plot for E<sub>1.1</sub>b) McCabe-Thiele plot for E<sub>1.3</sub>c) McCabe-Thiele plot for E<sub>1.5</sub>d) McCabe-Thiele plot for E<sub>1.7</sub>e) McCabe-Thiele plot for E<sub>2.0</sub>

**Figure 7.5:** Total Reflux Initial Steady State McCabe-Thiele Plots for the Case Study -1 Efficiency Curves.

The nature of the concentration-efficiency relationship also affects the time taken from startup, under total reflux, to reach steady state (equilibration time) for the chosen operating strategy. The equilibration times obtained using each of the Case Study –1 efficiency curves in simulation is shown in Table 7.1 based on the startup condition where the entire column contains the feed material at its bubble point temperature. Equilibrium is assumed when temperature and composition predicted on each tray remains unchanged (to the 4<sup>th</sup> decimal place), for 5 consecutive time intervals of integration.

**Table 7.1:** Equilibration Time Under Total Reflux for the Different Efficiency Curves.

Efficiency Curve	Equilibration Time (hrs)
E <sub>1.1</sub>	1.30
E <sub>1.3</sub>	1.30
E <sub>1.5</sub>	1.20
E <sub>1.7</sub>	1.40
E <sub>2.0</sub>	14.90

For curve E<sub>2.0</sub>, temperatures at the top of the column agree to the 2<sup>nd</sup> decimal place in less than 0.5 hours after startup, but Trays 3 to 7 take a much longer time to settle as is shown in Table 7.1. Temperatures in this section are in the region 66.1-71.5°C. These equilibration times represent a significant overhead in terms of the energy consumption of the column.

The pinch in the McCabe-Thiele diagram for E<sub>2.0</sub> in Figure 7.5e is seen to occur around Tray 2 which is also where the largest deviation from experimental data was observed in Figure 7.3a. The tray where the simulation results deviates greatest from experimental result is also seen to move up the column to Tray 7 in Figure 7.3b. Because this effect is seen to move up the column during the brief period of distillate withdrawal, it was decided to run the simulation so that all the methanol in the feed is distilled off, to investigate what effect this might

have on the distillate composition (as was observed with the distillate composition in Figure 7.4).

The simulation was run at total reflux until steady state is attained and product withdrawal was started at time  $t = 2.0$  hours. Equilibration times shown in Table 7.1 show that equilibrium as defined here is only achieved after 14.9 hours for efficiency curve  $E_{2.0}$ . Only a qualitative study is being made at this stage so, the distillate composition profile for  $E_{2.0}$  in Figure 7.6 is truncated where the distillate composition approaches 1.0 methanol mole fraction so that distillate withdrawal appears to start after 2hrs as in the other cases. This allows comparison of the behaviour of the distillate composition profile for  $E_{2.0}$  with the other efficiency curves during product withdrawal.

The results are shown in Figure 7.6, which reveals an unexpected behaviour in the distillate composition movement during product withdrawal.

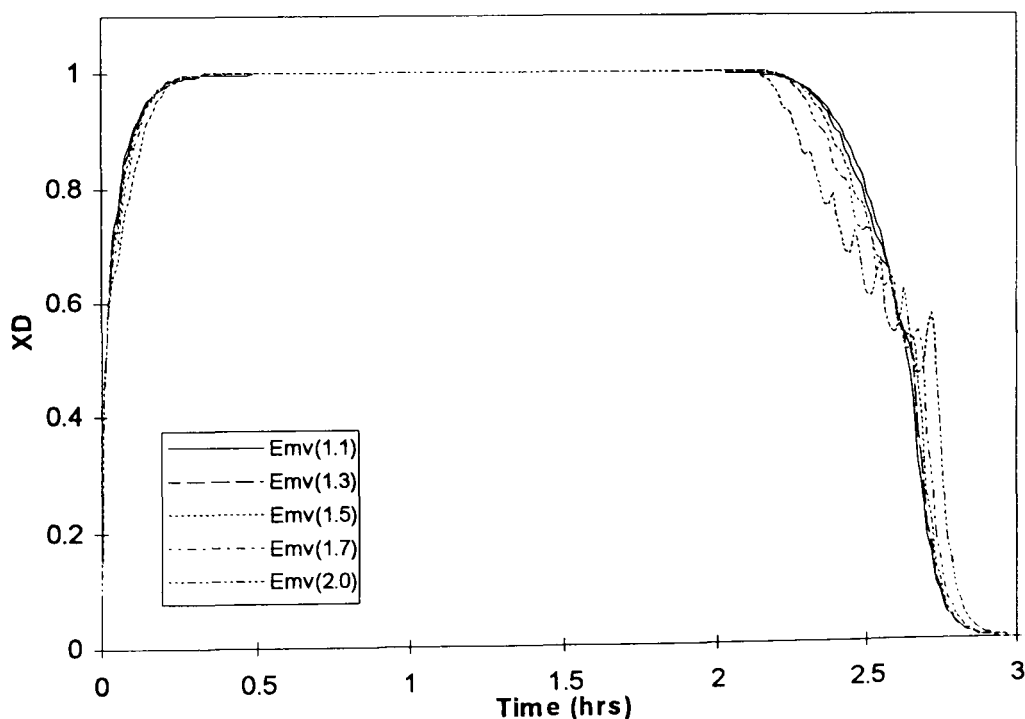


**Figure 7.6:** Distillate Composition Movements for Continuous Distillate Withdrawal after Steady State using Case Study -1 Efficiency Curves

The distillate composition for  $E_{1.1}$  falls smoothly from its steady state value, until all the methanol in the system has been withdrawn. The profile for  $E_{1.3}$  is also seen to fall gradually from its initial steady state value but is also seen to oscillate slightly at the start of the distillate withdrawal. The amplitude and duration of the oscillation increases as the efficiency-concentration relationship becomes more pronounced. In the extreme case ( $E_{2.0}$ ), the distillate composition profile oscillates with a high and increasing amplitude and finally, falls smoothly. Table 7.2 shows how long after distillate withdrawal is begun the distillate composition continues to oscillate, before it finally begins to fall off smoothly and the compositions at which the oscillations apparently stop.

**Table 7.2:** Duration of Distillate Composition Oscillation after Start of Product Withdrawal and the Distillate Composition at which Oscillations Apparently Stop.

	Duration of Oscillation	Distillate Composition
	(mins)	MeOH (mol frac)
$E_{1.3}$	37.26	0.5414
$E_{1.5}$	38.46	0.5313
$E_{1.7}$	40.26	0.5399
$E_{2.0}$	42.66	0.5722

From Figure 7.6 and Table 7.2, as the concentration-efficiency relationship becomes more severe (i.e. going from  $E_{1.1}$  to  $E_{2.0}$ ), the following observations are made:

- The composition around which the oscillation stops and the distillate composition drops off smoothly is almost the same for all the efficiency curves (between 0.53 - 0.54 MeOH mole fraction).

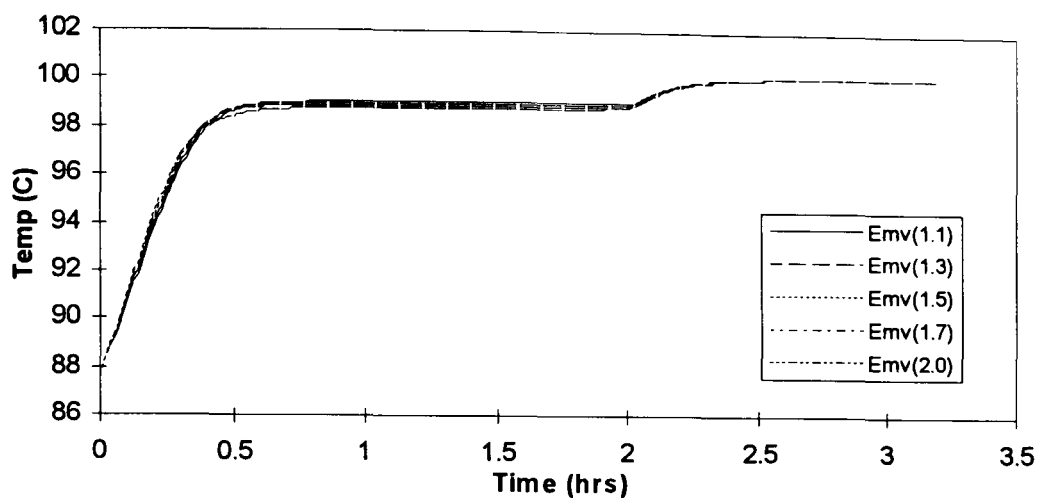
- As the efficiency-concentration relationship becomes more pronounced, the distillate composition oscillates over a longer period of time before falling off smoothly.
- After distillate withdrawal is begun, the methanol mole fraction in the distillate remains close to 1.0 for the milder efficiency curves ( $E_{1.1}$  and  $E_{1.3}$ ) for a longer time but drops below 1.0 almost immediately with the steeper curves (e.g.  $E_{2.0}$ ).
- Though the distillate composition began to fall sooner for the steeper efficiency curves, the average rate of its decay is much slower for these steeper efficiency curves than for the milder curves. As a result, it takes a longer time to exhaust the methanol charged to the system as the efficiency curve becomes steeper. This means that initially, the methanol concentration in the distillate is lower in the steeper efficiency curves until a crossover point. This crossover is seen to occur when the methanol mole fraction is between 0.53 and 0.54, which is also the region when the oscillating distillate composition steadies off. This is also close to the methanol concentration at which the efficiency curve passes through a minimum.
- All the efficiency curves produce a methanol mole fraction in the distillate of around 1.0 at steady state but it takes slightly longer to reach steady state as the efficiency curve gets steeper (1.2 minutes difference between  $E_{1.1}$  and  $E_{2.0}$ ).

This composition oscillation also occurs on the trays in the column, but is more pronounced towards the top of the column, the region with the higher methanol concentration. The amplitude of oscillation is also seen to increase as we move up the column. This is demonstrated in the temperature movements plotted in Figure 7.7 for each tray from startup, through steady state and distillate withdrawal until the entire methanol charged to the system is withdrawn. The observations listed above for the distillate composition trajectory also apply to the trays in the column.

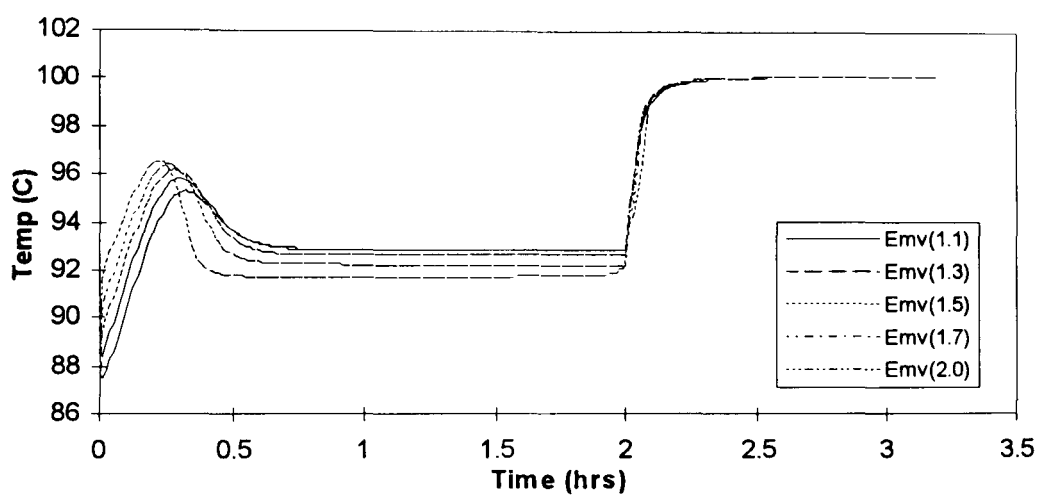
Figure 7.7 shows the movement of the temperature on each tray in the column, predicted using the different efficiency curves, from the initial steady states shown in Figure 7.3a until the methanol charged to the system is distilled off. In the lower section of the column, the steeper efficiency curves result in slightly lower steady state temperatures than the milder efficiency curves (also apparent in Figure 7.3a). Above Tray 3 however, the steady state temperatures are slightly higher for the steeper efficiency curves, except in the region towards the top of the column where all the efficiency curves predict the presence of pure methanol. This implies that the steeper efficiency curves predict a higher methanol concentration in the bottom section of the column than the milder curves and vice versa in the top section of the column. This indicates that the net effect of the steeper efficiency curves is to reduce the degree of separation achieved in the column.

A reduction in the degree of separation achieved in a column is characteristic of lower tray efficiencies and the steeper efficiency curves, which have the higher maximum also have the lower minimum efficiency values. This leads to the deduction that the minimum in the efficiency curve plays a more dominant role on the net effect of the efficiency curve, on the distillation process.

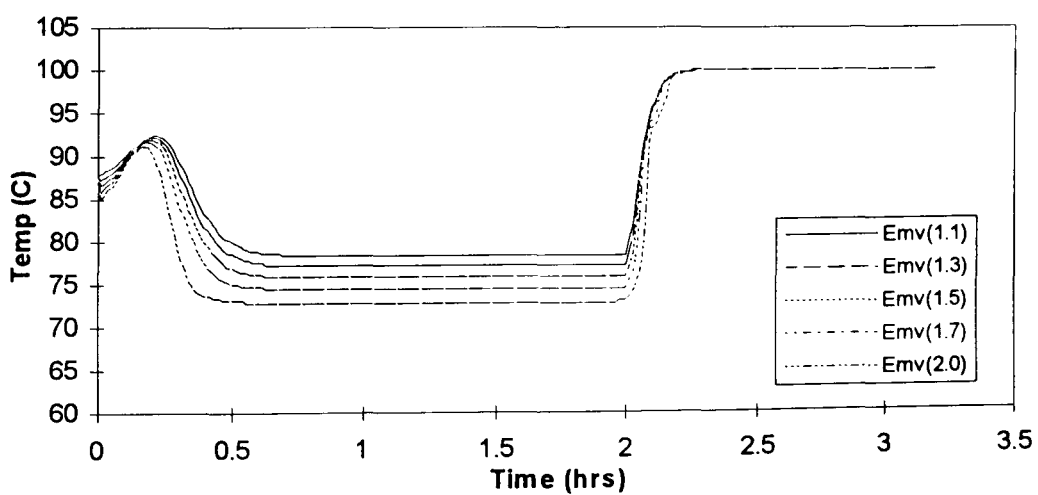
As was observed with the distillate composition movements in Figure 7.6, the temperature profiles for the steeper efficiency curves respond quicker than the shallower curves when distillate withdrawal commences. The average rate at which these temperatures rise are however slower than that of the shallower curves causing the profiles to crossover so that beyond a certain time, the temperature predicted for  $E_{2.0}$  will be lower than that for  $E_{1.7}$ ,  $E_{1.5}$ , etc. This crossover occurs between 71-72°C for all the trays, corresponding to a methanol mole fraction of about 0.54-0.59 (the range where the distillate compositions cross over in Figure 7.6).



a) Reboiler Profile

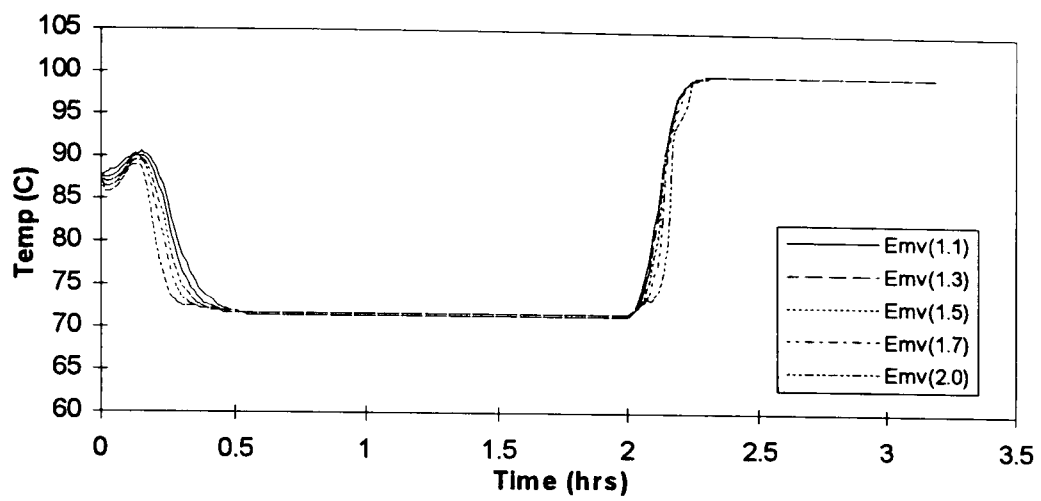


b) Tray 1 Profile.

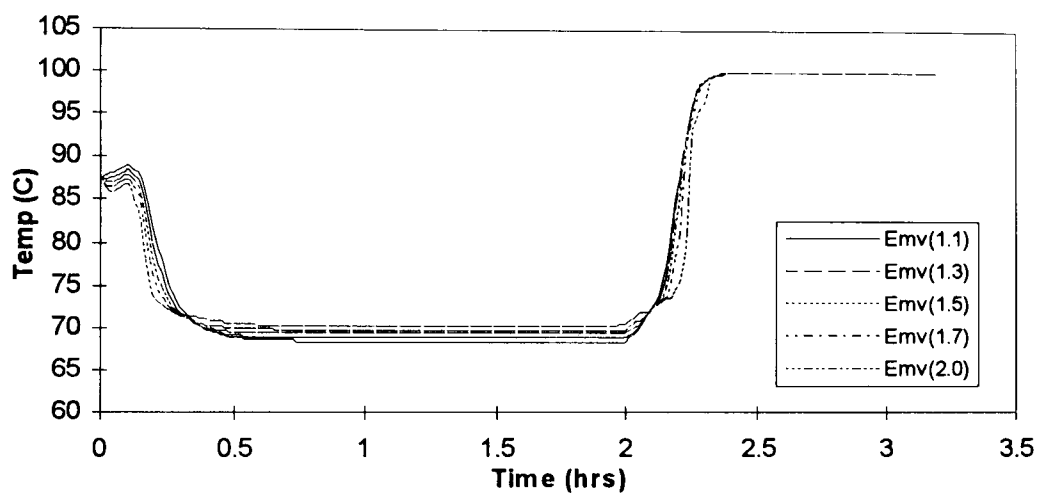


c) Tray 2 Profile

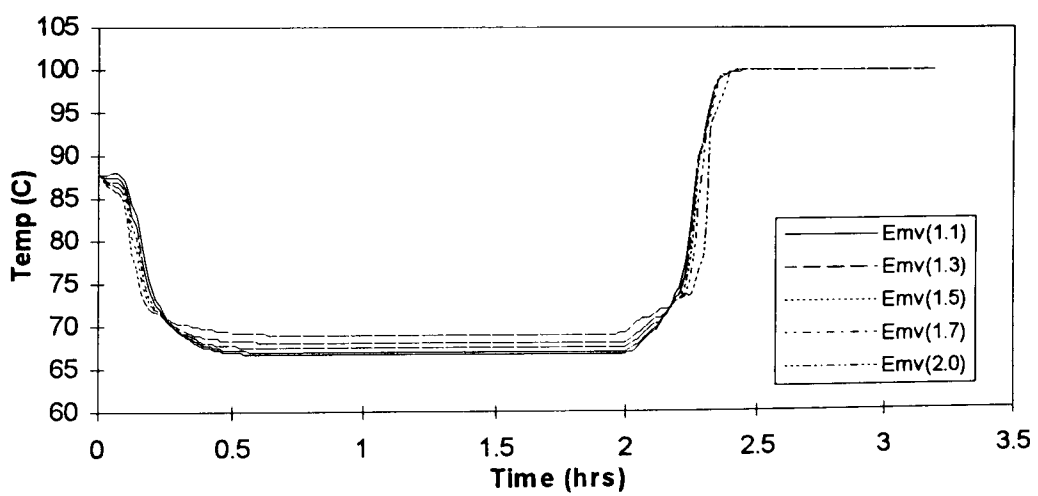
**Figure 7.7:** Transient Temperature Profile for Each Tray from Startup until All the Methanol Charged to the Column is Distilled off. Offtake Starts at Time,  $t = 2.0$  hours.



d) Tray 3 Profile

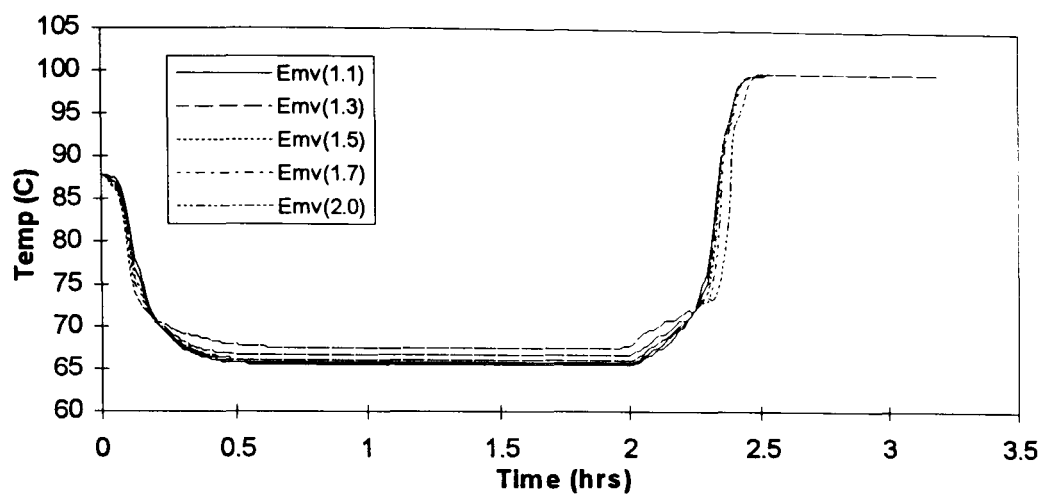


e) Tray 4 Profile

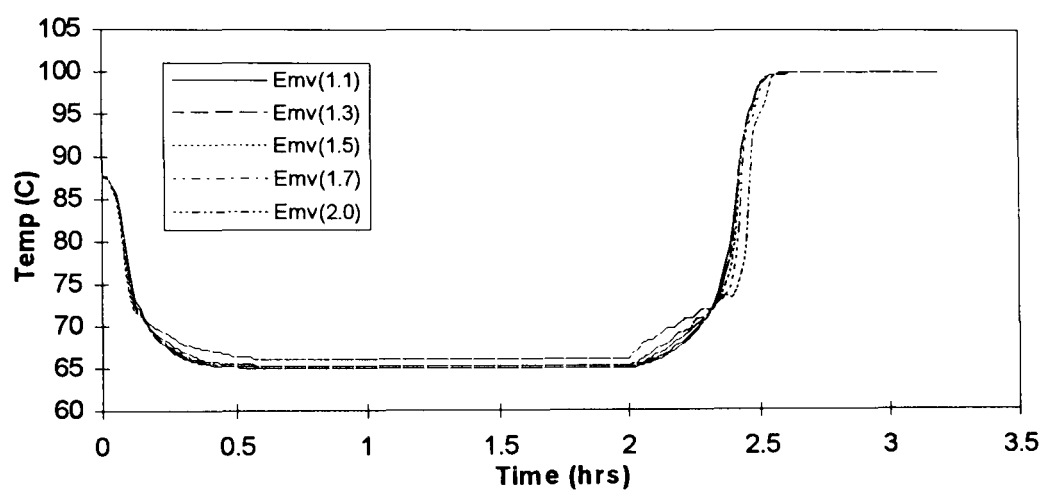


f) Tray 5 Profile

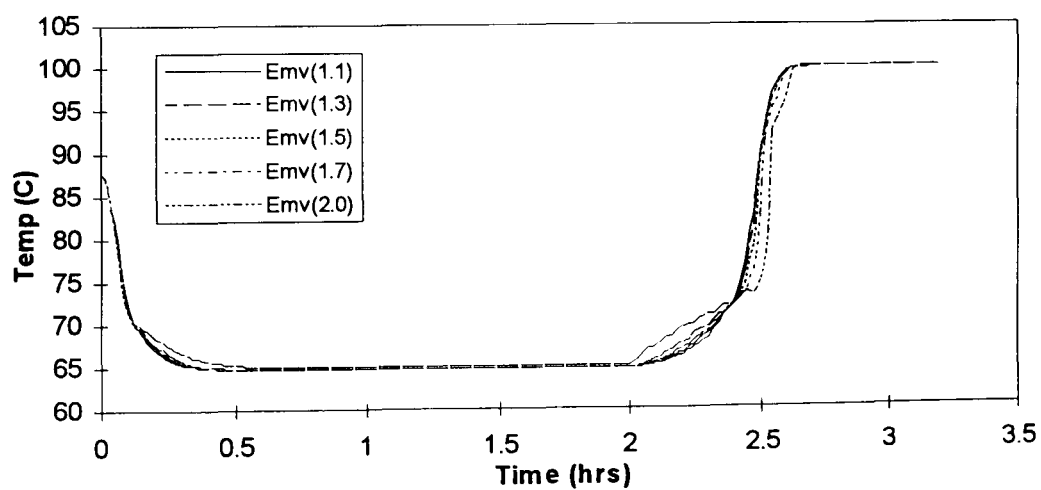
Figure 7.7 Continued . . .



g) Tray 6 Profile

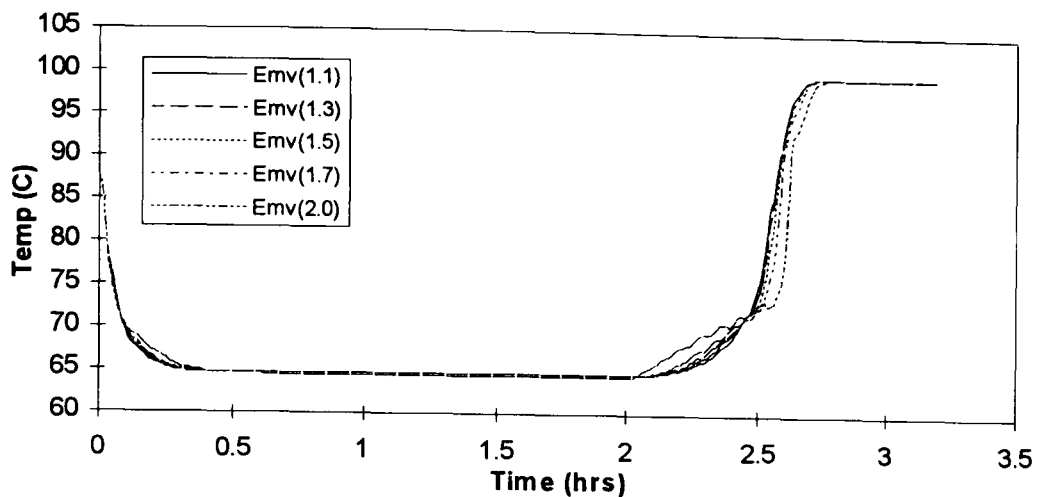


h) Tray 7 Profile

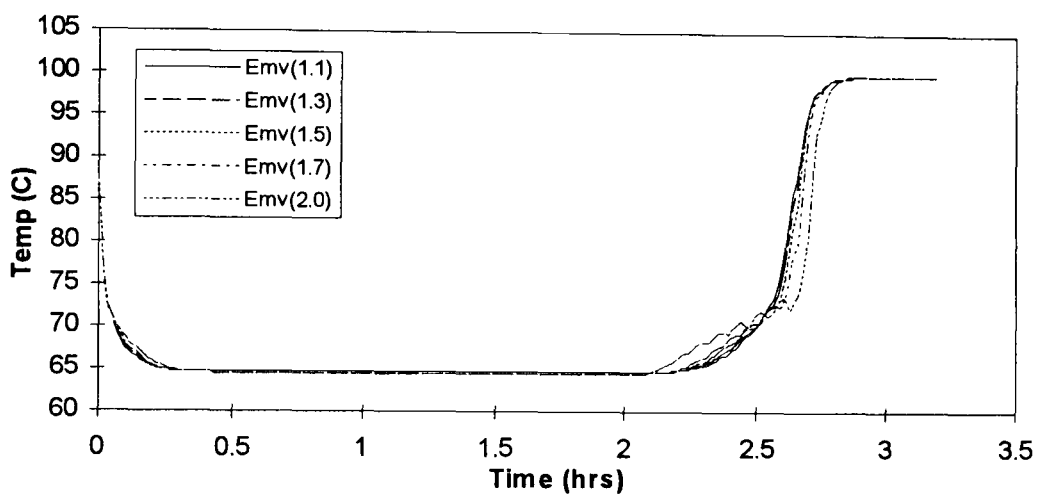


i) Tray 8 Profile

Figure 7.7 Continued . . .



j) Tray 9 Profile



k) Tray 10 Profile

Figure 7.7 Continued . . .

The simulation is also run under this fixed reflux ratio policy such that the column is not allowed to reach steady state before product withdrawal is begun. Instead, product withdrawal starts when methanol composition in the distillate reaches 92%. Because the reflux ratio is fixed, the distillate composition will continue to rise above 92%, and pass through a peak. Product withdrawal is stopped when the distillate concentration drops below 92%. The average concentration of the distillate collected is therefore higher than 92% and the peak distillate composition reached is different for each of the efficiency curves. The results are presented in Figure 7.8 and Table 7.3.

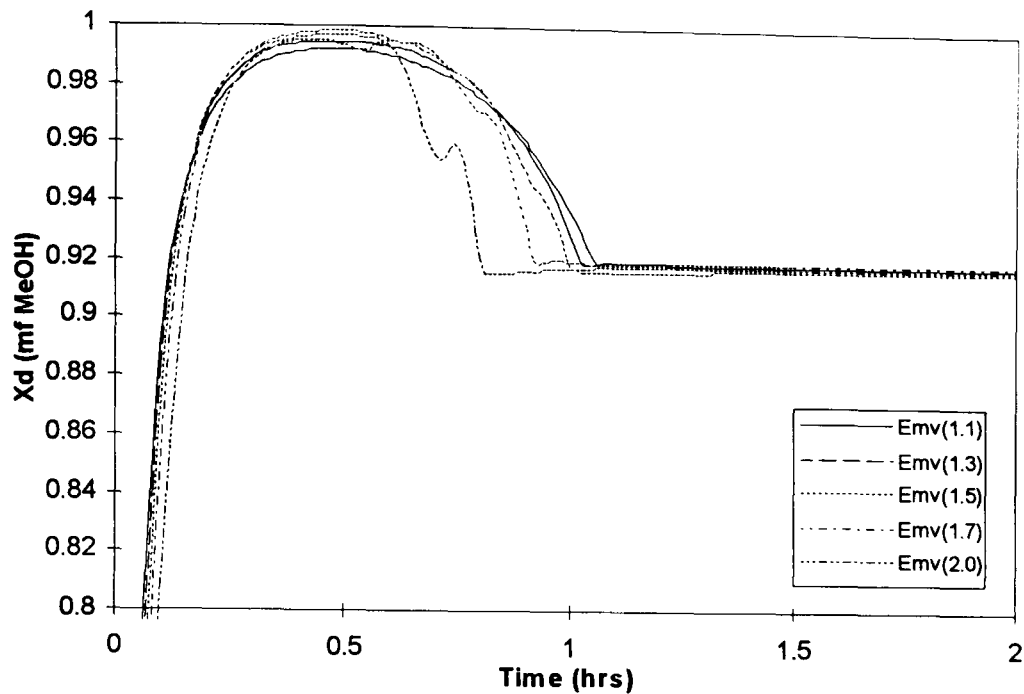


**Figure 7.8:** Distillate Composition Profile For Product Withdrawal When Distillate Composition is Over 92% Methanol.

**Table 7.3:** Product Details For Offtake When Distillate Composition is Over 92%

	Offtake Period	Peak Composition	Average Composition
	(mins)	(MeOH mol frac)	(MeOH mol frac)
$E_{1.1}$	56.28	0.9920	0.9737
$E_{1.3}$	54.00	0.9947	0.9772
$E_{1.5}$	52.02	0.9966	0.9788
$E_{1.7}$	47.52	0.9983	0.9813
$E_{2.0}$	38.82	0.9955	0.9770

As was observed previously, the distillate composition for efficiency curve  $E_{1.1}$  reaches 92% before  $E_{2.0}$ , but the peak composition is slightly lower. Also, the distillate composition remains above 92% for a longer period for  $E_{1.1}$ , compared with  $E_{2.0}$  and the other steeper curves. Because the reflux ratio and

steam rates to the still are similar for all the simulation runs, larger amounts of distillate is collected for runs with higher offtake times (i.e. more distillate is collected using curve  $E_{1.1}$  than that using  $E_{1.3}$  etc.)

The composition results in Table 7.3 do not show a straightforward trend in the peak distillate and average product compositions obtained for the different efficiency curves. However, both the peak distillate composition and the average product composition increase with increasing severity of the efficiency relationship until curve  $E_{1.7}$  but decrease beyond that (average composition for  $E_{2.0}$  is even lower than  $E_{1.5}$ )

### 7.1.1.2 Fixed Distillate Composition Simulation for Case Study –1

The runs described in the previous section are based on the fixed reflux ratio policy. The simulation model was also run using the fixed distillate composition policy which entails varying the reflux ratio to maintain a specified distillate composition. The feed specification was the same as that used for the fixed reflux ratio simulation in the Section 7.1.1.1 (i.e. a 1.168 kmol feed of 0.0925 methanol mole fraction). The feed and operating conditions are equivalent to that listed for Run 6 in Appendix A.

A maximum reflux ratio must be assigned when the column is to be run under the fixed distillate composition policy. This maximum is usually defined by economic parameters, as operation under very high reflux ratios results in energy wastage unless such high reflux ratios are justified by other (e.g. environmental) considerations. A maximum reflux ratio of 20:1 was chosen for this simulation. This value is rather high but was chosen as it gives a longer period of product withdrawal hence, more of the methanol in the feed is distilled off.

The simulation was run with a 92% methanol composition specification in the distillate. This means that the column does not reach steady state, but is run at

total reflux until the distillate composition reaches 92%. Product withdrawal is begun, at a liquid reflux rate given by Equation 4.20, which maintains the distillate composition at the target value. The resulting distillate composition and reflux ratio profiles are presented in Figure 7.9 for the various efficiency-concentration relationships. A similar simulation run is made for a distillate composition specification of 99% methanol and the distillate composition and reflux ratio profiles obtained are presented in Figure 7.10.

The interesting feature in Figure 7.9 and Figure 7.10 is that for the  $E_{1.1}$  efficiency curve, smooth distillate and reflux ratio profiles are obtained. However, for the other efficiency curves (where temperature oscillations were observed during distillate withdrawal under fixed reflux ratio), the reflux ratio profile oscillates in order to maintain the distillate composition at the specified value. The degree of oscillation of the reflux ratio profile also increases as the severity of the efficiency curve increases (ie going from curve  $E_{1.3}$  to  $E_{2.0}$ ).

In the simulation run, when the reflux ratio reaches 20:1, distillate collection is switched to another receiver. The resulting distillate is an off-specification product and is withdrawn at a very low reflux ratio of 2:1 and distillation continues until the still is dry. The product offtake times and quantity of specification product collected are different for each hypothetical efficiency curve. The offtake times and product quantities obtained from simulation are given in Table 7.4. Offtake time here refers to the time from start of distillate withdrawal until distillate composition falls below the specified value and is switched to the slop cut receiver.

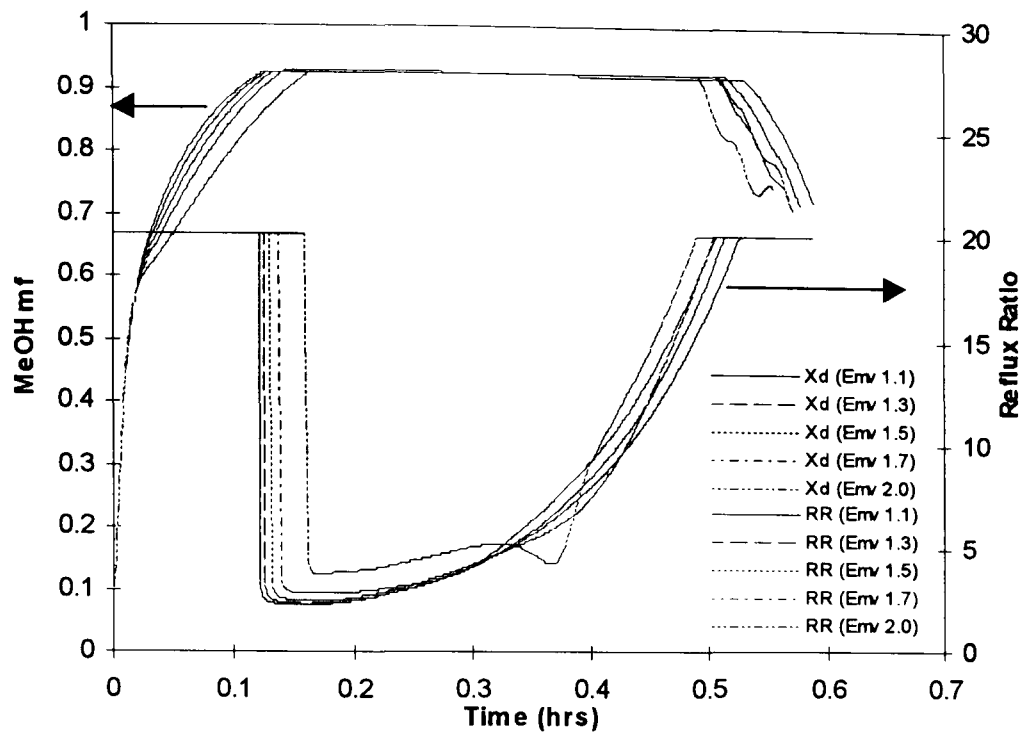


**Figure 7.9:** Case Study 1 Distillate Composition and Reflux Ratio Profiles For 92% MeOH Product - Fixed Distillate Composition Policy

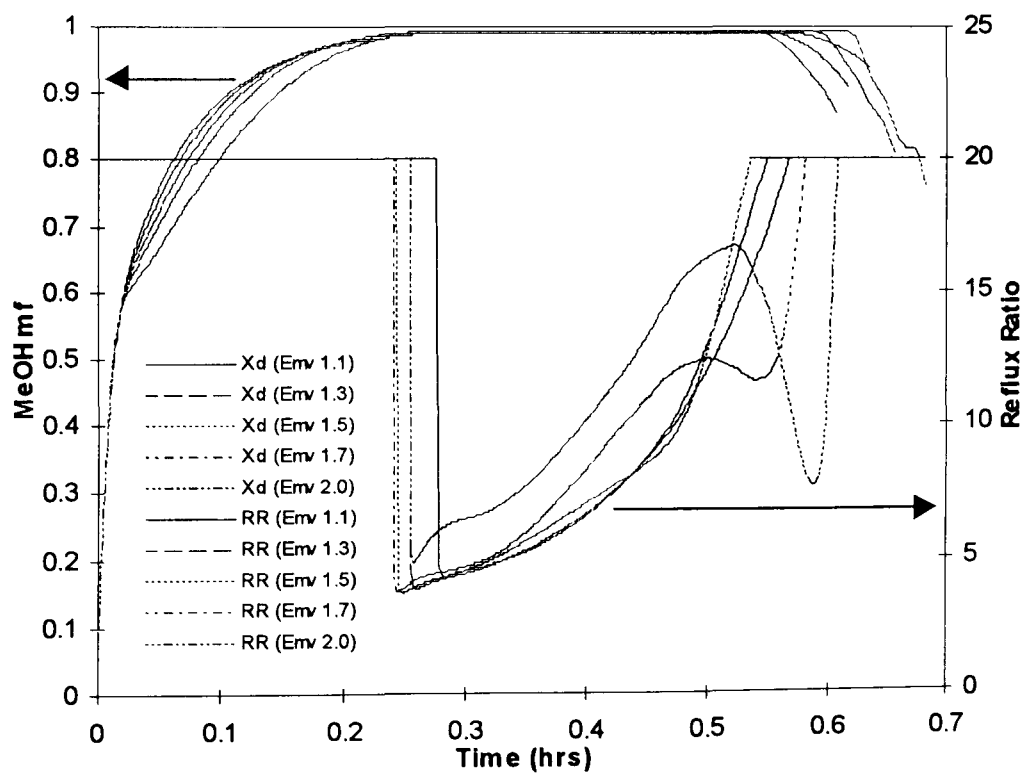


**Figure 7.10:** Case Study 1 Distillate Composition and Reflux Ratio Profiles For 99% MeOH Product - Fixed Distillate Composition Policy

**Table 7.4:** Production details for Fixed Distillate Composition Simulation for Case Study 1

	92% Methanol		99% Methanol	
	Offtake Time (mins)	Product (kmols)	Offtake Time (mins)	Product (kmols)
E <sub>1.1</sub>	24.48	0.0726	17.82	0.0365
E <sub>1.3</sub>	23.52	0.0699	18.12	0.0403
E <sub>1.5</sub>	22.68	0.0674	18.12	0.0420
E <sub>1.7</sub>	22.32	0.0615	21.24	0.0450
E <sub>2.0</sub>	19.98	0.0467	21.96	0.0384

For the 92% methanol product specification, the offtake time (hence amount of specification distillate withdrawn) reduces with increasing efficiency curve severity. With the 99% methanol product specification however, offtake time and amount of distillate collected increase with increasing efficiency curve severity. For curve E<sub>2.0</sub> however, offtake time is higher than that for E<sub>1.7</sub> but the amount of distillate produced is smaller than even that obtained using curve E<sub>1.3</sub>. This is a consequence of the significantly higher-value reflux ratio trajectory required to maintain the specified distillate composition, using curve E<sub>2.0</sub>. The practical significance of these results is investigated and analysed in Section 7.3.

## 7.2 CASE STUDY –2

The second case study is chosen so that the efficiency maximum for the different hypothetical efficiency curves is 1.0 at the ends of the concentration range. Because the efficiency curves of Case Study –2 are not allowed to exceed 1.0, they are related to the curves of Case Study –1 by their minimum. The curves are defined so that their minimum points are equivalent to the minimum points of the curves generated in Case Study -1. The curve equivalent to a maximum efficiency of 1.1 in Case Study –1 will therefore have a minimum

of 0.686, that which is equivalent to the 2.0 maximum will have a minimum of 0.236, etc. These curves are plotted in Figure 7.11 and labelled  $E_{1.1q}$ ,  $E_{1.3q}$ , etc. The subscripts indicate that the respective curves are “equivalent” to a Case Study-1 curve with maximum tray efficiency of 1.1, 1.3 etc.

The hypothetical tray efficiency curves of Case Study –2 are described by the equation

$$E_{mv} = a \sin \pi(2x - 1.5) + b \quad 7.3$$

where  $a = (1 - E_{\min})/2$

and  $b = 1 - a$

The constraint of Equation 7.2 does not apply in this case as the average efficiencies must vary if the maximum is fixed.

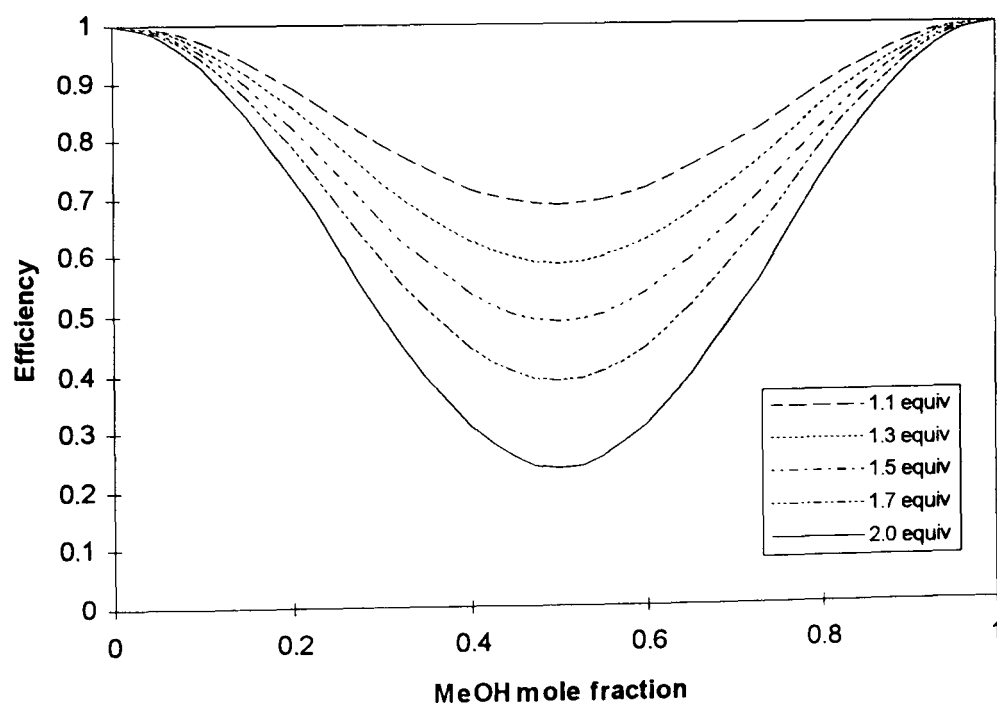


**Figure 7.11:** Assumed Tray Efficiency-Concentration Relationship used For Case Study –2 (Note: Values in legend link to “equivalent” values in Figure 7.2.)

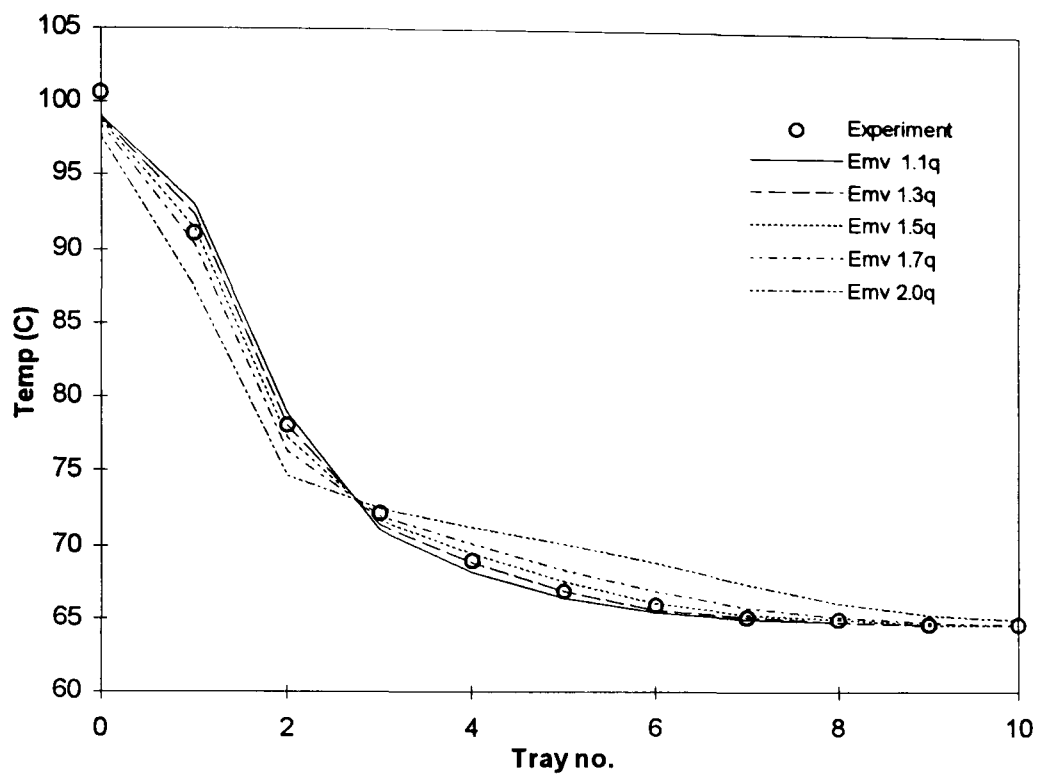
### 7.2.1 Case Study –2 Simulations

The tray efficiency-concentration curves of Case Study –2 are given by Equation 7.3 and the curves are plotted in Figure 7.11.

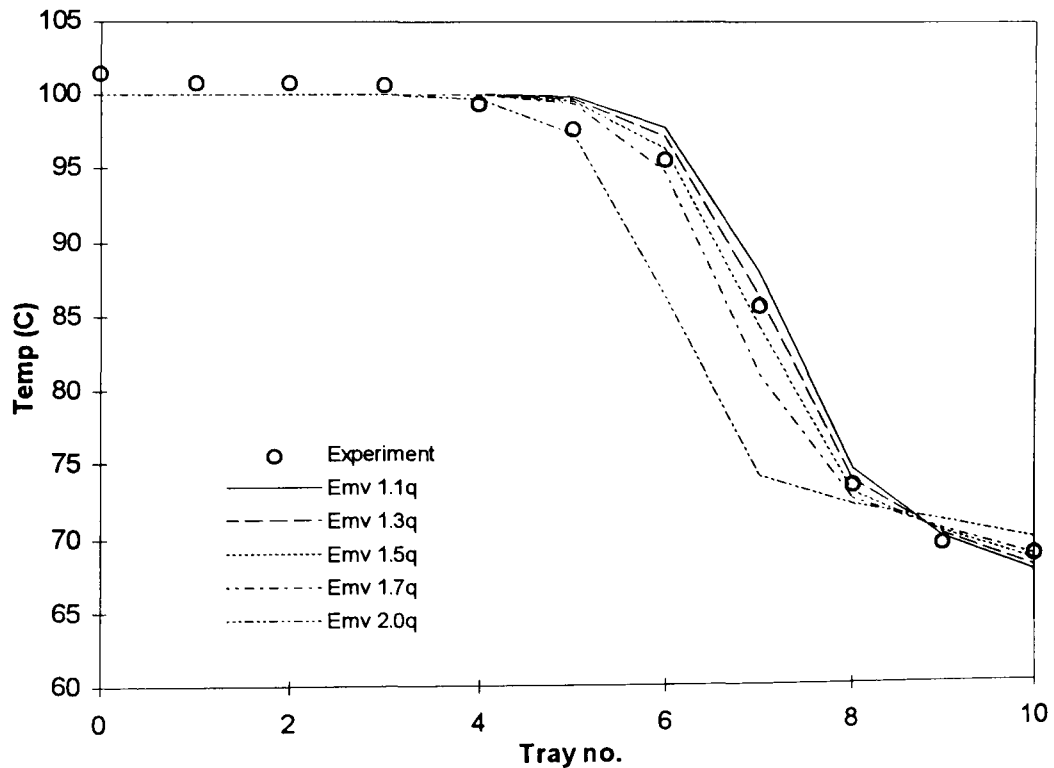
Using the same column setup, charge (1.168 kmols with 0.0925 mole fraction of methanol), and heat input (18 kg/hr steam flow rate at 2.2 bar) described in Section 7.1.1.1 for the Case Study –1 simulations, the simulation was run using the efficiency curves of Case Study –2. The fixed reflux ratio and constant distillate composition policies were considered.

#### 7.2.1.1 Fixed Reflux Ratio Simulation For Case Study –2

The temperature profiles predicted by the simulation for the initial steady state after total reflux startup and a new steady state after a 25 minute distillate withdrawal at a reflux ratio of 4.5, is given in Figure 7.12. The same general trend is observed in these steady state profiles as was obtained with the efficiency curves of Case Study –1 (Figure 7.3). The simulation was also run at a total reflux until steady state and then set to a reflux ratio of 4.5 until the still content was exhausted. Under this operating condition, the efficiency curves in the Case Study –1 simulations that gave the most severe oscillations (from Figure 7.6) were  $E_{1.7}$  and  $E_{2.0}$ . The results obtained for the  $E_{1.7q}$  and  $E_{2.0q}$  efficiency curves are compared with the equivalent Case Study –1 curves in Figure 7.13 and Figure 7.14 respectively. Only the composition profiles for the distillate and for Trays 1, 3, 5, 7 and 9 are shown for the sake of clarity. These profiles show that the steady state compositions predicted by the efficiency curves of Case Study –2 on each tray, are slightly lower than those predicted by the equivalent Case Study –1 curves. The oscillations in tray and distillate composition are also present in the Case Study –2 curves, but to a lesser extent. Also, the rate of depletion of the methanol at each of the locations shown, is slightly slower in Case Study –2 than it is in Case Study –1.



a) Initial Column Steady State after Total Reflux Startup.



b) Final Column Steady State Profiles after Product Withdrawal for 0.417hrs

**Figure 7.12:** Initial and Final Steady State Temperature Profiles for Case Study -2 Efficiency Curves with Different Severities of Tray Efficiency-Concentration Relationship.

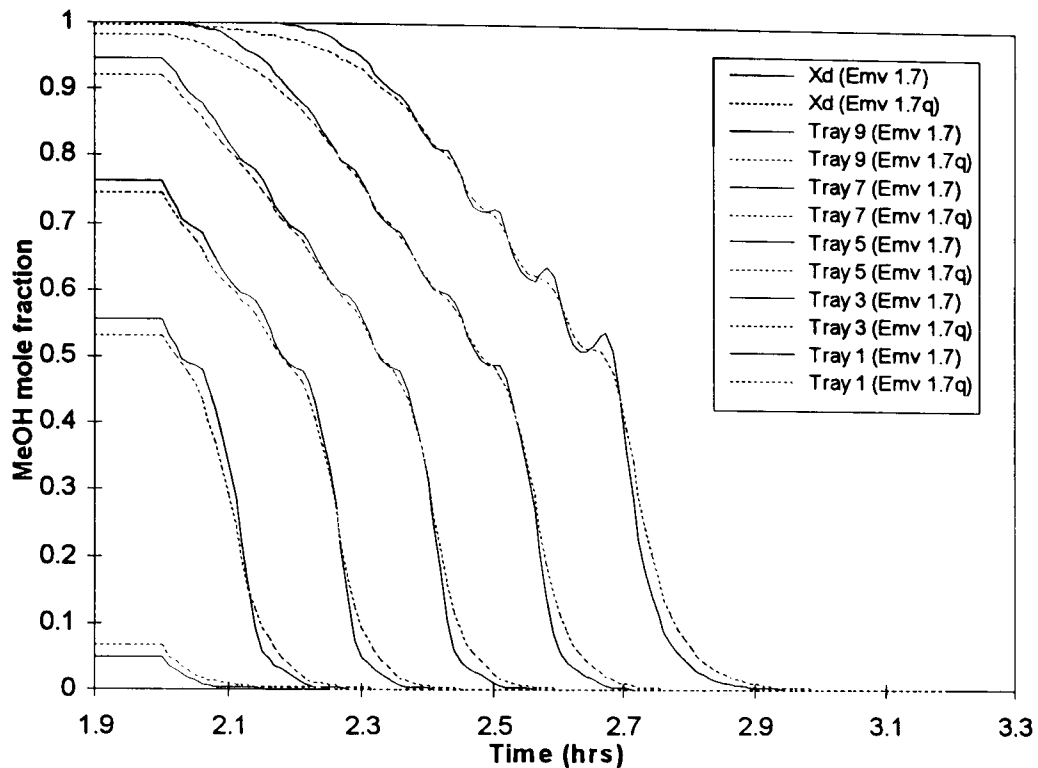


**Figure 7.13:** Transient Composition Profiles for Distillate and Trays 1, 3, 5, 7, 9 using Efficiency curves  $E_{1.7}$  and  $E_{1.7q}$

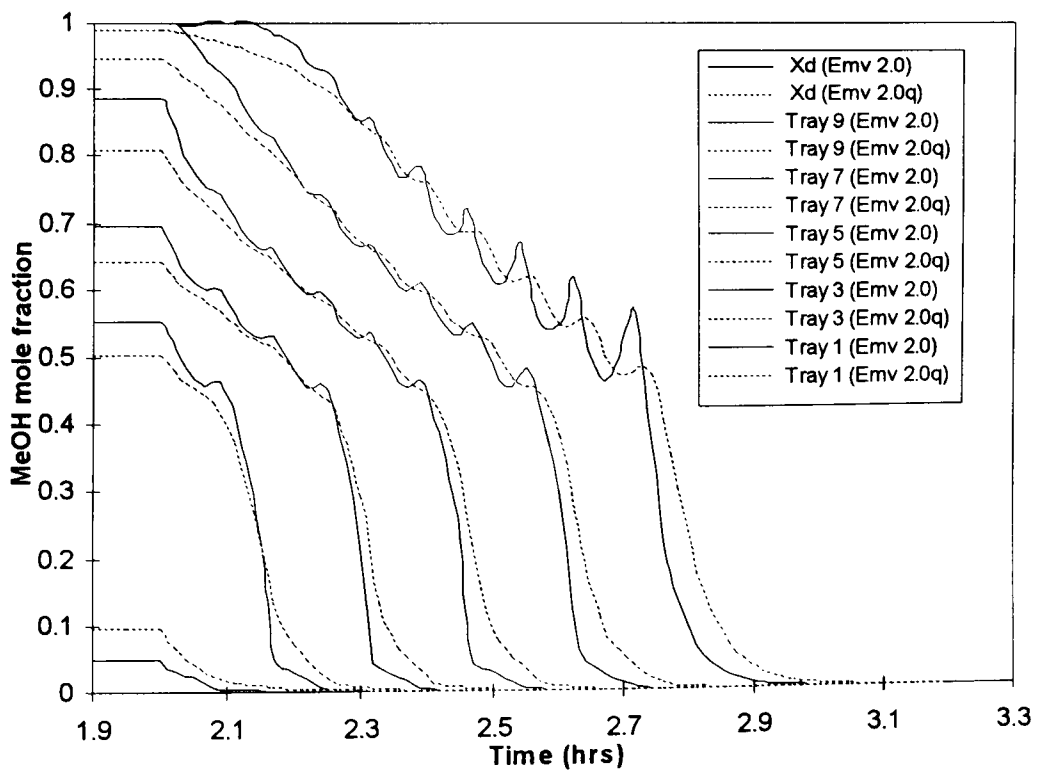


**Figure 7.14:** Transient Composition Profiles for Distillate and Trays 1, 3, 5, 7, 9 using Efficiency curves  $E_{2.0}$  and  $E_{2.0q}$

In Case Study –1, steady state was achieved after about 15 hours of simulation when the column is run at total reflux using efficiency curve  $E_{2.0}$ . In the equivalent curve,  $E_{2.0q}$  however, steady state was reached in 1.12 hours, about the same time it took using the other efficiency curves of Case Study –2.

To explain this anomaly, a look at Table 7.1 reveals a general trend of increasing equilibration time from startup, with increasing efficiency curve for the Case Study –1 curves but the effect is more pronounced for  $E_{2.0}$ . This is because the tray efficiency ranges from 2.0 to 0.236, a very wide range, and varies with composition. This results in a situation where the vapour enrichment is greatly enhanced in the top and bottom sections of the column (very low and very high methanol concentrations) and is greatly retarded in the midsection of the column where the efficiency curve passes through a minimum. These conflicting effects therefore cause a slower approach to steady state in the midsection of the column. For curve  $E_{2.0q}$  however, the range of efficiency values is half that of curve  $E_{2.0}$  and is therefore not greatly affected by this effect.

The distillate composition movement predicted for the different efficiency curves is presented in Figure 7.15. The result shows a similar trend as was observed using the Case Study –1 efficiency curves (Figure 7.6) but with less severe oscillation of the composition movement. Also, the steeper efficiency curve  $E_{2.0q}$  predicts an immediate drop in distillate composition at the start of distillate offtake, compared with the shallower curves. As product offtake progresses however, the distillate compositions predicted by the steeper curves become higher than the shallower curves and this crossover is observed to occur around a distillate composition of 0.53-0.54 methanol mole fraction. This coincides with the composition at which the crossover occurs in simulation using the Case Study –1 efficiency curves and is also in the composition region where the minimum in efficiency occurs.

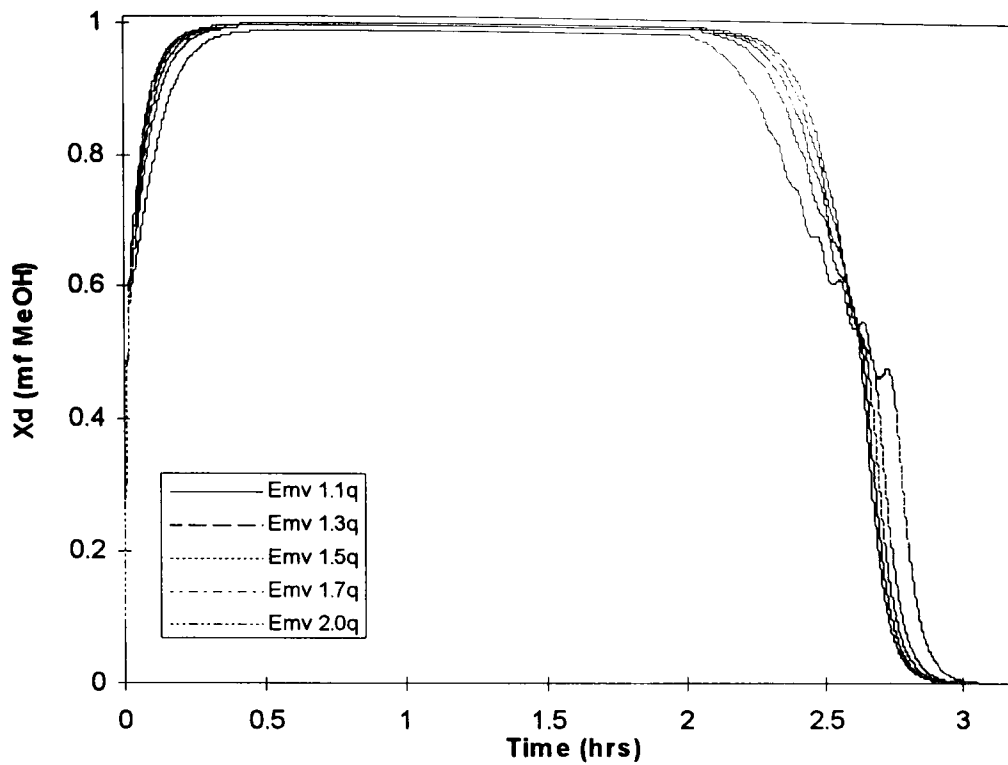


**Figure 7.15:** Distillate Composition Profiles for Case Study 2 with Distillate Withdrawal Start Time,  $t=2.0$  hrs at Reflux Ratio of 4.5.

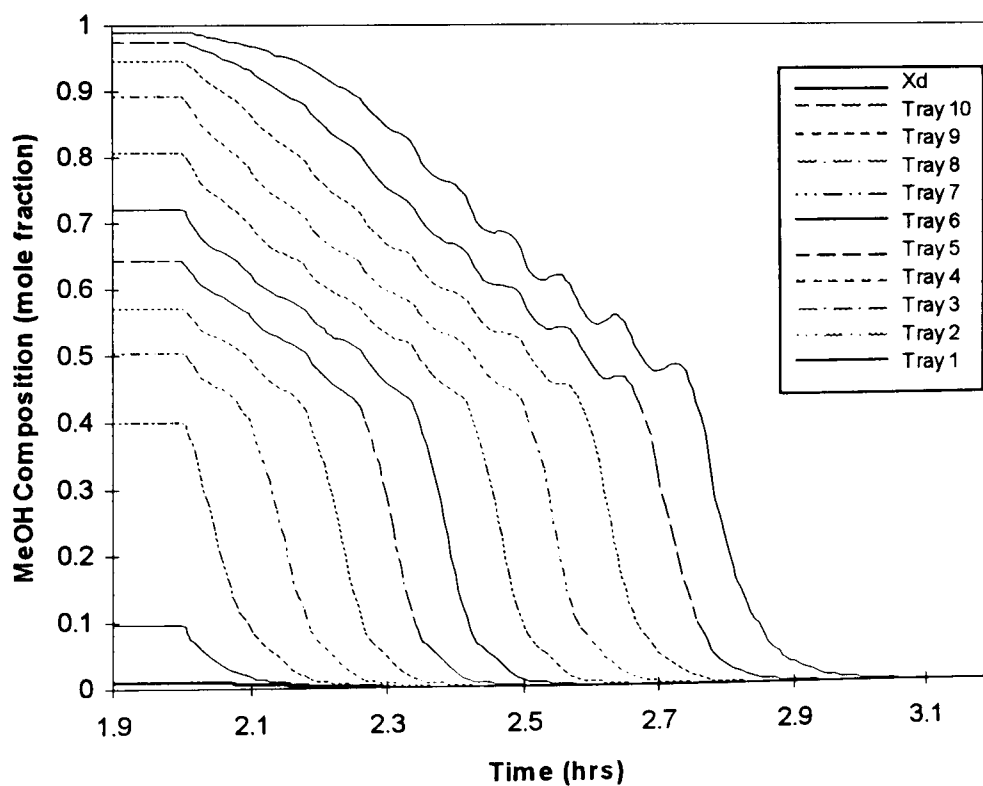


**Figure 7.16:** Composition Trajectory on All Trays during Product Withdrawal until all Methanol is Distilled for Efficiency Curve  $E_{2.0q}$ .

The oscillations are seen in Figure 7.16, to also occur throughout the column as was observed using the Case Study –1 efficiency curves. Also, the oscillations are seen to be more pronounced near the top section of the column.

Poor convergence of the Euler method may explain the oscillations observed but accuracy is improved when smaller time steps are used. However, integration using a step size of  $1 \times 10^{-6}$  hrs also produced oscillatory composition movements, which exactly match those presented in Figure 7.15. Other more sophisticated integration methods must be used to fully ascertain that the oscillations observed here do not arise from the integration method used.

#### 7.2.1.2 Fixed Distillate Composition Simulation For Case Study –2

The operation of the fixed distillate composition policy as described in Section 7.1.1.2 was simulated using the efficiency curves of Case Study –2. The reflux ratio is made to vary, up to a maximum of 20:1, to maintain the specified distillate composition. Beyond this value of reflux ratio (20:1), product withdrawn is diverted to a slop receiver. Distillate composition and reflux ratio profiles obtained are shown in Figure 7.17 and Figure 7.18 for a 92% and 99% methanol distillate specification respectively.

A major observation from these results is that for a 99% methanol product specification, simulation using the efficiency curve  $E_{2.0q}$  does not produce a distillate material of the specified purity. In Figure 7.17 and Figure 7.18, as in Case Study –1, the milder efficiency curves reach the specified distillate composition quicker than the steeper efficiency curves and product withdrawal is begun. But unlike Case Study –1 where product withdrawal for the steeper curves ended before the shallower curves, the trend is not as direct, using the Case Study –2 curves for the simulation. The product withdrawal times and amounts of product withdrawn are given in Table 7.5.

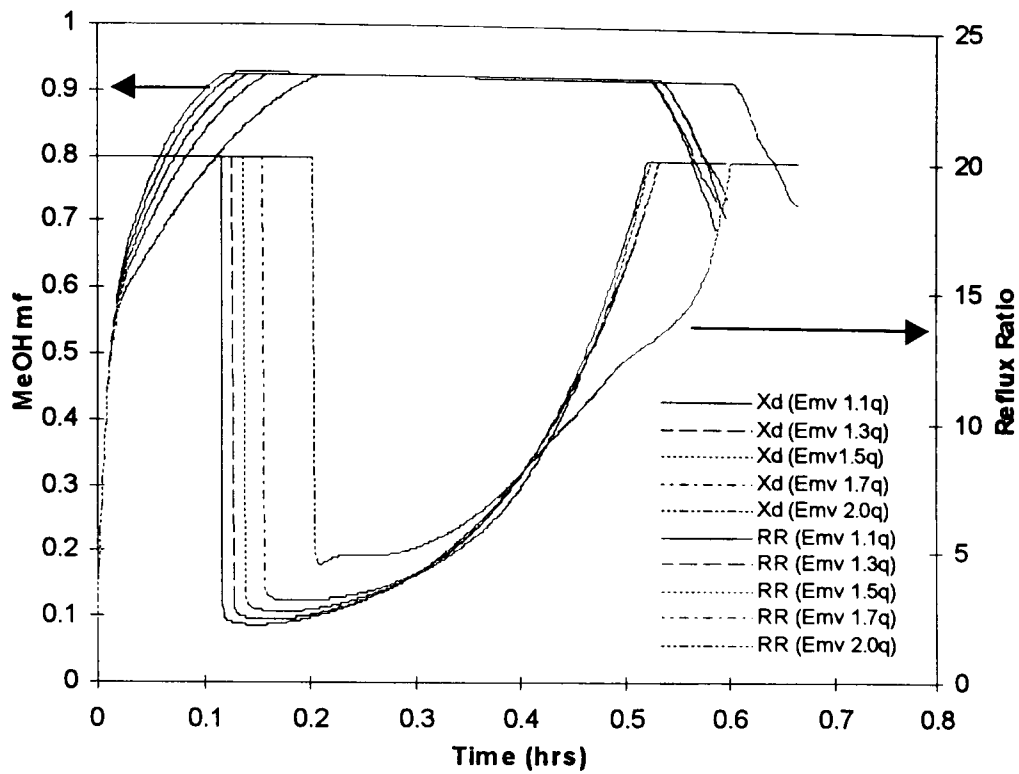


**Figure 7.17:** Case Study 2 Distillate Composition & Reflux Ratio Profiles For 92% MeOH Product - Fixed Distillate Composition Operation

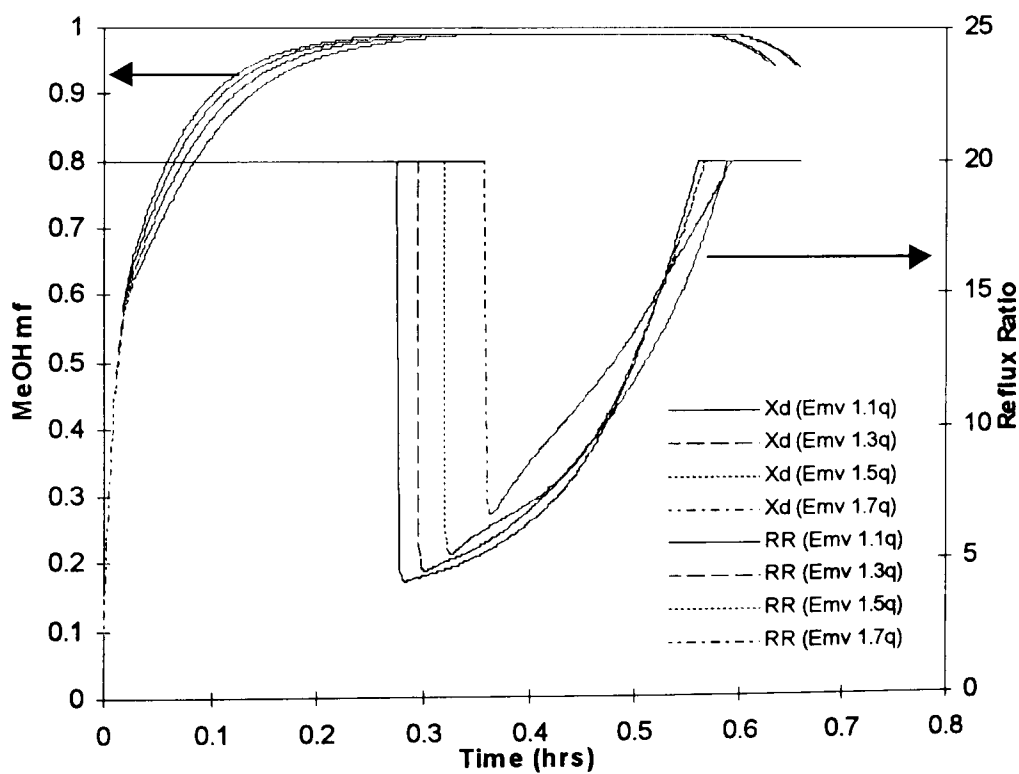


**Figure 7.18:** Case Study 2 Distillate Composition & Reflux Ratio Profiles For 99% MeOH Product - Fixed Distillate Composition Operation

**Table 7.5:** Production details for Fixed Distillate Composition Simulation for Case Study 2

	92% Methanol		99% Methanol	
	Offtake Time (mins)	Product (kmols)	Offtake Time (mins)	Product (kmols)
$E_{1.1q}$	24.66	0.0752	17.52	0.0362
$E_{1.3q}$	24.66	0.0708	17.94	0.0333
$E_{1.5q}$	23.40	0.0655	15.24	0.0269
$E_{1.7q}$	22.86	0.0584	14.28	0.0200
$E_{2.0q}$	24.12	0.0467	-----	-----
$E_{fix}$	26.70	0.0858	15.72	0.0295
$E_{RR}$	32.82	0.0970	7.44	0.0220

### 7.3 ECONOMIC PERFORMANCE IMPLICATIONS OF THE TRAY EFFICIENCY-COMPOSITION DEPENDENCE

The results in the previous sections are difficult to put into perspective without the use of some performance criterion. In order to gain some indication of the potential significance of tray efficiency variation in batch distillation operation, an economic study is performed.

In evaluating the economic performance of a distillation unit, the production costs must be evaluated. This should take into account, the fixed capital and working capital, cost components. Fixed capital includes the investment costs as well as cost of equipment and auxiliaries required until the unit is ready for commissioning. Working capital on the other hand is the additional capital needed, over and above the fixed capital investment, to start the unit up. The operating costs include cost of material, maintenance, operating labour, utilities and other annual capital charges required to keep it running.

The aim here is not to calculate real costs, but to assign a cost factor to the performance of the column when the simulation is run using the efficiency curves of both case studies. This aids the comparison of the economic performance of the column using a given efficiency curve, relative to its performance using a different efficiency curve. A few simplifications are therefore made:

- The analyses are carried out on the basis of an existing distillation plant and so no fixed capital cost components are considered.
- All the cases evaluated will incur similar labour costs so, labour cost is not accounted for in this economic evaluation.
- The feed costs for the case studies considered are all the same and is therefore not considered in the analysis.
- Cooling water costs are very small compared with other costs and will not be included in the cost components.

This reduces the items considered in the economic evaluation to steam utilities and finished product cost.

The performance factor used to analyse the potential significance of these efficiency-concentration relationships is the net product cost (or annual productivity),  $P_c$ . Based on a total operating time of 8000 hours per annum, the net product cost is defined by

$$P_c = \frac{8000}{\text{cycle time} + 0.5} \left( Q_p C_p - M_{st} C_{st} \right) \quad 7.4$$

where  $Q_p$  = amount of product distilled per batch (kg)

$C_p$  = Value of finished product (£/kg)

$C_{st}$  = cost of steam utility (£/kg)

$M_{st}$  = amount of steam used per batch (kg)

The cycle time is the total time taken from startup until all specification distillate is withdrawn. A half hour (0.5 hours) is added to the batch cycle time predicted by the model to account for the time taken to empty and re-charge the column between batches (i.e. column “turn-around” time). The costs and values of materials and utilities used are:

- Steam (low pressure)      £0.0024 / kg. (Pitt (1996))
- 92% methanol product      £0.2 / kg. (Pitt (1996))
- 99% methanol product      £0.3 / kg (assumed value).

Amount of product, steam usage and annual productivities are presented in Table 7.6 and Table 7.7 respectively for the 92% and the 99% methanol product purity specification for simulation using the efficiency curves of Case Study –1. Similar information for simulation using the Case Study –2 efficiency curves are presented in Table 7.8 and Table 7.9 for a 92% and 99% methanol product specification.

Annual productivities are also presented in Table 7.6 to Table 7.9 for simulation under fixed distillate composition policy using a fixed efficiency (Overall Column Efficiency Model) of 0.824 throughout the column (the average of the efficiencies obtained experimentally for a methanol/water mixture). The Overall Column Efficiency Model was also run (using an efficiency of 0.824) under fixed reflux ratio policy, at a reflux ratio of 4.5 and the results are also shown in Table 7.6 to Table 7.9. For the fixed reflux ratio operation, distillate withdrawal begins when the instantaneous distillate composition reaches the specified value and continues even after it falls below this value, until the average composition of the distillate collected, equals the specified composition. The results for the Overall Column Efficiency Model simulation is labelled  $E_{fix}$  for the constant distillate composition policy simulation and  $E_{RR}$  for the constant reflux ratio simulation.

**Table 7.6: Product and Utilities for 92% Methanol Purity Specification Using Case Study 1 Efficiency Curves**

	<b>Product per Batch (kg)</b>	<b>Steam Used per Batch (kg)</b>	<b>Batch Time (mins)</b>	<b>Annual Productivity (£/annum)</b>
<b>E<sub>1.1</sub></b>	2.3262	9.522	31.74	184.04
<b>E<sub>1.3</sub></b>	2.2397	9.306	31.02	176.68
<b>E<sub>1.5</sub></b>	2.1596	9.144	30.48	168.63
<b>E<sub>1.7</sub></b>	1.9706	9.180	30.60	137.66
<b>E<sub>2.0</sub></b>	1.4964	8.874	29.58	69.52
<b>E<sub>fix</sub></b>	2.7492	10.170	33.90	229.68
<b>E<sub>RR</sub></b>	3.1081	12.039	40.14	227.67

**Table 7.7: Product and Utilities for 99% Methanol Purity Specification Using Case Study 1 Efficiency Curves**

	<b>Product per Batch (kg)</b>	<b>Steam Used per Batch (kg)</b>	<b>Batch Time (mins)</b>	<b>Annual Productivity (£/annum)</b>
<b>E<sub>1.1</sub></b>	1.1695	10.332	34.44	76.64
<b>E<sub>1.3</sub></b>	1.2903	10.026	33.42	111.08
<b>E<sub>1.5</sub></b>	1.3458	9.828	32.76	128.38
<b>E<sub>1.7</sub></b>	1.4419	10.710	35.70	128.24
<b>E<sub>2.0</sub></b>	1.2304	11.178	37.26	71.97
<b>E<sub>fix</sub></b>	0.9452	10.890	36.30	16.08
<b>E<sub>RR</sub></b>	0.7049	7.228	24.12	33.71

**Table 7.8:** Product and Utilities for 92% Methanol Purity Specification Using Case Study 2 Efficiency Curves

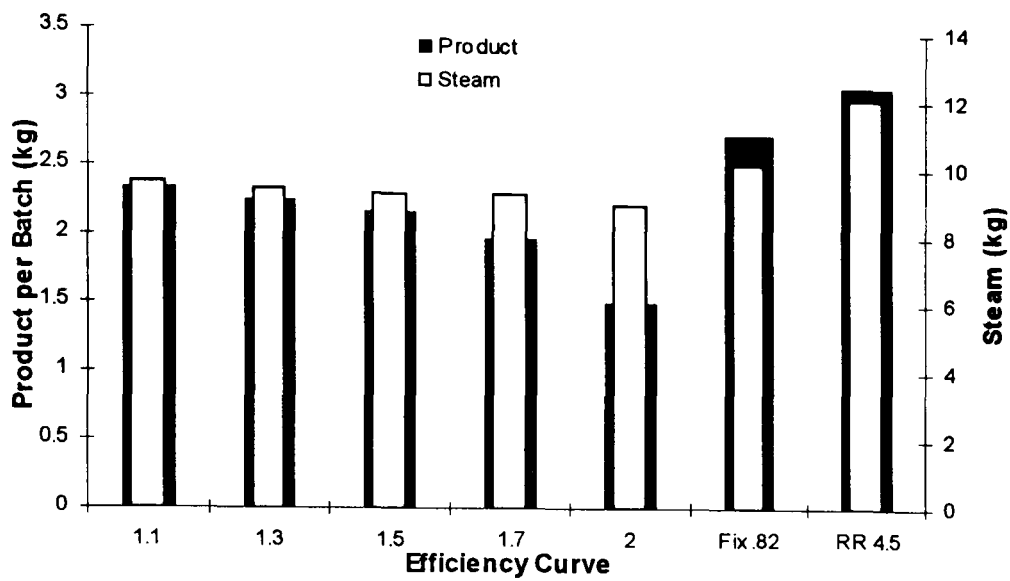
	<b>Product per Batch (kg)</b>	<b>Steam used per Batch (kg)</b>	<b>Batch Time (mins)</b>	<b>Annual Productivity (£)</b>
<b>E<sub>1.1</sub></b>	2.4096	9.486	31.62	198.05
<b>E<sub>1.3</sub></b>	2.2686	9.666	32.22	171.06
<b>E<sub>1.5</sub></b>	2.0988	9.504	31.68	149.15
<b>E<sub>1.7</sub></b>	1.8713	9.666	32.22	109.75
<b>E<sub>2.0</sub></b>	1.4964	10.890	36.30	27.45
<b>E<sub>fix</sub></b>	2.7492	10.170	33.90	229.68
<b>E<sub>RR</sub></b>	3.1081	12.039	40.14	227.67

**Table 7.9:** Product and Utilities for 99% Methanol Purity Specification Using Case Study 2 Efficiency Curves

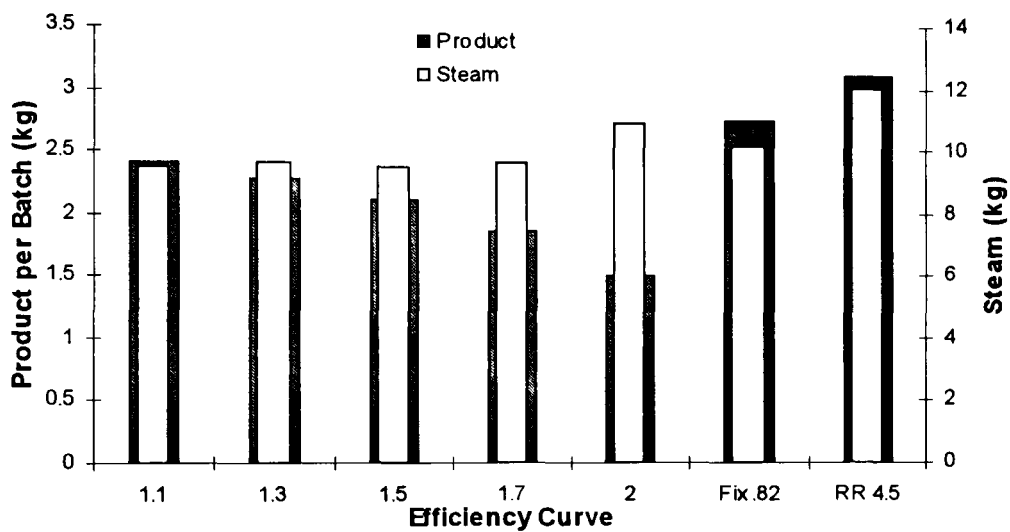
	<b>Product per Batch (kg)</b>	<b>Steam used per Batch (kg)</b>	<b>Batch Time (mins)</b>	<b>Annual Productivity (£)</b>
<b>E<sub>1.1</sub></b>	1.1599	10.224	34.08	76.85
<b>E<sub>1.3</sub></b>	1.0670	10.692	35.64	46.43
<b>E<sub>1.5</sub></b>	0.8619	10.332	34.44	7.90
<b>E<sub>1.7</sub></b>	0.6408	10.746	35.82	-47.88
<b>E<sub>2.0</sub></b>	----	----	----	----
<b>E<sub>fix</sub></b>	0.9452	10.890	36.3	16.08
<b>E<sub>RR</sub></b>	0.7049	7.228	24.12	33.71

A graphic representation of this data is given in Figure 7.19 to Figure 7.21. These results show that for the 92% methanol product purity specification, the highest column annual productivity is obtained using curve  $E_{1.1}$  in the Variable Efficiency Model simulations and the worst, using curve  $E_{2.0}$ . Simulation using the Overall Column Efficiency Model under fixed reflux ratio and fixed distillate composition policies give significantly better performance than the best performance obtained for the Variable Efficiency Model simulations using the different tray efficiency-concentration relationships. Closer observation shows that the fixed reflux ratio policy operation has the largest energy consumption but also produces the largest amount of specification product.

This is because when operating under the fixed reflux ratio policy, offtake starts when the distillate composition reaches the specified value. It continues to rise even after product withdrawal is begun until it reaches a maximum. The distillate composition will eventually begin to drop as the methanol in the system is depleted. Because distillate withdrawal continues until the average composition of the collected distillate equals the specified product purity, the fixed reflux ratio operation may not produce better performance at a higher purity requirement. This is evident in the results for a 99% methanol product purity specification where the column performance using the Overall Column Efficiency Model is generally worse than that using the Variable Efficiency Model simulation. In this case, some increase in the severity of the concentration efficiency relationship is seen to be beneficial (Figure 7.21).

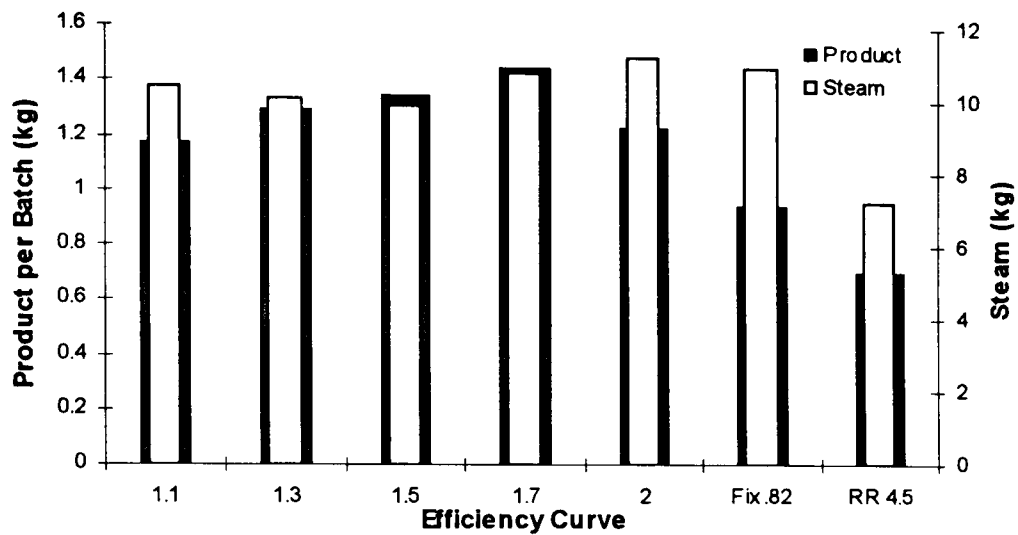


a) 92% Methanol Purity for Case Study 1 Efficiency Curves

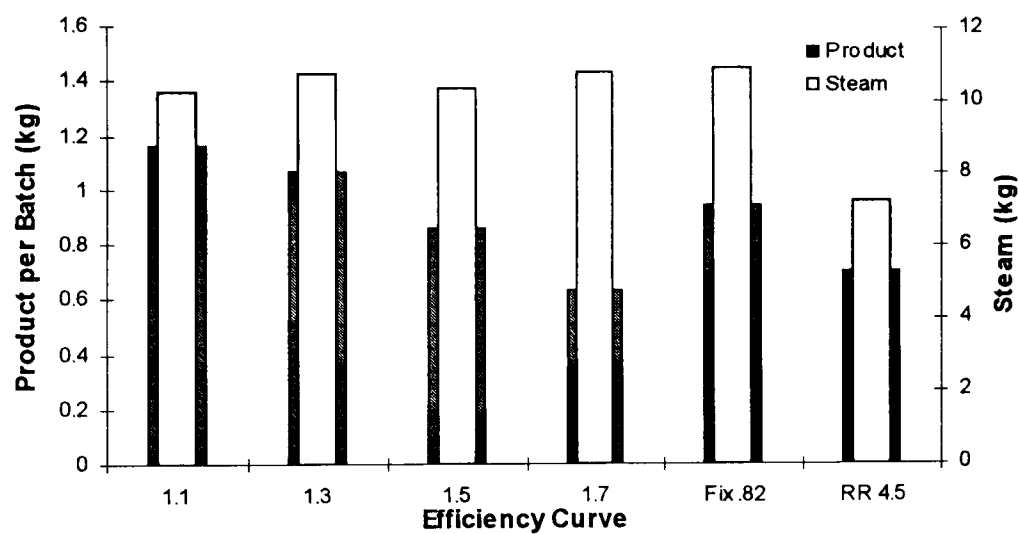


b) 92% Methanol Purity for Case Study 2 Efficiency Curves

**Figure 7.19:** Product and Steam Utilities for Simulation Using the Different Efficiency Curves for a 92% Methanol Specification



a) 99% Methanol Purity for Case Study 1 Efficiency Curves



d) 99% Methanol Purity for Case Study 2 Efficiency Curves

**Figure 7.20:** Product and Steam Utilities for Simulation Using the Different Efficiency Curves for a 99% Methanol Specification

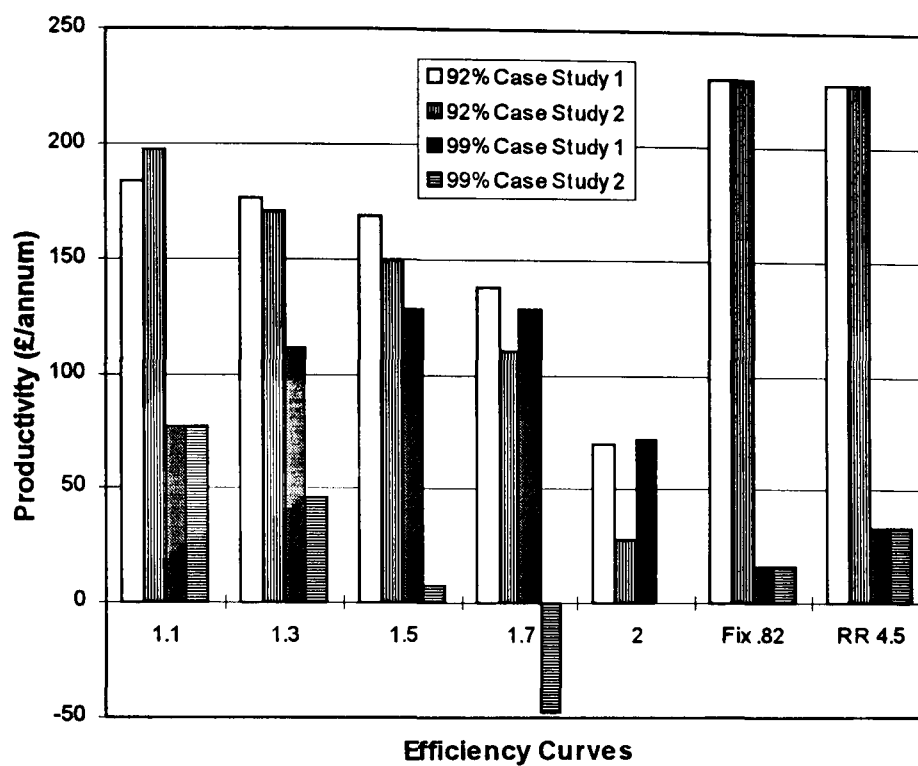


**Figure 7.21:** Annual Performance of the Different Efficiency Curves for a 92% and a 99% Methanol Specification.

# CHAPTER EIGHT

## RESULTS ANALYSIS

### 8.1 MODEL BEHAVIOUR AND ACCURACY

In the context of batch distillation, three different ways of accounting for tray efficiency have been considered in this study:

- the Overall Column Efficiency Models where a single value efficiency is used in the column.
- the Constant Efficiency Model where tray efficiencies are fixed on any tray but may differ from tray-to-tray.
- the Variable Efficiency Model where the efficiency on each tray is not constant but varies with time as a function of the concentration of the mixture on the tray.

The Overall Column Efficiency Model was run using an efficiency of 0.45. This value was obtained by a trial and error process to give an efficiency value that produces a temperature profile, which matches that observed experimentally. As the distillation progresses however, the column temperature profile predicted by the Overall Column Efficiency Model departs increasingly from the observed experimental profile. (Figure A.2). The Overall Column Efficiency Model was also run using an efficiency of 0.824, the average efficiency estimated from experimental data for a methanol/water mixture. Comparing the simulation with experimental results once more shows that this model gives a good agreement with the

experimental temperature profile at one stage during the distillation but not at all stages in the progress of the distillation (Figure 6.3).

The Constant Efficiency Model on the other hand, gives a good match with experimentally observed steady state temperature profiles at different stages during the progress of the distillation. It also predicts temperature movements on the trays during product withdrawal, which agrees with those observed experimentally (Figure 5.3 to Figure 5.7).

When the same simulation runs are carried out using the Variable Efficiency Model, a small but evident improvement was observed in the predicted column steady state temperature profiles (Figure 6.3 to Figure 6.6) for methanol/water mixture. In the transient period during product withdrawal, the constant and variable efficiency models predict very similar tray temperature movements but the final steady state temperatures predicted by the Variable Efficiency Model are closer to those obtained experimentally (Figure 6.7 to Figure 6.11).

The dependence of tray efficiency on composition for a methanol/water mixture is not very severe (Figure 6.2) and in order to facilitate the investigation of the potential effects of this tray efficiency-concentration relationship, two forms of efficiency vs concentration curves were assumed. These efficiency curves are hypothetical extensions of the relationship observed for methanol/water mixture and consider the case where tray efficiency may exceed 1.0 at the ends of the concentration range (Case Study –1) and that where it is restricted to a maximum of 1.0 (Case Study –2). The efficiency curves of both case studies pass through a minimum in the intermediate composition range.

The following is an analysis of the results from simulation, using the Variable Efficiency Model including the various efficiency-concentration curves of both case studies, presented in the preceding chapter.

### 8.1.1 Equilibration Time

In the simulations, equilibrium as defined in this work, is attained when consecutive predicted temperatures and compositions on all trays agree to the 4<sup>th</sup> decimal. In the results for the efficiency curve of Case Study 1, the average equilibration time for curves  $E_{1.1}$  to  $E_{1.7}$  was approximately 1.3 hours. For  $E_{2.0}$  however, equilibrium, as defined in this work, was only attained after 14.9 hours. The temperatures at the top and bottom of the column reach their steady state values after about 0.5 hours, just as with the other efficiency curves. In the mid-section of the column (between trays 3 and 7), the temperatures come to within 1°C of their steady state values within the same 0.5 hours but agreement to the 4<sup>th</sup> decimal only occurs after 14.9 hours.

The top and bottom of the column consists of almost pure methanol and water respectively, while the midsection of the column is the two-component region. In this section of the column, tray temperatures range between 66.1 and 71.5°C, corresponding to a methanol concentration of 90-58%. The efficiency curve approaches its minimum in this region, with values less than 0.3 at 58% methanol concentration, and this could offer an explanation for this sluggish advance towards steady state.

For the efficiency curves of Case Study 2, similar equilibration times were observed for the efficiency curves  $E_{1.1q}$  to  $E_{1.7q}$ , but simulation using efficiency curve  $E_{2.0q}$  did not produce a 99% methanol concentration distillate. This is a consequence of the nature of the efficiency curve. Using curve  $E_{2.0}$ , a 99% product purity is attainable because of the very high efficiency values at the concentration ends which compensates for the low values in the mid-composition region. In  $E_{2.0q}$  however, efficiency at the concentration ends is restricted to a maximum of 1.0 and is thus unable to compensate adequately for the low efficiencies of the mid-composition region.

### 8.1.2 Slope of the Equilibrium Line.

The effect of the tray efficiency-concentration dependence on the equilibrium lines is shown in the McCabe-Thiele diagrams of Figure 7.5 for the Case Study –1 efficiency curves. Curve  $E_{1.1}$ , which is closest to the actual efficiency-concentration curve observed for methanol/water mixture, produces an equilibrium line closest to the actual equilibrium line for the mixture. The apparent effect of the steeper efficiency curves is to move the equilibrium line closer to the operating line (which lies along the  $y = x$  line under total reflux operation). In the most severe efficiency curve  $E_{2.0}$ , a pinch almost occurs between the equilibrium and operating lines. This near-pinch condition occurs in the 0.5 methanol mole fraction region, corresponding to the composition at which the efficiency curve passes through a minimum.

The implication is that separation is easiest with the less severe efficiency curves (e.g.  $E_{1.1}$ ) and most difficult with the steeper curves ( $E_{2.0}$ ) despite the very high efficiencies at the concentration ends. This suggests that in the distillation of a given mixture, more stages will be required for a specified separation, the more severe the tray efficiency-concentration dependence.

The effect of the high efficiency at the concentration ends is also, more noticeable in the low methanol concentration region, where the enrichment of the vapour rising from a tray is significantly enhanced, compared to that from the other trays. In the high methanol composition region though, only a limited degree of enrichment is possible and the high efficiencies in this region do not have a significant effect.

The equivalent McCabe-Thiele plots for the Case Study 2 efficiency curves are not presented, but are very similar to the corresponding curves of Case

Study 1. The equilibrium line also moves towards the operating line with increasing severity of the efficiency dependence on concentration. The significant difference between the steady state profiles of the two case studies (comparing Figure 7.3a and Figure 7.12a) is that for the Case Study –2 efficiency curves, the same level of enrichment observed in the low methanol concentration region using the Case Study –1 efficiency curves was not obtained. This has the resulting effect that for  $E_{2.0q}$  a similar near-pinch situation occurs and the column reached equilibrium when run at total reflux from startup but distillate composition did not reach 99% methanol purity. The liquid and vapour compositions in the relevant sections of the column where the near-pinch condition occurs are presented in Table 8.1.

**Table 8.1:** Liquid and Vapour Composition at Near-Pinch Situation for the Efficiency Curves of Case Studies-1 and Case Study –2 with the Most Severe Composition Dependence ( $E_{2.0}$  and  $E_{2.0q}$ ).

Location	$E_{2.0}$		$E_{2.0q}$	
	Liq. mf	Vap. mf	Liq. mf	Vap. mf
Tray 1	0.0496	0.4824	0.0959	0.4001
Tray 2	0.4824	0.5544	0.4001	0.5047
Tray 3	0.5544	0.6210	0.5047	0.5725
Tray 4	0.6210	0.6956	0.5725	0.6416

Table 8.1 shows that the level of enrichment of vapour obtained for  $E_{2.0}$  between Trays 1 and 2 is obtained between Trays 1 and 3 for  $E_{2.0q}$  and this is attributable to the higher values of efficiency in  $E_{2.0}$  between 0.04 and 0.1 methanol mole fraction concentration. The near-pinch condition occurs on Tray 3 for  $E_{2.0}$  and  $E_{2.0q}$ . This pinch occurs in the concentration region where the efficiency curve passes through minimum (i.e. 0.5 mf).

### 8.1.3 Temperature and Composition Profiles

A peculiar trend in temperature and composition movements of the distillate and on the trays during product withdrawal results from simulation when the efficiency curves of both case studies are applied to the Variable Efficiency Model. During distillate withdrawal (after initial steady state) under a fixed reflux ratio simulation, the temperatures and compositions on the trays do not change smoothly. Instead, they oscillate at different amplitudes for the different tray efficiency-concentration curve severities. The amplitude of oscillation of the tray temperature movements increases with increasing efficiency curve severity (Figure 7.6 and Figure 7.8).

The resulting effect of this non-linear temperature movement on distillation is shown in Table 7.3 for a simulation run with product withdrawal when distillate composition is greater than or equal to 92 mole percent methanol. The results in Table 7.3 show that when the simulation was run with efficiency curves of increasing severity, off-take period, hence amount of distillate collected, decreases for the Case Study –1 efficiency curves. For the average product composition however, a similar linear trend was not obtained as efficiency curves of increasing severities are used in the simulation. The average product composition increases for simulation using efficiency curves of increasing severity only as far as curve  $E_{1.7}$ . Simulation using efficiency curve  $E_{2.0}$  results in a product with an average composition, even less than that obtained when curve  $E_{1.3}$  is used.

Similar results were obtained using the efficiency curves of Case Study 2. The oscillations in the temperature and composition movements during product withdrawal were however, not as pronounced as those obtained using the equivalent efficiency curves of Case Study 1 where efficiencies exceed 1.0. These oscillations in temperature movements do not occur only during product withdrawal, but also from the startup of the simulation before steady state is reached. The oscillations are therefore not peculiar to

the product withdrawal process but occur during any transient process in the simulation.

For the fixed distillate composition operation, the simulation was run with product purity specifications of 92% and 99% methanol concentrations and the resulting reflux ratio profile may be oscillatory in order to maintain the specified product purity (Figure 7.9, Figure 7.10, Figure 7.17, Figure 7.18). For a 92% methanol product specification, the efficiency curves of Case Study –1 result in smaller amounts of product in shorter off-take times as the efficiency curve severity increases (Table 7.4). A similar trend was obtained for the Case Study 2 curves in Table 7.5 except for  $E_{2.0q}$  where off-take time increases over  $E_{1.7q}$  (contrary to the trend) but the amount of product collected follows the trend and was less than that of  $E_{1.7q}$ .

When product purity was set to 99%, off-take time increases with increasing efficiency curve when using the Case Study 1 curves as does the amount of product collected, except for  $E_{2.0}$  which produces less distillate than even curve  $E_{1.3}$ . However, the reverse was observed using the efficiency curves of Case Study 2 with off-take times and product collected decreasing with increasing efficiency curve.

The interesting aspect of these fixed distillate composition simulation results is the contrary trends obtained from simulation using efficiency curves  $E_{2.0}$  and  $E_{2.0q}$ . Even when off-take time is higher for simulation using curve  $E_{2.0}$ , for 99% purity specification, the amount of product produced is small compared with that produced using the other efficiency curves. This is as a result of the significantly higher reflux ratios required to maintain the distillate composition at the specified purity (Figures 7.10 and Figure 7.18). Similarly, for curve  $E_{2.0q}$ , for a 92% product specification, the product withdrawal period is longer than that of the other Case Study 2 efficiency curves, but the least amount of product is withdrawn. This anomaly is also explained by the higher reflux ratios (hence lower distillate rates) during

product withdrawal for these efficiency curves with severe concentration dependence.

The severity of the oscillations in the reflux ratio profile is also a function of the severity of the tray efficiency-concentration dependence as is seen in Figure 7.9, Figure 7.10, Figure 7.17 and Figure 7.18. The oscillation in the reflux ratio profile becomes more pronounced with increasing efficiency curve severity. The most oscillatory reflux ratio profile was obtained from simulation using efficiency curve  $E_{2.0}$  (the efficiency curve with the most severe concentration dependence) when a 99% methanol product was specified. This reflux ratio oscillation is analogous to the oscillations in the distillate and tray composition movements during transient periods under the fixed reflux ratio policy.

The batch time (time from start of simulation until all specification product is withdrawn) and amount of product collected is quantified in terms of utility cost and finished product costs respectively. This is used as a basis for comparing the performance of the column when the simulation is run using the different tray efficiency-concentration dependence severities considered in the case studies.

To further investigate the cause of the oscillations in the distillate composition movements, an integration time step as low as  $1 \times 10^{-6}$  hrs was used in simulation and this also resulted in oscillations, which exactly match those obtained when a time step of 0.001 hrs was used. This does not however confirm that the oscillations are not due to the convergence characteristics of the numerical integration method. Simulation using other more sophisticated integration methods (such as the Runge-Kutta method or Gear's method) is required to verify that the oscillations are indeed a feature of the system and not as a result of the convergence characteristics of the Euler method used in the model developed for this work.

## 8.2 COLUMN PERFORMANCE ANALYSIS

Annual productivity, defined as the net returns expected on the specification distillate produced per annum (ie total product cost – cost of utilities), is used as the criterion for comparing the column performance using the different tray efficiency-concentration curves in simulation. Graphical presentations of the column performance for a 92% and 99% methanol product specification using the efficiency curves of both Case Studies –1 and 2 in the Variable Efficiency Model are shown in Figure 7.19 to Figure 7.21.

Generally, for a 92% product specification, the annual productivity of the column from simulation using an efficiency curve of Case Study –1 is higher than that obtained using the equivalent efficiency curve of Case Study –2. The exception is curve  $E_{1.1q}$  for Case Study –2, for which the column gives a higher productivity than  $E_{1.1}$  of Case Study –1. The general trend in both cases however is for the column performance (annual productivity) to decrease with increasing severity of the efficiency curve (Figure 7.21).

For the 99% product specification on the other hand, equal performance is obtained for simulation using efficiency curves  $E_{1.1}$  and  $E_{1.1q}$ . The general trend in the annual productivity of the column using the efficiency curves of Case Study –1 is for productivity to increase with increasing efficiency curve severity. However, curve  $E_{2.0}$  results in a lower productivity than even  $E_{1.1}$  (contrary to the trend as shown in Figure 7.21). Using the Case Study –2 efficiency curves however, the productivity decreases with increasing efficiency curve severity (Figure 7.21). The product specification of 99% methanol purity was not achieved using curve  $E_{2.0q}$ .

The performance of the column simulated using the Variable Efficiency Model is compared with the performance using the Overall Column

Efficiency Model. The Overall Column Efficiency Model was run using an efficiency of 0.824 under fixed reflux ratio ( $R = 4.5$ ) and fixed distillate composition policies.

For a 92% product specification, no appreciable difference is apparent in the performance of the Overall Column Efficiency Model run under fixed reflux ratio or fixed distillate composition policy. Comparing its performance to that of the Variable Efficiency Model however reveals that the column productivity is significantly higher when the Overall Column Efficiency Model is used regardless of the severity of the efficiency curves used in the Variable Efficiency Model (Figure 7.21).

Efficiency curve  $E_{1.1}$  approximates the true tray efficiency-concentration relationship observed for methanol/water and this observation suggests that the overall Column Efficiency Model, which is more commonly used in simulation, over-predicts the performance of the column when 92% methanol product purity is specified.

When 99% methanol product purity is specified for the Overall Column Efficiency Model, the column productivity is significantly higher under fixed reflux ratio simulation compared with the fixed distillate policy simulation (Figure 7.21). Comparing with the column performance using the Variable Efficiency Model reveals that the Variable Efficiency Model, using the efficiency curves of Case Study -1, predict higher productivities than the Overall Column Efficiency Model for 99% product specification. When the efficiency curves of Case Study -2 were used in the Variable Efficiency Model simulation however, only efficiency curves  $E_{1.1q}$  and  $E_{1.3q}$  predict higher productivities than the Overall Column Efficiency Model.

One striking observation from Figure 7.21 is that simulation using the Overall Column Efficiency Model, predicts higher productivities for the column than the Variable Efficiency Model when a 92% methanol purity is specified. When 99% methanol purity is specified however, the Variable

Efficiency Model generally predicts higher column productivities than the Overall Column Efficiency Model. This shows that simulation using the Overall Column Efficiency Model, which is the usual practice (instead of accounting for the variation of tray efficiency with composition) may over-predict or under-predict the column performance, depending on the product quality specified.

## CHAPTER NINE

### CONCLUSIONS

Tray efficiency has been shown to vary with the composition of the mixture on the tray. The form of the variation, observed experimentally for a methanol/water mixture, is for the tray efficiency to pass through a minimum at an intermediate composition. While the effect of concentration on tray efficiency is not important in continuous distillation where the column is run at steady state, concentration varies significantly in batch distillation and its effects on the performance of the column may be significant.

A general batch distillation model has been developed to assess the potential effects of the tray efficiency-concentration relationship on the performance of a batch distillation column. To this end, the model is run using three different efficiency models:

- Overall Column Efficiency Model – a single efficiency value is applied on all the trays in the column.
- Constant Efficiency Model – the tray efficiency is constant on each tray but may vary from tray to tray.
- Variable Efficiency Model – the efficiency on each tray is not constant but varies with time as a function of the concentration of the mixture on the tray.

From the results and analyses presented in the preceding chapters for the distillation of methanol/water mixtures of different compositions under different operating conditions, the following conclusions can be drawn:

- Batch distillation can be modelled using an Overall Column Efficiency Model to give a good match with experimentally observed steady state temperature profiles provided a good choice of the efficiency value is made.
- When the Overall Column Efficiency Model is used to model a batch distillation, the column steady state temperature profile predicted by the model may closely match that observed experimentally after the total reflux startup. The temperature profile predicted by the model may however, not match that observed experimentally at different stages during the progress of the distillation, using the same efficiency value.
- The use of the Overall Column Efficiency Model in batch distillation should be restricted to preliminary design studies and operational studies when temperature and composition measurements on the trays cannot be made.
- Unlike the Overall Column Efficiency Model, the column steady state temperature profile predicted by the Constant Efficiency Model matches the experimentally observed temperature profiles at different stages during the progress of the distillation of a given mixture. Correct choice of tray efficiencies is equally important in this model. The tray efficiencies used in this work were estimated from measured liquid compositions.
- The column steady state temperature profile and temperature movements on the trays during transient periods of product withdrawal predicted by the Constant Efficiency Model closely matches the temperature profile and movements observed experimentally. The Variable Efficiency Model however gives an even better match with experimental steady state temperature profiles and temperature movements than the Constant Efficiency Model.

- Improved model accuracy is obtained when the tray efficiencies in the model are allowed to change with the mixture composition on the tray. This however, requires a knowledge of the nature of the tray efficiency-composition variation.
- For a methanol/water mixture, the nature of the tray efficiency-concentration relationship is for the tray efficiency to take on high values at the ends of the concentration range and pass through a minimum at an intermediate composition.
- Although the liquid and vapour rates in a distillation column affect the tray efficiency, they do not affect the form of the efficiency-concentration relationship, for the different heat inputs (hence vapour rates) considered in the experiment work carried out.
- For a methanol/water mixture, tray efficiencies may exceed 1.0 at very high or very low methanol concentrations (Figure 5.2). This is in agreement with the findings of Hay and Johnson (1960), Mostafa (1979) and Lockett and Ahmed (1983).

To investigate the significance of the effect of composition on tray efficiency in the general context of batch distillation, the efficiency-concentration relationship obtained experimentally for methanol/water was extended to form two classes of efficiency curves:

Case Study -1: The hypothetical efficiency curves pass through a minimum at intermediate compositions and assume values greater than 1.0 at the ends of the concentration range. Efficiency curves with maximum efficiency values of 1.1, 1.3, 1.5, 1.7 and 2.0 were assumed and labelled  $E_{1.1}$ ,  $E_{1.3}$ ,  $E_{1.5}$ ,  $E_{1.7}$ ,  $E_{2.0}$ , respectively.

Case Study -2: The hypothetical efficiency curves pass through a minimum at intermediate compositions but do not go above 1.0 at the ends of the concentration range. Another five efficiency curves were

assumed which are related to the curves of Case Study –1 by their minimum in the mid-composition region and are labelled  $E_{1.1q}$ ,  $E_{1.3q}$ ,  $E_{1.5q}$ ,  $E_{1.7q}$ ,  $E_{2.0q}$  according to their equivalent Case Study –1 curve.

The performance of the column, modelled using the efficiency curves of both case studies, has been compared, using “annual productivity” (Section 7.3) as the performance criterion. The following conclusions can be drawn based on the simulation using the different efficiency curves and on the economic performance of the column.

- The tray efficiency-composition dependence introduces additional non-linearity to the process behaviour with the result that during product withdrawal, tray and distillate composition movements are oscillatory. These composition (hence temperature) movements become increasingly oscillatory as the efficiency-concentration dependence becomes more severe.
- The temperature and composition movements on the trays during product withdrawal are more oscillatory for the Case Study –1 efficiency curves (where efficiency may exceed 1.0) than the equivalent Case Study –2 efficiency curves.
- When the simulation is run under fixed distillate composition policy, the time profile of the reflux ratio may be oscillatory in order to maintain the set distillate composition. This reflux ratio profile becomes more oscillatory as efficiency curves of increasing severity are used and also when higher purity products are specified.
- At steady state during total reflux operation, the equilibrium line on an x-y diagram moves closer to the operating line ( $y = x$ ) as the severity of the efficiency curve used in the simulation increases. This is despite the high efficiencies at the concentration ends for the efficiency curves of Case Study –1. In fact, the most severe efficiency curve (with the

highest and lowest efficiencies at the concentration-ends and at intermediate compositions) moves the equilibrium line closest to the operating line, resulting in a near-pinch situation. The near-pinch condition occurs in the composition region where the efficiency curve passes through a minimum.

- The performance of the column using the Overall Column Efficiency Model compared with the performance of the Variable Efficiency Model is dependent upon the product purity specified. In the cases considered, the column performance predicted by the Overall Column Efficiency Model is higher than that predicted by the Variable Efficiency Model when low product purity is specified (92% methanol product). When a higher purity (99% methanol) is specified, the Overall Column Efficiency Model generally predicts a lower annual productivity for the column than the Variable Efficiency Model.
- For the methanol/water mixture (efficiency-concentration dependence is approximated by curve  $E_{1,1}$ ), modelling using a fixed column efficiency (as is commonly done) over-predicts the performance of the column at the lower methanol product specification simulation. At high product purity specification, simulation using a fixed column efficiency under-predicts the actual performance of the column.

The results of this work show that tray efficiency is an important factor affecting the fidelity of batch distillation simulation models and has generally been overlooked in published studies. Equally important is the numerical value of tray efficiency assigned and the manner of its representation. Models, which include the variation of tray efficiency with mixture composition, result in improved model fidelity. The findings of this study highlight the shortcomings of assuming fixed tray efficiencies in batch distillation simulation when the tray efficiency of the system varies significantly with mixture composition.

# CHAPTER TEN

## FURTHER WORK.

The model used in this work was developed for the pilot scale Kestner column described in Chapter 3, the efficiency-concentration relationship employed in the simulation was determined using experimental data from the column. Future work can focus on developing a generalised method of estimating tray efficiency as a function of mixture composition, which can be incorporated in the batch distillation model for use when experimental efficiency-concentration data is not available. Experiments can also be carried out on mixtures that exhibit a strong tray efficiency-concentration dependence to verify the column behaviour predicted by the model.

This work has focused on investigating the effect of the composition dependence of tray efficiency on the operation and performance of a batch distillation column. Further work can focus on investigating the effect of the composition dependence of tray efficiency on the design of a batch distillation column.

The model developed in this work can be extended for use in startup and shutdown simulations in future work. This will require the inclusion of the thermal dynamics of the still and the column as well as detailed liquid hydraulics correlations.

## NOMENCLATURE

a	-	Area reading from gas chromatograph (% of total area).
A,B,C	-	Antoine Constants.
D	-	Distillate rate (kmol/hr).
DP	-	Differential Pressure cell.
$E_{MV}$	-	Tray Murphree vapour-phase tray efficiency.
$E_{max}$	-	Maximum Murphree tray efficiency.
$E_{min}$	-	Minimum Murphree tray efficiency.
F	-	F factor, a parameter describing vapour load ( $m/s \sqrt{(kg/m^3)}$ ).
FUG	-	Fenske-Underwood-Gilliland calculation procedure for continuous distillation column design.
h	-	Integration step size (hrs).
$H_B$	-	Molar holdup in the still (kmols).
$H_D$	-	Molar holdup in the reflux receiver (kmols).
$H_n$	-	Molar holdup on tray n (kmols).
L	-	Liquid rate, (kmol/hr).
mf	-	Mole fraction, unit of concentration.
$N_G$	-	Number of vapour phase mass transfer units.
$N_L$	-	Number of liquid phase mass transfer units.
NC	-	Number of components.
NT	-	Number of trays.
P	-	Absolute Pressure (atm).
$P^\circ$	-	Saturated vapour pressure (atm).
$P_c$	-	Net Product Cost (£/kg of product).
$P^*$	-	Saturated vapour pressure (atm).
Q	-	Heat Duty (kJ/hr).
$Q_{PROD}$	-	Total amount of product obtained per batch (kg).
$Q_{st}$	-	Total amount of steam used per batch (kg).
R	-	Reflux Ratio.

---

RMM	-	Relative Molecular Mass (kg/kmol)
T	-	Temperature (C).
t	-	Time (hr).
V	-	Vapour rate (kmol/hr).
VLE	-	Vapour-Liquid Equilibrium.
w	-	Component weight fraction (%).
x	-	Liquid phase mole fraction.
y	-	Vapour phase mole fraction.
y*	-	Equilibrium vapour phase mole fraction.
Z	-	Moles of feed (kmol).

### Greek Characters

$\alpha$	-	Relative volatility.
$\gamma$	-	Activity coefficient.
$\lambda$	-	Latent heat of vaporisation (kJ/kmol).
$\Lambda$	-	Wilson coefficient.
$\rho$	-	Mass Density (kg/m <sup>3</sup> ).
$\rho_m$	-	Mass Density of mixture (kg/m <sup>3</sup> ).
$\rho_s$	-	Mass Density of steam at prevailing conditions (kg/m <sup>3</sup> ).
$\rho_w$	-	Mass Density of water (kg/m <sup>3</sup> ).
$\tau$	-	Column dynamic time constant (hr).
$v$	-	Volume holdup (m <sup>3</sup> ).

### Subscripts

B	-	Reboiler.
D	-	Distillate.

G	-	Vapour phase.
i	-	Component number.
L	-	Liquid phase.
NT	-	Top Tray.
n	-	Tray number.
max	-	Maximum value.
min	-	Minimum value.
tf	-	Stop time for distillate withdrawal (hrs).
ts	-	Start time for distillate withdrawal (hrs).

## REFERENCES

**Albet, J., LeLann, J.M., Joulia, X. & Koehret B. (1991)**

“Rigorous Simulation of Multicomponent Multisequence batch reactive distillation”, Proceedings COPE '91, Elsevier, Amsterdam, 75.

**Albet, J., LeLann, J.M., Joulia, X. & Koehret B. (1994)**

“Operational Policies for The Start-up of Batch Reactive Distillation Columns”, IChemE Symp. Ser. No. 133, 63.

**Anderson, N.J., & Doherty, M.F. (1984)**

“An Approximate Model for Binary Azeotropic Distillation Design”, Chem. Engng. Sci., 39, 11.

**Archer, D.J. & Rothfus, R.R. (1961)**

“The Dynamics and Control of Distillation Units and Other Mass Transfer Equipment”, Chem. Engng. Prog. Symp., n36, v57, 2.

**Bainbridge G.S., & Sawistowsky, H. (1964)**

“Surface Tension Effects In Sieve Plate Distillation Columns”, Chem. Eng. Sci., 19, 992.

**Barker, P.E. & Choudhury, M.H. (1959)**

“Performance of Bubble cap Trays”, British Chemical Engineering, 14, 348.

**Barolo, M., Guarise, G.B., Ribon, N., Rienzi, S., Trotta, A., & Macchietto, S. (1996a)**

“Some Issues in the Design and Operation of a Batch Distillation Column with a Middle Vessel”, Computers & Chem. Engng., 20, Supplement, S37.

**Barolo, M, Guarise, G.B., Ribon, N., Rienzi, S., Trotta, A., & Macchietto, S. (1996b)**

“Running Batch Distillation in a Column with a Middle Vessel”, *Ind. Engng. Chem. Res.*, 35, 12, 4612.

**Bernot, C., Doherty, M.F. & Malone, M.F. (1989)**

“Design Procedure for Multicomponent Batch Distillation”, American Institute of Chemical Engineers Annual Meeting, San Francisco.

**Bernot, C., Doherty, M.F. & Malone, M.F. (1990)**

“Patterns of Composition Change In Multicomponent Batch Distillation”, *Chem. Eng. Sci.*, 45, 1207.

**Bernot, C., Doherty, M.F. & Malone, M.F. (1991)**

“Feasibility and separation sequencing in multicomponent batch distillation”, *Chem. Eng. Sci.*, 46, 1311.

**Bernot, C., Doherty, M.F. & Malone, M.F. (1993)**

“Design and Operating Targets for Nonideal Multicomponent batch distillation”, *Ind. Eng. Chem. Res.*, 32, 293.

**Bidulph, M.W. (1975)**

“Multicomponent Distillation Simulation - Distillation of Air”, *AIChE Journal*, 21, 2, 327.

**Bidulph, M.W. & Ashton, N. (1977)**

“Deducing Multicomponent Distillation Efficiencies from Industrial Data”, *Chem. Engr. Journal*, 14, 7.

**Bogart, M.J.P. (1937)**

“The design of equipment for fractional Batch distillation”, *Trans. Am. Inst. Chem. Eng.*, 33, 139.

**Bonny, L., Domench, S., Floquet, P. & Pibouleau, L. (1994)**

“Strategies for Slop Cut Recycle in Multicomponent Batch Distillation”, *Chem. Engng. & Processing*, 33, 23.

**Bosley, J.R. & Edgar, T.F. (1994)**

“An Efficient Dynamic Model for Batch Distillation”, *J. Proc. Cont.*, v4, n4, 195.

**Bossen B.S., Jorgensen, S.B. & Gani, R. (1993)**

“Simulation, Design and Analysis of Azeotropic Distillation”, *Ind. Engng. Chem. Res.*, 32, 620.

**Boston, J.F. (1980)**

“Inside-out Algorithm for Multicomponent Separation Calculations”, Presented at the 178th Natn. Meeting of the Am. Chemical Soc. Washington DC. 1978.

**Boston, J.F., Britt, H.I., Jirapongphan, S. & Shah, V.B. (1981)**

“An Advanced System for Simulation of Batch Distillation Operations”, In *Foundations of Computer-aided Chemical Process Design*, Mah R.H.S., Seider, W. eds., Engineering Foundation, New York, v2, p203.

**Colburn, A.P. & Stearns, R.F. (1941)**

“The effect of column hold-up on Batch Distillation”, *Trans. Am. Inst. Chem. Eng.*, 37, 291.

**Chen G.X, Afacan, A., Xu, C. & Chuang, K.T. (1941)**

“Performance of Combined Mesh Packing and Sieve Tray in Distillation”, *Canadian Journal of Chem. Eng.*, 68, 382.

**Chiotti, O.J. & Iribarren, O.A. (1991)**

“Simplified Models for Binary Batch Distillation”, *Computers Chem. Engng.*, 15, 1.

**Choo, K.P. & Saxena, A.C. (1987)**

“Inferential Composition Control of an Extractive Distillation Tower”,  
Ind. Eng. Chem. Res., 26, 2442.

**Coulson, J.M. & Richardson, J.F. (1993)**

“Chemical Engineering -Vol. 6: Chemical Engineering Design”, 2nd  
ed., Pergamon.

**Coward, I. (1967)**

“The Time-Optimal Problem In Binary Batch Distillation”, Chem. Eng.  
Sci., 22, 503.

**Cuille, P.E., & Reklaitis, G.V. (1986)**

“Dynamic Simulation of Multicomponent Batch Rectification With  
Chemical Reactions”, Computers Chem. Engng., 10, n4, 389.

**Davidyan, A.G., Kiva, V.N., Meski, G.A., & Morari, M. (1994)**

“Batch Distillation In A Column With A Middle Vessel”, Chem. Engr.  
Sci., 18, 3033.

**Distefano, G.P. (1968)**

“Mathematical Modelling and Numerical Integration of  
Multicomponent Batch Distillation Equations”, AIChE J, 14, 190.

**Diwekar, U.M. (1994)**

“How Simple Can It Be? - A Look at The Models for Batch  
Distillation”, Computers & Chem. Engr., 18(S), S451.

**Diwekar, U.M., (1996)**

“Batch Distillation: Simulation, Optimal Design and Control”, Taylor &  
Francis, London.

**Diwekar, U.M. & Madhavan, K.P. (1991a)**

“Multicomponent Batch Distillation Column Design”, *Ind. Eng. Chem. Res.*, 30, 713.

**Diwekar, U.M. & Madhavan, K.P. (1991b)**

“BATCH-DIST: A Comprehensive Package For Simulation, design, Optimisation and Optimal Control of Multicomponent, Multifraction Batch Distillation Columns”, *Computers Chem. Engng*, 15, 833.

**Diwekar, U.M., Malik, R.K. & Madhavan, K.P. (1987)**

“Optimal Reflux rate Policy Determination for Multicomponent Batch Distillation Columns”, *Comput. Chem. Eng.*, 11, 6, 629-637.

**Domench, S., Guilglion, C. and Enjalbert, M. (1974)**

“Modele Mathematique D'une Colonne Rectification Discontinue II - Exploitation Numerique”, *Chem. Eng. Sci.*, 29, 7, 1529.

**Dribika, M.M. (1986)**

“Multicomponent Distillation Efficiencies”, PhD Thesis, University of Nottingham.

**Dribika, M.M. & Bidulph, M.W. (1986)**

“Scaling-up Distillation Efficiencies”, *AIChE Journal*, 32, n11, 1864.

**Egly, H., Ruby, V. & Seid, B. (1979)**

“Optimum Design and Operation of Batch Rectification Accompanied by Chemical Reaction”, *Computers Chem. Engng.*, 3, 169.

**Fair, J.R., Null, H.R. & Bolles, W.L. (1983)**

“Scale-up of Plate Efficiency From Laboratory Oldershaw Data”, *Ind. Eng. Chem. Proc. Des. Dev.*, 22, 1, 53.

**Fane, A.G., & Sawistowski, H. (1969)**

“Plate Efficiency in the Foam and Spray Regimes of Sieve plate Distillation”, IChemE Symposium Series No 32, 1, 8.

**Fell, C.J.D. & Pinczewski, W.V. (1977)**

“New Considerations In the Design of High Capacity Sieve Trays” The Chem. Engr., 1., 45.

**Foucher, E.R., Doherty, M.F. & Malone, M.F. (1991)**

“Automatic Screening of Entrainers for Homogenous Azeotropic Distillation”, Ind. Engng., Chem., Res., 30, 4, 760.

**Freshwater, D.C. (1994)**

“Why Batch? An Outline of the Importance of Batch Processing”, IChemE NW Branch Symposium papers, 3.

**Galindez, H. & Fredenslund, A.A. (1988)**

“Simulation of Multicomponent Batch Distillation Processes”, Computers Chem. Engng., 12, 281.

**Gerster, J.A., Bonnett, W.E & Hess, I. (1951)**

“Mass Transfer Rates on Bubble Plates, Part II”, Chem. Eng. Prog., 47, 621.

**Gmehling, J., Onken, U. & Arlt, W. (1981)**

“Vapour-Liquid Equilibrium Data Collection”, v1a, Frankfurt, Germany: DECHEMA.

**Hart, D.J. & Haselden, G.G. (1969)**

“Influence of Mixture Composition on Distillation-Plate Efficiency”, IChemE Symposium Series No. 32, 1, 19.

**Hay, J.M., & Johnson, A.I. (1960)**

“A Study of Sieve Tray Efficiencies”, *AIChE. Journal*, 6, 3, 373.

**Hirata, M., Ohe, S. & Nagahama, K. (1975)**

“Computer aided data book of vapour-liquid equilibria”, Kodansha, Tokyo.

**Hirst, J.N. (1996)**

“Revamp vs. New: Guess Which is Better! Fast Tracking Improved Project Efficiency”, *ICHEME NW Branch Papers*, 1.

**Hitch, D.M. & Rousseau, W.R. (1988)**

“Simulation of Continuous Contact Separation Processes: Multicomponent Batch Distillation”, *Ind. Eng. Chem. Res.*, 27, 1466.

**Holland C.D. (1963)**

“Multicomponent Distillation”, Prentice Hall, Englewood Cliffs, New Jersey.

**Holland C.D. & McMahon K.S. (1970)**

“Comparison of Vaporisation Efficiencies with Murphree-Type Efficiencies in Distillation-I”, *Chem. Eng. Sci.*, 25, 431.

**Houtman, J.P.W. & Husain, A. (1956)**

“Design Calculations for Batch Distillation Column”, *Chem. Eng. Sci.*, 5, 178.

**Huckaba, C.E. & Danly D.E. (1960)**

“Calculation Procedure for Binary Batch Rectification”, *AIChE J.*, 6, 335.

**Kalagnanam, J.R. & Diwekar, U.M. (1993)**

“An Application of Qualitative Analysis of Ordinary Differential Equations To Azeotropic Batch Distillation” *AI in Engineering*, 8, 1, 23.

**Kalbassi, M.A. (1987)**

“Distillation Sieve Tray Efficiencies”, PhD Thesis, University of Nottingham, UK.

**Krishnamurthy, R., & Taylor, R. (1985a)**

“A Nonequilibrium Stage Model of Multicomponent Separation Processes -Part I: Model Description and Method of Solution”, *AIChE J*, 31, n3, 449.

**Krishnamurthy, R., & Taylor, R. (1985b)**

“A Nonequilibrium Stage Model of Multicomponent Separation Processes -Part II: Comparison With Experiment”, *AIChE J*, 31, n3, 456.

**Krishnamurthy, R., & Taylor, R. (1985c)**

“A Nonequilibrium Stage Model of Multicomponent Separation Processes -Part II: The Influence of Unequal Component Efficiencies in Process Design Problems”, *AIChE J*, 31, n12, 1973.

**Kumana, J.D. (1990)**

“Run Batch Distillation Processes With Spreadsheet Software”, *Chem. Engr. Prog.*, 53.

**Langdon, W.M. & Keyes, D.B. (1943)**

“Plate Factors in Fractional Distillation of Isopropyl Alcohol-Water System”, *Ind. Engr. Chem.*, 35, n4, 464

**Lockett, M.J. (1986)**

“Distillation Tray Fundamentals”, Cambridge University Press.

**Lockett, M.J. & Ahmed, I.S. (1983)**

“Tray And Point Efficiencies From a 0.6 Metre Diameter Distillation Column”, Chem. Eng. Res. Des., 61, 110.

**Lockett, M.J. & Uddin, M.S. (1980)**

“Liquid Phase Controlled Mass Transfer on Sieve Trays”, Trans. Instn. Chem. Eng., 58, n3, 166.

**Logsdon, J.S. & Biegler, L.T. (1993)**

“Accurate Determination of Optimal Reflux Policies for the Maximum Distillate Problem in Batch Distillation”, Ind. Eng. Chem. Res., 32, 692.

**Logsdon, J.S., Diwekar, U.M. & Biegler, L.T. (1990)**

“On The Simultaneous Optimal Design and Operation of Batch Distillation Columns”, Chem. Eng. Res. Des., 68, 5, 434.

**Luyben, W.L. (1971)**

“Some Practical Aspects of Optimal Batch Distillation Design”, Ind. Eng. Chem. Proc. Des. Dev., 10, 54.

**Luyben, W.L. (1988)**

“Multicomponent Batch Distillation 1. Ternary Systems With Slop Recycle”, Ind. Eng. Chem. Res., 27, 642.

**Malenko, Yu I. (1970)**

“Physiochemical analysis of fractional distillation diagrams. III. Multicomponent (n-component) systems”, Russ. J. Phys. Chem., 44, 920.

**Martinez, C.L.M. (1997)**

“State Estimation for Improved Control In Batch Reaction and Distillation Processes”, PhD Thesis, University of Nottingham.

**Meadows, E.L. (1963)**

“Multicomponent Batch Distillation Calculations on a Digital Computer”, Chem. Eng. Prog. Sym. Ser., 59, 48.

**Medina, A.G., Ashton, N. & McDermott, C. (1978)**

“Murphree and Vaporisation Efficiencies in Multicomponent Distillation”, Chem. Eng. Sci., 33, 331.

**Medina, A.G., McDermott, C. & Ashton, N. (1979)**

“Prediction of Multicomponent Distillation Efficiencies”, Chem. Eng. Sci., 34, 861.

**Mehlhorn, A., Espuna, A., Bonsfills, A., Gorak, A & Puigjaner, L. (1996)**

“Modelling and Experimental Validation of Both Mass Transfer and Tray Hydraulics In Batch Distillation”, Computers Chem. Engng., 20S, S575.

**Mostafa, H.A. (1979)**

“Effect Of Concentration On Distillation Plate Efficiencies”, Trans IChemE, 57, 55.

**Mujtaba, I.M., & Macchietto, S. (1988)**

“Optimal Control of Batch Distillation”, Proceedings 12<sup>th</sup> IMACS World Congress, Paris, July 18.

**Mujtaba, I.M., & Macchietto, S. (1992)**

“An Optimal Recycle Policy For Multicomponent Batch Distillation”, Computers Chem. Engng., 16(S), S273.

**Mujtaba, I.M., & Macchietto, S. (1993)**

“Optimal Operation of Multicomponent Batch Distillation - Multiperiod Formulation and Solution”, *Computers Chem. Engng.*, 17, 12, 1191.

**Murphree, W.L. (1925)**

“Rectifying Column Calculations”, *Ind. Engng. Chem.*, 17, n7, 747.

**Ognisty, T.P. (1995)**

“Analyze Distillation Columns With Thermodynamics”, *Chem. Engr. Prog.*, 91, 2, 40.

**Pescarini, M.H., Barros, A.A.C. & Wolf-Maciel, M.R. (1996)**

“Development Of A Software For Simulating Separation Processes Using A Nonequilibrium Stage Model”, *Computers Chem. Engr.*, 20(S), S279.

**Pigford, R.L., Tepe, J.B. & Garrahan, C.J. (1951)**

“Effect of Column Holdup in Batch Distillation”, *Ind. Eng. Chem.*, 43, n11, 2592.

**Pitt, M..J. (1996)**

“Chemical And Utilities Cost Guide 1996”, IChemE, Education Subject Group, IChemE.

**Quereshi, A.K. & Smith W. (1958)**

“The Distillation of Binary and Ternary Mixtures”, *Journal Inst. Petrol.*, 44, 137.

**Quintero-Marmol, E. & Luyben W.L. (1990)**

“Multicomponent Batch Distillation 2. Comparison of Alternative Slop Handling and Operation Strategies”, *Ind. Eng. Chem. Res.*, 29, 1915.

**Rance, S (1993)**

“A PC-Based Data Acquisition System”, MEng Research Project, University of Nottingham.

**Rao, D.P., Prem Kumar, R.S., Pandit, P. & Das, D.A.S. (1940)**

“Multicomponent Tray Efficiencies Accounting For Entrainment”, Chemical Engineering Journal, 57, 237.

**Rayleigh, Lord. (1902)**

“On the Distillation of Binary Mixtures”, Philosophical Magazine (vi), 4, 23, 521.

**Reuter, E., Wozny, G., & Geromin, L. (1988)**

“Modelling of Multicomponent Batch Distillation Processes With Chemical Reaction and Their Control Systems”, Computers Chem. Engng., 13, n4/5, 499.

**Robinson, E.R. (1970)**

“The Optimal Control of an Industrial Batch Distillation Column”, Chem. Eng. Sci., 25, 921.

**Robinson, C.S. & Gilliland, E.R. (1950)**

“Elements of Fractional Distillation”, 4th ed., McGraw Hill, New York.

**Rose, A., O'Brien, V.J. (1952)**

“Effect of Holdup-Charge Ratio in Laboratory Ternary Batch Distillation”, Ind. Eng. Chem., 44, n6, 1480.

**Rose, A., Welshans, L.M. & Long, H.H. (1940)**

“Calculation of maximum sharpness of separation when Hold-up is appreciable”, Ind. Eng. Chem., 32, 673.

**Sawistowski, H. (1973)**

“Surface-Tension-Induced Interfacial Convection and its Effects on Rates of Mass Transfer”, *Chemie. Ing. Tech*, 45, 1093.

**Sawyer, P. (1993)**

“Computer Controlled Batch Processing”, IChemE, Rugby.

**Sharratt, P.N. (1997)**

“Handbook of Batch Process Design”, Sharratt, P.N. ed., Blackie Academic Professional.

**Shilling G.D., Beyer, G.H. & Watson, C.C. (1953)**

“Bubble-Plate Efficiencies in Ethanol-Water Fractionation”, *Chem. Engng. Prog.*, 49, n3, 128.

**Smoker, E.H. & Rose, A. (1940)**

“Graphic determination of batch distillation curves for binary mixtures”, *Trans. AIChE*, 36, 285.

**Snowden, P.N. (1981)**

“Practical Distillation - A Post Experience Course”, University of Leeds.

**Sorensen, E. & Oppenheimer, O. (1997)**

“Comparative Energy Consumption in Batch and Continuous Distillation”, *Computers Chem. Engng.*, 21(S), S529.

**Sorensen, E. & Prenzler, M. (1997)**

“A Cyclic Operating Policy for Batch - Theory and Practice”, *Computers Chem. Engng.*, 21(S), S1215.

**Sorensen, E. & Skogestad, S. (1994a)**

“Optimal Operating Policies of Batch Distillation With Emphasis on The Cyclic Operating Policy”, Proceedings Process Systems Engineering, Kyongju, Korea, May-June, 449.

**Sorensen, E. & Skogestad, S. (1994b)**

“Control Strategies for Reactive Batch Distillation”, Journal of Proc. Control, 4, n4, 205.

**Standart, G. (1965)**

“Studies on Distillation V- Generalised Definition of a Theoretical Plate or Stage of Contacting Equipment”, Chem. Eng. Sci., 20, 611.

**Standart, G. (1971)**

“Comparison of Murphree-type Efficiencies with Vaporisation Efficiencies”, Chem. Eng. Sci., 26, 985.

**Stewart, R.R., Weisman, E., Goodwin, B.M. & Speight, C.E. (1973)**

“Effect of Design Parameters in Multicomponent Batch Distillation”, Ind. Eng. Chem. Proc. Des. Dev., 12, 130.

**Sundaram, S. & Evans, L.B. (1993a)**

“Synthesis of Separation by Batch Distillation”, Ind. Eng. Chem. Res., 32, 500.

**Sundaram, S & Evans, L.B. (1993b)**

“Shortcut Procedure for Simulating Batch Distillation Operations”, Ind. Eng. Chem. Res., 32, 511.

**Taylor, D.L. (1962)**

MSc Thesis, Texas A & M University, U.S.A.

**Terwiesch, P., Agrawal, M., Rippin, D.W.T. (1994)**

“Batch Unit Optimisation With Imperfect Modelling: A Survey”,  
Journal of Process Control, 4, n4, 238.

**Tomazi (1957)**

“Limitations and Dynamics Imposed on Multicomponent Batch Distillation by Tray Hydraulics”, Ind. & Engng. Chem. Res., 36, 10, 4273.

**Toor, H.L. (1957)**

“Diffusion in Three-component Gas Mixtures”, AIChE J., 3, n2, 198.

**Toor, H.L., Burchard, J. (1960)**

“Plate Efficiencies in Multicomponent Distillation”, AIChE J., 6, n2, 202.

**Ukeje-Eloagu, C.I., Wilson, J.A. and Pulley, R.A. (1997)**

“Concentration Effects on Component Tray Efficiencies in Batch Distillation”, Proceedings of the 1997 IChemE Research Event, v2, 721.

**VanDongen, D.B. & Doherty, M.F. (1985)**

“Design and Synthesis of Homogenous Azeotropic Distillation - I: Problem Formulation for Single Column”, Ind. Engng. Chem. Fund., 24, 454.

**Vital, T.J., Grossel, S.S. & Olsen, P.I. (1984)**

“Estimating Separation Efficiency”, Hydrocarbon Processing, 63, n11, 147.

**Wilson, J.A., (1987)**

“Dynamic Model Based Optimisation in the Design of a Batch Process Involving Simultaneous Reaction and Distillation”, IChemE Symp. Ser. No 100., 163.

**Wilson, J.A., & Martinez, C.L.M. (1995)**

“Dynamic Model Based Optimisation in the Design of a Batch Process Involving Simultaneous Reaction and Distillation”, IChemE – Advances in Process Control 4, 155.

**Wittgens, B., & Skogestad, S. (1995)**

“Evaluation of Dynamic models of distillation columns with Emphasis on The Initial Response”, IFAC Symposium DYCORDER+ ‘95, Denmark.

**Zuiderweg, F.J. (1983)**

“Marangoni Effect In Distillation of Alcohol-Water Mixtures”, Chem. Eng. Res. Des., 61, 388.

**Zuiderweg, F.J. & Harmens, A. (1958)**

“The Influence of Surface Phenomena on The Performance of Distillation Columns”, Chem. Eng. Sci., 9, 89.

## **APPENDIX A.**

### **COLUMN TEST RUNS AND SUMMARY OF FEED AND OPERATING CONDITIONS FOR ALL THE EXPERIMENTAL RUNS**

The results of initial test runs of the column using water as the test fluid and the initial methanol/water runs are presented here. The water test runs were carried out to check the column integrity as well as the reboiler characteristics and condenser limits. The initial methanol/water runs were carried out to verify the proper operation of the ancillary devices and their calibration.

#### **A.1 WATER TEST RUNS**

The column was firstly run with water as the test mixture to check the integrity of the reboiler and column, the operation of the steam and cooling water and electrical services and to calibrate the column's ancillary instrumentation based on the test fluid at the prevailing conditions. The column was operated at total reflux until steady state. Temperatures, steam condensate and distillate flow rates were recorded for different runs, at various heat loads, permitting heat and material balance checks and testing the column's loading limits.

The net flow of heat to the reboiler is compared with the amount of vapour produced in the still in Figure A.1. The average discrepancy according to the data collected is less than 3% and thus, heat losses from the column were neglected in model.

Similarly, the data collected was used to plot calibration charts for the actual steam flow rates vs. controller steam flow output display and for the actual reflux flow rate vs. reflux rotameter reading.

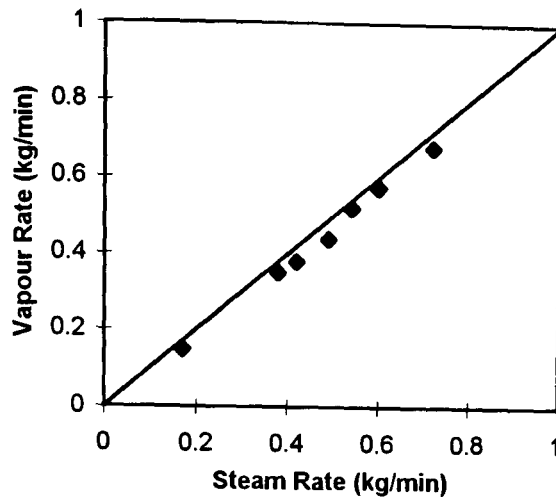


**Figure A.1:** Steam and Vapour Boilup Rates for the Column Using Water as a Test Fluid.

## A.2 METHANOL/WATER TEST RUNS

The feed mixture used in distillation studies here was methanol/water. The feed compositions used in the experiments described range from 0.082 to 0.12 mole fraction methanol. This range was chosen because for very low methanol concentration feeds, total reflux batch distillation of a methanol/water mixture in a 10-tray column will result in methanol accumulation in the topmost trays only. Similarly, with high methanol concentration feeds, the initial distribution of components in the column could result in almost pure methanol holdup on all the trays and would require long runs at partial offtake to obtain a two component mixture at the top of the column. Feeds in the chosen composition range produced a two component mixture on a large number of trays in the column, resulting in a distinct composition profile.

Column startup was ignored in the verification process, as the simulation model was not designed to include the startup period. The first methanol/water run in the column (Run 1) was carried out to verify the measurements of the ancillary devices by comparing temperature and composition readings obtained

at different stages of the distillation with expected values based on published Vapour-Liquid Equilibrium (VLE) data at the measured temperatures.

### A.2.1 Run T1

The column was charged with 30 litres of a 0.1 mole fraction methanol feed and run at total reflux until steady state was reached. It was then switched to partial offtake at a reflux ratio of 8:1 for 16 minutes and returned to total reflux until a new steady state was reached. It was once more set to partial offtake at a reflux ratio of 8:1, this time, for 9 minutes and returned again to total reflux until another new steady state was reached. This procedure provides extensive data with which to test the steady state behaviour of the column. Temperature readings and liquid samples were taken from the still, Tray 2 and the reflux return line only for the initial runs.

Temperature readings were recorded from the still and the column and using the T-x graphs of Gmehling et al (1981), mixture compositions were obtained at these measured temperatures. The compositions expected at the measured temperatures from the published VLE data are compared with the measured sample compositions in Table A.1.

**Table A.1: Mixture Compositions at Measured Temperatures for Run T1**

Measured Temp (°C)	Sample Composition (MeOH mol frac)	Calculated Composition from VLE data (MeOH mol frac)
63.6	0.903	0.880
63.6	0.905	0.880
64.1	0.830	0.800
70.2	0.668	0.640
77.3	0.342	0.320
93.9	0.043	0.041
94.4	0.041	0.039
95.2	0.034	0.032

The sample compositions are seen in Table A.1 to be close to, but consistently higher than, the expected composition based on the VLE data at the measured temperatures. This suggests that the thermocouple readings may be slightly lower than the actual bubble point temperatures of the sampled mixtures. The maximum difference between the compositions estimated from VLE data and that measured from collected samples is only 0.03 mole fraction, which in most practical instances is a negligible error. This confirms that the thermocouple readings give a good indication of the temperature on the tray and hence, the composition of the mixture.

A slight sub-cooling of the reflux liquid was also observed hence the occurrence of temperatures lower than the normal boiling point temperature of methanol (64.5°C) in Table A.1. This could have the effect of reducing tray temperatures near the top of the column (by increasing the internal reflux) but was necessary to ensure that all the vapour entering the condenser was totally condensed.

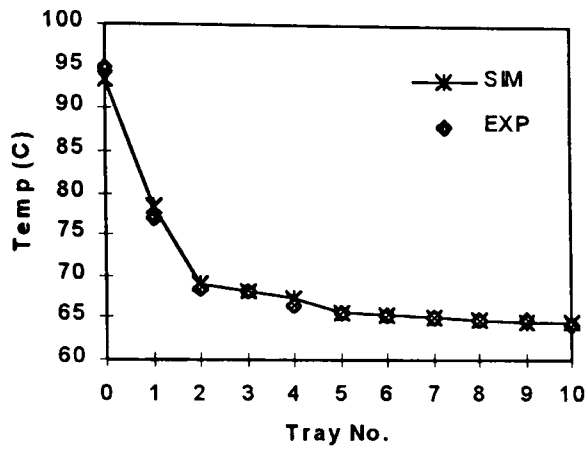
### A.2.2 Runs T2 and T3

At steady state during test run, Run T1, the measured still temperature and composition are 94.4°C and 0.041 methanol mole fraction respectively. A McCabe-Thiele calculation (not shown) using equilibrium trays and a still composition of 0.041 methanol mole fraction indicates that complete separation of the mixture is achieved in only five theoretical trays. For further runs therefore, a lower methanol concentration feed was used in order to produce a more distinct concentration profile through the column. Using a 1.499 kmol, 0.088 methanol mole fraction feed, the steam jacket was pressured up to 2.8 bar and the column was run at total reflux until steady state was attained. It was then set to run at partial offtake at a reflux ratio of 3:1 for 15 minutes and returned to total reflux and allowed to reach a new steady state. This partial offtake operation was repeated, this time at a reflux ratio of 2:1 for

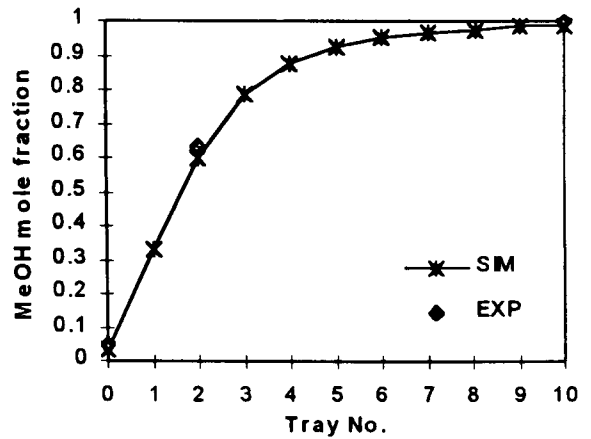
10 minutes and once more returned to total reflux and allowed to reach a new steady state. Temperature and composition measurements taken are compared with the results obtained from the simulation in Figure A.2. An identical run, performed to test the reproducibility of the experiments gave identical results (Runs T2 and T3) and only one set of results is shown.

At this stage, the tray efficiency used was a constant and equal value efficiency for all trays (Overall Column Efficiency Model) in the column and a value is assigned on a trial and error basis to match the simulation to the observed column temperature profile. A Murphree tray efficiency of 0.45 gave the best match between experimental and simulation temperature profiles after the initial startup total reflux operation (Figure A.2a). Samples were collected at only three locations on the column (the reboiler, reflux return line and Tray 2) and this is not sufficient to base a comparison of composition profiles on (Figure A.2). However, the agreement between sample compositions and estimated compositions (using published VLE data) in Run 1, suggest that a good match between experimental and simulation composition profiles in the column can be assumed when the temperature profiles match.

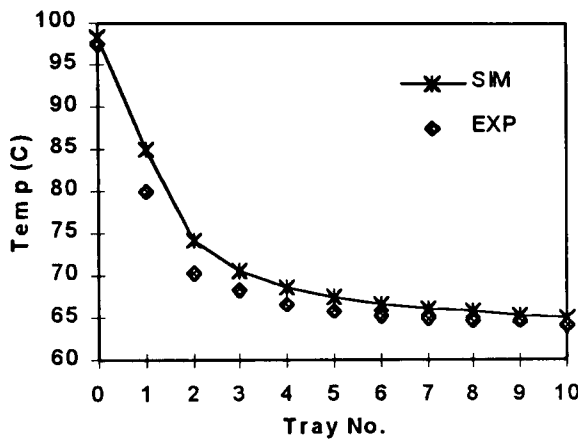
In Figure A.2c and e, the steady state temperature profiles at different stages of the distillation predicted by the model using a tray efficiency of 0.45 is seen to depart increasingly from the experimentally observed temperature profile as the distillation progresses. This suggests that the selection of a good efficiency value for use in the Overall Column Efficiency Model results in a good prediction of the experimental temperature profile at a specific point during the progress of the distillation and that compositions may be inferred from these temperatures. This efficiency will however not always produce temperature or composition profiles that match experimental results at all stages during the progress of the distillation.



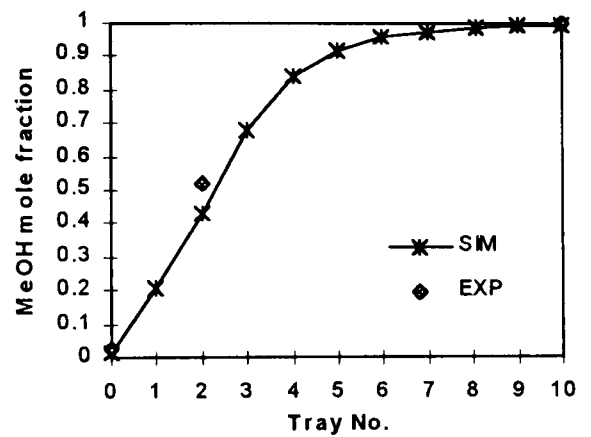
a) Initial Temperature Profile



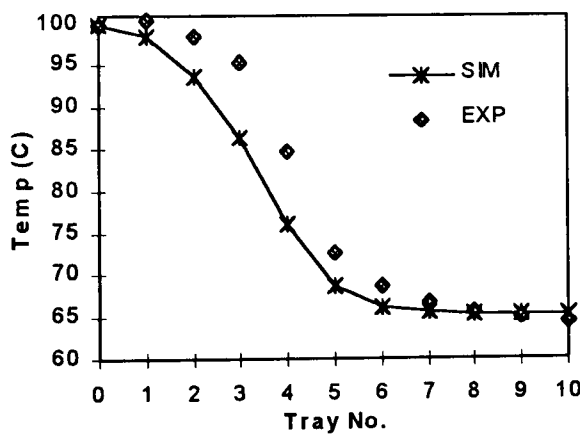
b) Initial Composition Profile



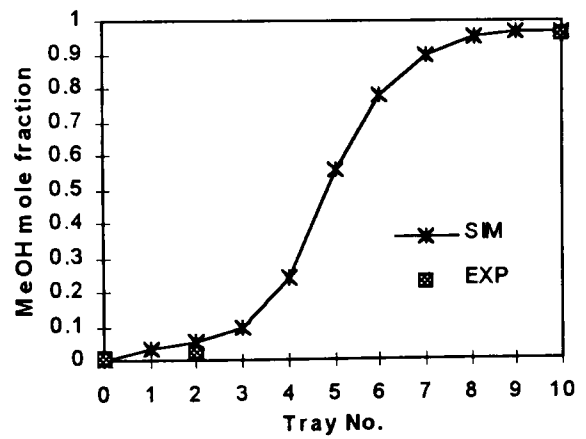
c) Temperature Profile After First Distillate Withdrawal Process



d) Composition Profile After First Distillate Withdrawal Process



e) Temperature Profile After Second Distillate Withdrawal Process



f) Composition Profile After 2<sup>nd</sup> Distillate Withdrawal Process

**Figure A.2:** Experimental and Simulation Steady State Temperature and Composition Profiles for Runs T2 and T3

### **A.3 SUMMARY OF THE FEED AND OPERATING CONDITIONS FOR THE EXPERIMENTAL AND SIMULATION RUNS**

The feed and operating conditions used for all the experimental runs are presented in Table A.2. The results obtained from running the simulation using the experimental setup and operating conditions are also presented.

The quantity of distillate collected during the partial offtake periods of Run 1 is measured but its composition is not shown in Table A.2. An error was made in the process of measuring the composition of the sample collected.

The runs described here were used in investigating the operation of the Constant Efficiency Model. For the Variable Efficiency Model however, only the operating and feed conditions of Run 6 was used for both the fixed reflux ratio and fixed distillate composition policy operations.

**Table A.2: Feed and Operating Conditions and Results of Experimental Runs and Equivalent Simulation Runs.**

	FEED	MeOH	STEAM		1 <sup>st</sup> Reflux Ratio		Product Collected		2 <sup>nd</sup> Reflux Ratio		Product Collected		
	(kmols)	mol frac.	(kg/hr)	(bar)	Value	Duration (mins)	Amount (moles)	MeOH mol frac	Value	Duration (mins)	Amount (moles)	MeOH mol frac	
Run T1	Exp	1.478	0.1000	24.0	3.20	8.0	16	0.0206	-	8.0	9	0.0100	-
	Sim	1.478	0.1000	24.0	3.20	8.0	16	0.0265	0.9830	8.0	9	0.0187	0.985
Run T2	Exp	1.499	0.0880	20.4	2.80	3.0	15	0.0562	0.9610	2.0	10	0.0499	0.7000
	Sim	1.499	0.0880	20.4	2.80	3.0	15	0.0825	0.9955	2.0	10	0.0402	0.7298
Run T3	Exp	1.499	0.0880	20.4	2.80	3.0	15	0.0562	0.9610	2.0	10	0.0499	0.7000
	Sim	1.499	0.0880	20.4	2.80	3.0	15	0.0825	0.9955	2.0	10	0.0402	0.7298
Run 1	Exp	1.540	0.0639	22.8	2.18	-	-	-	-	-	-	-	-
	Sim	1.540	0.0639	22.8	2.18	-	-	-	-	-	-	-	-
Run 2	Exp	1.580	0.0452	24.0	2.25	-	-	-	-	-	-	-	-
	Sim	1.580	0.0452	24.0	2.25	-	-	-	-	-	-	-	-
Run 3	Exp	1.540	0.0639	24.0	2.40	8.0	20	0.0773	0.9549	-	-	-	-
	Sim	1.540	0.0639	24.0	2.40	8.0	20	0.0694	0.9604	-	-	-	-
Run 4	Exp	1.375	0.0101	22.5	2.60	18.0	28	0.0276	0.5244	-	-	-	-
	Sim	1.375	0.0101	22.5	2.60	18.0	28	0.0276	0.4976	-	-	-	-
Run 5	Exp	1.148	0.1079	24.0	2.60	6.9	31	0.0879	0.9125	-	-	-	-
	Sim	1.148	0.1079	24.0	2.60	6.9	31	0.0849	0.9404	-	-	-	-
Run 6	Exp	1.168	0.0925	18.0	2.20	4.5	25	0.0780	0.9719	-	-	-	-
	Sim	1.168	0.0925	18.0	2.20	4.5	25	0.0743	0.9186	-	-	-	-
Run 7	Exp	1.206	0.0660	23.4	2.86	5.6	25	0.0675	0.9319	-	-	-	-
	Sim	1.206	0.0660	23.4	2.86	5.6	25	0.0602	0.9497	-	-	-	-

## **APPENDIX B.**

### **PROGRAM LISTING, INPUT DATA AND OUTPUT FILES**

Presented here, is a complete listing of the Fortran program code developed for this study and a sample data file containing the input data required to run the program. Variable names are assigned such that they are fairly self-explanatory.

#### **B.1 PROGRAM LISTING**

The main section of the program, presented in Figure B.1, controls the calls to the subroutines and sets all reflux ratio and printing flags. Actual vapour compositions on the trays are also calculated from the equilibrium vapour composition using Murphree tray efficiency values given, or calculated as a function of the tray composition.

The program allows interactive input of the name of the file which contains the input data required for running the program. This avoids the complications that may be encountered if program codes have to be changed whenever a different operating condition or column specification is to be simulated.

The Subroutine which estimates vapour-liquid equilibrium data using bubble point calculations governed by the Antoine equation is called BUBPT. It requires an iterative solution of the Antoine equations and liquid non-ideality is accounted for by the activity coefficient. Activity coefficients are estimated using Wilson's equation (Coulson and Richardson (1993)). A Newton-Raphson iteration is used and convergence is assumed when successive vapour compositions are exact to the 5<sup>th</sup> decimal place. The subroutine is presented in

Figure B.2 and also includes a subroutine, which estimates activity coefficients for the components of the mixture, using Wilson coefficients. Vapour pressure,  $P_{SAT}$ , is given in mmHg in this subroutine but the unit of pressure employed in other parts of the program is, atm. Conversion of pressure units is necessary to ensure consistency of units.

Subroutine INITIAL controls the data input to the model (see Figure B.3), reading data from the specified data file. Non-zero and other state variables are initialised here, as well as initial flag settings for reflux ratio control, product and slop withdrawal, operating procedures and the printing of results to file. Because the column is initially dry, the actual amount of feed in the reboiler on startup of the simulation is calculated as the total charge, less the moles of the feed material required to fill up the trays and reflux receiver. A constant volume holdup model is employed so actual molar holdup values are calculated in subroutine HOLDUP given in Figure B.4.

Details of column specification and feed composition and quantities, as well as operating conditions and efficiency data are stored in a data file which is read by the simulation using controls in subroutine INITIAL. A sample data file is presented in Section B.2.

The vapour rates, liquid rates and reflux ratios are calculated in Subroutine REBOIL. Vapour rates are calculated based on the amount of heat lost by the condensing steam in the reboiler jacket. For the fixed reflux ratio operation, liquid rates are calculated given the reflux ratio and vapour rates but in the fixed distillate composition operation, liquid flow rates are calculated using equation 4.20, which then defines the reflux ratio profile. The listing for this subroutine is shown in Figure B.5 and subroutine ENTH, for enthalpy calculations is given in Figure B.6.

The derivatives of the state variables, the liquid phase compositions are evaluated in subroutine DERIV for all trays, the still and the distillate. The subroutine listing is given in Figure B.7.

The Euler method is used for the integration of the state variables from one time step to the next using the specified time intervals. This subroutine EULER, at each time step, also updates the total amount of material left in the still and is presented in Figure B.8. A variable integration time step can be specified for a simulation run.

For the variable efficiency model, the tray efficiencies are given in the data file in a tabular manner at mixture compositions from 0 to 1.0 mole fraction, in steps of 0.05. The actual tray efficiency at any point in time (at any concentration), is calculated by linear interpolation. The subroutine that controls the estimation of these efficiencies with changing mixture composition is DYNEFF, shown in Figure B.9.

Subroutine DRAWDIST (Figure B.10) controls the distillate withdrawal aspect of the simulation runs. It sets and updates reflux ratio flags and diverts distillate between product receivers

The control of information output to the simulation result files (specified in the input data file) is carried out in subroutines PRES and PDRG, presented in Figure B.11 and Figure B.12 respectively.

```

C*****
C
C          *
C  BATCH DISTILLATION SIMULATION PROGRAM
C
C  For Batch Rectification of Ideal and Non-ideal Mixtures under fixed Reflux Ratio or
C  Fixed Distillate Composition Operating Policy and Variable tray Efficiencies.
C
C*****
C
C  DIMENSION X(100,3),Y(100,3),Z(3),BHXB(3),XD(3),EX(3)
C  DIMENSION XB(3),YB(3),DX(100,3),DBHXB(3),DXD(3),XX(3),YY(3)
C  DIMENSION XS1(3),HXS1(3),XBO(3),XS2(3),HXS2(3),YSTAR(100,3)
C  DIMENSION HL(100),HV(100),P(100),T(100),BPT(3),HN(100),EFFV(21)
C  CHARACTER*20 FILENAME(10)
C  CHARACTER*15 COMPNAME(3)
C
C  COMMON/COLUMN/NC,NT,TEST,TRAYEFF(100)
C  COMMON/PROPS/C1(3),C2(3),C3(3),AVP(3),BVP(3)
C  COMMON/INIDAT/HDX1,HDX2,HD1,HD2,HS1,HS2,HXS1,XS1,HXS2,XS2
C  OMMON/FLAGS/FLAGTE,FLAGP1,FLAGP2,FLAGS1,REFLAG1,REFLAG2,DEND
C  COMMON/DISTN/XD1AV,XD2AV,XB3AV,XD1,XD2,XB3,D,L,V,X,Y,QDIS
C  COMMON/TIMEX/TIME,TPRINT,DTPRN,TP1,TE,TSLOP1,TP2,DELTA,TSTOP,OD,CD
C  COMMON/HEAT/HVAPST,HVAP(3),MST,WILCO(3,3)
C  COMMON/ANTOINE/ANTA(3),ANTB(3),ANTC(3)
C  COMMON/ROLEX/TDRAW1,TDSTP1,TDRAW2,TDSTP2,RFIX(2),RMAX,RRTYPE
C  COMMON/HOLD/RHO(3),RMM(3)
C  COMMON/NAME/COMPNAME,FILENAME
C  COMMON/SETP/XD1SP,XD2SP,XB3SP
C  COMMON/DELTF/DELFLAG1,DELFLAG2
C  COMMON/SLOPS/HS1TOT,HS2TOT
C
C  REAL KC,L,MST
C  INTEGER RRTYPE
C
C  WRITE(*,*)' INPUT DATA FILE NAME - '
C  READ(*,10)FILENAME(1)
C  OPEN(3,FILE=FILENAME(1),STATUS='OLD')
C  OPEN(10,FILE='C:\TMP\SMOKER.RES',STATUS='UNKNOWN')
10 FORMAT(A20)
C
C  CALL INITIAL(Z,HBO,VN,VD,HD,HN,XD,XB,XBO,BH,P,TB,PB,PD,BHXB,EFFV)
C  CALL HEADER(NC)

```

**Figure B.1:** Main Program Listing.

```

IF(RRTYPE.EQ.0) R=RFIX(1)
  DELFLAG1=-1.
  DELFLAG2=-1.
  FLAGTE=-1.
  FLAGP1=-1.
  FLAGP2=-1.
  FLAGS1=-1.
  REFLAG1=-1.
  REFLAG2=-1.
  DEND=-1.
  ICHECK=0
  WRITE(*,*) XBO(J) =',(XBO(J),J=1,NC)
  WRITE(*,20)
20 FORMAT(/,'      OPERATING AT TOTAL REFLUX UNTIL PRODUCT SPEC
+ IS MET'/      One Moment Please !!!',/)

30 CALL BUBPT(XB,PB,YB,TB)
  CALL ENTH(TB,XB,YB,HBL,HBV)
  CALL REBOIL(NC,NT,XB,XD,R,RMAX,RRTYPE)

C Assume an initial temp on all trays, equal to still BUBPT Temp.
  IF(TIME.LT.DELTA) THEN
    DO 40 N=1,NT
40 T(N)=TB
  ENDIF

C Estimate Murphree tray efficiencies from concentration data.
  CALL DYNEFF(NT,X,EFFV,TRAYEFF)

  DO 50 N=1,NT
    DO 60 J=1,NC
60   XX(J)=X(N,J)
    CALL BUBPT(XX,P(N),YY,T(N))
    CALL ENTH(T(N),XX,YY,HL(N),HV(N))
    TOTY=0.
    DO 70 J=1,NC
      YSTAR(N,J)=YY(J)
      Y(N,J)=(YSTAR(N,J)-Y(N-1,J))*TRAYEFF(N)+Y(N-1,J)
      IF(N.EQ.1) Y(N,J)=(YSTAR(N,J)-YB(J))*TRAYEFF(N)+YB(J)
70   IF(J.LT.NC) TOTY=TOTY+Y(N,J)
      Y(N,NC)=1.-TOTY
50 CONTINUE
    ICHECK=ICHECK+1

C Operate at total reflux until DX(1) reaches XD1SP or calculate
  IF(TIME.LT.TPRINT) GOTO 80
  CALL PRES(T,TB,XB,XD,YB,HN,BH,XXB,R)
80 IF(TIME.GE.DELTA) GOTO 95

```

Figure B.1: Continued.

```

C
85 CALL EULER(HBO,BH,BHXB,XD,XB,YB,HN,HD,R,RMAX)

   IF(BH.LE.0.) GOTO 112
   SHN=0.
   DO 90 K=1,NT
   DO 100 M=1,NC
100 EX(M)=X(K,M)

CALL HOLDUP(NC,EX,VN,HN(K))
90 SHN=SHN+HN(K)
   CALL HOLDUP(NC,XD,VD,HD)
   GOTO 30

C   This section is dedicated to the refluc operation
95 IF(TIME.GT.TSTOP) GOTO 112
   CALL DRAWDIST(BH,HN,HD,XD,XB,YB,TB,R)
   IF(DEND)111,111,112
111 GOTO 85

112 TF=TIME
   SHN=0.
   DO 120 I=1,NT
120 SHN=SHN+HN(I)
   BHPSHN=BH+SHN
   CAP=(HD1+BHPSHN+HD2)/(TF+.5)

   WRITE(*,*)'ICHECK = ',ICHECK-1
   WRITE(*,*)' BH = ',BH,' HD1 = ',HD1
   WRITE(*,*)' P3 = ',BH+SHN,' SHN = ',SHN,' HD = ',HD
   WRITE(*,*)' HBO = ',BH+SHN+HD+HD1+HD2+HS1+HS2
   WRITE(6,130)HD1,HD2,BH+SHN+HD,TE,TP1,TSLOP1,TP2,TF,CAP
130 FORMAT('/ P1 = ',F8.5,' P2 = ',F8.5,' P3   = ',F8.5,/
+' TE = ',F5.2,3X,' TP1= ',F5.2,3X,' TSLOP1 = ',F5.2,/
+' TP2= ',F5.2,3X,' TF = ',F5.2,3X,' CAP   = ',F6.2)

C
   WRITE(6,140)HS1TOT,XS1
140 FORMAT(' S1 = ',F8.4,' XS1= ',3F8.5)
   IF(HS2TOT.GT.0.) THEN
   DO 150 J=1,NC
150 XS2(J)=(HS2*XS2(J)+HD*XD(J))/HS2TOT
   ENDIF

```

Figure B.1: Continued.

```
C
  CALL PDRG(NT,X,Y,XB,YB)
  WRITE(5,160)TIME
160 FORMAT(/2X,' AT TIME = ',F5.2//)
  WRITE(6,170)HS2TOT,XS2
170 FORMAT(' S2 =',F8.4,' XS2= ',3F8.5)

  STEAM=MST*18.015*TIME
  WRITE(6,180)STEAM
180 FORMAT(' Total Steam used =',F8.4,'kg')

  STOP
  END
```

**Figure B.1: Continued.**

```

SUBROUTINE BUBPT(X,P,Y,T)
C
  DIMENSION X(3),Y(3),PSAT(3),GAM(3)

  COMMON/COLUMN/NC,NT,TEST,TRAYEFF(100)
  COMMON/PROPS/C1(3),C2(3),C3(3),AVP(3),BVP(3)
  COMMON/ANTOINE/ANTA(3),ANTB(3),ANTC(3)

  LOOP=0

C Convert T to Kelvin and P to mmHg
  TK=T+273.
  PK=P*760
10 LOOP=LOOP+1
  IF(LOOP.GT.50) GOTO 30
  SUMY=0.

  CALL WILSON(X,NC,GAM)

C PSAT is given in mmHg
  DO 15 J=1,NC
    PSAT(J)=EXP(ANTA(J)-ANTB(J)/(TK+ANTC(J)))
    Y(J)=PSAT(J)*X(J)*GAM(J)/PK
15 SUMY=SUMY+Y(J)

  IF(ABS(SUMY-1.).LT..00001)THEN
    T=TK-273.15
    RETURN
  ENDIF

  F=SUMY*PK-PK
  DF=0.
  DO 20 J=1,NC
20 DF=DF+ANTB(J)*X(J)*PSAT(J)*GAM(J)/(TK+ANTC(J))**2

  TK=TK-F/DF
  GOTO 10
30 WRITE(6,40)
  WRITE(*,*) 'TEMP LOOP ERROR, T =',T
40 FORMAT(5X,'TEMP LOOP ERROR')

  CALL PDRG(NT,X,Y,XB,YB)

  STOP
  END

SUBROUTINE WILSON(X,NC,GAM)
  DIMENSION X(3),GAM(3)

  COMMON/HEAT/HVAPST,HVAP(3),MST,WILCO(3,3)
  REAL MST

```

**Figure B.2:** Bubble Point Temperature Subroutine Listing.

C Wilson Coefficients for MeOH (1) & Water (2) are :

```
C DATA (A(1,I),I=1,2)/1.0000,0.4180/
```

```
C DATA (A(2,I),I=1,2)/0.9699,1.0000/
```

```
DO 20 K=1,NC
```

```
Q1=0.
```

```
Q2=0.
```

```
DO 30 J=1,NC
```

```
30 Q1=Q1+X(J)*WILCO(K,J)
```

```
DO 40 I=1,NC
```

```
Q3=0.
```

```
DO 50 J=1,NC
```

```
50 Q3=Q3+X(J)*WILCO(I,J)
```

```
40 Q2=Q2+(X(I)*WILCO(I,K))/Q3
```

```
20 GAM(K)=EXP(1-LOG(Q1)-Q2)
```

```
RETURN
```

```
END
```

**Figure B.2: Continued.**

```

SUBROUTINE INITIAL(Z,HBO,VN,VD,HD,HN,XD,XB,XBO,BH,P,TB,PB,PD,
BHXB,EFFV)
C
C This sub initialises the column data

DIMENSION Z(3),XBO(3),XS1(3),HXS1(3),XS2(3),HXS2(3),XB(3),BHXB(3)
DIMENSION X(100,3),Y(100,3),XD(3),P(100),HN(100),EFFV(21),T1(3)
DIMENSION T2(3),VP1(3),VP2(3),CPL(3),CPV(3),BPT(3)
CHARACTER*20 FILENAME(10)
CHARACTER*15 COMPNAME(3)

COMMON/COLUMN/NC,NT,TEST,TRAYEFF(100)
COMMON/PROPS/C1(3),C2(3),C3(3),AVP(3),BVP(3)
COMMON/INIDAT/HDX1,HDX2,HD1,HD2,HS1,HS2,HXS1,XS1,HXS2,XS2
COMMON/DISTN/XD1AV,XD2AV,XB3AV,XD1,XD2,XB3,D,L,V,X,Y,QDIS

COMMON/TIMEX/TIME,TPRINT,DTPRN,TP1,TE,TSLOP1,TP2,DELTA,TSTOP,OD,CD
COMMON/HEAT/HVAPST,HVAP(3),MST,WILCO(3,3)
COMMON/ANTOINE/ANTA(3),ANTB(3),ANTC(3)
COMMON/ROLEX/TDRAW1,TDSTP1,TDRAW2,TDSTP2,RFIX(2),RMAX,RRTYPE
COMMON/HOLD/RHO(3),RMM(3)
COMMON/NAME/COMPNAME,FILENAME
COMMON/SETP/XD1SP,XD2SP,XB3SP
COMMON/SLOPS/HS1TOT,HS2TOT
REAL MST
INTEGER RRTYPE

READ(3,10)(FILENAME(J),J=2,6)
10 FORMAT(5A20)
20 FORMAT(A15)

OPEN(5,FILE=FILENAME(2),STATUS='UNKNOWN')
OPEN(6,FILE=FILENAME(3),STATUS='UNKNOWN')
OPEN(7,FILE=FILENAME(4),STATUS='UNKNOWN')
OPEN(8,FILE=FILENAME(5),STATUS='UNKNOWN')
OPEN(9,FILE=FILENAME(6),STATUS='UNKNOWN')

C INITILISE DATA
READ(3,25)NT,NC
READ(3,*)XD1SP,XD2SP,XB3SP,(Z(J),J=1,NC)
READ(3,*)TEST,TSTOP,OD,TPRINT,DTPRN
DELTA=OD
CD=DELTA/10.
READ(3,*)TDRAW1,TDSTP1,TDRAW2,TDSTP2
25 FORMAT(I3,I3)
DO 15 J=1,NC
READ(3,20)COMPNAME(J)
READ(3,*)RHO(J),RMM(J)
READ(3,*)T1(J),VP1(J),T2(J),VP2(J)
READ(3,*)CPL(J),CPV(J)

```

**Figure B.3:** Subroutine INITIAL Listing for Column Data Initialisation.

```

READ(3,*)BPT(J)
  READ(3,*)HVAP(J)
  READ(3,*)ANTA(J),ANTB(J),ANTC(J)
  C3(J)=CPL(J)
  C2(J)=CPV(J)
  C1(J)=HVAP(J)+BPT(J)*(C3(J)-C2(J))
  AVP(J)=(T1(J)+273.)*(T2(J)+273.)*ALOG(VP2(J)/VP1(J))/(T1(J)-T2(J))
15 BVP(J)=ALOG(VP2(J))-AVP(J)/(T2(J)+273.)

C Former data statement for feed(mols) and reflux & tray holdup (m3) resp.
  READ(3,*)HBO
  READ(3,*)VD,VN !324.612E-6 !215.00E-6
C Number of Trays in Column.
C "Pressure in Atmospheres"
  READ(3,*)PB,PD
C Constant Reflux ratio. Max of 2 RR's for the withdrawal of 2 prods.
  READ(3,*)RFX(1),RFX(2),RMAX,RRTYPE
C WST is the Steam flow rate in kg/hr and HVAPST, the Heat of vaptn.
  READ(3,*)WST,HVAPST ! From actual data
C Initial Estimate of Still (Bottoms) Temperature in Deg C
  READ(3,*)TB
C Read Wilson coefficients
  DO 30 I=1,NC
  30 READ(3,*)(WILCO(I,J),J=1,NC)
C Tray Efficiencies. Read values from data file from X=0 to X=1.
  READ(3,*)(EFFV(J),J=1,21)
  WRITE(*,*)(EFFV(J),J=1,21)

  WRITE(*,*)NC,NT,PD,PB,(TRAYEFF(N),N=1,NT)

  MST=WST/18.015

  ZTOT=0.
  DO 50 J=1,NC
  XBO(J)=Z(J)
  50 ZTOT=ZTOT+Z(J)
  IF(ZTOT.NE.1.)THEN
  WRITE(*,*) ' Normalised Feed Mole Fraction'
  DO 60 J=1,NC
  60 XBO(J)=XBO(J)/ZTOT
  ENDIF

  WRITE(5,65)(COMPNAME(J),J=1,NC)
  WRITE(6,65)(COMPNAME(J),J=1,NC)
  WRITE(7,65)(COMPNAME(J),J=1,NC)
  WRITE(8,65)(COMPNAME(J),J=1,NC)
  WRITE(9,65)(COMPNAME(J),J=1,NC)
  65 FORMAT(/1X,' DISTILLATION OF ',A,' / ',A,' / ',A,'" SYSTEM')
  WRITE(6,70)NT,HBO,XBO
  70 FORMAT(//,' NT = ',I4,' HBO = ',F8.4,' XBO = ',3F8.4)

```

Figure B.3: Continued.

```

WRITE(5,75)RFX(1),(EFFV(N),N=1,21)
  WRITE(6,75)RFX(1),(EFFV(N),N=1,21)
  WRITE(7,75)RFX(1),(EFFV(N),N=1,21)
  WRITE(8,75)RFX(1),(EFFV(N),N=1,21)
  WRITE(9,75)RFX(1),(EFFV(N),N=1,21)
75 FORMAT(' R = ',F4.1,3(' EFF =',7F8.3,/,10H    ))

C  INITIAL CONDITIONS

HDX1=0.
HDX2=0.
HD1=0.
HD2=0.
XD1AV=1.
XD2AV=1.
TP2=0.
HS1=0.
HS2=0.
HS1TOT=0.
HS2TOT=0.
TIME=0.

C  Estimate molar tray holdup (given vol holdup) or give fixed value!!
SHN=0.
DO 80 I=1,NT
  CALL HOLDUP(NC,XBO,VN,HN(I))
80 SHN=SHN+HN(I)
  CALL HOLDUP(NC,XBO,VD,HD)
  BH=HBO-HD-SHN
C  WRITE(*,*)' HBO,HD,SHN,BH',HBO,HD,SHN,BH
  WRITE(*,85)(HN(N),N=1,NT),HD
85 FORMAT(1X,'HN = ',(10F8.5,),' HD = ',F9.5)

DO 90 J=1,NC
HXS1(J)=0.
XS2(J)=0.
HXS2(J)=0.
XB(J)=XBO(J)

BHXB(J)=BH*XBO(J)
DO 95 N=1,NT
95  X(N,J)=XBO(J)
90 XD(J)=XBO(J)

C  Calculate Column Pressure Profile
DO 99 N=1,NT
99 P(N)=PB-(N*(PB-PD))/NT

RETURN
END

```

Figure B.3: Continued.

```
SUBROUTINE HOLDUP(NC,X,VN,TRHOLD)

DIMENSION X(3),W(3),Z(3)
COMMON/HOLD/RHO(3),RMM(3)

REAL M

SW=0.
DO 2 J=1,NC
  W(J)=X(J)*RMM(J)
2 SW=SW+W(J)
DO 4 J=1,NC
  4 Z(J)=W(J)/SW

RHOM=0.
RMMM=0.
DO 10 J=1,NC
  RHOM=RHOM+Z(J)*RHO(J)
10 RMMM=RMMM+X(J)*RMM(J)

M=RHOM*VN
TRHOLD=M/RMMM

RETURN
END
```

**Figure B.4:** Subroutine HOLDUP Listing.

```

SUBROUTINE REBOIL(NC,NT,XB,XD,R,RMAX,RRTYPE)

DIMENSION X(100,3),Y(100,3),XB(3),XD(3)

COMMON/DISTN/XD1AV,XD2AV,XB3AV,XD1,XD2,XB3,D,L,V,X,Y,QDIS

COMMON/FLAGS/FLAGTE,FLAGP1,FLAGP2,FLAGS1,REFLAG1,REFLAG2,DEND
COMMON/HEAT/HVAPST,HVAP(3),MST,WILCO(3,3)
COMMON/HOLD/RHO(3),RMM(3)
REAL MST,L
INTEGER RRTYPE

C Vapour rate is obtained from  $V=(HVAPs * Fs) / HVAPm$ , not a fixed Q.
HVAPM=0.
RMMM=0.
DO 10 I=1,NC
RMMM=RMMM+XB(I)*RMM(I)
10 HVAPM=HVAPM+XB(I)*HVAP(I)
V=HVAPST*MST/HVAPM
VMAS=V*RMMM

IF(RRTYPE.LT.1) THEN
IF(REFLAG1.GT.0..OR.REFLAG2.GT.0.) THEN
L=V*(R/(R+1.))
D=V-L
ELSE
D=0.
L=V
ENDIF
ELSE
IF(REFLAG1.GT.0..OR.REFLAG2.GT.0.) THEN
IF(D.GT.0..AND.R.GE.RMAX) GOTO 25
L=(V*(Y(NT,1)-Y(NT-1,1)))/(XD(1)-X(NT,1))
D=V-L
IF(D.GT.0.) R=L/D
25 IF(R.GE.RMAX) THEN
R=RMAX
L=0.5*V
D=V-L
ENDIF
GOTO 40
ELSE
GOTO 30
ENDIF
30 L=V
D=V-L
R=RMAX
ENDIF
40 CONTINUE
RETURN
END

```

**Figure B.5:** Subroutine REBOIL, Fluid rates and Reflux Ratio Calculation Listing.

```

SUBROUTINE ENTH(T,X,Y,HL,HV)

DIMENSION X(3),Y(3)

COMMON/COLUMN/NC,NT,TEST,TRAYEFF(100)
COMMON/PROPS/C1(3),C2(3),C3(3),AVP(3),BVP(3)

HL=0.
HV=0.
DO 10 J=1,NC
HL=HL+X(J)*C3(J)*T
HV=HV+Y(J)*(C1(J)+C2(J)*T)
10 CONTINUE
RETURN
END

```

**Figure B.6:** Subroutine ENTH, Enthalpy Calculations Listing.

```

SUBROUTINE DERIV(XD,YB,HN,HD,DX,DXD,DBH,DBHXB)

DIMENSION DBHXB(3),DXD(3),YB(3),XD(3),X(100,3),Y(100,3),DX(100,3)
DIMENSION HN(100)
COMMON/COLUMN/NC,NT,TEST,TRAYEFF(100)
COMMON/DISTN/XD1AV,XD2AV,XB3AV,XD1,XD2,XB3,D,L,V,X,Y,QDIS

REAL L

DBH=-D
DO 10 J=1,NC
DBHXB(J)=L*X(1,J)-V*YB(J)
DX(1,J)=(V*YB(J)+L*X(2,J)-V*Y(1,J)-L*X(1,J))/HN(1)
    DO 15 N=2,NT-1
15  DX(N,J)=(V*Y(N-1,J)+L*X(N+1,J)-V*Y(N,J)-L*X(N,J))/HN(N)
DX(NT,J)=(V*Y(NT-1,J)+L*XD(J)-V*Y(NT,J)-L*X(NT,J))/HN(NT)
IF(HD.EQ.0.0)THEN
DXD(J)=0.0
ELSE
DXD(J)=V*(Y(NT,J)-XD(J))/HD
ENDIF
10 CONTINUE

RETURN
END

```

**Figure B.7:** Subroutine DERIV Listing

```

SUBROUTINE EULER(HBO,BH,BHXB,XD,XB,YB,HN,HD,R,RMAX)

DIMENSION X(100,3),BHXB(3),XD(3),DBHXB(3),DXD(3),DX(100,3)
DIMENSION XB(3),YB(3),Y(100,3),EX(3),HN(100),XS1(3),HXS1(3),XS2(3)
DIMENSION HXS2(3),XDC(3)

COMMON/COLUMN/NC,NT,TEST,TRAYEFF(100)
COMMON/INIDAT/HDX1,HDX2,HD1,HD2,HS1,HS2,HXS1,XS1,HXS2,XS2
COMMON/DISTN/XD1AV,XD2AV,XB3AV,XD1,XD2,XB3,D,L,V,X,Y,QDIS

COMMON/TIMEX/TIME,TPRINT,DTPRN,TP1,TE,TSLOP1,TP2,DELTA,TSTOP,OD,C
D

COMMON/FLAGS/FLAGTE,FLAGP1,FLAGP2,FLAGS1,REFLAG1,REFLAG2,DEND
COMMON/SETP/XD1SP,XD2SP,XB3SP
COMMON/DELTF/DELFLAG1,DELFLAG2
COMMON/HOLD/RHO(3),RMM(3)

REAL L

CALL DERIV(XD,YB,HN,HD,DX,DXD,DBH,DBHXB)

TIME=TIME+DELTA
C Section for acc XD est by reducing "Dt" in the Const Xd case.
DO 5 J=1,NC
5 XDC(J)=XD(J)+DXD(J)*DELTA
IF(DELFLAG1.LT.0.)THEN
IF(REFLAG1.LT.0.AND.XDC(1).GT.XD1SP.OR.REFLAG2.GT.0.AND.XDC(2).GT.
+XD2SP) THEN
DELFLAG1=1.
DELTA=CD
ELSE
DELTA=OD
ENDIF
ENDIF

IF(DELFLAG1.GT.0..AND.(XDC(1)-XD1SP).GT.0.00001.AND.DELTA.GT.
+1.0E-5) THEN
DELTA=DELTA/10.
ENDIF
IF(D.GT.0..OR.R.GE.RMAX) DELTA=OD
SHN=0.
DO 10 I=1,NT
10 SHN=SHN+HN(I)
BH=HBO-HD-SHN-QDIS+DBH*DELTA ! QDIS includes slop cuts here.
IF(BH.LE.0.) THEN
WRITE(6,*)'----- STILL POT EMPTY -----'
WRITE(*,*)'----- STILL POT EMPTY -----'
RETURN
ENDIF

```

**Figure B.8:** Subroutine Euler Numerical Integration Program Listing.

```
DO 20 J=1,NC
  BHXB(J)=BHXB(J)+DBHXB(J)*DELTA
  XB(J)=BHXB(J)/BH
    DO 25 N=1,NT
      X(N,J)=X(N,J)+DX(N,J)*DELTA
      IF(X(N,J).GT.1.) X(N,J)=1.
      IF(X(N,J).LT.0.) X(N,J)=0.
25    CONTINUE
20  XD(J)=XD(J)+DXD(J)*DELTA
    SXBS=0.
    DO 22 J=1,NC-1
22  SXBS=SXBS+XB(J)
    XB(NC)=1.-SXBS

    IF(XB(1).LT..00001.AND.NC.EQ.3) THEN
      XB(1)=0.00001
      XB(3)=1.-XB(2)
    ELSE IF(XB(1).LT.0.00001) THEN
      XB(1)=0.00001
      XB(2)=1.
    ENDIF

    RETURN
  END
```

**Figure B.8: Continued.**

```
SUBROUTINE DYNEFF(NT,EX,EFFV,EFF)

DIMENSION EFFV(21),XV(21),X(100,3),EX(100,3),EFF(100)
DATA XV/0.,0.05,0.1,0.15,0.2,0.25,0.3,0.35,0.4,0.45,0.5,0.55,0.6,
+0.65,0.7,0.75,0.8,0.85,0.9,0.95,1./

DO 10 N=1,NT
COMP=EX(N,1)

DO 130 I=1,21
IF(COMP.LE.XV(I)) THEN
X2=XV(I)
X1=XV(I-1)
T2=EFFV(I)
T1=EFFV(I-1)
GOTO 140
ENDIF
130 CONTINUE
140 CONTINUE

TC=(COMP-X1)*((T2-T1)/(X2-X1))+T1
X(N,1)=COMP
10 EFF(N)=TC

RETURN
END
```

**Figure B.9:** Subroutine DYNEFF Listing.

```

SUBROUTINE DRAWDIST(BH,HN,HD,XD,XB,YB,TB,R)

DIMENSION X(100,3),Y(100,3),Z(3),BHXB(3),XD(3),HN(100)
DIMENSION XB(3),YB(3),DX(100,3),DBHXB(3),DXD(3),XX(3),YY(3)
DIMENSION XS1(3),HXS1(3),XBO(3),XS2(3),HXS2(3),YSTAR(100,3)
DIMENSION HL(100),HV(100),P(100),T(100),BPT(3)

COMMON/COLUMN/NC,NT,TEST,TRAYEFF(100)
COMMON/INIDAT/HDX1,HDX2,HD1,HD2,HS1,HS2,HXS1,XS1,HXS2,XS2
COMMON/FLAGS/FLAGTE,FLAGP1,FLAGP2,FLAGS1,REFLAG1,REFLAG2,DEND
COMMON/DISTN/XD1AV,XD2AV,XB3AV,XD1,XD2,XB3,D,L,V,X,Y,QDIS

COMMON/TIMEX/TIME,TPRINT,DTPRN,TP1,TE,TSLOP1,TP2,DELTA,TSTOP,OD,CD
COMMON/ROLEX/TDRAW1,TDSTP1,TDRAW2,TDSTP2,RFIX(2),RMAX,RRTYPE
COMMON/HEAT/HVAPST,HVAP(3),MST,WILCO(3,3)
COMMON/SETP/XD1SP,XD2SP,XB3SP
COMMON/SLOPS/HS1TOT,HS2TOT

REAL L,MST
INTEGER RRTYPE

R=R*1.
IF(FLAGTE.GE.0.) GOTO 20
IF(TIME.GE.TDRAW2.AND.TIME.LT.TDSTP2.OR.XD(2).GE.XD2SP) GOTO 60
IF(FLAGS1.GT.0.) GOTO 80

IF(XD(1).GE.XD1SP)THEN
CALL PDRG(NT,X,Y,XB,YB)
WRITE(5,5)TIME
5 FORMAT(/2X,' AT TIME = ',F5.2//)

FLAGTE=1.
REFLAG1=1.
TE=TIME
STEAM=MST*18.015*TIME
WRITE(6,10)TE,STEAM,TIME,D,TB,(XB(J),J=1,NC),(XD(J),J=1,NC),XD1AV,
+XD2AV
10 FORMAT(' START P1 WITHDRAWAL AT - ',F8.4,'hrs, ',F8.4,' Kg of Ste
+am used',/F5.2,F7.2,1X,F8.3,6F8.5,' <--- ',2F8.5)

WRITE(*,15)
15 FORMAT(/10X,'Withdrawing First Product'//5X,'PLEASE WAIT ..!/')
ELSE
RETURN
ENDIF
20 CONTINUE
C
IF(FLAGP1.GT.0.) GOTO 30
TP1=TIME
HD1=HD1+D*DELTA
QDIS=QDIS+D*DELTA
HXD1=HXD1+D*XD(1)*DELTA
IF(D.GT.0.)XD1AV=HXD1/HD1

```

**Figure B.10:** Subroutine DRAWDIST Listing.

```

C START SLOP CUT 1 WITHDRAWAL - FLAGP1=1 FOR SLOP 1 WITHDRAWAL!
  IF(XD1AV.LT.XD1SP) THEN
FLAGP1=1. ! Remove the Comment symbol to withdraw slop
  TP1=TIME
  STEAM=MST*18.015*TIME
  WRITE(6,25)TP1,STEAM,TIME,D,TB,(XB(J),J=1,NC),(XD(J),J=1,NC),XD1AV
  +,XD2AV
25 FORMAT(' END P1 WITHDRAWAL AT - ',F8.4,'hrs, ',F8.4,' Kg of Steam
  + used',F5.2,F7.2,1X,F8.3,6F8.5,' <--- ',2F8.5)
  WRITE(*,28)TP1
28 FORMAT(/10X,' END P1 WITHDRAWAL AT (TP1) = ',F8.4,/)
  ENDIF
30 IF(FLAGP1.LE.0.) RETURN
  IF(FLAGS1.GT.0.) GOTO 80

  HS1=0.
  DO 40 J=1,NC
  HXS1(J)=HXS1(J)+D*XD(J)*DELTA
40 HS1=HS1+HXS1(J)
  QDIS=QDIS+HS1
  HSITOT=HSITOT+HS1
  DO 50 J=1,NC
50 XS1(J)=HXS1(J)/HS1
C
C START P2 WITHDRAWAL - FLAGS1 = 1 !!!
  IF(NC.EQ.2)THEN
  XB3SP=XD2SP
  XB3=XB2
  GOTO 105
  ENDIF

60 CONTINUE
  FLAGS1=1.
  REFLAG2=1.
  TSLOP1=TIME
  WRITE(6,65)TSLOP1,TIME,D,TB,(XB(J),J=1,NC),(XD(J),J=1,NC),XD1AV,
  +XD2AV
65 FORMAT(' START P2 WITHDRAWAL AT (TSLOP1) = ',F8.4,/F5.2,F6.1,1X,
  +F8.3,8F8.5,' <---')
  WRITE(*,70)
70 FORMAT(/10X,'Withdrawing Second Product'//5X,'PLEASE WAIT ...!/')

80 IF(FLAGS1.LT.0.) RETURN
  IF(FLAGP2.GT.0.) GOTO 90
  XD2=XD(2)
  HD2=HD2+D*DELTA
  QDIS=QDIS+D*DELTA
  HXD2=HXD2+D*XD2*DELTA
  IF(HD2.GT.0.)XD2AV=HXD2/HD2

```

Figure B.10: Continued.

```
IF(RRTYPE.EQ.0.AND.TIME.GE.TDSTP2)THEN
  FLAGP2=1.
  GOTO 115
ENDIF

90 IF(FLAGP2.LT.0.) GOTO 105
  HS2=0.
  DO 95 J=1,NC
    HXS2(J)=HXS2(J)+D*XD(J)*DELTA
  95 HS2=HS2+HXS2(J)
    QDIS=QDIS+HS2
  DO 100 J=1,NC
  100 XS2(J)=HXS2(J)/HS2
  105 SUM=0.
    SHN=0.
    DO 110 N=1,NT
      SHN=SHN+HN(N)
  110 SUM=SUM+X(N,NC)*HN(N)
      SUM=SUM+XB(NC)*BH
      XB3AV=SUM/(BH+SHN)
    RETURN
  115 IF(FLAGP2.GT.0.) THEN
    HS2TOT=HD+HS2
    ELSE
    BH=BH+HD+HS2
    ENDIF
    WRITE(*,120)
  120 FORMAT(/10X,'Bottom Product Specification Reached'//5X,
    +'Distillation will Terminate Now !!')

    IF(FLAGP2.LT.0.) THEN
      HTEST=HD+HD2
      XTEST2=(HXD2+HD*XD2)/HTEST
      IF(XTEST2.GT.XD2SP) THEN
        HD2=HD2+HD
        HS2TOT=0.
        DO 130 J=1,NC
  130   XS2(J)=0.
        ENDIF
      ENDIF
    DEND=1.

    RETURN
  END
```

**Figure B.10: Continued.**

```

SUBROUTINE PRES(T,TB,XB,XD,YB,HN,BH,XXB,REF)

C For timed write to output file.

DIMENSION XB(3),XD(3),YB(3),T(100),X(100,3),Y(100,3),YSTAR(100,3)
DIMENSION TC(100),HN(100)
COMMON/COLUMN/NC,NT,TEST,TRAYEFF(100)
COMMON/DISTN/XD1AV,XD2AV,XB3AV,XD1,XD2,XB3,D,L,V,X,Y,QDIS
COMMON/TIMEX/TIME,TPRINT,DTPRN,TP1,TE,TSLOP1,TP2,DELTA,TSTOP,OD,CD

REAL L

SHN=0.
DO 10 N=1,NT
10 SHN=SHN+HN(N)
  WRITE(6,15)TIME,V,TB,(XB(J),J=1,NC),(XD(J),J=1,NC),XD1AV,XD2AV
15 FORMAT(F5.2,F7.2,1X,F8.3,8F8.5)
20 FORMAT(1X,'T =',F5.2,' HN = ',2(5F8.5,/),' HD = ',F8.5)
  WRITE(8,25)TIME,TB,(T(N),N=1,NT)
25 FORMAT(F5.2,11(1X,F8.3))
  TPRINT=TPRINT+DTPRN
  WRITE(*,35)TIME,BH,XD(1),T(5),V,L !,R
35 FORMAT(1X,6(F10.6,2X))

DO 40 N=0,NT
IF(N.EQ.0) THEN
WRITE(7,50)XB(1),XB(1),YB(1),XB(1),XB(1),XB(1),YB(1),YB(1),N
ELSE IF(N.EQ.1) THEN
WRITE(7,50)X(N,1),X(N,1),Y(N,1),YB(1),X(N,1),X(N,1),Y(N,1),Y(N,1),
+N
ELSE
WRITE(7,50)X(N,1),X(N,1),Y(N,1),Y(N-1,1),X(N,1),X(N,1),Y(N,1),Y(N,
+1),N
ENDIF
50 FORMAT(4(F8.4),/4(F8.4),I5)
40 CONTINUE
  WRITE(7,50)Y(10,1),Y(10,1),Y(10,1),Y(10,1)
  WRITE(7,55)TIME
55 FORMAT(' TIME = ',F8.4,/))

YB(1)=YB(1)
IF(D.GT.0.)THEN
RRR=L/D
ELSE
RRR=REF
ENDIF
WRITE(9,30)TIME,XB(1),XXB,X(5,1),X(6,1),X(10,1),QDIS,XD(1),REF
30 FORMAT(F6.3,5F8.4,2X,F7.4,2F8.4)

RETURN
END

```

**Figure B.11:** Subroutine PRES Listing for Output of Simulation Results.

```
SUBROUTINE PDRG(NT,X,Y,XB,YB)

DIMENSION X(100,3),Y(100,3),YSTAR(100,3),YB(3),XB(3)

DO 10 N=0,NT
IF(N.EQ.0) THEN
WRITE(5,20)N,(XB(J),J=1,3),(YB(J),J=1,3)
ELSE
WRITE(5,20)N,(X(N,J),J=1,3),(Y(N,J),J=1,3)
ENDIF
20 FORMAT(15,2(3(F8.4),3H ))
10 CONTINUE

RETURN
END
```

**Figure B.12:** Subroutine PDRG Listing, for Output of Composition Results

```

SUBROUTINE HEADER(NC)
□
□
WRITE(5,10)
□
10 FORMAT(1X,'TRAY',3X,'X(N,1)',2X,'X(N,2)',2X,'X(N,3)',5X,'Y(N,1)',2
□
+X,'Y(N,2)',2X,'Y(N,3)')
□
IF(NC.EQ.2)THEN
□
WRITE(6,20)
□
20 FORMAT(' TIME D    TB  XB1  XB2  XD1  XD2  XD1A
+V  XD2AV')
ENDIF
IF(NC.EQ.3)THEN
WRITE(6,30)
30 FORMAT(' TIME D    TB  XB1  XB2  XB3  XD1  XD2
+  XD3  XD1AV  XD2AV')
ENDIF
WRITE(7,50)
50 FORMAT(2X,'X(N,1)',2X,'X(N,1)',2X,'Y(N,1)',2X,'Stages',2
+X,'TRAY')
WRITE(8,35)
35 FORMAT(/,1X,'TIME',5X,'TB',7X,'T1',7X,'T2',7X,'T3',7X,'T4',7X,'T5'
+,7X,'T6',7X,'T7',7X,'T8',7X,'T9',7X,'T10')
WRITE(9,40)
40 FORMAT(/,'TIME  XB(1)  XS  X(5,1) X(6,1) X(10,1) QDIS
+  XD  REF')

RETURN
END

```

**Figure B. 13:** Subroutine Header Listing for Writing Output File Headers.

## B.2 SAMPLE INPUT DATA AND OUTPUT FILES

The simulation model developed is able to handle a variety of batch rectification column specifications. For greater ease of operation, a standalone program is created which can be run on any Personal Computer. This made it necessary to write the simulation in a manner such that data is input either interactively or from a data file. The data file option was chosen for this model

and a sample data file for the run using the efficiency curve with a maximum efficiency of 1.3 (i.e. efficiency curve  $E_{1.3}$ ) is shown in Table B. 1.

A description of the data values shown in the sample data file are as described below:

*Line1:* Names of the files to which simulation results are written.

*Line2:* Number of trays in the column and number of components in the mixture used.

*Line3:* Product purity specifications for components 1, 2 and 3 and feed mole fractions of components 1, 2 and 3.

*Line4:* Start time, Stop time, Integration step size (in hours), time to start writing results to file and time interval between writing results to file.

*Line5:* Start and stop times for first distillate offtake operation and start and stop times for second distillate offtake operation, for fixed reflux ratio policy simulation runs.

*Line6:* Name of component 1

*Line7:* Density and Molecular weight of component 1.

*Line8:* Temperature-1, Vapour pressure at Temperature-1 (in atm), temperature-2 and vapour pressure at temperature-2 (used in enthalpy calculations) for component 1.

*Line9:* Liquid and vapour heat capacities for component 1.

**Table B. 1: Sample Data File For the Simulation**

1)	T1-3.DRG	T1-3.ANS	T1-3.MCB	T1-3.TEM	T1-3.CMP				
2)	10	2							
3)	0.99	1.9995	0.00	0.0925	0.9075	0.00			
4)	0.0	3.2	0.001	0.00	0.01				
5)	3.200	3.2	10000	10000					
6)	METHANOL								
7)	747.486	32.042							
8)	65.302	760	83.8107	1551.02					
9)	90.5927	48.8223							
10)	64.54								
11)	35855.8								
12)	18.5875	3626.55	-34.29						
13)	WATER								
14)	990.500	18.015							
15)	100.0	760	121.308	1551.02					
16)	75.9716	36.8242							
17)	100.00								
18)	40653.8								
19)	18.3036	3816.44	-46.13						
20)	1.1678								
21)	1.23E-4	364.24E-6							
22)	1.0037	1.0024							
23)	04.50	2.00	20	1					
24)	18.00	39510.90							
25)	80.0								
26)	1.0000	0.4180							
27)	0.9699	1.0000							
28)	1.300	1.164	1.043	0.936	0.843	0.765	0.700	0.650	0.615
	0.593	0.586	0.593	0.615	0.650	0.700	0.765	0.843	0.936
	1.043	1.164	1.300						

*Line10:* Normal boiling point temperature of component 1 (in °C).

*Line11:* Heat of vaporisation of component 1.

*Line12:* Antoine constants A, B and C for component 1.

*Line13:* Name of component 2.

*Line14:* Density and Molecular weight of component 2.

*Line15:* Temperature-1, Vapour pressure at Temperature-1 (in atm),  
temperature-2 and vapour pressure at temperature-2 for component 2.

*Line16:* Liquid and vapour heat capacities of component 2.

*Line17:* Normal boiling point temperature of component 2.

*Line18:* Heat of vaporisation of component 2.

*Line19:* Antoine constants A, B and C for component.

For a multicomponent mixture, lines 13 to 19 are repeated for each new component before the next data items are entered into the data file.

*Line20:* Total moles of feed charged to the column.

*Line21:* Tray and reflux receiver, constant volume holdup values.

*Line22:* Pressure (in atm), at the top and the bottom of the column.

*Line23:* Reflux ratio for first offtake operation, reflux ratio for second offtake operation (for fixed reflux ratio policy), the maximum allowable reflux ratio (for fixed distillate composition policy), choice of operating policy (constant or variable reflux ratio).

The fourth data item on line 23 represents the choice of operating policy. A value of "0" indicates a fixed reflux ratio operation while "1" indicates a fixed distillate composition (variable reflux ratio) policy operation.

*Line24:* Steam flow rate in kg/hr and the heat of vaporisation of the steam at the operating jacket pressure.

*Line25:* Initial guess temperature for still content bubble point calculations.

*Line26:* Wilson coefficients  $\Lambda_{1j}$  for binary pairs of component 1 and other components,  $j$  in the mixture where  $j = 1, 2, \dots, NC$ . A value of '1.0' is entered for the coefficient of any component, paired with itself.

*Line27:* Wilson coefficients  $\Lambda_{2j}$  for binary pairs of component 2 and other components,  $j$  in the mixture where  $j = 1, 2, \dots, NC$ .

For a multicomponent mixture, a new line is added for each component.

*Line28:* The tray efficiency of component 1, given for all molar compositions from 0.0 to 1.0 in steps of 0.05.

Again, for a multicomponent mixture, more lines are added giving the information of line 28 for the other components up to component  $NC-1$ , where  $NC$  is the total number of components in the mixture.

For each simulation run, results are written to five output files for different sets of data. For the sample input data shown in Table B. 1, two sample output files T1-3.ANS and T1-3.DRG are presented in Table B. 2 and Table B. 3.

Table B. 2: Sample Output File T1-3.ANS

DISTILLATION OF "METHANOL / WATER /								
NT = 10	HBO =	1.1678	XBO =	.0925	.9075	.0000		
R = 4.5	EFF =	1.300	1.164	1.043	.936	.843	.765	.700
	EFF =	.650	.615	.593	.586	.593	.615	.650
	EFF =	.700	.765	.843	.936	1.043	1.164	1.300
TIME	D	TB	XB1	XB2	XD1	XD2	XD1AV	XD2AV
.00	.98	87.670	.09250	.90750	.09250	.90750	1.0000	1.0000
.01	.98	87.975	.08898	.91102	.44691	.55309	1.0000	1.0000
.02	.98	88.282	.08553	.91447	.58907	.41093	1.0000	1.0000
.03	.98	88.589	.08218	.91782	.65485	.34515	1.0000	1.0000
.04	.98	88.927	.07859	.92141	.70705	.29295	1.0000	1.0000
.05	.98	89.234	.07541	.92459	.74726	.25274	1.0000	1.0000
.06	.98	89.541	.07232	.92768	.78220	.21780	1.0000	1.0000
.07	.98	89.848	.06931	.93069	.81239	.18761	1.0000	1.0000
.08	.98	90.154	.06638	.93362	.83873	.16127	1.0000	1.0000
.09	.98	90.429	.06381	.93619	.85961	.14039	1.0000	1.0000
.10	.98	90.734	.06103	.93897	.87980	.12020	1.0000	1.0000
.11	.98	91.037	.05833	.94167	.89715	.10285	1.0000	1.0000
.12	.98	91.338	.05571	.94429	.91224	.08776	1.0000	1.0000
.13	.98	91.637	.05318	.94682	.92515	.07485	1.0000	1.0000
.14	.98	91.934	.05072	.94928	.93620	.06380	1.0000	1.0000
.15	.98	92.227	.04834	.95166	.94566	.05434	1.0000	1.0000
.16	.98	92.518	.04603	.95397	.95364	.04636	1.0000	1.0000
.17	.98	92.804	.04381	.95619	.96047	.03953	1.0000	1.0000
.18	.98	93.086	.04167	.95833	.96631	.03369	1.0000	1.0000
.19	.98	93.364	.03960	.96040	.97122	.02878	1.0000	1.0000
.20	.98	93.637	.03762	.96238	.97539	.02461	1.0000	1.0000
.21	.98	93.905	.03571	.96429	.97892	.02108	1.0000	1.0000
.22	.97	94.167	.03387	.96613	.98190	.01810	1.0000	1.0000
.23	.97	94.422	.03211	.96789	.98446	.01554	1.0000	1.0000
.24	.97	94.672	.03043	.96957	.98664	.01336	1.0000	1.0000
.25	.97	94.915	.02882	.97118	.98849	.01151	1.0000	1.0000
.26	.97	95.151	.02728	.97272	.99006	.00994	1.0000	1.0000
START P1	WITHDRAWAL AT - .2600hrs, 4.6800 Kg of Steam used							
.26	.00	95.151	.02728	.97272	.99006	.00994	1.0000	1.0000
.27	.97	95.375	.02584	.97416	.99063	.00937	.99050	1.0000
.28	.97	95.616	.02432	.97568	.99067	.00933	.99058	1.0000
.29	.97	95.829	.02299	.97701	.99068	.00932	.99061	1.0000
.30	.97	96.036	.02172	.97828	.99069	.00931	.99063	1.0000
.31	.97	96.238	.02051	.97949	.99070	.00930	.99064	1.0000
.32	.97	96.433	.01934	.98066	.99072	.00928	.99065	1.0000
.33	.97	96.621	.01823	.98177	.99073	.00927	.99066	1.0000
.34	.97	96.804	.01717	.98283	.99074	.00926	.99067	1.0000
.35	.97	96.980	.01616	.98384	.99076	.00924	.99068	1.0000
.36	.97	97.149	.01520	.98480	.99077	.00923	.99069	1.0000

Table B. 2 Continued.

□	.37	.97	97.312	.01429	.98571	.99079	.00921	.99069	1.0000	
□	.38	.97	97.468	.01342	.98658	.99080	.00920	.99070	1.0000	
	.39	.97	97.618	.01260	.98740	.99082	.00918	.99071	1.0000	
	.40	.97	97.761	.01182	.98818	.99084	.00916	.99072	1.0000	
	.41	.97	97.898	.01108	.98892	.99085	.00915	.99072	1.0000	
	.42	.97	98.029	.01038	.98962	.99087	.00913	.99073	1.0000	
	.43	.97	98.153	.00972	.99028	.99088	.00912	.99074	1.0000	
	.44	.97	98.271	.00909	.99091	.99090	.00910	.99074	1.0000	
	.45	.97	98.384	.00850	.99150	.99092	.00908	.99075	1.0000	
	.46	.97	98.490	.00795	.99205	.99093	.00907	.99075	1.0000	
	.47	.97	98.592	.00743	.99257	.99095	.00905	.99076	1.0000	
	.48	.97	98.687	.00694	.99306	.99097	.00903	.99077	1.0000	
	.49	.97	98.778	.00648	.99352	.99099	.00901	.99077	1.0000	
	.50	.97	98.863	.00604	.99396	.99100	.00900	.99078	1.0000	
	.51	.97	98.944	.00564	.99436	.99102	.00898	.99078	1.0000	
	.52	.97	99.020	.00526	.99474	.99104	.00896	.99079	1.0000	
	.53	.97	99.091	.00490	.99510	.99106	.00894	.99079	1.0000	
	.54	.97	99.159	.00456	.99544	.99107	.00893	.99079	1.0000	
	.55	.97	99.222	.00425	.99575	.99108	.00892	.99080	1.0000	
	.56	.97	99.281	.00396	.99604	.99110	.00890	.99081	1.0000	
	.57	.97	99.334	.00370	.99630	.98806	.01194	.99071	1.0000	
	.58	.97	99.384	.00345	.99655	.98221	.01779	.99019	1.0000	
	END P1 WITHDRAWAL AT -				.5830hrs, 10.4939 Kg of Steam used					
	.58	.49	99.394	.00340	.99660	.98069	.01931	.98992	1.0000	
	.59	.97	99.422	.00327	.99673	.97343	.02657	.98992	1.0000	
	.60	.97	99.427	.00324	.99676	.96116	.03884	.98992	1.0000	
	.61	.97	99.392	.00342	.99658	.94502	.05498	.98992	1.0000	
	.62	.97	99.291	.00391	.99609	.92566	.07434	.98992	1.0000	
	.63	.97	99.020	.00526	.99474	.90074	.09926	.98992	1.0000	
	.64	.97	97.608	.01265	.98735	.87547	.12453	.98992	1.0000	
	----- STILL POT EMPTY -----									
	P1 =	.04789	P2 =	.00000	P3 =	.17075				
	TE =	.26	TP1 =	.58	TSLOP1 =	.00				
	TP2 =	.00	TF =	.64	CAP =	.19				
	S1 =	.9487	XS1 =	.93449	.06551	.00000				
	S2 =	.0000	XS2 =	.00000	.00000	.00000				
	Total Steam used = 11.6099kg									

Table B. 3: Sample Output file T1-3.DRG.

DISTILLATION OF "METHANOL / WATER /									
R =	4.5	EFF =	1.300	1.164	1.043	.936	.843	.765	.700
		EFF =	.650	.615	.593	.586	.593	.615	.650
		EFF =	.700	.765	.843	.936	1.043	1.164	1.300
TRAY	X(N,1)	X(N,2)	X(N,3)	Y(N,1)	Y(N,2)	Y(N,3)			
0	.0273	.9727	.0000	.1862	.8138	.0000			
1	.0301	.9699	.0000	.2047	.7953	.0000			
2	.0463	.9537	.0000	.2884	.7116	.0000			
3	.1337	.8663	.0000	.4980	.5020	.0000			
4	.3747	.6253	.0000	.6416	.3584	.0000			
5	.5640	.4360	.0000	.7462	.2538	.0000			
6	.6933	.3067	.0000	.8324	.1676	.0000			
7	.7979	.2021	.0000	.9006	.0994	.0000			
8	.8804	.1196	.0000	.9482	.0518	.0000			
9	.9382	.0618	.0000	.9762	.0238	.0000			
10	.9726	.0274	.0000	.9905	.0095	.0000			
AT TIME = .26									
0	.0414	.9586	.0000	.2550	.7450	.0000			
1	.0164	.9836	.0000	.0883	.9117	.0000			
2	.0094	.9906	.0000	.0706	.9294	.0000			
3	.0073	.9927	.0000	.0554	.9446	.0000			
4	.0061	.9939	.0000	.0480	.9520	.0000			
5	.0057	.9943	.0000	.0459	.9541	.0000			
6	.0103	.9897	.0000	.0907	.9093	.0000			
7	.0828	.9172	.0000	.4228	.5772	.0000			
8	.4276	.5724	.0000	.6219	.3781	.0000			
9	.6045	.3955	.0000	.7527	.2473	.0000			
10	.7435	.2565	.0000	.8574	.1426	.0000			
AT TIME = .64									

## APPENDIX C.

### PROPERTIES OF COMPONENTS

**Table C.1:** Table of Antoine Constants (Coulson and Richardson (1993))

	Antoine Constants			Antoine Constants Valid Range (°C)
	A	B	C	
Methanol	18.5875	3626.55	-34.29	-16 - 91
Ethanol	18.9119	3803.98	-41.68	-3 - 96
Propanol	17.5439	3166.38	-80.15	12 - 127
Cyclohexane	15.752	2766.63	-50.50	7 - 107
Toluene	16.0137	3096.52	-53.67	7 - 137
Water	18.3036	3816.44	-46.13	11 - 168

Antoine equation:  $\ln P^\circ = A - B / [(T + 273) + C]$  with T in °C and P° in mmHg.

**Table C.2:** Physical Properties of the Mixture Components

	Molecular Weight	Density (kg/m <sup>3</sup> )	Boiling Temp (°C)	Heat Capacity (J/mol.K)		Heat of Vaporisation (J/mol)
				Liq	Vap	
Methanol	32.042	747.486	64.54	90.59	48.82	35856.2
Ethanol	46.069	736.448	78.29	139.14	76.38	37895.6
Propanol	60.096	735.529	97.15	193.20	104.92	41223.5
Cyclohexane	84.162	723.547	80.73	180.59	133.28	30097.7
Toluene	92.141	780.316	110.63	185.38	136.87	33032.1
Water	18.015	999.989	100.00	75.97*	36.82*	40654.2*

\* - The heat capacity and heat of vaporisation of steam used for each simulation run was dependent on the prevailing steam pressure and temperature

**Table C.3:** Wilson Coefficients,  $\Lambda_{ij}$  for Methanol-Water System (Hirata et al (1975))

$i \backslash j$	Methanol	Water
Methanol	1.0000	0.4180
Water	0.9699	1.0000

**Table C.4:** Wilson Coefficients,  $\Lambda_{ij}$  for Methanol-Ethanol-Propanol System (Hirata et al (1975))

$i \backslash j$	Methanol	Ethanol	Propanol
Methanol	1.0000	1.8539	1.8450
Ethanol	0.6091	1.0000	1.1291
Propanol	0.4024	0.6801	1.0000

**Table C.5:** Wilson Coefficients,  $\Lambda_{ij}$  for Cyclohexane-Toluene System (Hirata et al (1975))

$i \backslash j$	Cyclohexane	Toluene
Cyclohexane	1.0000	1.3002
Toluene	0.4822	1.0000